Evolution of Black Holes and Anisotropic Neutron Stars under Late Time Cosmic Acceleration

A Thesis is submitted to JADAVPUR UNIVERSITY
for the award of the degree of

DOCTOR OF PHILOSOPHY
in
SCIENCE (PHYSICS)

by

MAYUKH BANDYOPADHYAY

(Regn. No.: $SOPHY1105522$**, Index No.:** $55/22/PHYSICS/27$**)**

JADAVPUR UNIVERSITY(FACULTY OF SCIENCE)
DEPARTMENT OF PHYSICS
KOLKATA-700032
WEST BENGAL, INDIA

KOLKATA
May, 2024

CERTIFICATE FROM THE SUPERVISOR(S)

This is to certify that the thesis entitled "Evolution of Black Holes and Anisotropic Neutron Stars under Late Time Cosmic Acceleration" submitted by Sri MAYUKH BANDYOPADHYAY (Index No.: 55/22/PHYS./27) who got his name registered on February 18th , 2022 for the award of Ph. D. (Science) degree of Jadavpur University, is absolutely based upon his own work under the supervision of Prof. Subenoy Chakraborty (Supervisor) and Assistant Prof. Ritabrata Biswas (Co-Supervisor) and that neither this thesis nor any part of it has been submitted for either any degree / diploma or any other academic award anywhere before.

Subenoy Chakraborty 10/5/2024

(Signature of the Supervisor, date with official seal)

Ritabrata Biswas 10/5/2024

(Signature of the Co-Supervisor, date with official seal)

Dr. Ritabrata Biswas
Assistant Professor
Department of Mathematics
[illegible] University of [illegible]

DECLARATION BY THE AUTHOR

I do hereby declare that the thesis entitled "**Evolution of Black Holes and Anisotropic Neutron Stars under Late Time Cosmic Acceleration**" is composed independently by me at the Jadavpur University, Kolkata. The entire work, reported in this thesis which is carried out under the supervision of my main guide, **Dr. Subenoy Chakraborty, Professor, Department of Mathematics, Jadavpur University, Kolkata-**700032**, West Bengal, India** and my co-guide, **Dr. Ritabrata Biswas, Assistant Professor (Stage-*II*), Department of Mathematics, The University of Burdwan, Purba Bardhaman-**713104**, West Bengal, India**, is original.
I further declare that the subject matter in the thesis has not been submitted for awarding any degree/diploma/associateship/fellowship or any other qualifications at any other university or institution. All the figures presented in this thesis have been produced by the author using MATHAMETICA, C-Programming and GNUPLOT software. The thesis has been checked several times with utmost alertness to make it free from all discrepancies and typos. Even then the vigilant readers may find some mistakes and various sections of this thesis may seem unwarranted or mistaken. The author takes the sole liability for those undesired oversight.
Ultimately, I state that, to the best of my knowledge, all the facilitation taken in to prepare this thesis has been duly recognized.

Place: Jadavpur, Kolkata

Mayukh Bandyopadhyay 10/05/2024

Mayukh Bandyopadhyay
(Ph.D. Candidate)
Department of Physics
Jadavpur University

ASTROPHYSICS and COSMOLOGY

Evolution of Black Holes and Anisotropic Neutron Stars under Late Time Cosmic Acceleration

Ph.D. Thesis-May 2024

Author: Mayukh Bandyopadhyay

Supervisor: Prof. Subenoy Chakraborty

Co-Supervisor: Assistant Prof. Ritabrata Biswas

Location: Jadavpur, Kolkata

"God gave me nothing I wanted, he gave me everything I needed.
The gift of knowledge is the highest gift in the world."

– **Swami Vivekananda**

Dedicated
to my beloved guruma, ***Sri Sri MA ANANDAMAYI*** *and the departed soul of my loving maternal grandmother,* ***Smt. DEEPTI BANERJEE***

ACKNOWLEDGEMENTS

I have been incredibly fortunate these last five years to work with and have the facilitation of so many amazing people. Foremost, I would like to acknowledge my enormous debt to my advisor, **Prof. Subenoy Chakraborty**. His vision and tireless dedication to astronomy were inspiring and led to the topics in this thesis being at the forefront of astrophysics. Our styles contrasted, but his energy, open advice and support, made for a very rewarding collaboration. In this same vein, I am grateful to my co-advisor, **Dr. Ritabrata Biwas**, whose ideas and open door made the last 3 years incredibly enjoyable. I also express my gratitude for his immense support, insights and patience throughout this entire journey. I am fortunate enough to get such two friends, philosopher and guide.

I wish to express my warm and sincere thanks to Professor Anup Bandyopadhyay, subject expert, from the department of mathematics, Jadavpur University, Professor Kalyan Kumar Chattopadhyay and Professor Nabin Baran Manik, Head of the Department of Physics, Jadavpur University for their important guidance during each and every step of my research and studies. Their ideas and concepts have had a remarkable influence on my entire research career in the field of compact stars (Black Holes and Neutron Stars).

I am indebted to all the excellent faculty members and staff (of the Department of Physics as well as Mathematics, Jadavpur University and the Department of Mathematics, The University of Burdwan) for their care, support and understanding which helped me to carry out the research. I would like to pledge my gratitude and deep obligation to all my teachers in different stages of my educational career, for their con-

tinuous inspiration and support without which I could not reach in such a position and whatever I am. I am really blessed to get luminary teachers like Ashoke Mahanta, Dipak Roy, Anadai Chatterjee, Gadadhar Ghoshchowdhury, Sukumar Ghoshchowdhury, Debashis Bhattacharaya, Prodip Majhila, Kaliprasad Bandyopadhyay, Taraknath Sarkar, Shaymol Banerjee, Sanjoy Mahanta, Partha Sam and Rajarshi Banerjee during my high school days.

I have also had the privilege of working with a number of talented people on a wide variety of topics. I feel myself to be quite lucky in the sense that from the very first day of this journey, I found many people around me who constantly assisted me in various occasions like Mr. Kishor Kumar Bhattacherjee and Mrs. Bandana Bhattacherjee. I can still remember the love and care of my grandmother Santi Rani Bandyopadhyay, as my sweetest childhood memories. Actually, her stories (mythological) of various stars from "Suktara" and "Chand-Mama" from my childhood attracted me toward the wonder of our Universe.

I fondly remember a few of my friends like Soumya Da, Shantanu, Ramanuj, Shrabanti, Jhumki, Saptorshi, Tanu, Asish Da, Debasrita, Laltu, Toto, Probir, Sujit, Mansa, Suvendu Da, Avijit Da, Shamima, Suvo, Buddhadeb, Ayan Da, Samriddhi, Ismaile Da, Chandan and Gadadhar, for their unbound love and unconditional support during my journey from the school to the university. I can still remember the discussions on physical ideas with Koushik Da during the university days, from which I have learnt a lot. Best wishes for their career ahead.

I am grateful to other Ph.D. students like Sandip Da, Promila, Giri, Akash Da, Dipankar, Gopal Da, Roshni, Madhu, Shriton, Ayan and Dhriti for their helpful assistance whenever it was required for me. I would like to convey my gratitude to all of my friends with whom I have shared the colorful moments during these past years. Best wishes for their research career ahead.

I owe much to those who invited me to contribute on equal terms in their field of expertise and thereby made my research enjoyable. I am threatful for the sharing of information, the professional guidance and the skilled feedback of those who became involved in my work.

I wish to express my warm and sincere thanks to my sisters Purba and Tinni, my nephew Sayan and obviously my aunt, Asima, Purabi and Chobi. Aunt Asima with her vast deep knowledge in mathematics, always has become an inspirational character

to me from my childhood. The religious lifestyle shown by Aunt Purabi has inspired me to be more passionate about my work and to find the real goal of life. My late maternal grandmother Deepti Banerjee had given me a lot of enthusiasm for higher study and unconditional love from my childhood. Unfortunately she would not be able to see this thesis but I know that she is always with me.

I would also like to thank the IUCAA (Inter University Centre for Astronomy and Astrophysics, Pune, India) that got me thinking hard about astrometry and also for providing fooding, lodging and all kinds of facilities for carrying my research during my visits. I specially acknowledge the updated facilities at IUCAA library. The calm and quiet environment at the library helped me a lot during my deep study and realization, calculations.

Most importantly I owe my most sincere gratitude to thank my family. My mother, Mrs. Tultul Bandyopadhyay for her endless love and support through this whole journey, and my father, Mr. Utpal Bandyopadhyay for his timely advice and insights. For me, their sacrifice knows no bounds. My grandmothers through their life made me understand the value of life. None of this would have been possible without my amazing partner, Sukanya, whose caring, loving support knows no bounds - thank you for taking this journey with me.

During my research, I have received the scholarships and stipends grant under "Swami Vivekananda Merit Cum Means" scholarship by the government of West-Bengal. I gratefully acknowledge the financing.

At last but not the least I thank almighty God and my Gurudev(Gurumaa) for all the grace and love received during the entire journey.

Mayukh Bandyopadhyay
(Ph.D Candidate, J.U.)

PUBLICATIONS

1. "Repulsive gravitational force and quintessence field in $f(T)$ gravity: How anisotropic compact stars in strong energy condition behave." by **Mayukh Bandyopadhyay** and R. Biswas. *Modern Physics Letters A*, **36(07) (2021) 2150044**.
https://doi.org/10.1142/S0217732321500449.

2. "Generalized model of interacting dark energy and dark matter: Phase portrait analysis for evolving Universe." by G. Deogharia, **Mayukh Bandyopadhyay** and R. Biswas. *Modern Physics Letters A*, **36(40) (2021) 2150275**.
https://doi.org/10.1142/S0217732321502758.

3. "Impacts of modified Chaplygin gas on super-massive neutron stars embedded in quintessence field with $f(T)$ gravity." by **Mayukh Bandyopadhyay** and R. Biswas. *International Journal of Modern Physics D*, **32(03) (2023) 2350006**.
https://doi.org/10.1142/S0218271823500062.

4. "Investigation on the stability and quantum phase transition of the charged rotating Kiselev Black Hole embedded in Quintessence field with quantum fluctuation of entropy." by **Mayukh Bandyopadhyay** and R. Biswas. *International Journal of Geometric Methods in Modern Physics*, **21(01) (2024) 2450021**.
https://doi.org/10.1142/S021988782450021X.

5. "Nuclear Matter Equation of State and Stability of Charged Compact Stars Embedded in $f(T)$ Modified Gravity, under Cosmic Acceleration." by **Mayukh Bandyopadhyay** and R. Biswas. *International Journal of Geometric Methods in Modern Physics*, **21(05) (2024) 2450097**.
https://doi.org/10.1142/S021988782450097X.

6. "Investigating the Equation of state, Stability and Mass-Radius relationship of Anisotropic and Massive Neutron Stars embedded in $f(R,T)$ modified gravity." by **Mayukh Bandyopadhyay** and R. Biswas. *International Journal of Geometric Methods in Modern Physics*, (2024) 2450203.
https://doi.org/10.1142/S0219887824502037.

Evolution of Black Holes and Anisotropic Neutron Stars under Late Time Cosmic Acceleration

—Mayukh Bandyopadhyay

May, 2024

ABSTRACT

The dissertation actually focuses on the theoretical study of the cosmic evolution of black holes and the neutron stars (mainly high massive neutron stars) with the primary observational manifestation, through the present accelerated universe under the framework of modified gravity theories. Black holes (BHs) and Neutron stars (NSs) are incredibly high dense relativistic objects that have given a unparalleled semblance of physics in utmost physical environments. These objects are a powerful source of electromagnetic radiation and relativistic particles. General relativity (GR hereafter) exhibits good agreement and to work fully enough during the local weak field tests of gravity. However, difficulties and challenges come when applied to the massive relativistic objects, the entire Universe including dark entities and the singularities of space-time.

It is believed that quantum gravity can resolve these complications but a commonly adopted theory is still absent. So, modifications of GR which may indicate the quantum corrections are extensively argued. During my research, I have also studied the stability and phase transitions of the rotating BHs embedded in dark energy where quantum corrected thermodynamic parameters of the BHs are investigated. GR can also be constructed by using the tetrad field as the dynamical variable instead of the metric where the torsional scalar T is considered to be the underlying Lagrangian. The corrections corresponding to the higher energy scale may appear as terms of higher order of torsion with a nonlinear function of T. The $f(T)$

gravity may possess new features and provide new angles to supervise the geometry of space-time. Further we have also employed the concept of minimal matter-gravity coupling through the modified $f(R,T)$ gravity to model the massive NSs where R is the Ricci scalar and T denotes the trace of energy-momentum tensor. This $f(R,T)$ theory is the generalization of $f(R)$ modified theories of gravity where the coupling between geometry and matter plays a crucial role to realize space-time geometry.

On the other hand, a series of observational evidence have put the standard cosmology in a dilemma. Scientists are in confusion in the choice of perfect gravity theory and in the choice of the matter contained. The standard cosmology with Einstein gravity and normal matter can not support the present cosmic acceleration phase of the Universe. Cosmologists are trying to accommodate the observational prediction of the present accelerated Universe by applying the following two options : (i) Einstein gravity with some exotic matter having large negative pressure known as dark energy (DE) (ii) modified gravity theory with usual matter. Again modified gravity theory, comes in a natural way to accommodate the tensions in the present expansion rate of the Universe and as an alternative way to modifying the standard model of particle physics through dark matter, which has also been tested to explain the late-time cosmic acceleration and it supports the local gravitational tests.

Einstein's GR become quite successful in predicting various gravitational phenomena related to the solar system observations and also in case of strong-field situations but it faces difficulty to solve the mysteries related with DE and other puzzles. Besides, few questions in modern cosmology remain unsolved. Moreover, it is also shown by the scientists that as a quantum field theory, GR is renormalizable only if we can include higher order curvature terms in its action. Further, applications of GR become not necessary at small time and length scales and also for Planck energy scales. In this scenario, scientists have successfully argued that by incorporating changes in the geometric part of Einstein's GR theory can explain the early-time inflation and also late time accelerated expansion of the Universe.

One promising route to investigate these relativistic stars is to study their physical properties of matter by which they are formed. For the stellar matter if energy is conserved, can be approximated by the perfect fluid and a correlation between the space-time metric and the stellar structure can be found. In GR, this is famous Tolman-Oppenheimer-Volkoff (TOV hereafter) equation. Further, the equation of state (EoS hereafter) of the core matter is also necessary for understanding the interior structure of the stars. A mathematical co-relation between matter density and pressure is very much needed to close the system of differential equations. Physically, EoS represents the connection between the pressure and density which can describe the properties of the core stellar matter. For the stars like a NS in which the matter is so dense that a total relativistic treatment is required for understanding their properties. However, the modified theories of gravity essentially change the TOV equations and as a result of that astrophysical properties of the compact stars (e.g., maximum mass, moment of inertia, mass-radius relation etc.) are also varied in some way.

In recent times, there are very firm arguments on the presence and impacts of anisotropy (unequal tangential and radial pressure at the interior of the NSs) on the massive NSs with core nuclear matter at extremely high pressures and densities. Scientists have also demonstrated that the existence of anisotropy can cause crucial changes in the principal properties as well as characteristics of the neutron stars. Recent observations on compact stars (NICER survey) strongly indicate and also disclose various evidences for the presence of anisotropic fluid inside the core in case of massive NSs. The presence of anisotropy is very crucial because the anisotropic repulsive force allows larger mass and more compact structure of the NSs compared to an isotropic fluid in GR. In our work we have introduced modified Chaplygin gas (MCG) as an anisotropic fluid at the interior of the NSs. The MCG can unify the dark matter (DM) and DE significantly. The anisotropic compact stars can accommodate more mass than their general relativistic counterparts. This thesis investigates computational and mathematical methods of our theoretical understanding about the physics of the NSs. The study focuses on the macroscopic properties, relativistic behavior

and various important observable characteristics of the NSs. Further, the mass-radius relation, tidal deformability of the binary NS systems etc. are also very interesting properties to study for the researchers.

The EoS helps to understand the properties of the core nuclear matter of the compact stars at extremely high density and pressure. But still the EoS is not fully understood and the hunt for a general and realistic EoS continues. Different models of the NSs have proposed various types of EoS depending on the underlying physics. The recent discovery of gravitational waves by LIGO from the compact binary coalitions and few highly massive pulsars from the NICER survey have put some constraints on several properties and EoS of the NSs. These can predict several crucial quantities, such as the maximum stable mass, lowest possible radius, spherically stable equilibrium configuration etc., which allow them to rule out various non-physical models based on various astronomical observations and measurements.

This current work exhibits a natural way to write a general and realistic EoS with few parameters that can reduce and approximate various other different EoS. Astronomical observations and measurements are then used to constrain different parameter values systematically. For spherically symmetric compact star structures there are various known solutions of Einstein's field equations which are very popular. I have applied the famous Krori-Barua (KB) and Tolman-Kuchowicz (TK) solutions in modeling realistic NSs during my research. In these types of singularity free solutions the space-time metric meets the physical requirements of a real compact star under spherical symmetry and in the background of modified gravity theories.

The main aim for considering the TK and KB space-time solutions are to investigate the gravitational theories that deviate from the standard GR or beyond the conventional framework. These metrics can regenerate a substitute metric that can be applied to explain the space-time geometry for some specific cases. By culturing this space-time we want to explore its implications and effective applications in realizing gravity, cosmology, nature of space-time and other related phenomena. In my work, I have

introduced the existence of modified Chaplygin gas (MCG) as an exotic fluid inside the core of these NSs as a candidate of DE and also solved the Einstein-Maxwell field equations. Also the effect of the quintessence field is examined. I have also incorporated modified TOV equations under modified gravity. Furthermore, we have matched the interior space time of the spherical star to the exterior Schwarzschild line element at its surface to obtain the unknown constants of our working model. For a charged compact star the exterior metric is chosen as the Reissner-Nordström metric.

I have found out that, exotic fluids have a great impact on the EoS of the core nuclear matter and even on the stability of the compact stars. Pressure anisotropy reduces the tidal deformability of the charged neutron stars in an appreciable amount and helps to get a more compact structure. We have also found out that it leads to a certain phase transition between the core and crust of the NSs. But surprisingly, the compact stars are still able to maintain their spherically stable and equilibrium configuration. Further, we can put constraints on several macroscopic parameters of the compact stars. Additionally, to establish the physical viability of our constructed model, we have evaluated various significant properties of the NSs like mass-radius relationship, tidal deformability, compactness, sound velocity, anisotropy, energy density, effective pressure, adiabatic index, energy conditions, surface redshift etc. During my research, in order to confirm the reliability of the NS models which I have constructed, I have applied two different tests to investigate the stability of the obtained model in modified gravity. First, I have analyzed the relativistic adiabatic indices of the NSs under spherical symmetric space-time for an anisotropic fluid. Second, I have demonstrated the validity of the modified TOV equations considering the spherical stellar system under hydrostatic equilibrium where all the acting forces on the system neutralize each other. We defined all the different forces as given by the Tolman mass formula. I have also confronted the models with data from other neutron stars to examine its validity with a broad extent of astrophysical observations. The mass-radius relationship, I obtained from different models, corresponding to diverse selection of the boundary density is compatible with the nuclear saturation density as required boundary con-

ditions, depicts the consistency of these models. These models can predict masses in the lower mass gap between $2.2 - 5.3 M_{\odot}$. Furthermore, I have confronted the compactness parameter as predicted by these models with the compactness bound given by Buchdahl. Again, by using the DEC restriction, I have calculated the maximum allowed mass and lowest possible radius of the massive anisotropic compact stars. We also have confronted all the necessary restrictions on the EoS and different properties of the massive NSs based on recent astronomical observations like gravitational wave detection and NICER data. Further, recent observations of NICER survey on the pulsars PSR$J0030 + 0541$ and PSR$J0740 + 6020$ have put forward a surprising fact that these two pulsars have nearly the same size but the later pulsar contains more mass (more compact structure) than the former pulsar. This observation offers evidence against more squeezable models of the NSs. But significantly, the existence of anisotropic force at the interior of the NSs at tremendous high density and pressure, which I have found during the research, can justify the non-squeezability of the NSs as its mass increases. The presence of MCG type fluid inside the core of the NSs may also support this non-squeezable nature of the NSs as I have got evidence of that during my research.

I have got an explicit scenario of the evolution of rotating black holes and various types of massive and anisotropic neutron stars through accelerating space-time in the background of modified gravity. The NS models which I have constructed can even explain the existence of super massive NSs by applying the modified $f(T)$ and $f(R, T)$ gravity theories in the mass range between $2.2 - 5.3 M_{\odot}$. Surprisingly, the current astronomical observations by LIGO-VIRGO-KAGRA detectors also can predict the existence of highly massive NSs which is detected through the observations of gravitational wave, $GW190814$ with mass $2.68 M_{\odot}$ and with a linear EoS and the surface density consistent with nuclear saturation density. Further the detected gravitational wave $GW230529$, also indicates the existence of massive intermediate object with mass in between $2.5 - 4.5 M_{\odot}$, which is widely believed as the NS by the scientists. Interestingly, from the current models and investigations during the research, all the derived outcomes

have become compatible with physically adopted regimes which reveals the physical viability of my present work.

PREFACE

I am of the opinion that everyone at least once during his life, grasps the necessity to create his or her personal class : this is what happened to me and here is the result, which, however, should be seen as a work still in progress. Actually, this class is not completely original, but it is a blend of all the best ideas that I have found in a number of guides, tutorials, blogs and tex.stackexchange.com posts. In particular, the main ideas come from two sources :

- My own study of various research papers, articles and books and
- The research work done at the Jadavpur University, under the supervision of Professor Subenoy Chakraborty (Supervisor) and at the University of Burdwan, under the supervision of Dr. Ritabrata Biswas (Co-Supervisor).

This thesis is based on several papers and organised in *seven parts*. *The first Chapter*, the only one chapter under **Part** I, is introductory and covers the most essential features of the thesis as *Chapter 1*. Next, there is a bunch of chapters, devoted to all reports of my entire research work, which are under the **Part** II **to Part** VI. These different parts comprise the chapters based on research outputs of 5 separate papers jointly published with Dr. Biswas and 4 research papers which are under review. The **Part** II and **Part** III each comprises two chapters upto *Chapter 5*. The *Chapter 6* and *Chapter 7* are two separate chapters under **Part** IV and **Part** V respectively. The rest of the chapters (4 chapters) upto *Chapter 11* all are under the **Part** VI.

I have to point out my contributions to the studies reported in this thesis. I was the

principal author and contributor and Ritabrata Biswas was co-author for all the published papers in various international peer-reviewed journals. I conceived and planned the study, performed the literature review, wrote up the discussion of the literature, interpreted findings and wrote the paper. Dr. Biswas conceived and planned the study, collected and analyzed parts of the data, interpreted findings and was responsible for reviewing the entire work and writing a few pages. On the other hand I can gratefully point out that Professor Chakraborty also has contributed significantly to the research design and study, interpretation and presentation of results with final layout. Dr. Ritabrata also significantly contributed to the submission and revision process. The last **Part** VII comprises the final *Chapter 12* of the thesis, is a summary of the research conducted and also a brief discussion on the scope and future application of the present work.

In the course of my research, I learned that no task can be completed in professional isolation without any interaction with the others. discussions arising from differences of opinion or approach, and most particularly any criticism, can of course be time consuming and even painful to deal with, but I believe it has not only kept me from making mistakes, but also added clarity.

Here is just a outline of the design of this entire thesis for easy and clear understanding as follows :

• Part I : The Chapter **1** is the introduction chapter of this thesis work.

• Part II : Chapter **2** and Chapter **3** contain material from the research articles as mentioned below:

"Repulsive gravitational force and quintessence field in $f(T)$ gravity: How anisotropic compact stars in strong energy condition behave." by **M. Bandyopadhyay** and R. Biswas. *Mod. Phys. Lett. A*. ($February$, 2021).
https://doi.org/10.1142/S0217732321500449.

"Impacts of modified Chaplygin gas on super-massive neutron stars embedded in quintessence field with $f(T)$ gravity." by **M. Bandyopadhyay** and R. Biswas. *Int. J. Mod. Phys. D*. ($January$, 2023).
https://doi.org/10.1142/S0218271823500062.

"Confrontation of $f(T) = T + \xi T^2$ Modified Gravity with Charged X-ray Binaries Embedded in modified Chaplygin gas under Tolman-Kuchowicz Spacetime" by **M. Bandyopadhyay** and R. Biswas. (*UnderReview, January* 2024).

"Investigating the Equation of state, Stability and Mass-Radius relationship of Anisotropic and Massive Neutron Stars embedded in $f(R,T)$ modified gravity" by **M. Bandyopadhyay** and R. Biswas. *Int. J. Geom. Methods Mod. Phys.* (*Accepted*, *April* 2024).
https://doi.org/10.1142/S0219887824502037.

• Part III : In Chapter **4**, I have briefly discussed the implications of General Relativity theory and its consequences w.r.t. the present scenario of the accelerating phase of the Universe. In Chapter **5**, I have made a detailed discussion on the basic construction of $f(T)$ and $f(R,T)$ modified gravity theories with their active applications in astrophysical studies and cosmology.

• Part IV : Chapter **6** is based on the research paper

"Future of the accelerating Universe: Estimation of the Hubble parameter and Deceleration parameter under current Observations" by **M. Bandyopadhyay** and R. Biswas. (*UnderReview, March,* 2024).

• Part V : Chapter **7** is based on the research article

"Investigation on the stability and quantum phase transition of the charged rotating Kiselev Black Hole embedded in Quintessence field with quantum fluctuation of entropy." by **M. Bandyopadhyay** and R. Biswas. *Int. J. Geom. Methods Mod. Phys.* (*September*, 2023).
https://doi.org/10.1142/S021988782450021X.

• Part VI : The Chapters **8** to **11** contains the materials from the below research papers:

"Nuclear Matter Equation of State and Stability of Charged Compact Stars Embedded in $f(T)$ Modified Gravity, under Cosmic Acceleration." by **M. Bandyopadhyay** and R. Biswas. *Int. J. Geom. Methods Mod. Phys.*. (*December*, 2023).
https://doi.org/10.1142/S021988782450097X.

"Confrontation of $f(T) = T + \xi T^2$ Modified Gravity with Charged X-ray Binaries Embedded in modified Chaplygin gas under Tolman-Kuchowicz Spacetime" by **M. Bandyopadhyay** and R. Biswas. (*UnderReview*, *January* 2024).

"Investigating the Equation of state, Stability and Mass-Radius relationship of Anisotropic and Massive Neutron Stars embedded in $f(R,T)$ modified gravity" by **M. Bandyopadhyay** and R. Biswas. *Int. J. Geom. Methods Mod. Phys.* (*Accepted*, *April* 2024).
https://doi.org/10.1142/S0219887824502037.

"Isolated Compact Star $RXJ1856.5-3754$ in $f(R,T)$ Modified Gravity in Tolman-Kuchowicz Spacetime" and R. Biswas.
(*UnderReview*, *February* 2024).

- Part VII : The Chapters **12** contains the conclusion of the entire thesis work.

Kolkata, May 2024

NOTATION AND CONVENTIONS

The notations and conventions used in this thesis are as follows:

• Throughout the thesis, we take the natural units by requiring $c = 1$.

• The fundamental constants $16\pi G$, $\hbar$ have been set to unity (Sometimes, when $G = 1$ units, it will be mentioned specifically).

• We have chosen the signature of the metric $g_{\mu\nu}$ to be (+, -, -, -)

• The mass per baryon is taken as, $m_b = 1.66 \times 10^{-27}$ kg.

• Nuclear density is taken as $2.7 \times 10^{14}\ g\ cm^{-3}$.

• The relation between gravitational constant G with the reduced Planck mass M_P and the Planck mass M_{PL} is $M_P = \frac{1}{\sqrt{8\pi G}} = 2.4357 \times 10^{18}\ GeV$ and $M_{PL} = \frac{1}{\sqrt{G}} = 1.2211 \times 10^{19}\ GeV$ respectively.

• The symbol $\kappa^2 = 8\pi G$.

• We set $c = 1$ in thermodynamic discussions and the pressure p is chosen as $\frac{P}{c^2}$ in units of $g\ cm^{-3}$.

• In GR we have take the Christopher symbol as

$$\Gamma^{\alpha}_{\lambda\mu} = \frac{g^{\alpha\nu}}{2}(g_{\mu\nu,\lambda} + g_{\nu\lambda,\mu} - g_{\lambda\mu,\nu}) \quad .$$

The Riemann tensor is given as

$$R^{\lambda}_{\mu\nu\kappa} = \Gamma^{\lambda}_{\mu\nu,\kappa} - \Gamma^{\lambda}_{\mu\kappa,\nu} + \Gamma^{\sigma}_{\mu\nu}\Gamma^{\lambda}_{\sigma\kappa} - \Gamma^{\sigma}_{\mu\kappa}\Gamma^{\lambda}_{\sigma\nu} \quad .$$

The Ricci tensor: $R_{\mu\kappa} = R^{\lambda}_{\mu\lambda\kappa}$.

The Ricci scalar: $R = g^{\mu\nu}R_{\nu\mu}$.

The Einstein-Hilbert action: $S_{EH} = \frac{R}{16\pi G}\int d^4x\sqrt{-g}$.

The energy momentum tensor can be derived via $\delta S_m = \frac{\sqrt{-g}}{2}\int d^4x T^{\mu\nu}\delta g_{\mu\nu}$.

(All terms are discussed properly in the text of the related chapter respectively.)

• In $f(T)$ gravity, the fundamental variables that describe the manifold geometry are the vierbein fields $e_A(x^\mu)$. They form an orthonormal basis for the tangent space-time at each point x^μ, i.e., $e_A \cdot e_B = \eta_{AB}$ where $\eta_{AB} = diag(+1, -1, -1, -1)$ is the Minkowski metric for the tangent space-time.

The component form of the vierbein vector is given by $e_A = e_A^\mu \partial_\mu$.

The metric of physical space-time can be expressed as $g_{\mu\nu}(x) = \eta_{AB} e_\mu^A(x) e_\nu^B(x)$.

Moreover, the vierbein components follow the relations $e_A^\mu e_\nu^A = \delta_\nu^\mu$, $e_A^\mu e_\mu^B = \delta_A^B$.

The Weitzenböck connection is defined as $\hat{\Gamma}_{\mu\nu}^\lambda \equiv e_A^\lambda \partial_\nu e_\mu^A = -e_\mu^A \partial_\nu e_A^\lambda$.

• The torsion tensor: $T_{\mu\nu}^\lambda \equiv \hat{\Gamma}_{\mu\nu}^\lambda - \hat{\Gamma}_{\nu\mu}^\lambda = e_A^\lambda(\partial_\mu e_\nu^A - \partial_\nu e_\mu^A)$.

• The difference between the Levi-Civita and Weitzenböck connections is known as the contortion tensor, which becomes $K_\rho^{\mu\nu} = -\frac{1}{2}\left(T_\rho^{\mu\nu} - T_\rho^{\nu\mu} - T_\rho^{\mu\nu}\right)$.

• The superpotential is defined as $S_\rho^{\mu\nu} = \frac{1}{2}\left(K_\rho^{\mu\nu} + \delta_\rho^\mu T_\alpha^{\alpha\nu} - \delta_\rho^\nu T_\alpha^{\alpha\mu}\right)$.

• The torsion scalar is defined as $T \equiv S_\rho^{\mu\nu} T_{\mu\nu}^\rho$.

"There are many modes of thinking about the world around us and our place in it. I like to consider all the angles from which we might gain perspective on our amazing Universe and the nature of existence."

– **John A. Wheeler**

"Don't take rest after your first victory because if you fail in second, more lips are waiting to say that your first victory was just luck ".

—Dr. A.P.J. Abdul Kalam

LIST OF FIGURES

LIST OF TABLES

CONTENTS

Part I

INTRODUCTION AND MOTIVATION

"The imagination is more important than knowledge."

—Albert Einstein

CHAPTER 1

BRIEF OVERVIEW ON COMPACT STARS

1.1 Astrophysics of Compact Stars : Evolution under Cosmic Acceleration

1.1.1 Basic Ideas

To know the unknown and to see the unseen is inborn to humans.

The quest begins with the death of a star and looking after its remarkable evolution through accelerated spacetime of the Universe.

It is very amazing that few super massive stars are about the current age of the Universe. These stars during their whole life span keep a lot of information about the Universe. So, undoubtedly studying on their evolution process is the best way to understand the Universe as well as to reveal its secrets.

The first ever direct detection of the gravitational waves (GWs hereafter) took place in the year 2015 by the two detectors of LIGO observatory. A new field of gravitational wave astronomy and possible cosmology has opened up by the observed GWs signal from a coalescing binary black hole. Further, GWs from the coalescence of a binary NS

in August 2017, by LIGO and Virgo interferometers have also been observed along with the detection of Γ ray burst by Fermi-GBM and by INTEGRAL. So, in this way, GW astronomy has been opened for scientists to look at the secrets of the Universe through it. In recent times, due to the improvements in the sensitivities of the ground based interferometers, cosmologists expect that GWs from various astrophysical sources (like black holes and neutron stars) will soon be observed. Moreover, several other detectors, such as pulsar timing arrays, LISA space interferometer, Einstein Telescope etc. will explore the Universe up to cosmological distances. Thus, its very exciting for the scientists that we are indeed in a period for GW astrophysics and cosmology.

Molecular clouds or better to say, collapsing clouds of dust and gas are the birth-place of the stars, over the course of a million years or more. During these years a protostar settles down to a main-sequence star. The life-span of a star from a few million years to trillions of years depends on the initial mass. When the star is young or in main sequence, although the super strong gravity drags matter inside but the nuclear reactions (fusion) of hydrogen atoms at the core radiate energy in the outward direction. As a result enough pressure is produced to retain the proper size of the star as well as a stable equilibrium structure. During this sub-giant phase, the star gradually prospers in size until it achieves the red-giant phase. Eventually, however, as soon as the nuclear fuel in the core becomes exhausted, the fusion halts, and the outward pressure starts to drop rapidly. Except for the pressure, core of the star collapses by itself until something else provides support. The outer layers of the star are banished as a planetary nebula and left the remnant behind. For most of the stars, those around $(1-8)$ times the solar mass ($M_\odot$), the assistance comes from the gas of electrons surrounding the nuclei as the pressure from degenerate electrons which is enough to support the core. These stars are usually composed of carbon and oxygen and result is a low mass white dwarf. If the progenitor star has the mass in the range $(8-10)M_\odot$ "oxygen-neon-magnesium" stars can form, but they are rare. The number of white dwarfs in the Galaxy is expected to be of the order of 10^{10}.

But for larger mass stars, the gravitational pull overcome the electron degeneracy pressure inside the core and electrons are pushed to merge with protons in the nuclei

and as a result neutrons are produced. Now, the nuclei becomes more unstable with extra neutrons and then neutrons start to drip out of the nuclei and mix with the gas of electrons that surrounds them. Mainly, the stars with the mass around ten or more times the mass of the Sun can fulminate in a supernova and their inert core enriched with iron collapse into the utmost dense neutron star or black hole (Fig. 1). In case of NSs, neutron degeneracy pressure supports against the further collapse.

$Fig - 1$

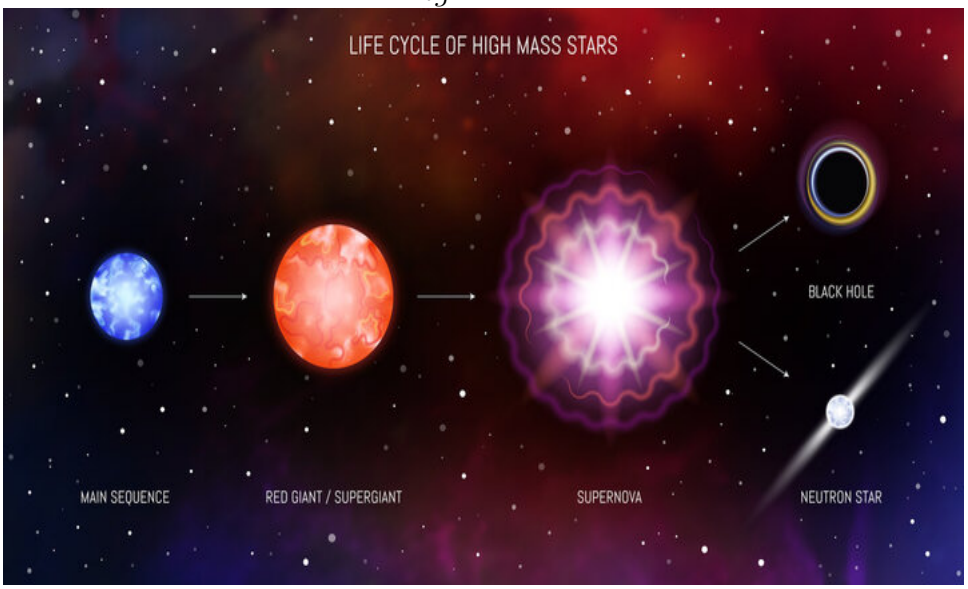

Figure 1.1: *Schematic diagram shows the different stages of the life cycle of a massive star. Figure credit: Veronika Bychkova.*

The neutron stars actually result from the supernova explosion of a massive star, combined with gravitational collapse. Mainly, these stars are the collapsed core of the massive giant stars of mass around ten to twenty-five times the mass of the Sun or even more depending on its metal rich core. It is the densest known class of stellar objects except black holes. Theoretically from Chandrasekhars limit, in general, these neutron stars have a radius of the order of 10.1 kilometers and a mass about $1.4M_{\odot}$. But from the "Tolman-Oppenheimer-Volkoff" limit (or TOV limit hereafter) gives the precise range of upper bound to the cold, non-rotating neutron stars as 2.2 to 2.5 times solar masses, before further collapse to a denser form, most likely a black hole, as explained in Chapter 9. This limit is also under rigorous investigation after the detection of the

first gravitational wave from the two merging neutron stars to have collapsed into a black hole as discussed in Chapter 10.

For the case of a rapidly spinning neutron star, the idea of an upper bound of the mass is still under investigation. Till now, as we do not know the exact equation of state (EoS hereafter) of the core nuclear matter of the neutron stars, we cannot say anything conclusively about any of the observed properties of the neutron stars. So, everything is under minute research and the quest continues. Furthermore, at present time, as our universe is under accelerated expansion phase, how these stars evolve and what impact they have imprinted is a matter of immense interest (Fig. 2).

$Fig - 2$

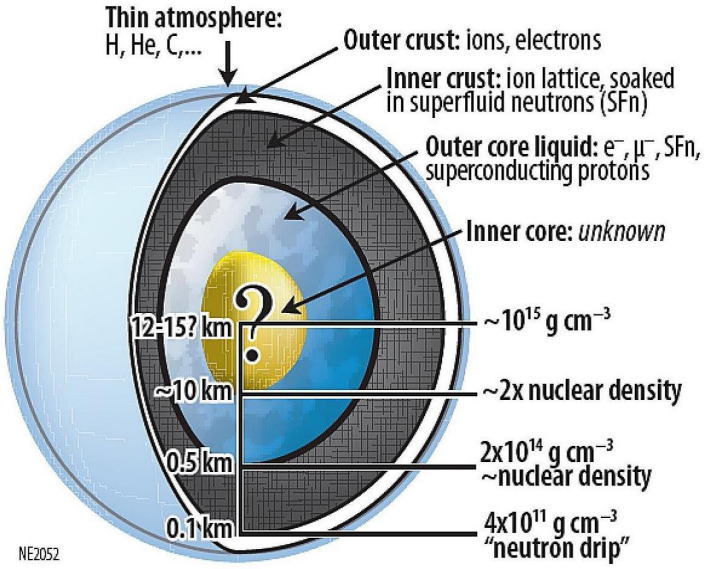

Figure 1.2: *Schematic presentation of the possible composition of a NS. Figure credit: K.C. Gendreau et al.* (2012), $SPIE$, 8443, 13.

1.1.2 Astrophysics of the Neutron Stars

After the end of the thermonuclear evolution of a star, the internal pressure can no longer sustain the inward gravitational attraction and the star collapses. If the mass of the progenitor star is in between $8M_{\odot}$ to $20M_{\odot}$, i.e., $8M_{\odot} < M < (20 - 30)M_{\odot}$, the evolutionary path of the star is different. The exothermic nuclear reactions can proceed all the way to Fe^{56}. Indeed, no element heavier than Fe^{56} can be generated

by fusion of lighter elements through exothermic reactions. The reaction process in which the Fe^{56} produces, starts with silicon burning as

$$Si^{28} + Si^{28} \rightarrow Ni^{56} + \gamma \quad ,$$
$$Ni^{56} \rightarrow Co^{56} + e^{+} + \nu_e \quad and$$
$$Co^{56} \rightarrow Fe^{56} + e^{+} + \nu_e \quad .$$

The Ni^{56} which forms in the reaction becomes unstable and decays again to form Co^{56} which is unstable again and decays further to form stable Fe^{56}, at last.

In addition, due to the increase in core density, the inverse β-decay stars to occur through which electrons are captured by protons forming neutrons and neutrinos becomes more and more efficient. These endothermic reactions subtract energy to the star through huge number of neutrino emission. The neutrinos are forming through the process as follows:

$$e^{-} + p \rightarrow n + \nu_e \quad ,$$

A huge number of neutrinos are created both in the silicon burning reactions and in the inverse β-decay process and leave the star, subtracting energy from the core. Again, γ photons are also produced in the reaction. At very high temperature about 10^{10} K, the number of high energy photons ($> 8MeV$) is enough to ignite the iron photo-disintegration process as

$$\gamma + Fe^{56} \rightarrow 13He^{4} + 4n \quad .$$

It is also an endothermic process which helps to subtract further energy to the core of the star and process also produces enormous number of neutrons.

1.1.2.1 An Overview

Neutron stars are the natural laboratories of cold matter with highest densities (almost nuclear density) in the Universe. The matter at the core of the neutron stars is at extreme densities such as central densities can reach or even exceed $10^{15} gm\ cm^{-3}$ and may reach upto $10^{16} gm\ cm^{-3}$ which is almost hundred times the density of the nucleus of an atom but surprisingly in its lowest possible energy configuration. These compact

objects have given the opportunity to test the general relativity (GR hereafter) theory and offered unique insight to astrophysics of the compact stars as well as physics of matter.

Various astronomical observations and also different experiments in the laboratory have constrained the EoS of the super dense matter at the core. We don't realize how this cold dense matter (CDM) operates and behaves exactly. It does not exist on the Earth even. The fundamental physical models such as standard cosmological model or the theory of quantum chromodynamics (QCD) can describes the interactions of the color-charged quarks and gluons that make up protons and neutrons and other particles is tabulated in Table 1., is valid at these large scales. The uncertainty in case of these models does not matter so much. The different phases of matter described by quantum chromodynamics, is given in Fig. 3 as a schematic diagram.

Table 1.

Sl No.	Name of Particles	Examples of Particles
1	Fermions	Leptons (neutrinos, electrons, muons,..) and Quarks
2	Bosons	force mediators, photons, gluons,..
3	Baryons (fermionic)	Nucleons (neutrons, protons) and Hyperons
4	Meson(bosonic)	pions, kaons

Table 1.1: Example of the different particles in the classes relevant to NSs cores and ground states

$Fig - 3$

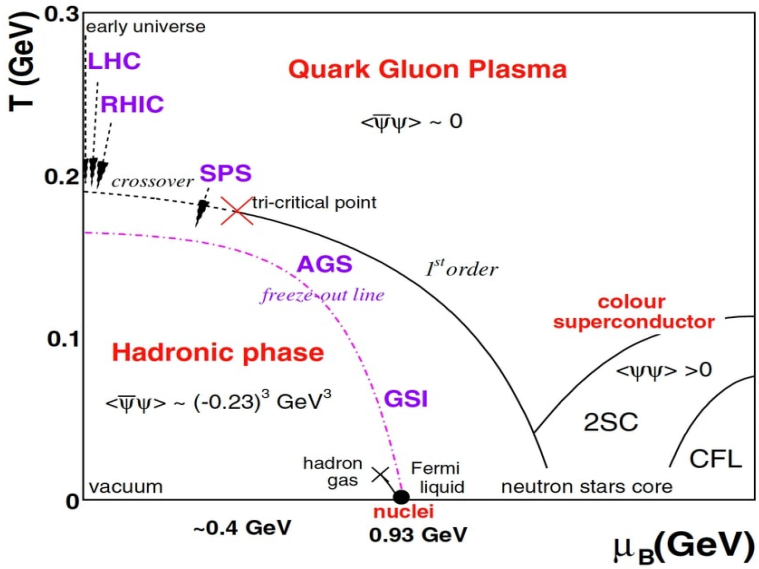

Figure 1.3: *Schematic representation of the phases of matter as described by quantum chromodynamics. QCD phase diagram in the temperature vs. baryochemical potential* (T, μ_B) *plane. The arrows indicate the expected crossing through the confinements transition during the expansion phase in heavy-ion collisions at different accelerators. The (dashed) freeze-out curve indicates where hadro-chemical equilibrium is attained in the final stage of the collision. The ground-state of nuclear matter at* $T = 0$ *and* $\mu_B = 0.93$ *GeV and the approximate position of the QCD critical point at* $\mu_B \approx 0.4$ *GeV are also indicated. Figure credit: A. K. Topaksu.*

The ultra strong magnetic field of a neutron star can be approximated as a dipole (as a bar magnet). This strong magnetic field probably originated in the progenitor star. At the time of supernova, this field becomes compressed and concentrated by the gravitational collapse, which gives birth to the neutron star. Like our Earth, the magnetic dipoles of the neutron stars are not aligned with the axis of rotation. At the star-surface, the magnetic poles are in different places than the poles of rotation as shown in Fig. 4. As the star rotates rapidly, a pulse of radiation is observed every time when one of the magnetic poles passes through the field of view of an observer. Depending on orientation, an observer can see one or two pulses for every rotation. Till now, most observed NSs are the pulsars which are rapidly spinning with relativistic electrons emitting radiation in cones from their magnetic poles.

$Fig - 4$

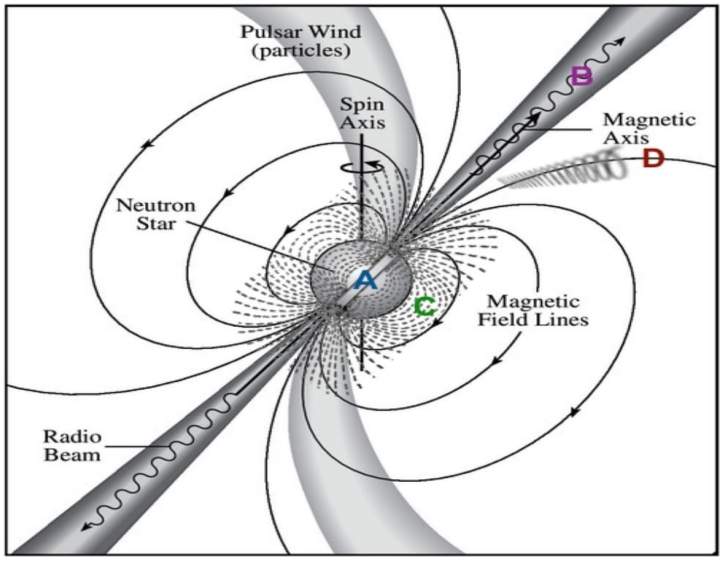

Figure 1.4: *Schematic diagram of rotating magnetised neutron star and its magnetosphere. Note that, the magnetic field is that of a dipole inclined* 40° *to the vertical rotation axis. Also the proposed regions for generation of pulsed radiations are indicated. Figure credit: Kaspi et al.* (2006).

If the NS is in a binary system, the orbital motion modulates the pulse frequency. If the companion star in the binary system is also a NS, the orbital dynamics become highly relativistic and very much complicated. This type of inspiralling NSs gives birth to the most fascinating natural event of the production of gravitational waves and whenever they start to coalesce. Observations on gravitational redshift, tidal deformability, pulse period, and the advance over time of the orbital period allow precise determination of the two NS masses as well as their moment of inertia, I. Hulse and Taylor, in the year 1975 first discovered the binary system composed of a neutron star and a pulsar [1], but the first double-pulsar system, PSR $J07373039$, was discovered in 2003 [2].

1.1.2.2 Choosing the Neutron Stars

The first ever direct detection of the gravitational waves (GWs hereafter) took place in the year 2015 by the two detectors of LIGO observatory. A new field of gravitational wave astronomy and possible cosmology has opened up by the observed GWs signal

from a coalescing binary black hole. Further, GWs from the coalescence of a binary NS in August 2017, by LIGO and Virgo interferometers have also been observed along with the detection of Γ ray burst by Fermi-GBM and by INTEGRAL. So, in this way, GW astronomy has been opened for scientists to look at the secrets of the Universe through it. In recent times, due to the improvements in the sensitivities of the ground based interferometers, cosmologists expect that GWs from various astrophysical sources (like black holes and neutron stars) will soon be observed. Moreover, several other detectors, such as pulsar timing arrays, LISA space interferometer, Einstein Telescope etc. will explore the Universe up to cosmological distances. Thus, its very exciting for the scientists that we are indeed in a period for GW astrophysics and cosmology.

Further, during the inspiral phase of two NSs in a binary system, NS deformation can occur by the tidal gravitational field of the companion star. Interestingly, this tidal deformability also depends on the EoS of the interior of the NS. This in turn affects the phase of the GW signal in such a way that we are able to detect it through advanced interferometers, uncovered the possibility of obtaining trace on the EoS of the NS. This leading milestone when the LIGO/Virgo detectors observed the GW signal named $GW170817$ from a the coalescence of NS-NS binary. A large number of telescopes also identified the total transient electromagnetic spectrum that strengthened the association with a NS-NS merger. This sensational event then marked the beginning of the era of multi-messenger astrophysics.

From our perspective, the neutron star is a bizarre state of matter. A mass about equal to that of the Sun to a region 20 km to 30 km in diameter. The core material is almost all neutrons as predicted so far. The density of the core material is of the order of nuclear density at the center. It's almost impossible to imagine from being on the Earth. The gravitational field near to the surface of the neutron star is enormous and the tidal force will pulverize to dust any solid object which approaches closer than a few thousand kilometers. We know these stars exist and we can predict masses of a few which are in binary systems. There is no straightforward measure of the radii or the internal structure. We would dearly like to know more.

So, needless to say that these stars really have an evolved mechanism at the interior.

Various astronomical observations like detection of gravitational waves, super massive pulsars from the $NICER$ sky survey etc. have also revealed very interesting and new features on these stars which have put constraints on the behavior of several parameters of the neutron stars. Their mass and radius is still unpredictable and there is no such a particular theory to describe them precisely. At the same time merging neutron star systems has created a lot of enthusiasm and a lot of questions on their evolution through spacetime under an accelerated Universe. As we still don't know the exact EoS of the core nuclear matter of these stars, our hunt continues. The key topic of investigation in this thesis is to study of evolution of the neutron star through accelerated spacetime and to get a precise EoS of the core nuclear matter.

By comparing the obtained result from various models with the astronomical observations, we can get the idea of mass, radius and various other important properties of the NSs out there in the Universe. These observations help us to put constraints or even rule out different non-physical theories used to describe such dense systems at extremely high pressure, density and temperature. We can also test the EoS which can perfectly describe the core matter and high nuclear densities. Thus, NSs serve as an excellent astronomical laboratory for studying how the laws that govern our Universe cause matter to behave under extreme physical environments with high densities and energies. We can inspect the effect of dark matter and dark energy originating from the large-scale modern cosmology by measuring the $M - R$ relations of the massive NSs with extreme compactness but in spherically stable and equilibrium configuration.

1.1.2.3 Theory to the Discovery

As proposed by Landau, just after the discovery of neutrons by sir J. Chadwick in 1932 that, in analogy to the white dwarfs which are supported by the electron degeneracy pressure, these stars are also supported by the neutron degeneracy pressure. We already aware from the Paulis Exclusion Principle that any two electrons can not occupy the same energy state. This in turn produces the degeneracy pressure that supports the core of the star against further collapse. Neutron stars as being the remnants of supernova is first suggested by Baade and Zwicky in the year 1934 [3]. In

1939, using Einstein's general relativity theory, Tolman introduced a theoretical stellar structure applying the relativistic equations of stellar structure [4]. This pioneering work of Tolman, has given the concept of maximum mass possessed by a neutron star. Interestingly, this maximum mass limit becomes the same order as the Chandrasekhar mass of white dwarf that subsists in Newtonian Gravity. Later, from further theoretical investigations, it was realized that neutron stars are rapidly rotating and possess an intense magnetic field around themselves. Pacini predicted that the strong magnetic field of the rapidly rotating neutron stars can produce radio waves [5]. But, we have to wait till 1967, when Bell and Hewish discovered the first radio pulsar to get the confirmation of the real existence of the neutron stars [6]. Just after that discovery, Gold has investigated the neutron stars and gave a model of rapidly rotating and intense magnetized neutron star with extreme compactness [7].

1.1.2.4 The Magnetic Fields

One very important property of neutron stars is that they have nearly infinite electrical conductivity i.e., they are superconductors. Therefore, electric current flow with essentially no resistance and magnetic fields diffuse very little in superconductors; fields do not diffuse in or out of them. So, the magnetic field within them is said to be frozen into the stellar matter. This means that any field line that passes through a given fluid element (stellar matter) is trapped in that fluid element and moves and deforms with it. A magnetic field that is deformed i.e., stretched or compressed responds by applying a restoring Lorentz force on the fluid. We can find the strongest magnetic field B (in Gauss), at the poles of the neutron stars. We can measure the magnetic field strength of a neutron star as

$$B = \left[\frac{3c^2 I P \dot{P}}{8\pi^2 r^6}\right]^{\frac{1}{2}} \quad , \tag{1.1}$$

where c is the velocity of light, r denotes the radius, time period P and I denotes the rotational moment of inertia of the neutron star. We are still not sure exactly how strong the magnetic field is before the supernova. The natural magnetic field at

the Earth's surface is about 0.7 G whereas in the case of a neutron star's surface it is of the order of 10^{12} G. This is stronger than any field in our experience. Even in the laboratory we can create a steady magnetic field of strength about 10^7 G. The materials available on the Earth are not capable of retaining such a strong field. Thus when from the other stellar core, the neutron star formed after the collapse, the magnetic field that already trapped in the core is enhanced by a factor of $(\frac{R_i}{r_f})^2$. This factor almost becomes 10^{12} times. Indeed the highest observed magnetic field of the neutron stars reaches nearly 10^{15} G but a more typical value is of the order of 10^{12} G.

Surprisingly, even a 10^6 G electromagnet would crush itself because the steel would not be strong enough to hold it up. The magnetic field of the neutron stars is high enough that the atoms of its core material have a normal structure and instead the electron orbits become highly distorted and flattened. The neutron stars with super strong magnetic fields are called magnetars, which generate bursts of gamma rays due to sudden re-arrangements of the magnetic field. Unfortunately we do not know much about them. But investigations are going on to realize their nature and EoS of the core nuclear matter.

1.1.2.5 Radiation from the Neutron Stars

If we consider a simple model of a pulsar with magnetic dipole moment μ and rotating at frequency Ω, then the radiated power of the electromagnetic radiation can be measured as

$$L_{em} = \frac{2}{3c^2}\mu_\perp^2\Omega^4 \quad , \tag{1.2}$$

where $\mu_\perp$ denotes the component of dipole moment transverse to the rotational axis. This energy comes from the rotational energy of the pulsar as

$$E_{rot} = \frac{I}{2}\Omega^2 \quad , \tag{1.3}$$

where I denotes the moment of inertia of that NS (pulsar). The spindown luminosity $\frac{-dE_{rot}}{dt}$ of the pulsar can be measured as

$$-\frac{dE_{rot}}{dt} = -\frac{d}{dt}\left[\frac{I}{2}\Omega^2\right] = 4\pi^2 I\frac{\dot{P}}{P^3} \quad , \tag{1.4}$$

where Ω is denoted as $\frac{2\pi}{P}$.

Two regions have been proposed by the scientists as the origin of the high energy radio pulses. The polar-cap model of the neutron stars assume pair production in the magnetosphere at the pole where the magnetic field is the strongest. It predicts photon generation by the inverse-Compton process or by curvature radiation, close to the surface of the star. The particles which are traveling back to the surface and heating the polar-cap region are the main source for this type of radiation. But another model assumes that the origin of the radio pulses is the region between the last open field lines and null-charge surface which is denoted as outer-gap. The origin of the radiating particle is a pair cascade. Again, some heating is expected from the energetic particles returning to the surface. These models are also not fully successful to explain the predicted spectra and pulse shape.

Most of the pulsars with low P and high $\dot{E}$ emit pulsed X-rays. This spectra may be either thermal or non-thermal depending on the origin. The X-rays are produced from the hot surface of the stars whereas the magnetosphere gives the non-thermal spectrum. There are two pulses per cycle at all energies from radio to gamma rays and no such a variation is noticed between the wavebands for the pulse shape and phase. As a matter of interest, the pulsed radiation represents only approx 1 percent of the pulsar's spin down energy.

In the case of a rotating magnetized neutron star, the production of non-thermal pulses has been investigated by Kaspi et al. in the year 2006 [8]. A rotating and highly magnetized neutron star has a strong surface charge. Electric fields pull these charges from the surface to fill sections of the magnetosphere. The magnetosphere is filled with regions of negative and positive charge divided by the null-charge surface where the magnetic field is perpendicular to Ω. The magnetic field and the space-charge co-

rotate with the neutron star out to the radius where the co-rotation velocity becomes maximum ($\simeq c$). At a very far distance co-rotation must be stopped.

Traditionally, this speed-of-light cylinder is supposed to be the origin of emission of the radio pulses. Thus a pulse of radiation is only shown when one of the magnetic poles rotates through the observer's line of sight. Radio waves are elevated by the synchrotron process when the electrons co-rotating and move along the magnetic field lines but still the width of the resultant beam of electromagnetic radiation is not fully understood.

Only thermal radiation is understood better. The interior of a young neutron star is expected to be very hot ($\simeq 10^{12}$ K) and surrounded by the crust which is insulating in nature. Heat is conducted along, rather across field lines, the magnetic poles should be hotter than the rest of the star surface. The temperature is expected to be in the range $10^5 - 10^6$ K after a few years of formation, because of huge neutrino emission from the core. In this low temperature most of the light the star emits is in X-rays. According to GR, a strong gravitational field above the surface may bend pulses from the far side of the star towards the observer.

1.1.2.6 Rotation and Spin Down

The intense low-frequency electromagnetic radiation of the neutron stars produces a torque which slows the rotation. A large fraction of energy in this low-frequency radiation is transferred quickly to high energy electrons and magnetic fields. These electrons form a relativistic wind flowing outwards from the neutron stars. But, unfortunately till now the exact mechanism behind this creation of high energetic accelerated electrons is not understood and further investigations are going on.

A rotating magnetic dipole of the neutron star with period P radiates electromagnetic energy at the rotational frequency $\Omega = \frac{2\pi}{P}$. The torque associated with the radiation which slows down the rotation of the neutron stars. This is how the rotational energy is converted to radiation and the star starts to spin more slowly. It is assumed that the torque is proportional to Ω^n, where n is denoted as the "braking index". This index is a measure of how well the slowing neutron star follows this strictly electro-

magnetic behavior. In case of few pulsars we can even measure the rate of change of time period $\dot{P}$ and using this, we can calculate the breaking index as

$$n = \frac{\Omega\ddot{\Omega}}{\dot{\Omega}^2} = \left[2 - \frac{P\ddot{P}}{\dot{P}^2}\right] \quad , \tag{1.5}$$

where $\dot{\Omega}$ can be denoted as

$$\dot{\Omega} = -\kappa\Omega^n \quad , \tag{1.6}$$

where κ and n are the time independent free parameters and κ is given as

$$\kappa = \frac{2\mu_\perp^2}{3Ic^3} \quad , \quad n = 3 \quad . \tag{1.7}$$

In case of only electromagnetic radiation from the neutron star, the value of n becomes 3. The value $n < 3$ indicates that some of the torque is from the particles accelerated in the magnetosphere and the source of the relativistic wind. After integrating the above equation from an initial time $t = 0$, we get

$$\kappa t = \frac{1}{n-1}\left[\frac{1}{\Omega^{n-1}(t)} - \frac{1}{\Omega_0^{n-1}}\right] \quad , \tag{1.8}$$

where $\Omega_0 = \Omega(t_0)$ denotes the angular velocity at birth. Using this equation we can measure the age of the pulsars. The age of the neutron stars can be calculated as

$$\tau_{age} = \frac{P}{(n-1)\dot{P}}\left[1 - \left(\frac{P_0}{P}\right)^{n-1}\right] \quad , \quad \Omega(t) \ll \Omega(t_0) \quad . \tag{1.9}$$

When the axis of the magnetic dipole becomes perpendicular with the axis of rotation, the torque becomes maximum. We can obtain several quantities related to the neutron stars from the observed time period P(measured in seconds) and the rate of spin down ($\dot{P}$). We can calculate the rotational moment of inertia I from the proposed EoS of the nuclear material at the core of the neutron stars. Usually, the value of I is around $10^{45} gm\ cm^2\ s^{-2}$ for a typically proposed neutron star of mass $1.4M_\odot$ with radius about 10km. We can calculate the rotation energy (E in ergs) and the rate of loss

of this energy ($\dot{E}$ *in ergs* s^{-1}) can be calculated by following equation (1) where the negative sign in $\dot{E}$ indicates the loss of rotational energy. The X-ray emitting neutron stars generally have a high value of $\dot{E}$.

$$E = \frac{2\pi^2 I}{P^2} \quad and \quad \dot{E} = -\frac{4\pi^2 I \dot{P}}{P^3} \quad . \tag{1.10}$$

1.1.2.7 The Glitch

In the case of pulsars, a regular period which increases steadily with time, may become discontinuous somehow. This discontinuity is called glitches in the timing. During a glitch, the frequency of radio pulsations, ν, increases suddenly by ≈ 1 part in 10^6 and the derivative in frequency, $\dot{\nu}$, increases by ≈ 1 part in 10^2 and then recovers steadily from this transient change. Duration of this change is almost 10 to 100 days. As for example, a glitch is monitored in vela pulsar to occur roughly in every 2.5 years.

The core-crust concept (Fig. 5) of the neutron stars as also in our work, may be the most possible explanation of this observed phenomenon of glitch, in the case of pulsars. Just imagine a star quake changing the shape of the crust and suddenly lowering the I by a small amount. It is then obvious from the conservation of angular momentum, to increase its spin rate. The crust then settles back to a new equilibrium configuration.

$Fig - 5$

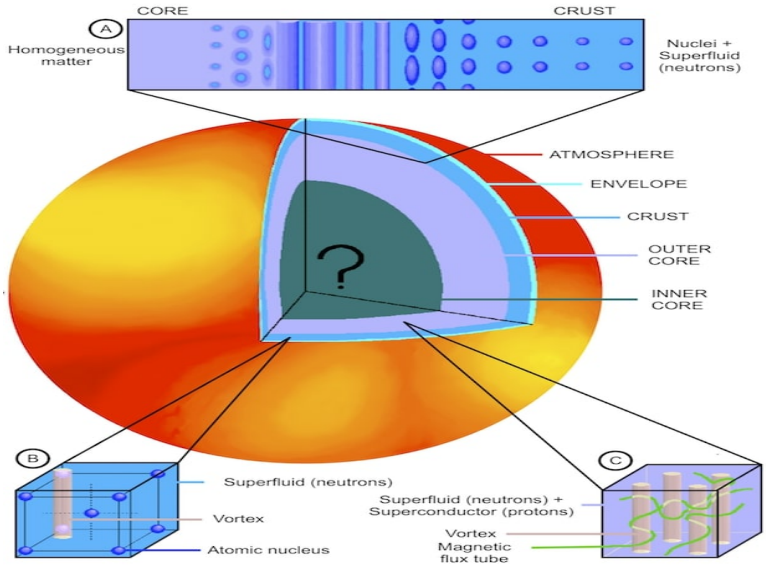

Figure 1.5: *Schematic diagram of core and crust of a rotating magnetised neutron star. Figure credit: Chandra X-ray Observatory (Supernova Remnant Cassiopeia A).*

Glitches exhibit a rare opportunity to realize about the interior structure of the neutron stars. But, much has been learned from radio-timing data alone [9]. A glitch which can have a duration of < 1 minute, indicates a sudden change in configuration of the solid crust and/or a change in the coupling in the crust, which rotates at the observed rate, to the loosely coupled stellar interior. Some part of the interior, not tied strongly to the torque-producing magnetic field, gets a little ahead of the crust, then suddenly locks to and speeds the rotation of the crust. Current theory favors superfluid protons as the loose component in the inner crust. Whatever the mechanism behind the glitch, during glitch, rotational energy should be dissipated in the interior and will heat the interior region of the neutron star where the change occurred. The timescale of the flow of energy to the surface depends on the size of the neutron star, the nature of the glitch mechanism and the structure of the outer layers. The amount of thermal energy generated and conducted to the surface could be enough to cause an observable increase in the temperature of the star's surface. Moreover, useful information can be acquired about the glitch mechanism from the observations of X-ray, emitting from the surface of the neutron stars.

1.1.2.8 Neutron Star Cooling

The core of a neutron star cools by neutrino emission whereas the crust of the star cools by the process of conduction. The highly massive neutron stars cool more rapidly. The temperature of the core of a newly born young neutron star is about $10^{11} - 10^{12}$ K. But the star starts to radiate energy at a high rate through the neutrino emission from the core at a huge amount. As a result, it starts to cool down rapidly and almost after $10 - 100$ years of formation, its temperature becomes $10^6 - 10^7$ K. It is believed that, this cooling process by neutrino emission dominates and continues upto the age about 10^6 years but after that the star starts to cool through the process of photon emission.

Upto the age of about 100 years, the crust of the NS star is thermally coupled with the core which is almost transparent to neutrinos but after that age it turns to a major X-ray source at about 10^6 K. The temperature of the surface of the neutron star can be measured from its luminosity as a function of its age as $L_X = 4\pi r^2 \sigma T^4$, by considering it as a black body and using a reasonable value of the radius. Investigations suggest that the cooling curve of a neutron star is independent of its EoS of the core nuclear matter.

For the neutron stars of mass around $1.4M_\odot$, neutrinos are emitted by the process of modified Urca process. This process is comparatively slower than the direct Urca process. The modified Urca process needs a third nearby particle for the conservation of both energy and momentum. The direct Urca process occurs for neutron stars with higher mass and very high core density with the presence of plenty of photons inside the core. In this process the rate of cooling is very fast and neutrino emission also increases.

Rapid neutrino emission during the cooling of the neutron star may also occur due to the presence of exotic particles inside the core such as mesons at very high nuclear density. The atmosphere surrounding the neutron star is thick enough to absorb the X-rays. The higher energy photons coming from deeper layers may have the possibility to be absorbed by the atmosphere. So, to determine the surface temperature of the star through spectrum analysis is not so reliable. The observed spectra from the

neutron stars which almost fits with the blackbody spectra, yield surface temperatures sometimes 2 times higher than the actual value of it. The presence of a very strong magnetic field may also have a crucial effect on the ejected X-ray spectra from the neutron stars.

1.1.2.9 Neutron Star Accretion

In our Universe, accreting compact objects have offered us the unique insights into the core astrophysical ideas of the last stages of stellar evolution and to culture the physics of matter at extreme environment or physical conditions [10]. Till now, we have discovered but not fully understood the thermonuclear flashes from the surface and periodic pulsation in X-rays emitted by the rapidly spinning neutron stars. The mass measurement process of the neutron stars is still under question but provides the strongest evidence for the existence of black holes in the Universe. A compact star can also accrete matter from a companion star if the companion star is losing its mass in the form of a stellar wind and does not fill its Roche Lobe. The companion star should have the mass $\geq 10M_{\odot}$ in order to drive a strong stellar wind.

1.1.2.10 Neutron Stars as the Powerful Source of the Gravitational Waves

The NSs can be excited by a small perturbation that oscillates into a set of normal modes. Again, these normal modes can also be excited during various astrophysical processes, such as the formation of a proto-NS, collapse of a compact binary NS system. The strong oscillations can be found from the hot and differentially rotating proto-NSs. Further, if there is major rearrangements in the internal structure (during giant flares of magnetars) of the NSs or during the glitches we can also get the oscillations of excited normal modes. These coherent vibrations in turn becomes the significant source of gravitational radiation. As for examples during core collapse and bounce the consecutive compressions and expansions of the core density induces oscillations in the new-born proto-NS. During this process, the non-linear coupling between the normal modes of the proto-NS produces the GWs. The computation of these normal modes of a NS is quite complicated. It involves both perturbations of the metric around and

inside the NS. Moreover, in also involves the perturbations of the variables of the core matter of the NSs.

Further, during the inspiral phase of two NSs in a binary system, NS deformation can occur by the tidal gravitational field of the companion star. Interestingly, this tidal deformability also depends on the EoS of the interior of the NS. This in turn affects the phase of the GW signal in such a way that we are able to detect it through advanced interferometers, uncovered the possibility of obtaining trace on the EoS of the NS. This leading milestone when the LIGO/Virgo detectors observed the GW signal named $GW170817$ from a the coalescence of NS-NS binary. A large number of telescopes also identified the total transient electromagnetic spectrum that strengthened the association with a NS-NS merger. This sensational event then marked the beginning of the era of multi-messenger astrophysics.

1.1.3 Shortcomings of General Relativity Theory

It is very interesting as well as very enthusiastic to understand that when Newtonian gravity was discovered no one knew and also never imagined that it was just a weak field limit of a more complex theory of gravity as GR. In the same way, it feels, after getting the evidence of the accelerated Universe, that GR is the limit of some more complex theory of gravity that we still do not know. This may be like history is repeating itself.

General Relativity (GR) theory has been developed by Albert Einstein between the years 1907 to 1915. According to this theory, the effect of gravitation between masses is due to the warping of spacetime surrounding them by themselves only. GR has flourished as a vital tool in modern astrophysics [11]. It supports the base of understanding of black holes. GR is also a crucial part of the framework of construction of the standard "Big Bang model" of cosmology.

GR is quite successful in describing the gravitational interactions in the standard ΛCDM model. It provides the best formalism to describe spacetime geometry. It has shown remarkable agreement to the local tests such as perihelion precession tests of gravity done within the Solar System. At the same time, it has also passed all other experimental and observational tests of gravity such as Lunar laser ranging experiments,

anomalous perihelion of Mercury, classical test of gravitational redshift, lensing of light from the background of the stars, gravitational time dilation etc. Even outside the solar system, This theory also has a very good agreement with the tests like changes in the orbital period of binary pulsars as for producing gravitational waves which has been discovered recently [12]. The GR theory shows us how the presence and motion of matter (mass) affect the spacetime curvature [13].

Despite these outstanding successes, however, there still remains few reasons to suspect GR as not a complete theory. Some unresolved issues still remain there which shows that GR is not providing us the full scenario. One main reason is the presence of singularity in the study of various cosmological phenomena leading to a predictability loss. GR is not providing agreements with the observed results for the large scales (larger than the Solar system), i.e., the deviations from GR on cosmological scales. The size of such types of deviations should be constrained. Besides, horizons in GR possess temperature, entropy etc. without any natural explanation of these thermodynamic properties. On the other hand, we still don't have any quantum theory of gravity like other known interactions (electromagnetic, weak and strong) already have. This is conclusive enough to say that, either we need to modify our understanding of quantum field theory or the understanding of GR or both.

1.1.3.1 The ΛCDM model and arising Problems

Till at present time, ΛCDM model is considered to be the best fit model of cosmology. It is widely accepted also by the cosmologists. According to this model, our Universe has evolved through some different phases with time after the Big-Bang and the stages of evolution of our Universe can be distinguished as first inflation, then our Universe enters in a radiation dominated era which follows a matter dominated (Baryonic and Dark matter) epoch and in the last states finally a DE dominated epoch at late times (Fig. 6).

$Fig - 6$

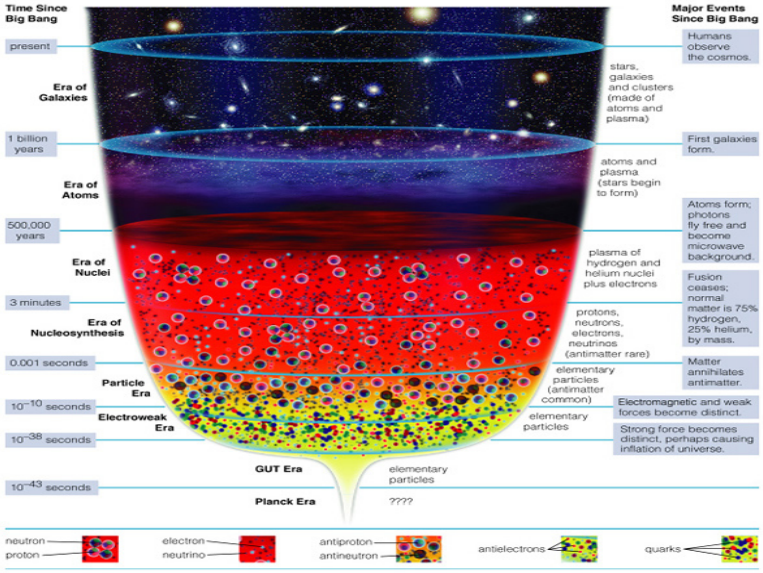

Figure 1.6: *Schematic diagram of the expanding Universe with its different stages. Figure credit: D. E. Gary, Intro to astronomy, Lecture* (26).

Now, assuming matter as a perfect fluid (isotropic and homogeneous) and considering energy conservation ($\nabla^{\mu} T_{\mu\nu} = 0$),the Friedmann equation yields

$$\dot{\rho} + 3H\rho(1+\omega) = 0 \quad , \tag{1.11}$$

where for the perfect fluid, $\omega = \frac{P}{\rho}$ and $\omega_{\Lambda} = -1$, the vacuum pressure ($P = -\rho$). the solution of the above equation can be written as

$$\rho = \rho_0 \left(\frac{a_0}{a}\right)^{3(1+\omega)} \quad , \tag{1.12}$$

where the integration constant a_0, ρ_0 are their respective values at present time. So, the critical density in terms of Hubble constant H can be written as

$$\rho_c = \frac{3}{8\pi G} H_0^2 \quad as \quad H_0 = H(t_0) \quad . \tag{1.13}$$

Again, by using the density parameter and the friedmann equation we will get the

equation that gives the percentage contributions of different epoch to our Universe as

$$\Omega_R + \Omega_M + \Omega_k + \Omega_\Lambda = 1 \quad , \quad (\Omega_k \quad and \quad \Omega_R) \ll 1 \quad . \tag{1.14}$$

Though, still now the controversy amongst the cosmologists persists about the exact shape of the Universe, various present dat study from independent sources like CMBR from WMAP [14], BOOMERanG [15] and the data from the Planck telescope [117] confirms that our Universe is flat. Data from CMB confirms that the contribution of radiation dominated and curvature dominated epochs are negligible. So, the above equation (8) reduces to $\Omega_\Lambda + \Omega_M = 1$. The best fit values we get in the present day from cosmic microwave background radiation (CMBR) data is that $\Omega_M \sim 0.3$ and $\Omega_\Lambda \sim 0.7$ [119]. All these results are obtained by applying the GR and from the ΛCDM model so far.

Various cosmological observations are successfully explained by using the ΛCDM model and it has become a very satisfying model till date. But, the problem arises when we go for the calculations of energy contributions of the accelerating Universe. This model predicts that around 70% of the Universe is dominated by an unknown form of energy with large negative pressure. This energy is something that still needs observational evidence for its existence and is named as dark energy (DE). The same goes for the dark matter which also contributes around 25% of the Universe. However, even though these components have yet to be detected, it does not indicate about the inaccuracy of the model. This may change our concept of the composition of the Universe. Furthermore, the real issue with this model is that we also don't know how these components interact. This model also doesn't provide that fundamental view either. Besides, this model faces some problems due to the included cosmological constant Λ. One issue is the cosmological coincidence problem [109](the energy densities associated with DE and DM are of the same order in this present epoch) and another one is the fine tuning problem. Also the tension in Hubble constant in cosmology is considered widely as a major problem for the ΛCDM model.

1.1.4 Modifications of GR Theory: The Motivation to study

Despite tremendous success, *GR* still has faced some challenges during its application, in order to explain some observed astrophysical phenomenon. We have already discussed it earlier. We can also think that in few cases of observation GR is not providing the full picture and modification of this theory is needed. At the same time, a few questions also arise which lead me to think about modified gravity theories instead of GR. The main questions which arise in my mind are as follows:

1. Is GR giving correct results or predictions on large scales as it is not well tested in cosmological scales ?

2. Why gravity can not have any quantum background? As GR also does not have any well defined quantum limit as well.

3. In order to explain the accelerated Universe, the concept of dark energy has been postulated by the scientists which have a large negative pressure and the concept of "repulsive gravity" is just opposite to our conventional idea of Einstein's gravity. Why?

Again, the idea of modified gravity can explain the concept of accelerated expansion of the Universe which GR does not. So, the modifications or corrections to GR are very much required indeed.

In order to provide the solution to the accelerated Universe incorporating dark energy, instead of using cosmological constant Λ, we can use the idea of modified gravity [19]. GR is not well tested in the large universal scales also. The consideration of the presence of dark matter is required to explain the rotational curves of the galaxies. The modified gravity theories can also be used to explain dark matter [20]. But here, in this work of the thesis we will mainly focus on tackling the problem of dark energy by using the concept of modified gravity. This thesis will try to show how these modified gravity theories may be applied to provide answers for the late time cosmic acceleration.

The main aim of the modified gravity theory is to address the current issues facing the ΛCDM model and to focus on the current accelerated expansion of the Universe. These theories are actually the modifications of GR theory and can take any form of it. The main goal of these theories is to provide a general theory that can reproduce

the results of GR over small distances for astronomical masses (where GR undoubtedly shows success) and that clearly relate large scale observations like accelerated Universe. These theories help us to think about GR in a new way and give a deeper understanding of the theory indeed. The models in modified gravity also divulge how those theories precisely work. There are indeed a few ways to modify gravity and in this thesis we are mainly focusing on two main examples only. One method will look at finding higher orders of the Torsional scalar in the action in $f(T)$ gravity, similar to $f(R)$ gravity but possess new features with new angle of investigations. The other will look to modify the curvature of spacetime through the minimal coupling between the matter and geometry of space-time in $f(R,T)$ gravity.

Throughout this thesis we will work with a $(-,+,+,+)$ metric signature.

1.1.4.1 GR in a nutshell: A Brief Review of Previous Reading

The modified gravity theories are nothing but the modifications of the GR theory. So, it is more convenient to use the term "modified GR", instead of "modified gravity". Actually for any theory of gravity if it goes beyond GR, we generally use the term "modified gravity". Now, before coming to deal with the modified gravity theory, it's best to make a fleeting recap on GR. GR actually provides a geometrical interpretation of gravity.

The description of GR can be made by an action as

$$S = \int d^4x\sqrt{-g}\left[\frac{R}{16\pi G} + L_M(\psi, g_{\mu\nu})\right] \quad , \tag{1.15}$$

where g denotes the determinant of the metric tensor field $g_{\mu\nu}$ of rank 2, R is denoted as the Ricci scalar and L_M is the Lagrangian density which describes various forms of energy such as dark matter, baryons, radiations etc (collectively described by ψ). The whole integration is taken over the four dimensional spacetime x^μ $(\mu = 0, 1, 2, 3)$.

From the above equation (5), we can derive the Einstein's field equations as

$$G_{\mu\nu} \equiv R_{\mu\nu} - \frac{R}{2}g_{\mu\nu} = 8\pi G T^m_{\mu\nu} \quad where \quad T_{\mu\nu} = T_{\nu\mu} \quad , \tag{1.16}$$

where $R_{\mu\nu}$ is the Ricci tensor and $T_{\mu\nu}$ is the energy-momentum tensor associated with L_M. The L.H.S. of the equation takes on purely geometric terms whereas the R.H.S. of the equation specifies the energy that subsists in the Universe. According to GR, the Einstein tensor $G_{\mu\nu}$ is divergence free which confirms the conservation of energy and momentum, i.e., $\nabla_\nu G^{\mu\nu} = 0 \Rightarrow \nabla_\nu T^{\mu\nu} = 0$.

In order to build up any new sets of equations one needs to change either or both sides of the Einstein's field equations. In cosmology, the energy-momentum tensor, $T_{\mu\nu}$ for any perfect fluid takes the form as

$$T_{\mu\nu} = (P + \rho)u_\mu u_\nu - P g_{\mu\nu} \quad , \tag{1.17}$$

where P, ρ and u_μ are the pressure, density and four velocity of the fluid. Here we have neglected the fluid's heat flux and anisotropic stress. Again, motivated by the cosmological principle, the line element of the spatially flat Friedmann-Lemaitre-Robertson-Walker spacetime metric (under spherical symmetry) took the form as

$$ds^2 = -dt^2 + a^2(t)\left[\frac{dr^2}{1 - kr^2} + r^2 d\omega^2\right] \quad where \quad k = 0, \pm 1 \quad , \tag{1.18}$$

where $a = \frac{1}{1+z}$ is the cosmological scale factor in terms of redshift factor z. The value of k defines the curvature of the Universe. $k = 0$ denotes the flat Universe whereas $k = 1$ for positively curved hyper surface and $k = -1$ gives the negative curvature of the Universe.

1.1.4.2 Concept of Dark Energy: Idea of the Accelerated Universe

Now, from the energy-momentum conservation, $\nabla_\mu T^{\mu\nu} = 0$, we can get the equations of our expanding Universe as

$$H^2 \equiv \left(\frac{\dot{a}}{a}\right)^2 = 8\pi G\rho \quad , \tag{1.19}$$

$$\left(\frac{\ddot{a}}{a}\right) = -\frac{4}{3}\pi G(\rho + 3P) \quad and \tag{1.20}$$

$$\dot{\rho} = -3H(\rho + P) \quad , \tag{1.21}$$

where the "overdot" denotes the derivative of the quantity w.r.t. physical time t and H is the "Hubble" constant ($\frac{\dot{a}}{a}$). These above equations actually specify the rate at which our Universe expands. The equation (15) gives the idea of the matter dominated Universe with $a = 1$. Solving equations (13) and (15), we can find the present day value of the scale factor ($a(t)$ describes the relative change in the size of the Universe with time) at present time. The matter dominated era of the Universe is now almost well understood.

But, in the present situation, what actually matters is to explain the observed accelerated expansion of our Universe. Moreover, the present accelerated expansion of the Universe has put the standard cosmology in dilemma. There is a conflict in the choice of gravity theory or in the choice of the matter that exists. The standard cosmology with normal matter (obeying the strong energy condition) and applying GR can not support this accelerated phase. So, in this situation, either Einstein's gravity with some exotic matter (possessing large negative pressure known as dark energy) or modified gravity theory with usual matter, may be applicable to explain this situation. Scientists have postulated the existence and concept of repulsive gravity through the presence of dark energy to explain the accelerated Universe. GR can only explain the radiation and matter dominated era of the universe till now. However, hope is there that we can make corrections in the existing GR theory which can accommodate the effects of dark energy as what we think of it possess. But unfortunately, we are still unaware of it.

Now, in this critical situation, the equation (14) has put some focus on how to solve this puzzle of the Universe. This equation gives us the concept of dark energy (DE). Only this equation shows us that the Universe is under acceleration if and only if $\ddot{a} > 0$. But at the same time this same equation also implies that the Universe should be dominated by a mysterious form of energy characterized by $\frac{P}{\rho} < -\frac{1}{3}$. Currently we are not aware about any form of this energy which can show this behavior and also its exact nature is still a mystery to us. It is believed that this dark energy

is uniform across space and avail almost 68% of the total energy of the present day observable Universe. DE is also considered as the dominant energy component as well. Cosmologists are trying endlessly to solve this maze by incorporating various models such as "Quintessence Model" of dark energy but still not getting the success in hand.

1.1.4.3 Key Equations of Modified Gravity

The new equations in modified gravity actually adds something new in the Einstein's field equations. Let us consider the best fit model of cosmology at present, the ΛCDM model. The field equations of this model can be written from the action

$$S = \int d^4x\sqrt{-g}\left[\frac{R}{16\pi G} + L_M(\psi, g_{\mu\nu}) - \frac{\Lambda}{8\pi G}\right] \quad as \tag{1.22}$$

$$G_{\mu\nu} + \Lambda g_{\mu\nu} = 8\pi G T^m_{\mu\nu} \quad , \tag{1.23}$$

which generally contains something new. The extra term, Λ in the above equation (17) leads to changes on the background quantities of the expansion equations (13 to 15) of the Universe and also the Poisson equation (relates matter density with gravitational potential), which are relevant to the structure formation of the Universe, given as

$$\nabla^2\Phi = 4\pi G\partial\rho_m \quad , \tag{1.24}$$

where $\partial\rho_m = \rho_m - \bar{\rho_m}$ and Φ is the gravitational potential. In "Quintessence Model" of the accelerated Universe incorporating the effects of dark energy, shows that the density fluctuations of such types of scalar field (filed produces due to the effect of DE) propagates through space with the speed of light ($c_s^2 = 1$), i.e., the field does not have noticeable amount of density fluctuations on sub-horizon scales as it still under GR theory of gravity. The presence of this field is only detectable in the change of background pressure and density but indirectly through its effect on the expansion rate of the Universe H.

In modified gravity the relation between matter density and gravitational potential

can be written as

$$S = \int d^4x\sqrt{-g}\left[\frac{R}{16\pi G} + L_M(\psi, g_{\mu\nu}) - \Lambda_\varphi\right] \quad which\ implies \tag{1.25}$$

$$G_{\mu\nu} = 8\pi G\left[T^m_{\mu\nu} + T^\varphi_{\mu\nu}\right] \quad , \tag{1.26}$$

where Λ_φ is the general scalar Lagrangian and associated energy-momentum tensor is denoted by $T^\varphi_{\mu\nu}$. Now, here comes the interesting fact of using modified gravity as this scalar field can develop appreciable density fluctuations in the sub-horizon scales. In this model of scalar field of DE, the gravitational potential counts for both the contributions of matter and arbitrary chosen scalar field as

$$\nabla^2\Phi = 4\pi G\left[\partial\rho_m + \partial\rho_\varphi\right] \quad . \tag{1.27}$$

The scalar field is said to be "minimally coupled" to the metric. It is more practical to say that, the action of the scalar field φ is coupled with the $\sqrt{-g}$ term only. At the same time, modified gravity can also accommodate additional degrees of freedom non-minimally coupled to the metric.

Now, the equations (12) and (17) simultaneously gives the Friedmann equation as

$$H^2 = \frac{8}{3}\pi G\rho + \frac{\Lambda}{3} - \frac{k}{a^2} \quad , \tag{1.28}$$

where H is the Hubble parameter and its present time value is believed to be about 70 $km\ s^{-1}\ Mpc^{-1}$

The matter density of the universe at present time ($\rho = 9 \times 10^{-27} kg\ m^{-3}$) is not enough alone to achieve a flat Universe at $k = 0$. So, a vacuum energy provided by the extra term Λ to make up the shortfall for this. The present observations such as Luminosity distance of Type Ia supernova, baryon acoustic oscillations (BAO), CMBR anisotropies etc. strengthened the presence of dark energy in the cosmological model.

1.1.5 Black Holes : A Brief Review

A black hole (BH hereafter) is a region of spacetime where gravity is so strong that nothing, including light and other electromagnetic waves, can escape from its tremendous gravitational pull. Einstein's theory of general relativity predicts that a sufficiently compact massive object can deform spacetime surrounding it, to form a BH. BHs are the simplest among the families of compact stars. Einstein's general relativity, where a central singularity and some inner horizons such as Cauchy horizons, Innermost Stable Circular Orbit (ISCO) etc are intertwined by an event horizon, can be used to treat these objects. Quantum fluid studies also uncover the fact that they even can radiate, named as "Hawking radiation". Vacuum perturbations, which generate virtual pairs of particles, are the origin of this BH radiation. At one time, tidal forces draw them aloof, one falls in and the other escapes away giving this radiation. This idea leads us to consider the BHs as thermodynamic systems. In physics, BH thermodynamics is the area of study that seeks to reconcile the laws of thermodynamics with the existence of the BH event horizon. Also, a BH may stop to evaporate and then it may become stable at the quantum ground state. Thermodynamics and related topics are emergent ways to culture BH physics.

A BH acts like an ideal black body, as it reflects no light. Moreover, quantum field theory (QFT) in curved spacetime predicts that event horizons emit Hawking radiation, with the same spectrum as a black body of a temperature inversely proportional to its mass. This temperature is of the order of billionths of a kelvin for stellar black holes. BHs are essentially impossible to observe directly. BH parameters like mass, charges, angular momenta etc. are the thermodynamic variables of the first law. One of the best ways to look into what happened to the BH at the quantum scale is to study the thermal fluctuations which is discussed in Chapter 7. We get the knowledge about the microscopic origin of entropy from it. As a matter of fact, it is statistical fluctuation that may be illustrated as the quantum corrections. We need a theory of quantum gravity for practicing this type of quantum corrections in a strong gravitational system. It can be done via some quantum theories of gravity like string theory

or loop quantum gravity. Meanwhile, it is found that leading order corrections to the BH entropy may be logarithmic. It is actually an important term when the BH's size is small. Consequently, it can be considered to test quantum gravity. Such thermal fluctuations can be considered as small perturbations around the equilibrium temperature of the BH.

The idea of such a compact object with such a strong gravitational field was first considered in the 18th century by John Michell and Pierre-Simon Laplace. Again, in 1916, Karl Schwarzschild found the first modern solution of GR that would characterize a BH. David Finkelstein, in 1958, first published the interpretation of "black hole" as a region of space from which nothing can escape. BHs were long considered a mathematical curiosity- it was not until the 1960s that theoretical work showed they were a generic prediction of GR. The discovery of NS by Jocelyn Bell Burnell in 1967 sparked interest in gravitationally collapsed compact objects as a possible astrophysical reality. The first BH known was $CygnusX-1$, identified by several researchers independently in 1971.

1.1.6 The Scope of the Work

The title of the thesis reflects the main focus is to develop a flexible and modular framework or model, for investigating both BHs and NSs structure with their various properties to get a clear picture of their evolution through accelerated spacetime. Ongoing theoretical research aims to refine our understanding of the behavior of matter under these extreme conditions. We have modeled the NSs such that it can easily expandable also to include more and exciting physics in the future. At the same time, we have also built up a realistic NS model with precise EoS of the core nuclear matter, incorporating the effect of dark matter under the accelerated phase of the Universe. Not only that, we have also investigated the thermodynamic parameters of the rotating black holes through the quantum approach of gravity where we have applied the generalised uncertainty principle to understand the evolution of the parameters related to the black holes under dark energy dominated Universe. Here, we will also discuss the scope of this thesis work briefly.

Neutron stars are one of the most utmost compact objects of the Universe. The densities of these types of stars can even exceed those of atomic nuclei and gravitational fields also. Their observable physical properties and structure have created a lot of mystery as well as enthusiasm amongst the researchers. If we can realize the exact EoS of their constituent core matter, it is possible to explore a new era of astrophysics and cosmology. Various theoretical and observational research on NSs have revealed plenty of information but still very little is understood. It is obvious that the structural characteristics of these compact objects can be determined by the EoS which clearly depicts how its density, energy and pressure are related to each other. Various observational research on these stars, such as measurements of their masses and radii, can provide valuable constraints on the properties of the EoS.

The physical properties of the NSs are also of immense interest to researchers. Neutron star pulsation and emission of electromagnetic waves (X-rays and Gamma rays) may be the effect of their heavily strong magnetic field. Thermal properties of the NSs are also a matter of great interest due to its very high surface temperature. Observations on their gravitational fields can test the GR as well. Various observational researches are going on by using a variety of techniques, including telescopes (radio and X-ray), gravitational wave detectors and optical telescopes.

These observations are often combined with theoretical models to gain a more complete understanding of the properties of neutron stars and black holes. In a nutshell, this is the main focus of this thesis. Actually I have a few quarries regarding the black holes as well as neutron stars. throughout this research, I have tried to find out the most possible answers of those questions. The questions which have driven me to make a rigorous study on these mysterious compact objects are as follows :

•Why general theory of relativity is not enough for studying those compact objects under accelerated Universe?

•Does any alternative theory of GR is possible to develop for the study of those objects?

•Does the modified gravity theories are suitable enough to investigate those objects?

•What are the advantages of modified gravity theory over general relativity theory?

Which theory is more suitable then?

•Is it possible to investigate the evolution of the rotating charged black holes embedded in dark energy, through measuring the quantum corrected thermodynamic parameters?

•How these compact objects evolved through dark energy dominated Universe?

•What kind of effect the dark energy have on those compact objects?

1.1.7 Organization of the Thesis

We shall provide a chapter wise summary of the thesis now. This thesis is composed of seven different parts comprising a total of twelve chapters.

1. The introductory part of this thesis includes a single chapter, *Chapter 1*, where a brief review of some necessary background topics have been discussed.

2. The second part comprises of two chapters, *Chapter 2 and Chapter 3*.

3. The third part comprises of two chapters, *Chapter 4 and Chapter 5*.

4. The fourth part comprises of one chapter, *Chapter 6*.

5. The fifth part also comprises of only one chapter, *Chapter 7*.

6. The sixth part comprises of four chapters, *Chapter 8 to Chapter 11*.

7. The concluding part seven contains a single chapter, *Chapter 12* giving the summary of the thesis and presenting the future outlook.

The results presented in this thesis are derived from the work done in the following papers:

1. "Repulsive gravitational force and quintessence field in $f(T)$ gravity: How anisotropic compact stars in strong energy condition behave." by **M. Bandyopadhyay** and R. Biswas. *Mod. Phys. Lett. A*. (*February*, 2021).

2. "Impacts of modified Chaplygin gas on super-massive neutron stars embedded in quintessence field with $f(T)$ gravity." by **M. Bandyopadhyay** and R. Biswas. *Int. J. Mod. Phys. D*. (*January*, 2023).

3. "Investigation on the stability and quantum phase transition of the charged

rotating Kiselev Black Hole embedded in Quintessence field with quantum fluctuation of entropy." by **M. Bandyopadhyay** and R. Biswas. *Int. J. Geom. Methods Mod. Phys.*. (*September*, 2023).

4. "Nuclear Matter Equation of State and Stability of Charged Compact Stars Embedded in $f(T)$ Modified Gravity, under Cosmic Acceleration." by **M. Bandyopadhyay** and R. Biswas. *Int. J. Geom. Methods Mod. Phys.*. (*December*, 2023).

5. "Future of the accelerating Universe: Estimation of the Hubble parameter and Deceleration parameter under current Observations" by **M. Bandyopadhyay** and R. Biswas. (*UnderReview*, *March*, 2024).

6. "Confrontation of $f(T) = T + \xi T^2$ Modified Gravity with Charged X-ray Binaries Embedded in modified Chaplygin gas under Tolman-Kuchowicz Spacetime" by **M. Bandyopadhyay** and R. Biswas. (*UnderReview*, *February* 2024).

7. "Investigating the Equation of state, Stability and Mass-Radius relationship of Anisotropic and Massive Neutron Stars embedded in $f(R,T)$ modified gravity" by **M. Bandyopadhyay** and R. Biswas. *Int. J. Geom. Methods Mod. Phys.* . (*Accepted*, *April* 2024).

8. "Isolated Compact Star $RXJ1856.5-3754$ in $f(R,T)$ Modified Gravity in Tolman-Kuchowicz Spacetime" and R. Biswas. (*UnderReview*, *February* 2024).

Part II

THEORETICAL FOUNDATION OF THE NEUTRON STARS

"Things changed with the discovery of neutron stars and black holes - objects with gravitational field so intense that dramatic space and time-warping effects occur".

—Paul Charles William Davies

CHAPTER 2

THE STRUCTURE OF NEUTRON STARS

2.1 The Stellar Structure: Spherical Symmetric Configuration

It's nothing but the mysterious and beautiful gravity that governs the life-cycle (life and death) of stars, and the balance between gravity and pressure, accompanying a lot of tussles. They have started to form initially from sparse collapsing clouds of gas and dust due to gravity. The pressure of this collapsing cloud later converts into energy due to which fusion reactors starts and illuminates the whole Universe. In case of the massive stars like NSs, gravity starts to govern their lives from the beginning. NSs are the examples of final defense against the crushing force of gravity in the nature. These stars are the most compact configuration matter in the Universe that may be compressed into before imploding, forming a black hole. In order to model the compact stellar structure of the NSs, a thorough understanding on the process about the balance of gravity and pressure is very much needed. Due to the extreme gravitational fields in the NSs, we should incorporate the relativistic effects from Einsteins general theory

of relativity (GR), which modifies the concept of Newtonian gravity.

We are mainly investigating static NS structure under spherical symmetry and equilibrium. Thus, we only need to consider hydrostatic physics and related equations. Our aim for this chapter is to obtain the basic equations to construct the structural profile of the NSs and to investigate their evolution under accelerated Universe. In this chapter we will only confine our interest on the internal structure of the neutron star, i.e., mainly three regions such as outer crust, an inner crust and a core.

The cold matter EoS ascertain the macroscopic properties of NSs, which can be potentially extractable from various astrophysical measurements and observations. It is expected that the NSs can be traced by applying the same one parameter EoS. In order to establish this EoS, data on multiple NS observations are required by the help of which we can constrain the properties of the single NS EoS. Isolated NSs are mainly characterized by their mass, radius, and spin frequency but in case of massive binary pulsars, the spin-orbit coupling is very important to understand the moments of inertia of the NSs. At the same time, atmospheric and crust properties are very much required to determine the behavior of bursts, glitches and also other properties of the NSs. Observations of such astronomical processes are very sensitive to realize the NSs physics beyond the cold EoS. In this chapter, we will only focus to investigate the $M - R$ relation of the NSs instead of investigating the properties that derive from the core EoS (specifically the EoS which are well-constructed by using the perfect fluid concept with cold high-density equilibrium matter).

2.1.1 Inner Structure of Neutron Stars

The interior of a NS can be modeled, as in Figure 7 which is widely accepted configuration. The interior can be divided into various layers of distinct composition and thickness which surrounds the unknown mysterious core. The interior of a NS mainly consists of three regions. Starting from the exterior region, we will first get an outer crust with thickness about 0.3 km, an inner crust region with thickness around 0.5 km, and at last the innermost core region which extends about 10 km. The assumed temperature of the core matter at the NS interior is $T = 0K$ and that matter is transparent

to neutrinos as already mentioned in the previous chapter. The first assumption is justified because at extreme high densities of typical NSs, neutrons have a Fermi energy $E_F = kT_F$ which corresponds to temperatures T_F about $3 \times 10^{11-12}$ K, whereas shortly after almost one year of their birth NSs reach temperatures as $T \leq 10^9 K << T_F$. The other assumption depends on the fact that the mean free path of neutrinos in the core nuclear matter of the NSs at $T \leq 10^9$ K is very much larger than the typical radius of a NS.

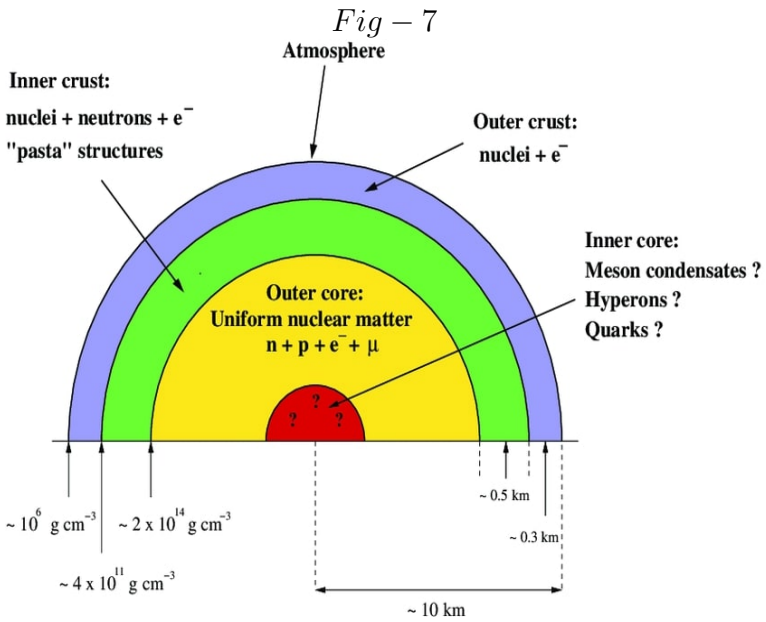

Figure 2.1: *Schematic diagram of cross section of a neutron star illustrating various regions. See text for more discussions. Figure credit: G. F. Burgio and I. Vidana, August,* 2020.

2.1.1.1 The Outer Crust Region

Several models on neutron stars have shown that the interior of the neutron star can be divided into main two regions - crust and core. We have also investigated the "crust-core" concept of the neutron star interior but in $f(T)$ modified gravity, a completely different approach compared to normal GR based investigations on neutron stars [21]. Our model strongly supports the "crust-core" structure of the neutron stars. We have also got the evidence of this type of internal structure as we have found out the region which can divide the interior of the neutron star into two different regions like core and

crust. Significantly we have also shown in our research that, in this particular region, the pressure and density of the neutron star matter shows a significant behavior. These two crucial parameters show a step-like phase transition in this region which can divide the interior of the neutron star. The step-like phase transitions occur in the region which is almost at a distance half of the radius of the massive neutron star. The graphical variations of these parameters with radius clearly depicts the fact. Our investigations show that for massive neutron stars with a radius around 12.1 km, this region lies at a distance of about 6.5 km.

The density of matter in the outer crust region ranges from $10^7 gm\ cm^{-3}$ to $4 \times 10^{11} gm\ cm^{-3}$. It's made up of a heavy nuclei lattice immersed in an electron gas. These electrons can move freely through the crust. In this region, at such a density, nucleons are formed individual nuclei to minimize the Coulomb repulsive force and stabilize against the β decay. As we go from the external boundary region to the internal one, the density increases and in turn inverse β-decay process becomes more and more efficient and a huge number of neutrons are produced. The newly produced neutrinos leave the star as usual. In this region pressure is mainly due to the degenerate electron gas. As the density reaches around $\rho = 4 \times 10^{11} gm\ cm^{-3}$ all bound states available in the nuclei for neutrons are filled up. Neutrons can no longer live bound to nuclei and start leaking out which is called neutron drip. The composition of this region can be found out by making Gibbs free energy of the nucleons minimum. So, it is very essential to know about the nucleus binding energy for different isotopes and isobars. But we have not studied that during our research. The interior crust region of the neutron star is also divided into two parts as outer crust region and inner crust region. Here, we have discussed only the interior structure of the massive neutron stars.

2.1.1.2 The Inner Crust Region

In this region, the density becomes of the order of nuclear density as $3 \times 10^{14} g\ cm^{-3}$ and the neutron gas gives the dominant contribution to the high pressure. In this region, the stellar matter is the mixture of two phases: one phase is rich in protons, indicated as "Proton Rich Matter" and the another phase is superfluid neutron rich

matter. Moreover, the electron gas exists to secure charge neutrality condition. So, to determine the fundamental state of the stellar matter in this region one has to specify the density of these two phases. The spherical drops of nuclei which is surrounded by a gas of electrons and neutrons, ensures the minimum energy condition. But as soon as the density becomes of the order of nuclear density, it is not possible to separate these two phases. At super high nuclear density, a homogeneous fluid as a mixture of protons, neutrons and electrons is formed.

From our constructed model in modified $f(T)$ gravity with quintessence field as dark matter, we have found that in this region density can reach upto of the order of $10^{15} gm\ cm^{-3}$ and the pressure of this region also becomes of the order of $10^{36} dyne\ cm^{-2}$ [88]. At these high densities the properties of core matter can be obtained from experimental data on neutron rich nuclei. Conversely, densities that exist in the core are presently unreachable in a laboratory. Consequently the available models of EoS at supranuclear densities are based on theoretical models only and partially constrained by empirical data. The EoS proposed to culture the core nuclear matter of the NSs is beyond the scope of this chapter. We will discuss and give some focus on it in the next chapter of this thesis.

2.1.1.3 The Mysterious Core Region

The core of a neutron star is still acting as a mysterious region. The composition of the core nuclear matter is still unknown and several researches are going on and several models are building up. But unfortunately we still know a very little about the core. The EoS of the core nuclear matter can help us to investigate and realize about different macroscopic properties of the neutron star like its mass, radius, spin, tidal deformability etc. different researchers can only guess about the core matter composition and structure as shown in Fig 8.

$Fig - 8$

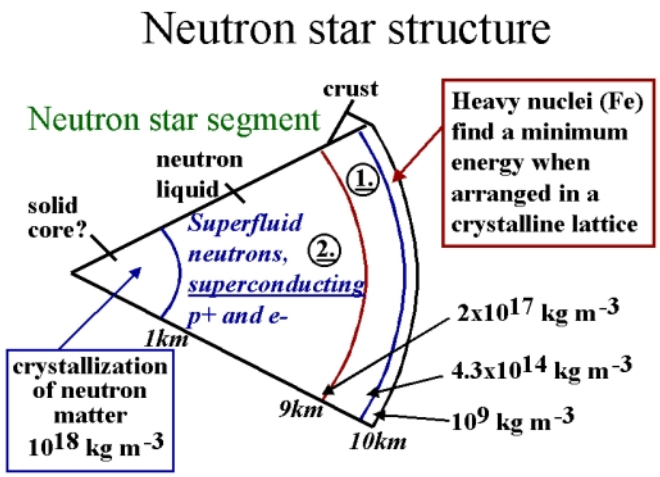

Figure 2.2: *Schematic diagram of the structure of a neutron star. The diagram shows a segment through a neutron star. The core extends out to about* 1 *km and has a density of* $10^{18}\ kgm^{-3}$. *Its substance is not well known however it could be a neutron solid, quark matter or a pion concentrate. It may not even exist. From* 1 *km out to* 9 *km, there is a "neutron fluid", a superfluid made up of neutrons and superconducting protons and electrons. The density in this region is between* 2×10^{17} *and* $10^{18}\ kgm^{-3}$. *In the inner crust, there is a lattice of neutron-rich nuclei with free degenerate neutrons and a degenerate relativistic electron gas. The neutron fluid pressure increases as the density increases. The outer crust is solid and its matter is similar to that found in white dwarfs, ie heavy nuclei (mostly Fe) forming a Coulomb lattice embedded in a relativistic degenerate gas of electrons. The density falls away relatively quickly in this region, down to a billion* kgm^{-3} *in the outer crust. On the very surface of the neutron star, densities fall below a billion* kgm^{-3} *and matter consists of atomic polymers of* Fe^{56} *in the form of a close packed solid. The atoms become cylindrical, due to the effects of the strong magnetic fields. Stresses and fractures in the crust cause the glitches in the pulse period. Figure credit: Lecture notes on "Neutron star structure", University College London, July,* 2011.

The density of the core matter may beyond nuclear density as $\rho_{core} > 10^{14} g\ cm^{-3}$. the core nuclear matter is composed of a homogeneous fluid of proton, neutron and electron, in β-equilibrium. If it is possible to make the Gibbs free energy minimum to find that matter in the core under stable condition. It is possible only if protons are about 10% of the total. Several processes may develop at this type of higher density core. For instance, electrons become more energetic and their kinetic energy increases

and so does the chemical potential. Indeed the chemical potential is the energy needed to insert in a gas in equilibrium, a new particle in the same state, and this energy increases if the state is more energetic. Thus, at some high density the electrons chemical potential become larger than the rest mass of the muon $m_{\mu^-} = 105MeV$. At this point neutron decay may occur and neutrinos are produced which can easily escape from the core but the other particles like neutrons, electrons and protons are trapped inside the core. The neutrons are in a superfluid state inside the core at such high density and pressure. So, neutrons must be treated as ultra-relativistic particles. Moreover, the main and maximum contribution to the core pressure comes from neutrons. Since they are more massive than electrons, the total energy also will be now provided by the neutrons themselves.

Neutrons are also the fermions. However, the pressure they generate cannot be associated with the Pauli exclusion principle. Because at the core densities we can no longer treat neutrons as non interacting particles, as we did for the degenerate electron gas in white dwarfs. Indeed, if we would assume that the neutron star is composed of non interacting neutrons, we would find a maximum mass of $0.7M_{\odot}$, which is exceedingly too low. It is lower than the Chandrasekhar limit and also lower than the mass of any observed neutron star. Depending on the particular way researchers choose to model neutron interaction for a different composition. For instance in some models heavy baryons may form. Through the transitions different types of bosons may form, disobeying Pauli's exclusion principle, which leads to Bose-Einstein condensate may form at the deepest region of the core. Further, since nucleons are known to be composite objects of size around $0.5 - 1.0\ fm$, corresponding to a density about $10^{15} g\ cm^{-3}$, if the density in the core reaches this value, matter undergoes a transition to a new phase, in which quarks are no longer confined into nucleons or hadrons.

So, from the above information about the interior structure of a massive neutron star, it is quite clear that, at the densities that are expected to occur in the inner core of a neutron star, the EoS of matter at this supranuclear densities depends on the modeling of neutron interactions. The model predicts the typical mass and radius in the range within $(1.1-3.2)M_{\odot}$ and $(10-14)$ km respectively. Thus, the surface gravity

is of the order of $\frac{GM}{c^2R} \approx 10^{-1}$ and therefore GR must be used to determine the structure of such stars. But, at the same time application of GR in modeling these types of stars can not provide a singularity free solution for the relativistic stars. Again at the same time, due to the accelerating universe, GR can not also accommodate the tension in the Hubble parameter. In this situation, modifications of GR theories provide a unique way to model these massive relativistic compact objects avoiding the above mentioned problem which arises with GR. So, keep this in mind we have introduced the idea of $f(T)$ and also $f(R,T)$ modified gravity in our research and quite successfully modeled the massive neutron stars with their stable equilibrium configuration. Furthermore, the derived results from our model are highly compatible with other observations on Neutron stars. In what follows we shall first introduce the tools that are needed to describe perfect fluids in modified general relativity, then we shall derive the equilibrium equations of a compact star, on the assumption that the fluid in the interior behaves as a perfect fluid.

2.1.2 The Newtonian Stellar Structure of Neutron stars

For any stable star against self-gravitating collapse, the strong inwards force of gravity must be countered by an equal outward force of pressure. For different static models of the NSs, one can solve for the one-dimensional structure of the star at any time by balancing these forces radially throughout the profile from the core to the surface. As long as the net force acting in each volume element of the star is zero, the star is in equilibrium. In the Newtonian formulation, gravity is an ordinary force acting on both objects, described as

$$\vec{F} = \frac{GMm}{r^2}\hat{r} \quad , \tag{2.1}$$

where G denotes the gravitational constant, M and m are denoted as center of mass of two different objects, r is the distance between the objects and $\hat{r}$ denotes the unit vector in the direction of the gravitational force acting between the two bodies. Now, if we choose $\phi(r)$ as the gravitational potential through which the force of gravity acts

between the stars, then Poissons equation in Newtonian gravity gives

$$\nabla^2\phi(r) = 4\pi\rho(r)G \quad , \tag{2.2}$$

where $\rho(r)$ is the mass density and ∇^2 is the Laplace operator. As we have considered the spherically symmetric configuration of the neutron stars, we have used spherical polar coordinates, the only nonzero component of the gradient of the potential, $\nabla\phi$ is the radial part, $\frac{d\phi}{dr}$. So, the Newtonian gravitational potential can be expressed as

$$\frac{d\phi}{dr} = \frac{Gm(r)}{r^2} \tag{2.3}$$

where $m(r)$ is interpreted as the cumulative mass inside radius r of the star and is given by

$$\frac{dm(r)}{dr} = 4\pi r^2\rho \quad . \tag{2.4}$$

So, from this above equation we can easily point out the mass, M of a star with spherical structure of radius R as

$$M = 4\pi\rho\int_0^R r^2 dr \quad . \tag{2.5}$$

Now, for the star to be in equilibrium, the gravitational force must be balanced by a pressure force. So, we get

$$\frac{dP(r)}{dr} = -\rho\frac{d\phi}{dr} = -\rho\frac{Gm}{r^2} \quad , \tag{2.6}$$

where $P(r)$ is the pressure inside the star. In this way the interior gets an equilibrium.

We have now introduced all the fundamental variables, such as mass, radius, density and pressure, we need to describe the structure profile of our modeled NSs. These above coupled equations (3), (4) and (6) governing the stellar structure under hydrostatic equilibrium (Newtonian). They describe the mass and gravitational potential, along with the counterbalancing pressure, all as a function of radial distance from the core. However, we seemingly have no equation for the actual density of the NSs. During my

research, we have modeled the NSs in modified gravity in order to find a realistic and general EoS for the stars. This topic has been discussed in the following Chapter 3 elaborately.

Various attempts have been made, and are continuously worked at, to improve the shortcomings of GR theory and give alternating explanations of gravity for some of the uncomfortable consequences of applying this theory to the whole Universe, where we have discovered the need for substances like dark matter and dark energy to explain the reality we observe around us like accelerating phase of the Universe, CMBR, BAO etc. So far these alternative theories of gravity have had little success at describing as many of the different ways our Universe behaves and are able to simplify the problems that arises with Einsteins GR theory. It is very interesting to show from our research on neutron stars using $f(T)$ and $f(R,T)$ modified gravity theories, these newly proposed alternative gravity theories can accommodate the effect of dark matter as well as dark energy and also can produce a singularity free solution to the stars. Even these modified gravity theories can accommodate the tension in the Hubble parameter as well. As such, the theory described in the Chapter 4, with emphasis on the remaining relativistic version. Thus, when studying NSs, the main variable is in fact how we choose to model the EoS, which we will come back in chapter 3.

2.1.3 Law of conservation of Baryon Number

A fundamental equation in the study of stellar structure is the conservation of particle number. Let us consider a perfect fluid with fixed chemical composition and in thermodynamic equilibrium. The motion of the fluid is described by a vector field, the four-velocity u^α. Let us also consider a fluid element of volume V with n number of particles. So, the volume V contains nV particles, therefore, if τ is the proper time associated to the pressure P of the flow of the fluid, the conservation of particles number can be written as

$$\frac{d}{d\tau}(nV) = 0 \quad . \tag{2.7}$$

The above equation is not covariant. So, as generalization of the above law for any reference frame can be written as

$$(nu^{\alpha})_{;\alpha} = 0 \quad . \tag{2.8}$$

In case of a star, n denotes the baryon number density which is conserved by all interactions. As baryons are much heavier than electrons and neutrinos, the "rest mass" of the star is assumed to be the contribution of baryons only. If it is assumed that the star does not contain antimatter and the contribution of mesons are negligible then baryon number coincides with n^3.

2.1.4 Static, Spherically Symmetric Neutron Star Structure in $f(T)$ Gravity

2.1.4.1 Mathematical Formulation of Covariant $f(T)$ Gravity

The simplest model of a neutron star is a spherically symmetric, non-rotating perfect fluid, supported against gravitational collapse by its pressure. The general form of spacetime metric as

$$g = g_{\mu\nu} dx^{\mu} dx^{\nu} \quad . \tag{2.9}$$

Now, in tetrad formalism, after transformation, tangent space metric η becomes

$$\eta = \eta_{ij} \theta^{i} \theta^{j} \quad . \tag{2.10}$$

The component wise relation between g and η can be written as

$$g_{\mu\nu} = \eta_{ij} \theta^{i}_{\mu} \theta^{j}_{\nu} \quad , and \quad \eta_{ij} = g_{\mu\nu} e^{\mu}_{i} e^{\nu}_{j} \quad , \tag{2.11}$$

where

$$\eta_{ij} = diag[-1, 1, 1, 1] \quad and \quad e^{\mu}_{i} e^{\nu}_{i} = \delta^{\mu}_{\nu}. \tag{2.12}$$

So, using proper tetrad formalism componentwise, the torsion tensor takes the form as

$$T^{\alpha}_{\mu\nu} = e^{\alpha}_{i}\left(\partial_{\mu}e^{i}_{\nu} - \partial_{\nu}e^{i}_{\mu}\right) = \Gamma^{\alpha}_{\mu\nu} \quad , \tag{2.13}$$

where $\Gamma^{\alpha}_{\mu\nu}$ is the non-vanishing Christoffel symbols. Now, the torsional scalar after contraction becomes

$$T = T^{\alpha}_{\mu\nu}S^{\mu\nu}_{\alpha} \quad , \tag{2.14}$$

where after considering super potential, the term $S^{\mu\nu}_{\alpha}$ becomes

$$S^{\mu\nu}_{\alpha} = \frac{1}{4}\left(T^{\mu\nu}_{\alpha} + T^{\nu\mu}_{\alpha} - T^{\mu\nu}_{\alpha}\right) + \frac{1}{2}\left(\partial^{\mu}_{\alpha}T^{\beta\nu}_{\beta} - \partial^{\nu}_{\alpha}T^{\beta\mu}_{\beta}\right) \quad . \tag{2.15}$$

Now in TEGR, taking torsion T as the Lagrangian and $\sqrt{-g}$ as the tetrad determinant, $f(T)$ gravity is expressed as follows

$$S[e^{i}_{\mu}, \Phi_{A}] = -\frac{1}{2}\int d^{4}xe\left[\sqrt{-g}f(T)\right] + \int d^{4}xe\left[\sqrt{-g}L_{M}(\Phi_{A})\right] \ , \tag{2.16}$$

where $G = c = 1$ and $L_M(\Phi_A)$ is matter Lagrangian. Now, if we take the variation of the above equation (15) w.r.t. the tetrad, we get

$$\frac{2}{\sqrt{g}}\partial_{\beta}\left(\sqrt{g}S^{\mu\nu}_{\sigma}e^{\sigma}_{i}f_{T}\right) + \frac{f}{2}e^{\mu}_{i} = \sqrt{g}T^{\mu}_{\beta}e^{\beta}_{i} \quad , \tag{2.17}$$

where $\sqrt{g}T^{\mu}_{\beta}e^{\beta}_{i}$ is the energy-momentum tensor related to the matter, denoted as $T^{matter}_{\mu\nu}$ and f_T denotes $\frac{df}{dT}$.

So, according to our model in $f(T)$ gravity, Einstein equation can be written in terms of matter, quintessence field and electromagnetic field as

$$G_{\mu\nu} = 8\pi G\left(T^{matter}_{\mu\nu} + T^{q}_{\mu\nu} + T^{EM}_{\mu\nu}\right) \quad , \tag{2.18}$$

where $T^{q}_{\mu\nu}$ corresponds to the energy-momentum tensor of the quintessential field whose EoS parameter becomes ω_q as $(-1 < \omega_q < -\frac{1}{3})$ and the energy-momentum tensor of

the electromagnetic field is given by

$$E_{\mu\nu}^{EM} = \frac{1}{4\pi}\left(g^{\delta\omega}F_{\mu\delta}F_{\omega\nu} - \frac{1}{4}g_{\mu\nu}F_{\delta\omega}F^{\mu\delta}\right) \quad , \tag{2.19}$$

where Maxwell Field tensor is denoted by $F_{\mu\nu} = \Phi_{\nu,\mu} - \Phi_{\mu,\nu}$. So, electromagnetic field equations of Maxwell are

$$(\sqrt{-g}F^{\mu\nu})_{,\nu} = 4\pi J^{\mu}\sqrt{-g}, F_{[\mu\nu,\delta]} = 0 \quad , \tag{2.20}$$

where, four-vector of current is denoted as J^{μ} , holds $J^{\mu} = \sigma u^{\mu}$, with charge density parameter σ. Now, the energy-momentum tensor of the ordinary matter analogous to anisotropic fluid becomes

$$T_{\mu\nu}^{matter} = \sqrt{g}T_{\beta}^{\mu}e_{i}^{\beta} = (\rho + p_t)u_{\mu}u^{\nu} - p_t g_{\mu\nu} + (p_r - p_t)v_{\mu}v^{\nu} \quad , \tag{2.21}$$

where u^{μ} and v^{μ} are the four-velocity and the radial four-vector respectively. Further, they also holds $u_{\mu}u^{\nu} = 1$, $v_{\mu}v^{\nu} = -1$ and $u_{\mu}v^{\mu} = 0$. In the above equation (13), energy density is denoted by ρ , p_r and p_t are radial pressure and transverse pressure respectively.

2.1.4.2 Spherically Symmetric Stellar Equations

In case of relativistic massive neutron stars, if we consider that they are in spherical symmetry, for interior space-time, we can take into account the metric as

$$ds^2 = -e^{a(r)}dt^2 + e^{b(r)}dr^2 + r^2\left(d\theta^2 + \sin^2\theta d\phi^2\right) \quad , \tag{2.22}$$

where $a(r)$ and $b(r)$ are the unknown metric functions rely on the radial coordinate r. Here, in case of our investigation, we choose $a(r)$ and $b(r)$ as

$$a(r) = Br^x + Cr^y \;\; and \;\; b(r) = Ar^z \quad , \tag{2.23}$$

where applying physical conditions and choosing suitable values of x, y *and* z, we can find out the arbitrary constants like A, B and C of our model. In case of some early investigations in this covariant $f(T)$ gravity spin parameter is set to zero. But later, modern researches have upgraded tetrad metric with restoring the spin parameter. Now, we can choose the proper tetrad under Lorentz transform, for the above metric as

$$[e^i_\mu] = diag\left[e^{\frac{a(r)}{2}}, e^{\frac{b(r)}{2}}\sin\theta\cos\phi, -r\sin\theta\sin\phi, r\sin(\theta)\right] \quad . \tag{2.24}$$

So, for the above metric, $T(r)$ and $T'(r)$ can be written as

$$T(r) = \frac{2e^{-b(r)}}{r^2}\left(e^{\frac{b(r)}{2}} - 1\right)\left(e^{\frac{b(r)}{2}} - 1 - ra^{'}(r)\right) \quad and \tag{2.25}$$

$$T'(r) = -\frac{2e^{-b(r)}}{r^2}\left(e^{\frac{b(r)}{2}} - 1\right)\left[a^{''}(r) + \frac{2b^{'}(r)}{r}\left(e^{\frac{b(r)}{2}} - \frac{1}{r} - ra^{'}(r)\right)\right] \quad , \tag{2.26}$$

where prime $'$ denotes the derivative w.r.t. r. Therefore, with the 4−velocity and equation (13), the anisotropic fluid EoS along with quintessence field in $f(T)$ gravity takes the form,

$$4\pi\rho_q + E^2 = \frac{f}{4} - \frac{f(T)}{r^2e^b}\left\{\left(e^{\frac{b}{2}} - 1\right)(2 + a^{'}r) + rb^{'}\right\}f_T + \frac{2f_{TT}}{re^b}T^{'} + \frac{e^{-b}}{r^2}(e^b + rb^{'} - 1) \quad , \tag{2.27}$$

$$4\pi p_r - E^2 = -\frac{f}{2} - \frac{1}{r^2e^b}(1 - e^b + ra^{'})\frac{f_T}{2} - \frac{f_T}{2r^2}\left(2e^{\frac{b}{2}} - 1 - 2ra^{'}\right) \quad and \tag{2.28}$$

$$\begin{aligned} 4\pi\left\{p_t + (3\omega_q + 1)\rho_q\right\} + E^2 = &-\frac{f}{2} + r^2a^{'2} - 2(rb^{'} + r^2a^{''}) \\ &- \frac{f_{TT}}{4re^b}T^{'}\left(4 - 4e^{\frac{b}{2}} + 4e^b - 6ra^{'}\right)f_T \\ &- \frac{1}{4re^b}\left(ra^{'2} + b^{'}(2 + ra^{'} + 2ra^{''})\right) \quad , \end{aligned} \tag{2.29}$$

where f_{TT} denotes $\frac{d^2f}{dT^2}$.

Now, we can consider the electric field E inside the sphere of radius r with $q(r)$ as

the total charge inside, as

$$E(r) = \frac{1}{r^2}\int_o^r 4\pi r^2 \sigma e^{\frac{\lambda}{2}} dr = \frac{1}{r^2} q_0 r^{\epsilon} \quad , \quad q_o \; and \; \epsilon > 0 \quad . \tag{2.30}$$

In our model, we gave taken the anisotropic fluid as MCG. So, the EoS of MCG becomes

$$p(r)_{MCG} = \chi\rho - \frac{\psi}{\rho^{\xi}} \quad , \quad \xi = 1 \;\; and \;\; \chi \neq -1 \quad . \tag{2.31}$$

where χ, ψ and ξ are the free parameters. We have also chosen the torsional scalar $f(T)$ in case of our model as

$$f(T) = T + \alpha T^2 \quad . \tag{2.32}$$

So, solving the above equations (15), (18), (21), (23) and (24), we get the expression of energy density of MCG as

$$\begin{aligned} \rho_{(MCG)} =& \alpha e^{-Ar^z} \frac{\tau + \sqrt{\alpha^2\tau^2 y^2 e^{-2Ar^z} + 4\pi r^2 \psi(1+\chi)}}{4\pi^2 r^2 (1+\chi)^2} \\ &+ \frac{1}{4\pi}\left(\frac{\psi e^{-Ar^z}(1+\chi)}{Br^2} + \frac{\alpha y B r^x}{r^2(1+\chi)^2}\right) \quad , \end{aligned} \tag{2.33}$$

where τ is given as $\tau = (xBr^x + yCr^y + zAr^z)$.

After that, we can also found the expressions of radial pressure, p_r and transverse pressure, p_t as

$$\begin{aligned} p_r =& \alpha\chi e^{-Ar^z}\frac{\tau}{4\pi} + \frac{\psi\sqrt{\alpha^2\tau^2 e^{-2Ar^z}}}{4\pi^2 r^2(1+\chi)^2} \\ &- \frac{B\alpha e^{-Ar^z}\psi}{4r^2}\left(\frac{\pi r^2(1+\chi)}{\alpha\tau + \sqrt{\alpha^2\tau^2(1+\chi)}e^{-2Ar^z}}\right) + \frac{e^{-2Ar^z}(1 - rA + e^{-2Ar^z})}{r^2} \quad and \end{aligned} \tag{2.34}$$

$$p_t = \frac{\alpha\tau e^{-Ar^z}}{8\pi}\left[\frac{\chi\tau x(x-1)Br^{x-2}}{2} - \frac{(3\omega_q+1)e^{-Ar^z}\alpha}{16\pi r^2} + \tau(rzAr^z + y(y-1)Cr^{y-2})\right] - \frac{q^2}{r^4} - \frac{\psi e^{-2Ar^z}}{4\pi(1+\chi)} \quad . \tag{2.35}$$

So, the quintessence field density ρ_q becomes

$$\rho_q = \frac{1}{8\pi}\left[\frac{\alpha\tau\psi e^{-Ar^z}}{4\pi r^2(1+\chi)}(zAr^z-1) - \frac{q^2}{r^4}\right] - \frac{\alpha\tau e^{-Ar^z}}{16\pi^2 r^2(1+\chi)} + \frac{\tau + \sqrt{\alpha^2\tau^2 y^2 e^{-2Ar^z} + 4\pi r^2\psi(1+\chi)}}{4\pi^2 r^2(1+\chi)^2} \quad . \tag{2.36}$$

2.1.4.3 The Trace-Energy Tensor for Perfect Fluid: MCG

In our study, we have considered the form of $f(T)$ as, $f(T) = T + \alpha T^2$ for simplicity. Here, in this model, we can get the Einstein tensor in the form as

$$g_{\mu\nu} = T^{\alpha}_{\mu\nu} + \tilde{T}^{\alpha}_{\mu\nu} \quad , \tag{2.37}$$

where the effective energy-momentum tensor $\tilde{T}^{\alpha}_{\mu\nu}$, after absorbed all the non linear terms of effective $f(T)$ fluid, can be written as

$$\tilde{T}^{\alpha}_{\mu\nu} = \frac{1}{2}(f_T T - f)g_{\mu\nu} - S^{\mu\nu}_{\sigma} e^{\sigma}_{i} f_T + (1 - f_T)g_{\mu\nu} \quad . \tag{2.38}$$

Now, from the above equation (36), we get that if we choose $\alpha = 0$, we get, $f_T = 1$ and $(f_T T - f) = 0$ and also $\tilde{T}^{\alpha}_{\mu\nu} = 0$. Only in this condition of $f(T)$ gravity in our model, the above equation reduces to Einstein equations. So, we can say from our model that when $\alpha = 0$, our NS model becomes equivalent to the GR model of NSs.

2.1.4.4 Conservation of the Trace-Energy Tensor for Perfect Fluid

The law of conservation is satisfied by the stress-energy tensor, i.e., $T^{\mu\nu}_{;\nu} = 0$. Now, as we know that

$$u_\mu (u^\mu)_{;\nu} = \frac{1}{2}(u_\mu u^\mu)_{;\nu} = 0 \quad , \tag{2.39}$$

So, the stress-energy tensor under contraction can be written as

$$u_\mu T^{\mu\nu}_{;\nu} = u_\mu u^\mu u^\nu (p+\rho)_{,\nu} + (p+\rho)(u_\mu u^\mu u^\nu_{;\nu} + u_\mu u^\mu_{;\nu} u^\nu) + u^\nu p_{;\nu} = -u^\nu \rho_{,\nu} - (p+\rho) u^\nu_{;\nu} = 0 \quad . \tag{2.40}$$

On the other hand, baryon number conservation gives

$$u^\nu \rho_{,\nu} = -(p+\rho) u^\mu_{;\nu} = \frac{p+\rho}{n} u^\nu n_{,\nu} \tag{2.41}$$

which implies

$$\frac{d\rho}{d\tau} = \frac{p+\rho}{n}\frac{dn}{d\tau} \quad ; \tag{2.42}$$

Again, from the first law of thermodynamics we have

$$\frac{d\rho}{d\tau} = \frac{p+\rho}{n}\frac{dn}{d\tau} + nT\frac{ds}{d\tau} \quad , \tag{2.43}$$

the above two equations are compatible if and only if

$$\frac{ds}{d\tau} = 0 \quad , \tag{2.44}$$

which means that a fluid element does not exchange heat with its surroundings, as it must be for a perfect fluid. Thus, the contraction of the stress-energy tensor conservation law with the fluid four velocity and the baryon number conservation, implies that a perfect fluid is isentropic.

2.1.4.5 The Maximum Mass with Stability: Matching of Matrices with Boundary Conditions

Now, we will Apply matching condition between interior space-time metric of the neutron star with the Reissner-Nordstrm's exterior region metric given as

$$ds^2 = -\left(1 - \frac{r_g}{r} + \frac{q^2}{r^2}\right) dt^2 + \left(1 - \frac{r_g}{r} + \frac{q^2}{r^2}\right)^{-1} dr^2 + r^2 \left(d\theta^2 + \sin^2\theta d\phi^2\right) \quad , \quad (2.45)$$

where $0 \leq \theta \leq \pi$, $0 \leq \phi \leq 2\pi$ and $r_g = 2m(r)$ with m being the mass of the compact star, q is charge within the boundary of the compact star, r is the radius of the compact star. We took that at the boundary, $r = R$ with $g_{tt}^- = g_{tt}^+$ and $g_{rr}^- = g_{rr}^+$.

Now in this condition, from the above matching conditions of two metrics, we get

$$1 - \frac{r_g}{R} + \frac{q^2}{R^2} = e^{BR^x + CR^y} \quad and \quad (2.46)$$

$$1 - \frac{r_g}{R} + \frac{q^2}{R^2} = e^{-AR^z} \quad . \quad (2.47)$$

So, after solving those above equations and also applying boundary conditions we obtain,

$$A = -\frac{1}{R^z} \ln\left(1 - \frac{r_g}{R} + \frac{q^2}{R^2}\right) \quad , \quad (2.48)$$

$$B = \frac{1}{R^{x(x-y)}} \left[-y \ln\left(1 - \frac{r_g}{R} + \frac{q^2}{R^2}\right) + 2\left(\frac{m}{r} - \frac{q^2}{R^2}\right)\left(1 - \frac{r_g}{R} + \frac{q^2}{R^2}\right)^{-1}\right] \quad and \quad (2.49)$$

$$C = \frac{1}{R^{y(x-y)}} \left[x \ln\left(1 - \frac{r_g}{R} + \frac{q^2}{R^2}\right) - 2\left(\frac{m}{r} - \frac{q^2}{R^2}\right)\left(1 - \frac{r_g}{R} + \frac{q^2}{R^2}\right)^{-1}\right] \quad . \quad (2.50)$$

Now, first putting all the values of m, R, and q we find out the values of A, B and C. After that using the values of A, B and C we obtain the values of different parameters for our model.

We know that, because of the non-linear nature of the gravitational field, instead of the total mass, effective mass of these compact stars comes into play which is the material mass combined with the energy of the gravitational field associated with that star. But, as we know the energy density ρ_R of these massive NSs, we can define the active mass of these NSs in $f(T)$ gravity quite easily by using the equation

$$m(R) = 4\pi \int_0^R \rho(R) R^2 dR \quad . \tag{2.51}$$

According to our model the above equation takes the form as

$$m(R) = \int_0^R \left[\alpha e^{-Ar^z} \frac{\tau + \sqrt{\alpha^2\tau^2 y^2 e^{-2Ar^z} + 4\pi r^2 \psi(1+\chi)}}{\pi(1+\chi)^2} + \left(\frac{\psi e^{-Ar^z}(1+\chi)}{B} + \frac{\alpha y B r^x}{(1+\chi)^2} \right) \right] dR \quad . \tag{2.52}$$

Now, using the above equation, we can easily calculate the active mass of the massive NSs (see Table 2) numerically after applying the values our model parameters and we can effectively find out the impact of MCG and $f(T)$ gravity, on the mass of those massive neutron stars.

Actually in GR, "ADM" mass gives the active mass at a asymptotic flat space-time and as in case of null infinity this mass is calculate as "BS" mass. But, in case of a finite hyper-surface active mass can be calculated as "MS" mass which can reduce to asymptotically in BS or ADM mass as well in certain conditions. In fact, these types of masses has utilized only the field equations of gravitation and change the gravitational energy and material mass into space-time geometry. If we have any known solution of the material source and the metric, then it is possible to find out the active mass in terms of density (ρ) and pressure(p) as using any chosen EoS. These masses are closely related with the gravitational field equations because active mass can be calculated by using various integrations of field equations. This idea is used in case of modified gravity theories in order to find out gravitational mass of any relativistic objects. We also uses the same idea in our work in case of calculating gravitational mass of those compact stars (see Fig 9). The very important "mass-radius" relation of the neutron stars with the presence of modified chaplygin gas a the core, under $f(T)$ modified

gravity is shown in the Fig. 10 [23].

Table 1..

Sl No.	NSs	M ($M_\odot$)	M' ($M_\odot$)	R (km)	R'(km)
1	PSR J1614-2230	1.97	1.98684	13.01	12.27
2	PSR J0348+0342	2.01	2.08723	13.01	12.12
3	PSR J1748-2446ad	2.10	2.16247	17.01	12.01
4	PSR J0740+6620	2.08	2.12579	12.39	12.08
5	PSR J2215+5135	2.27	2.29963	13.01	11.89

Table 2.1: Values of Observed Mass M, Mass from Model M', Observed Radius R and Radius from Model R' of few NSs from our model.

$Fig - 9$

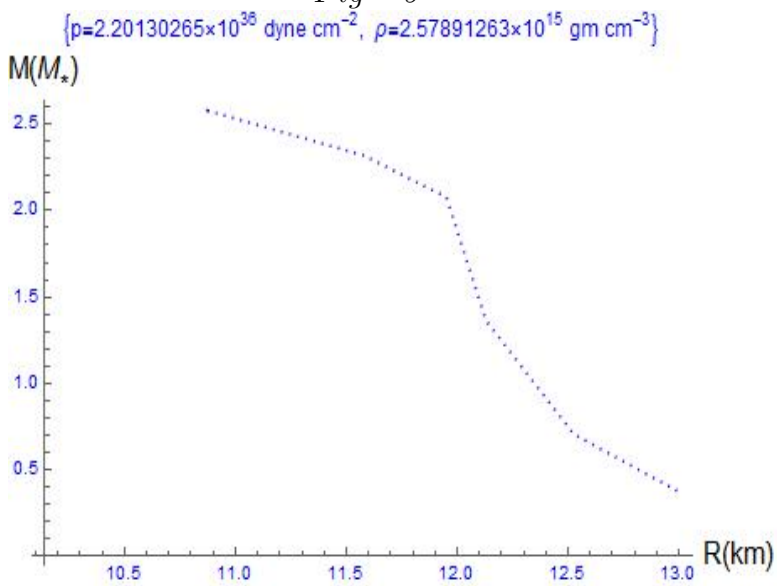

Figure 2.3: *Represents the variation of mass with radius of massive compact stars under critical pressure and density.*

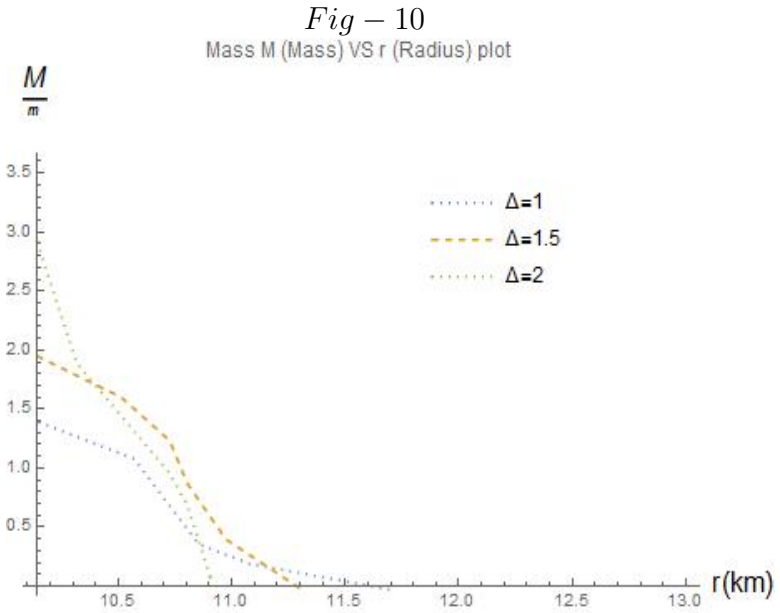

Figure 2.4: *Represents the variation of mass with radius of massive compact stars as a function of anisotropic force at the interior of the neutron star.*

2.1.5 The Buchdahl Theorem: Limit of Compactness for Neutron stars

A theorem proved by Buchdal in the year 1959 establishes that the maximum value that the ratio $\frac{M}{R}$ in case of a star of constant energy-density should be less than $\frac{4}{9}$, i.e., $\frac{M}{R} < \frac{4}{9}$, is much more general. The theorem is based on the only assumption that the star is static, and that the energy density is positive, and monotonically decreasing function of the radial coordinate, i.e.,

$$\rho \geq 0 \quad and \quad \frac{d\rho}{dr} \leq 0 \quad . \tag{2.53}$$

No assumption is made on the EoS that relates ρ and the pressure p.

From the theorem, we also get the idea that $R > \frac{4}{9}$ and science the Schwarzschild radius is $R_S = 2M$, this means that a star cannot have radius smaller than the Schwarzschild radius. The variation of the compactness factor of the massive neutron stars in the framework of $f(R,T)$ gravity is shown in the Fig. 11. [24].

$Fig - 11$

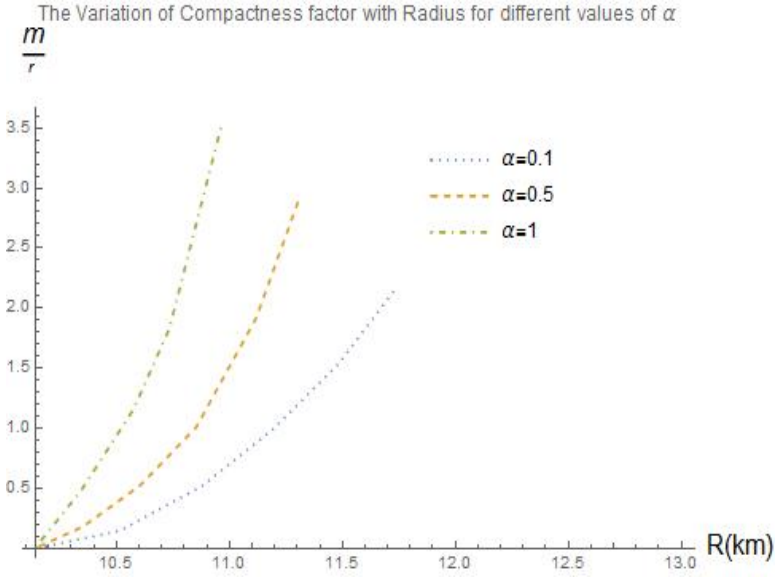

Figure 2.5: *Represents the variation of compactness factor with radius of super massive compact stars as a function of matter-geometry coupling parameter* α.

"The cosmos provides the only laboratory where sufficiently extreme conditions are ever achieved to test new ideas on particle physics.....By studying things like neutron stars, we are in effect learning something about fundamental physics".

—Martin John Rees

CHAPTER 3

THE EQUATION OF STATE FOR NEUTRON STARS

3.1 The Equation of State of Core Matter of Neutron Stars: The Microphysics

In physics, an equation of state (EoS) is a governing equation that describes the state of matter under a given set of conditions (external, internal or both). First of all, a rough idea about what type of matter can be found in the deep core of a NS and what might be the composition of this mysterious matter, we have discussed in the previous chapters 1 and 2. Matter is everything made of stuff that has a nonzero rest mass, and occupies some volume in spacetime. Up close, stuff is molecules, atoms, and particles, like neutrons, protons, and electrons. Massless particles, like photons, are usually not considered as matter, but are rather categorized as radiation. As we will see a particular example in the following chapters, some types of matter are given special names because of the way they behave. Fig. 12 shows the schematic presentation of the neutron star core.

$Fig - 12$

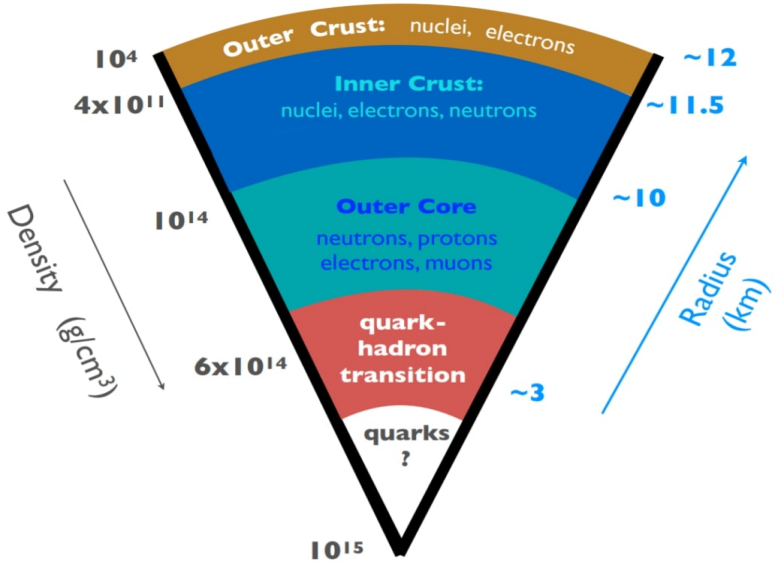

Figure 3.1: *Internal structure of a NS. Phase transitions to states of matter containing deconfined quarks, hyperons and meson condensates are possible at the densities encountered in the inner core. Figure credit: 3G Science White Paper.*

So an EoS describes different states of a given distribution of matter and for the different phases the EoS becomes distinct as well. As for example, the matter distribution, in the case of water in different phases as liquid, solid or gas can be assigned an appropriate and distinct EoS. Such phase transitions usually infer a discontinuous change in behavior. For the EoS of the core matter of the NSs, we are looking at in this current chapter, we have included possible phase transitions of pressure and density throughout the profile of our investigated (modeled) NSs.

The particle composition at the core of the NSs is still uncertain, including the possible states and phase transitions of the expected composition. As already mentioned, this is the ultimate variable in studying NSs and is the connection between the structural part of chapter 2 and the following chapters. We are for now modeling the neutron star to be of pure neutrons. The core matter densities of the NSs of masses range from one to two times of the solar mass, is much higher than the central densities of terrestrial atomic nuclei. At such extreme densities, scientists are expecting the presence of quarks and hadrons inside the core of the neutron stars. But the possibility of phase transition and also the nature of hadron to quark phase transition is still

beyond the reach of the researchers.

As in case of our research model in $f(T)$ modified gravity on the massive neutron stars with mass about $2M_{\odot}$, we have find out the presence of anisotropic force which is repulsive in nature, due to the pressure difference radial and tangential direction at the interior of these massive compact stars [88]. The anisotropic force along with the internal hydrostatic force encounters the effects the of forces due to modified gravity as well as sufficiently high the attractive pull of gravitational forces to maintain the hydrostatic equilibrium inside the star [26]. All these forces are produced from the modified TOV equation of our model in $f(R,T)$ modified gravity. The production of hydrostatic equilibrium condition also supports the more compact structure of the star under stable and spherical equilibrium configuration of the compact stars with existence of anisotropy inside the star as well. We can see the graphical plots of all these forces which create the hydrostatic equilibrium at the interior of the compact system in Fig. 13.

$Fig - 13$

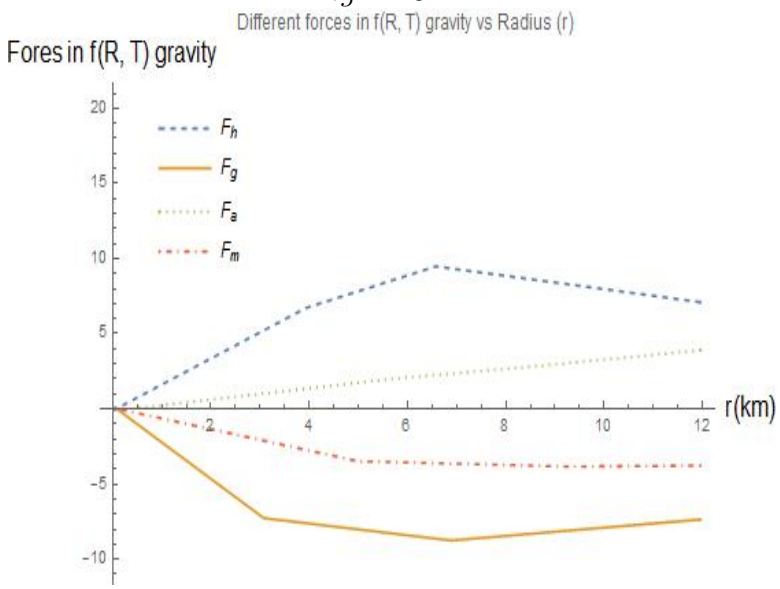

Figure 3.2: *Represents the various forces of the modified TOV equation with radius r, creating equilibrium. See text for more discussions.*

3.1.1 The Properties of Core Matter

The behavior of the core matter is responsible for the structural evolution and dynamics of the NSs. Further, the properties exhibited by the NSs are also greatly affected by the EoS of the core matter. During most of the time in the life-cycle of a NS, the bulk of its core matter is cold and degenerate, i.e., the matter is at temperatures below the Fermi temperature of its constituent particles. So the particles are in their respective ground states. We can estimate the Fermi temperature also.

If we consider μ_0 as the chemical potential at the temperature $T = 0$ K and r_F as the radius of the chosen Fermi sphere in momentum space which is scaled by $\hbar$, then we have $\mu_0 = \frac{(\hbar r_F)^2}{2m}$ for any particle of mass m. Now, with the spatial volume V and for the number of states N, the Fermi sphere is $2(2\pi)^{-3}V(\frac{4}{3}\pi r_F^3)$ for the particles with the spin $\frac{\hbar}{2}$. So, it is clear that at $T = 0$ K, this N defines the total number of particles in the volume V. Again, the Fermi temperature T_F can be written as

$$T_F = \frac{\hbar^2}{2mk}(3\pi^2\frac{N}{V})^{\frac{2}{3}} \quad , \quad \mu_0 = kT_F \quad . \tag{3.1}$$

So, at below this temperature the particles are degenerate and their total energy and chemical potential will be approximately equal to those calculated at $0K$ temperature [27]. Above nuclear density, the temperature of the nucleons is about $T_F \geq 10^{11}K$. Though the NSs are born with very high temperatures of about $10^{11}K$ but they cool to 10^8K within a month and in less than a million years the temperature falls to 10^6K [28]. The region which is temperature dependent for an isolated NS is a layer of thickness about 1 m and this region contains only a small fraction of the NS matter. The EoS of the core matter of the NSs at $0K$ temperature almost entirely determines the structure of the star. We have also considered the non-magnetic NS matter. This approximation is very appropriate for the NSs with the magnetic field $B < 10^{16}G$ because the magnetic energy density is very much smaller than the pressure density.

3.1.2 Thermodynamics of Neutron Star: Application of First and Second Law of Thermodynamics

3.1.2.1 Thermodynamic Variables to Study the Neutron Star Interior

The structure of the NSs at large scales will depend on averaged properties of the small piece of matter chosen as the thermodynamic variable. For the degenerate matter, these properties are totally determined by n which denotes the average number density of baryons measured in the comoving frame. Now, with the total energy density ρ measured in this frame and applying the first law of thermodynamics we get the heat gained per baryon, dQ as

$$dQ = d(\frac{\rho}{n}) + pd(\frac{1}{n}) \quad , \tag{3.2}$$

where $\frac{1}{n}$ denotes the volume per baryon, energy per baryon is doted by $\frac{\rho}{n}$ and p is the pressure. In case of the reversible process, $dQ = Tds$, where s is denoted as the entropy per baryon and T is the temperature of the system.

On the other hand, from the second law of thermodynamics, we have

$$d\rho = \rho T ds + \frac{p+\rho}{n} dn \quad , \tag{3.3}$$

where $\rho = m_b n$ is denoted as average rest mass per baryon of the NS matter, dispersed to infinity. Again, if the ground state energy density of a NS is $\rho(n)$ then the pressure of the matter via the first law of thermodynamics, as

$$p_m = n^2 \frac{d\frac{\rho}{n}}{dn} \quad . \tag{3.4}$$

Below the Fermi temperature, the entropy per baryon is almost uniform over the star. So, the increase in density and pressure will be approximated as isentropic, with $ds = 0$. Thus both processes are adiabatic and reversible. Thus now we have

$$d\rho = \frac{p+\rho}{\rho} d\rho \quad , \tag{3.5}$$

which gives

$$\frac{p+\rho}{\rho}\frac{dp}{d\rho} = \Gamma \quad , \tag{3.6}$$

where Γ is denoted as the adiabatic index which characterizes the change in pressure per change in volume when entropy becomes constant. Under equilibrium condition, Γ also characterizes the response of matter to density perturbations as long as the perturbations are slow enough. The sound speed in the fluid is given as

$$v_s = \frac{\partial p}{\partial \rho} \quad . \tag{3.7}$$

3.1.3 The Equation of State under Modified Gravity

The EoS of matter in NSs is usually described by using $p(\rho)$. A well defined EoS (pressure as a function of energy density) is very much essential to solve the equations for stellar structure which is the main focus in this chapter. The microscopic stability of matter requires a monotonically increasing EoS, i.e., $\frac{dp}{d\rho} \geq 0$, otherwise the star will start to collapse. For the matter to satisfy causality condition, the sound speed v_s as given in above equation, through the matter must be less than 1, i.e., $v_s < 1$.

For NSs, the core matter will be in equilibrium under various reactions involving both nuclear and electromagnetic interactions. But the timescales of achieving chemical and nuclear equilibrium are all short compared to the lifetime of NSs. In the context of nuclear physics, the EoS is generally constructed to minimize the internal energy per baryon as a function of number density.

3.1.3.1 The Equation of State with the presence of both Quintessence field and Modified Chaplygin Gas in $f(T)$ Gravity

Many cosmologists are exploring the possibility that the vast majority of the energy in the universe is in the form of an undiscovered substance called "quintessence", about which we have discussed in detail in the next Chapter. By numerous observations and experiments, now they reshape the field also. In cosmology, quintessence is a real form of energy distinct from any normal matter or radiation, or even "dark matter".

Its bulk properties energy density, pressure etc. lead to novel behavior and unusual astrophysical phenomena. So far its existence has only been inferred indirectly from a range of observations, but a number of current and planned experiments will make direct searches for this elusive form of energy. Radial pressure is not equal to the tangential pressure in case of the compact stars and as the density of the stars exceeds the nuclear density, it is obvious that the pressure at the interior becomes anisotropic which proves the electromagnetic field and mass distribution inside the compact stars.

We actually got the singularity free solution for a charged fluid sphere in general relativity using KB metric so it is quite easy to incorporate $f(T)$ gravity, which gives linear relations between various parameters in case of study of the compact stars. It is known to us that quintessence has the striking physical characteristic that it causes the expansion of the universe to speed up. Most forms of energy, such as matter or radiation, cause the expansion to slow down due to the attractive force of gravity. For quintessence, however, the gravitational force is repulsive, and this causes the expansion of the universe to accelerate in this type of field. We also know that quintessence differs from the cosmological constant. Quintessence in the explanation of dark energy becomes dynamic and it changes over time, unlike the cosmological constant which does not change. Quintessence can be either attractive or repulsive depending on the ratio of its kinetic and potential energy. For this type of repulsive force it is evident that a more massive distribution of matter would exist which can be explained in our work as the existence of quintessence fields and dark matter and its distribution inside the compact stars.

Now, the matter energy-momentum tensor corresponding to anisotropic quintessence fluid becomes

$$T_{\mu\nu}^{Matter} = (\rho + p_t)u_\mu u^\nu - p_t g_{\mu\nu} + (p_r - p_t)v_\mu v^\nu \quad , \tag{3.8}$$

where, u^μ is the four-velocity, v^μ is the radial four-vector and they are satisfying $u_\mu u^\nu = 1$, $v_\mu v^\nu = -1$ and $u_\mu v^\mu = 0$. Here ρ is the energy density, p_r is the radial pressure and p_t is the transverse pressure and $T_{\mu\nu}^q$ is the energy momentum tensor which consists of

ρ_q the quintessential field energy density and state parameter ω_q $(-1 < \omega_q < -\frac{1}{3})$. So, with the presence of anisotropic fluid, the field equations in $f(T)$gravity take the form as

$$4\pi\rho + E^2 = \frac{f}{4} - \left\{T - \frac{1}{r^2} - \frac{e^{-b}}{r}(a' + b')\right\}\frac{f_T}{2} \quad , \tag{3.9}$$

$$4\pi p_r - E^2 = \left(T - \frac{1}{r^2}\right)\frac{f_T}{2} - \frac{f}{4} \quad , \tag{3.10}$$

$$4\pi p_t + E^2 = \left[\frac{T}{2} + e^{-b}\left\{\frac{a''}{2} + \left(\frac{a'}{4} + \frac{1}{2r}\right)(a' - b')\right\}\right]\frac{f_T}{2} - \frac{f}{4} \quad . \tag{3.11}$$

We have chosen the $f(T)$ gravity as

$$f(T) = \beta T + \beta_1 \quad , \tag{3.12}$$

where β and β_1 are integrating constants and to simplify the equation we took $\beta_1 = 0$. We also took strange core matter equation of state as "MIT BAG model",

$$p_r = \frac{1}{3}(\rho - 4B_m) \quad . \tag{3.13}$$

Now, in our work we have chosen three unknown parameters as- ρ, P_r, p_t. Solving the above field equations (Einstein-Maxwell field equations) we can derive these parameters as follows

$$\rho = \frac{3(A + B)}{16\pi}e^{-Ar^2}\beta + B_m \quad , \tag{3.14}$$

$$p_r = \frac{(A + B)}{16\pi}e^{-Ar^2}\beta - B_m \quad , \tag{3.15}$$

$$p_t = \frac{1}{8\pi}\left[\left(\frac{7}{2}B - \frac{3}{2}A + B^2r^2 - ABr^2 + \frac{1}{r^2}\right)e^{-Ar^2}\beta - \frac{1}{r^2}\right] + B_m \quad . \tag{3.16}$$

We can even calculate the anisotropic parameter inside the core of the neutron star

due to the presence of quintessence field as

$$\Delta = [p_t - p_r] = 2B_m - \frac{\beta}{8\pi r^2} + \frac{1}{8\pi}\left(3B - 2A + B^2r^2 - ABr^2 + \frac{1}{r^2}\right)e^{-Ar^2}\beta \quad . \quad (3.17)$$

The variations of radial pressure p_r, transverse pressure p_t and the energy density ρ is shown in the Fig. 14, Fig. 15 and Fig. 16 respectively.

$Fig - 14$

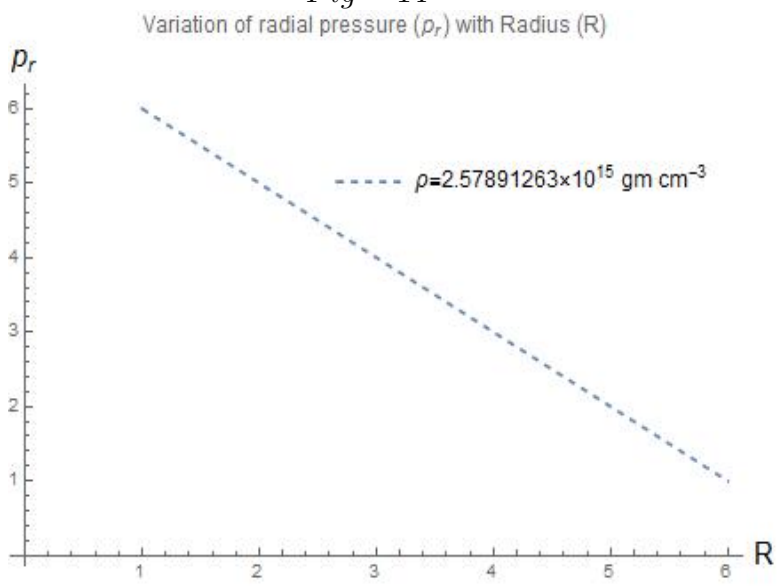

Figure 3.3: *Represents the variation of the radial pressure p_r dyne cm^{-2} with the radius R (km) of the neutron star.*

$Fig - 15$

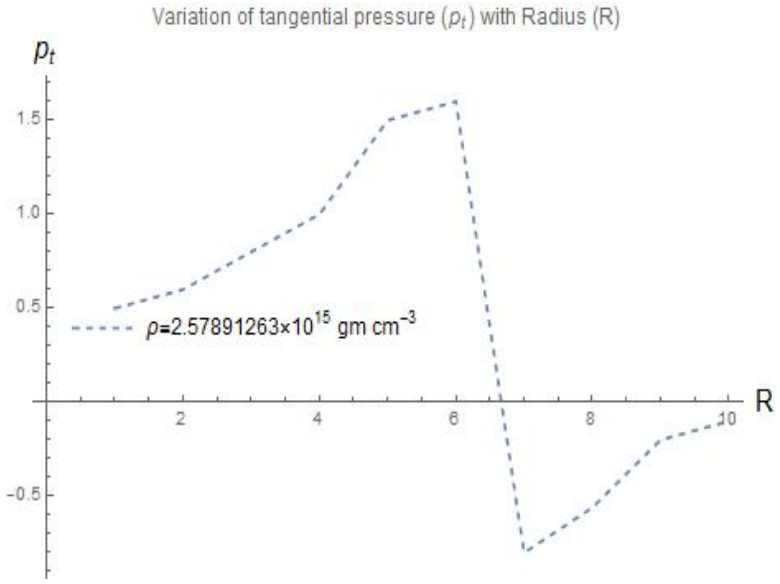

Figure 3.4: *Represents the variation of the transverse pressure p_t dyne cm^{-2} with the radius R (km) of the neutron star.*

$Fig - 16$

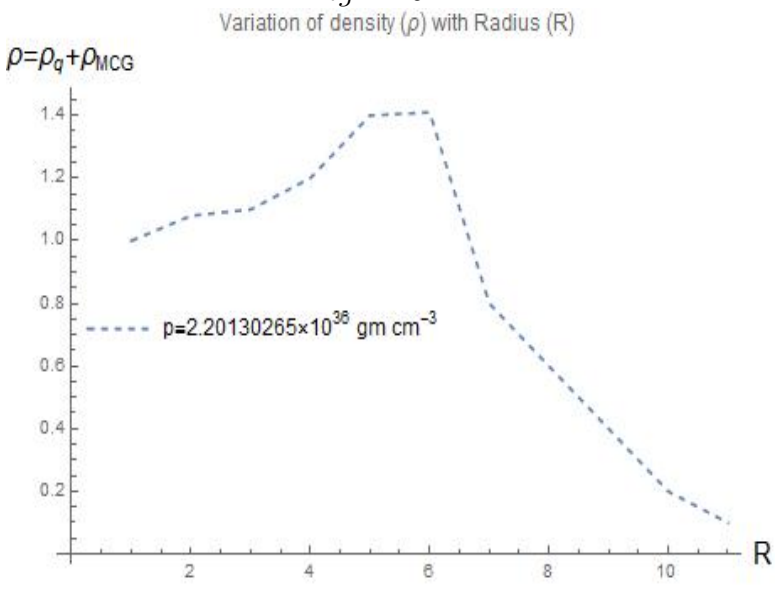

Figure 3.5: *Represents the variation of the core energy density ρ with radius R (km) of the massive neutron star.*

3.1.3.2 The Equation of State with Modified Chaplygin Gas in $f(T)$ Gravity

The torsional scalar T, for the spherically symmetric structure of the compact stars is given by

$$T = \frac{2}{r^2} e^{-B} \left(e^{\frac{B}{2}} - 1\right) \left(e^{\frac{B}{2}} - 1 - rA'\right) \quad . \tag{3.18}$$

EoS of the chosen fluid MCG is given as

$$p(r)_{MCG} = \left(\varphi\rho - \frac{\psi}{\rho^{\zeta}}\right) \quad , \quad \zeta = 1 \quad and \quad \varphi \neq -1 \quad , \tag{3.19}$$

where φ, ψ and ζ are free parameters and energy density is denoted by ρ. The effective energy-momentum tensor $\tilde{\tau}_{\mu\nu}$, analogous to the $f(T)$ fluid, becomes

$$\tilde{\tau}_{\mu\nu} = \frac{1}{2}(f_T T - f) g_{\mu\nu} - 2S^{\sigma}_{\mu\nu}\partial_{\sigma} + (1 - f_T) G_{\mu\nu} \quad . \tag{3.20}$$

The above equation in the form of an anisotropic fluid, effectively can be written as

$$\tilde{\tau}_{\mu\nu} = [(\rho + p_t) u_\mu u^\nu - p_t g_{\mu\nu} + (p_r - p_t) v_\mu v^\nu] \quad , \tag{3.21}$$

where u^μ and v^μ denotes four velocity and space like four vector respectively. They also follows, $u_\mu u^\nu = 1$, $v_\mu v^\nu = -1$ and $u_\mu v^\mu = 0$. Besides, radial pressure and the transverse pressure is denoted by p_r and p_t respectively.

In this model in $f(T)$ modified gravity, the expressions of effective energy density ρ, radial pressure p_r and transverse pressure p_t at the interior of the compact object can be written as

$$\begin{aligned} \rho =& \frac{\alpha}{2} f + \frac{2\psi}{r^2} e^{-B} \left[\left(e^{\frac{B}{2}} - 1\right)(2 + rA')\psi(1 + \varphi) + rB'\right] f_T \\ &+ \left[\frac{2\alpha^2}{r(1+\varphi)} e^{-B} \left(e^{\frac{B}{2}} - 1\right)\right] T' f_{TT} \\ &+ \left[\frac{\psi(1+\varphi)}{4r^2} e^{-B} \left(e^{B} - 1 + rB'\right)\right] \quad , \end{aligned} \tag{3.22}$$

$$
\begin{aligned}
p_r = &-\frac{\alpha}{2}f - \left[\frac{\psi(1+\varphi)^2}{4r^2}e^{-B}\left(1-e^{B}+rA'\right)\right] \\
&-\frac{2\alpha^2}{r(1+\varphi)}e^{-B}\left[2\left(e^{\frac{B}{2}}-1\right)+\psi\left(e^{\frac{B}{2}}-2\right)rA'\right]f_T \quad and
\end{aligned}
\tag{3.23}
$$

$$
\begin{aligned}
p_t = &-\frac{\alpha}{2}f + \frac{\psi}{4r^2}e^{-B}\left[4-8e^{\frac{B}{2}}+4e^{B}-2\varphi\left(e^{\frac{B}{2}}-3\right)rA'\right]f_T \\
&+\frac{\psi}{4r^2}e^{-B}\left[\psi(1+\varphi)r^2A'^2-rB'\left(2+rA'\right)+2\psi r^2A''\right]f_T \\
&-\left[\frac{\alpha^2}{r(1+\varphi)}e^{-B}\left(2e^{\frac{B}{2}}-2-rA'\right)\right]T'f_{TT} \\
&-\left[\frac{\psi(1+\varphi)^2}{4r}e^{-B}\left(2A'+rA'^2-B'(2+rA')+2rA''\right)\right] \quad .
\end{aligned}
\tag{3.24}
$$

Now, according to this new model, the variations of radial pressure p_r, transverse pressure p_t and the energy density ρ is shown in the Fig. 17, Fig. 18 and Fig. 19 respectively.

$Fig-17$

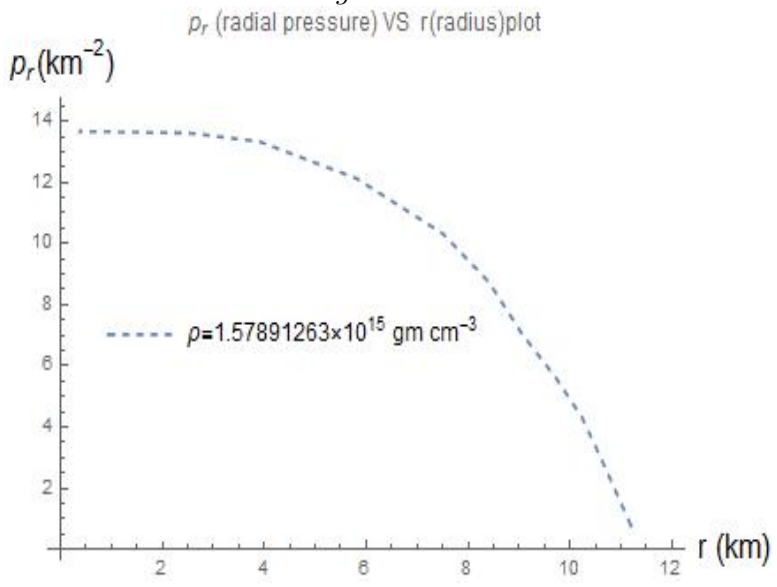

Figure 3.6: *Represents the variation of the radial pressure p_r dyne cm^{-2} with the radius R (km) of the neutron star.*

$Fig - 18$

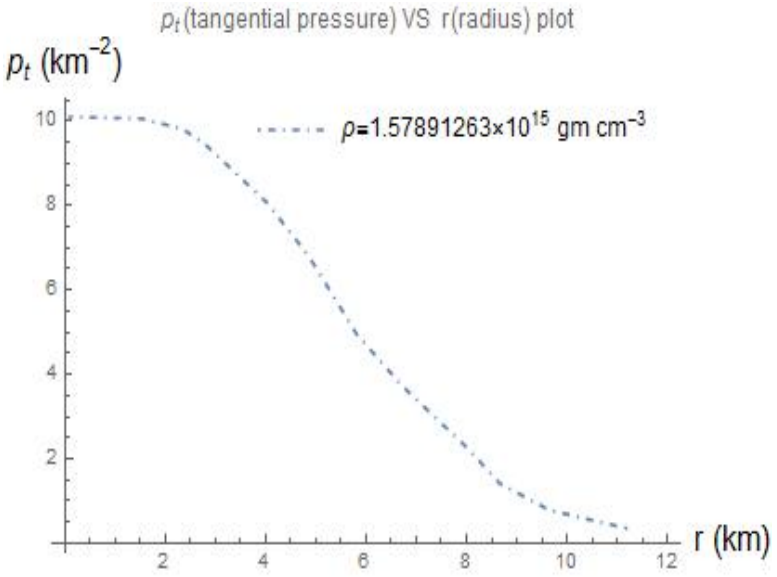

Figure 3.7: *Represents the variation of the transverse pressure p_t dyne cm^{-2} with the radius R (km) of the neutron star.*

$Fig - 19$

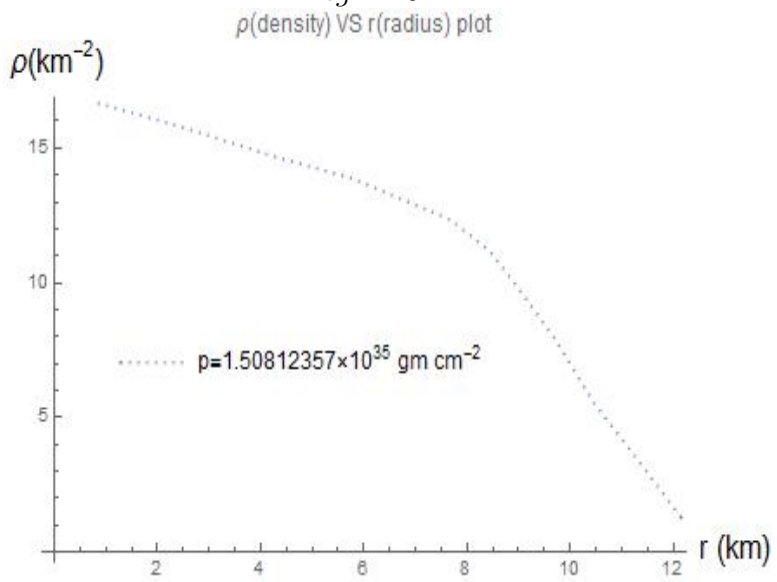

Figure 3.8: *Represents the variation of the core energy density ρ with radius R (km) of the massive neutron star.*

3.1.3.3 The Equation of state with Modified Chaplygin Gas in $f(T)$ Gravity under Tolman-Kuchowicz Spacetime

Here, the static spherically symmetric interior space-time metric is chosen as

$$ds^2 = -e^{A(r)}dt^2 + e^{B(r)}dr^2 + r^2d\Omega^2 \quad , \tag{3.25}$$

where the unknown metric potentials, $A(r)$ and $B(r)$ are purely radial and $d\Omega^2 = sin^2\theta d\phi^2 + d\theta^2$. The range of r is from 0 to ∞ and $0 \leq \theta \leq \pi$, $0 \leq \phi \leq 2\pi$.

As our main aim is to get a singularity free and physically reasonable model of the charged compact star, for our study, we have chosen the following Tolman-Kuchowicz (TK) ansatz as

$$e^{B(r)} = 1 + ar^2 + br^4 \quad and \quad e^{A(r)} = C^2e^{Dr^2} \quad , \tag{3.26}$$

where a, b, C and D are constants.

Now, using this matter distribution and from the above space-time metric, the Tolman-Oppenheimer-Volkoff (TOV hereafter) equations can be written in modified form as

$$\frac{dp_r}{dr} = -\frac{(\rho + p_r)}{r\{r - 2m(r)\}}\left(m + 4\pi r^3 p_r\right) + \frac{2}{r}(p_t - p_r) + \frac{\xi}{(2 + 4\pi)}\left[\frac{d\rho}{dr} + \frac{dp_r}{dr} + 2\frac{dp_t}{dr}\right] \tag{3.27}$$

and

$$\frac{dm(r)}{dr} = 4\pi r^2\rho \quad , \tag{3.28}$$

where $m(r)$ is the enclosed mass within the radius r. Now for the above metric, the proper tetrad is chosen as

$$[e^a_\alpha] = diag\left[e^{\frac{A(r)}{2}}, e^{\frac{B(r)}{2}}sin\theta cos\phi, -rsin\theta sin\phi, rsin\theta\right] \quad . \tag{3.29}$$

So, the torsional scalar T, for the above metric is given by

$$T = \frac{2}{r^2}e^{-B(r)}\left(e^{\frac{B(r)}{2}} - 1\right)\left(e^{\frac{B(r)}{2}} - 1 - rA'(r)\right) \quad . \tag{3.30}$$

Again, in our model we have chosen the modified gravity in the form of $f(T)$ as

$$f(T) = T + \xi T^2 \quad and \quad \xi > 0 \quad , \tag{3.31}$$

where ξ is a small positive constant and for $\xi \to 0$ generates the GR field equations.

Now, for the line element of the spherical metric, the field equations in $f(T)$ modified gravity becomes

$$8\pi\rho^{EG} + \frac{q^2}{r^4} = \frac{e^{-B}}{r}B^{'}(r) + \frac{1}{r^2}(1 - e^{-B(r)}) \quad , \tag{3.32}$$

$$8\pi p_r^{EG} - \frac{q^2}{r^4} = \frac{1}{r^2}(e^{-B(r)} - 1) + \frac{A^{'}(r)}{r}e^{-B(r)} \quad and \tag{3.33}$$

$$8\pi p_t^{EG} + \frac{q^2}{r^4} = \frac{1}{4}e^{-B(r)} + [2A^{''}(r) + A'^2 - B'(r)A'(r) + \frac{1}{r}(A'(r) - B'(r))] \quad , \tag{3.34}$$

where the quantities ρ^{EG}, p_r^{EG} and p_t^{EG} are the density, radial pressure and transverse pressure in Einstein Gravity respectively and can be written as

$$\rho^{EG} = \rho + \frac{\xi}{8\pi}(\rho - p_r - 2p_t) \quad , \tag{3.35}$$

$$p_r^{EG} = p_r + \frac{\xi}{8\pi}(\rho + 3p_r + 2p_t) \quad and \tag{3.36}$$

$$p_t^{EG} = p_t + \frac{\xi}{8\pi}(\rho + p_r + 4p_t) \quad . \tag{3.37}$$

Our main focus is to find out the solutions of the system, governed by the above equations, which entirely specify the behaviour of the interior of the X-ray binaries. ρ, p_r and p_t are the density, radial pressure and tangential pressure in modified $f(T)$ gravity respectively. The differentiation w.r.t. r is denoted by prime.

Now, employing the metric coefficients as chosen by TK ansatz, in the above field

equations, we have obtained the following sets of equations as

$$8\pi\rho^{EG} + \frac{q^2}{r^4} = \frac{3a + (a^2 + 5b)r^2 + 2abr^4 + b^2r^6}{\tau^2} \quad , \tag{3.38}$$

$$8\pi\rho^{EG} - \frac{q^2}{r^4} = -\frac{a - 2D + br^2}{\tau} \quad and \tag{3.39}$$

$$8\pi\rho^{EG} + \frac{q^2}{r^4} = \frac{1}{\tau^2}[-a + 2D + (D(a + D) - 2b)r^2 + aD^2r^4 + bD^2r^6] \quad , \tag{3.40}$$

where τ is the function of r and is given by

$$\tau = (1 + ar^2 + br^4) \quad . \tag{3.41}$$

So, according to our current model, the effective components, i.e, effective density, radial and transverse pressure of the X-ray binaries respectively in $f(T)$ modified gravity, can be written as

$$\begin{aligned}\rho =& \frac{\xi}{2}f + \frac{2\psi}{r^2}\left[(2b + aD)\left(2 + r(a + b)\right)\psi(1 + \varphi) + r(2b + D)\right]\frac{f_T}{\tau} \\ &+ \frac{1}{\tau^2}\left[\frac{2\xi^2}{r(1 + \varphi)}(bD)\left(a + D + (2b + aD)\right)\right]T'f_{TT} \\ &+ \left[\frac{\psi(1 + \varphi)}{4r^2}(a + D)\left(b - 1 + r^2D\right)\right] \quad ,\end{aligned} \tag{3.42}$$

$$\begin{aligned}p_r =& -\frac{\xi}{2}f - \left[\frac{\psi(1 + \varphi)^2}{4r^2}\left(1 - (a + D) + r^2(2b + aD)\right)\right] \\ &- \frac{2\xi^2}{r(1 + \varphi)}\left[2\left(a + b + 2D\right) + \psi\left(a + b\right)br^4\right]\frac{f_T}{\tau} \quad and\end{aligned} \tag{3.43}$$

$$
\begin{aligned}
p_t = &-\frac{\xi}{2}f + \frac{\psi}{4r^2}\left[4\{a+b+(2b+aD)r\}+4aD-2\varphi\{b+D-2a\}\right]\frac{f_T}{\tau} \\
&+\frac{\psi}{4r^2}\left[\psi(1+\varphi)r^2 - r(a+b)\{2+r(b+D)\}\right]\frac{f_T}{\tau} \\
&-\left[\frac{\xi^2}{r(1+\varphi)}\left(2e^{\frac{B}{2}}-2-r^4(b+aD)\right)\right]T'f_{TT} \\
&-\frac{1}{\tau^2}\left[\frac{\psi(1+\varphi)^2}{4r}\{2a+rb-D(2+rb)+2r^2(a+D-1)\}\right] \quad .
\end{aligned}
\tag{3.44}
$$

3.1.3.4 The Equation of State with Modified Chaplygin Gas in $f(R,T)$ Gravity under Tolman-Kuchowicz Spacetime

In this work, we have chosen the spherically symmetric metric as

$$
ds^2 = -e^{A(r)}dt^2 + e^{B(r)}dr^2 + r^2d\Omega^2 \quad , \tag{3.45}
$$

where the unknown metric functions, $A(r)$ and $B(r)$ are purely radial (r varies from 0 to ∞) and $d\Omega^2 = sin^2\theta d\phi^2 + d\theta^2$, $0 \leq \theta \leq \pi$, $0 \leq \phi \leq 2\pi$. Here, for our purpose to get a singularity free and stable compact star model, we have chosen the metric potentials according to the Tolman-Kuchowicz ansatz as

$$
e^{A(r)} = \tau(r) = 1 + ar^2 + br^4 \quad and \quad e^{B(r)} = C^2e^{Dr^2} \quad , \tag{3.46}
$$

where a, b, C and D are constants (model parameters). Again, to incorporate matter-curvature coupling effect, we have considered the $f(R,T)$ modified gravity in the form

$$
f(R,T) = f_1(R) + f_2(T) = R + 2\xi T \quad as \quad f_1(R) = R \quad and \quad f_2(T) = 2\xi T \quad , \tag{3.47}
$$

where ξ is the coupling constant (small and positive) and $\xi = 0$ can reproduce the GR field equations. The term $2\xi T$ induces a time dependent coupling between matter and curvature.

In modified gravity, the field equations along the line element, can be written as

$$8\pi\rho^{eff}+\xi(3\rho-p)=\left[\frac{B^{'}(r)}{r}e^{-B(r)}+\frac{1}{r^2}\left(1-e^{-B(r)}\right)\right] \quad , \tag{3.48}$$

$$8\pi p_r^{eff}-\xi(\rho-3p)=\left[\frac{A^{'}(r)}{r}e^{-B(r)}+\frac{1}{r^2}\left(e^{-B(r)}-1\right)\right] \quad and \tag{3.49}$$

$$8\pi p_t^{eff}-\xi(\rho-3p)=\frac{1}{4}e^{-B(r)}\left[2A''(r)+A'^2(r)-A'(r)B'(r)+\frac{2}{r}(A'(r)-B'(r))\right] \quad , \tag{3.50}$$

where prime ($'$) represents the derivative w.r.t. r. ρ^{eff}, p_r^{eff} and $8\pi p_t^{eff}$ are effective density, radial pressure and transverse pressure respectively in Einstein's gravity and can be written as

$$\rho^{eff}=\rho+\frac{\xi}{8\pi}(\rho-p_r-2p_t) \quad , \tag{3.51}$$

$$p_r^{eff}=p_r+\frac{\xi}{8\pi}(\rho+3p_r+2p_t) \quad and \tag{3.52}$$

$$p_t^{eff}=p_t+\frac{\xi}{8\pi}(\rho+p_r+4p_t) \quad . \tag{3.53}$$

Now, the modified TOV equation in modified gravity can be written as

$$-\frac{A^{'}(r)}{2}(\rho+p_r)-\frac{dp_r}{dr}+\frac{2}{r}(p_t-p_r)+\frac{\xi}{(2\xi+8\pi)}\left[\frac{d\rho}{dr}+\frac{dp_r}{dr}+2\frac{dp_t}{dr}\right]=0 \quad , \tag{3.54}$$

where $m(r)$ is the total mass enclosed within the radius r of the NS $RXJ1856.5-3754$. Here, conservation equations of Einstein's gravity can be reconstructed by putting $\xi=0$. Now, applying the metric potentials, we have obtained

$$\left[8\pi\rho^{eff}+\xi(3\rho-p)\right]\tau^2=\left[3a+(a^2+5b)r^2+2abr^4+b^2r^6\right] \quad , \tag{3.55}$$

$$\left[8\pi p_r^{eff} - \xi(\rho - 3p)\right]\tau = -(a - 2D + br^2) \quad and \tag{3.56}$$

$$\left[8\pi p_t^{eff} - \xi(\rho - 3p)\right]\tau^2 = \left[-a + 2D + (D(a+D) - 2b)r^2 + aD^2r^4 + bD^2r^6\right] \quad . \tag{3.57}$$

In this present model, we have taken the existence of MCG at the core of this star. The EoS of this fluid takes the form

$$p(r)_{MCG} = \varphi\rho - \frac{\psi}{\rho^{\zeta}} \quad , \quad 0 \leq \zeta \leq 1 \quad and \quad \varphi \neq -1 \quad , \tag{3.58}$$

where φ, ψ and ζ are free parameters and ρ is the energy density and $p(r)$ is the radial pressure.

Now, we have solved the above field equations and got the matter density and pressure in Einstein's gravity as

$$\rho^{eff} = \psi + \frac{3\varphi\left(a + D + (2b + aD)r^2 + bDr^4\right)}{16\pi\tau^2} \quad , \tag{3.59}$$

$$p_r^{eff} = -\psi + \frac{\varphi\left(a + D + (2b + aD)r^2 + bDr^4\right)}{16\pi\tau^2} \quad and \tag{3.60}$$

$$\begin{aligned} p_t^{eff} =& \psi + \frac{\varphi}{16\pi\tau^2}\left[-5a + 7D + \left(-2a^2 - 8b + aD + 2D^2\right)r^2\right] \\ &+ \frac{\varphi}{16\pi\tau^2}\left[\{3bD + 2a(-2b + D^2)\}r^4 + 2b(-b + D^2)r^6\right] \quad . \end{aligned} \tag{3.61}$$

Now, we have solved the above equations and obtained the expressions of matter density, radial pressure and transverse pressure in $f(R,T)$ modified gravity as

$$\rho = \frac{1}{3}\left[3\psi + \frac{\varphi\left(a + D + (2b + aD)r^2 + bDr^4\right)}{(\xi + 4\pi)\tau^2}\right] \quad , \tag{3.62}$$

$$p_r = \left[-\psi + \frac{\varphi\,(a + D + (2b + aD)r^2 + bDr^4)}{(\xi + 4\pi)\tau^2}\right] \quad and \tag{3.63}$$

$$\begin{aligned} p_t =& \frac{1}{2(\xi+4\pi)^2}\left[\psi(\xi+4\pi)^2 + \frac{1}{\tau}\{-D(\xi-12\pi) - 2a(\xi+4\pi) + 2(-b+D^2)\}(\xi+4\pi)r^2\right] \\ &+ \frac{\varphi}{2(\xi+4\pi)^2}\left[\frac{1}{\tau^2}[4D(\xi+4\pi) - 2b(7\xi+12\pi)r^2 + a\{2D(\xi+4\pi)r^2 - (7\xi+12\pi)\}]\right] \quad . \end{aligned} \tag{3.64}$$

Part III

FOCUSING ON THE ALTERNATIVE THEORIES OF GRAVITY: THE MODIFIED GRAVITY

"Because gravity shapes space and time, it allows space-time to be locally stable but globally unstable".

—Stephen William Hawking

CHAPTER 4

THEORY OF GENERAL RELATIVITY : A CONCISE OVERVIEW

4.1 Einstein's Theory of Gravity: An Overview on General Relativity and Accelerating Universe

4.1.1 General Relativity Theory: A Brief Proposition

In the year 1979, the unified theory of three fundamental forces (out of four) of nature (Electromagnetic force, Strong Nuclear force and Weak Nuclear force) has been established by the scientists. These all four fundamental forces are believed to be related and unite into a single force at a very high energy scale, i.e., Plank scale. But unfortunately scientists can not unify the remaining force of gravitation in the "Grand Unified Theory" [29]. The gravitational force is described as the curvature of spacetime by famous scientist Albert Einstein in his renowned "General theory of Relativity" (GR) [30]. The fundamental forces which are already mentioned, except gravity, all have their discrete quantum field and their interactions can be moderated

through elementary particles as described by the standard model of particle physics. So, at present it's a challenge to the researchers to find the quantum gravity theory to quantize the gravitational field. Till now one of the best known theories in the way of unifying all these four fundamental forces is the "String Theory" [31].

In the special theory of relativity, Einstein incorporated Newtonian gravity theory in the relativistic framework, in 1905. But in 1915, almost a decade after, he published his pioneering work, the general theory of gravity which deals with the geometrical approach of gravitational force. Gr actually treats gravity as the property of spacetime. The idea of basic differences between the local inertial frame of reference to the rotating reference frame leads to the proposition of GR, which was also motivated by the laws given by Ernest Mach on observing distant stars in the galaxy. GR is completely different from classical approaches in several cases like during the measurement of gravitational lensing, gravitational red-shift etc. of distant stars. Nowadays it's the main concern to find the quantum aspect of GR which will be self consistent. GR relates the energy-momentum of matter (present in the Universe) to the geometry of spacetime. Einstein specified this relation through a system of nonlinear partial differential equations (PDE) which are popularly known as "Einstein's Field Equations" (EFE hereafter) which is a symmetric tensor equation in 4 dimension and each tensor has ten independent components [30]. One can determine the geometry of the space-time/gravitational field by using EFE similarly to find the electromagnetic fields by applying Maxwell's electromagnetic equations. The EFE can be written in the form

$$R_{\mu\nu} - \frac{R}{2} g_{\mu\nu} + \Lambda g_{\mu\nu} = \frac{8\pi G}{c^4} T_{\mu\nu} \quad , \tag{4.1}$$

where $R_{\mu\nu}$, $g_{\mu\nu}$ and $T_{\mu\nu}$ are the Ricci curvature tensor, metric tensor and stress-energy tensor respectively. c is the speed of light in vacuum and G and Λ denote the Newton's gravitational constant and Einstein's cosmological constant respectively. Here, $R = g_{\mu\nu} R^{\mu\nu}$ is the scalar curvature. From the above equation Newton's law of gravitational force can also be recovered if the speed between the objects is very less than c along with a weak gravitational field. When $T_{\mu\nu}$ becomes zero, the field equation describes a

vacuum. The main interesting term Λ, was introduced by Einstein in 1917 to explain the static and finite Universe which was later rejected by him in 1931 when the idea of expanding Universe has came in front by the observations the redshift of distant galaxies and most physicists agreed to set it zero. But interestingly this constant has been reintroduced again in 1998 by the physicists believing it might be positive from the observational evidence of accelerating expansion of the Universe. The current standard cosmological model, the ΛCDM model (See Fig. 20) which incorporates the cosmological constant Λ again, is the simplest model to explain the present accelerated expansion of our Universe dominated by the DE ($\sim 68\%$) (See Fig. 21).

$Fig - 20$

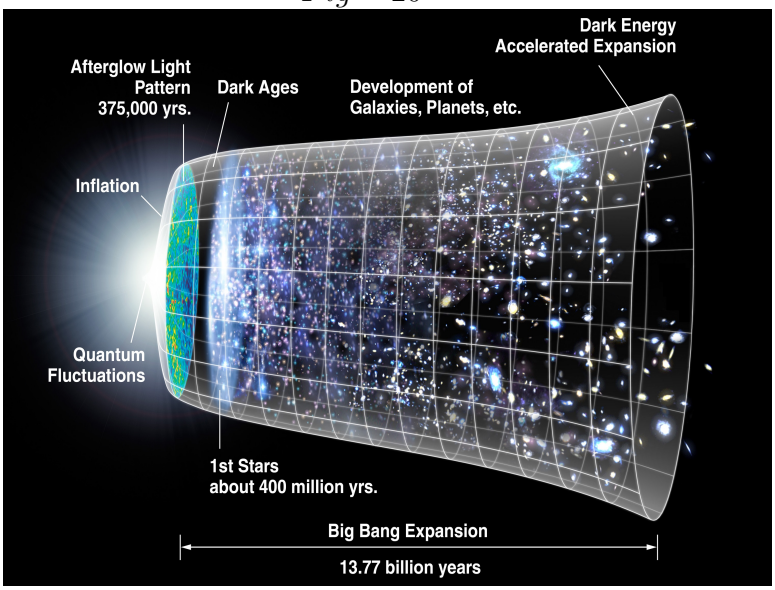

Figure 4.1: *Represents the schematic representation of the timeline of the Universe in the ΛCDM model. The last third of the timeline represents the accelerated expansion with dark energy dominated era. Figure credit: NASA/ LAMBDA Archive / WMAP Science Team.*

$Fig - 21$

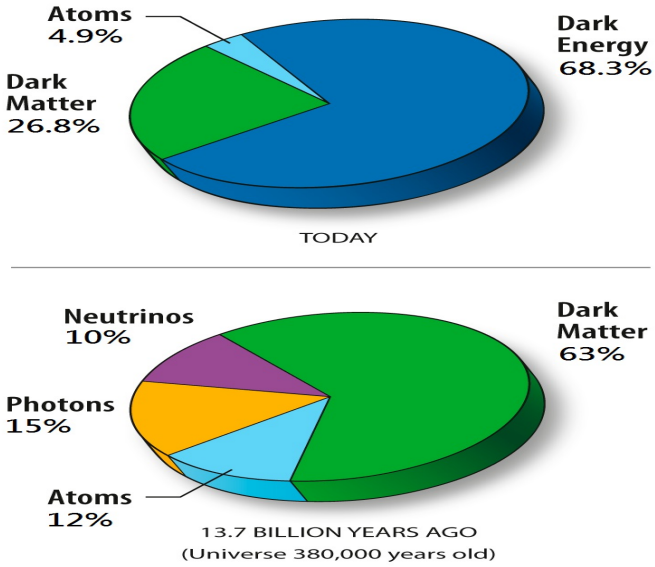

Figure 4.2: *Represents the estimated ratios of dark matter and dark energy in the Universe. Figure credit: WMAP results.*

GR has become the most essential tool for astrophysical studies in modern times. It provides the foundation of the basic understandings of black holes. GR also helps to construct the standard "Big Bang" model of cosmology and provides the foundation of the ΛCDM model of cosmology. But a few problems also arise during explanation of the accelerating expansion of the Universe using GR. One of the main contradictions with quantum field theory is known as "cosmological constant problem".

4.1.2 The Schwarzschild Spacetime: The concept of interior Schwarzschild metric for non-rotating spherical objects

Einstein's description about geometry of curved spacetime using GR has the most compulsive consequence of spacetime singularities, at intense gravity which exists at the junction between GR and quantum mechanics. Gravitational singularities are the main concern for the objects with tremendous high density (like at the core of black holes). GR predicts the formation of singularity inside any object collapsing beyond a certain point would form a BH. For the stars this is known as "Schwarzschild radius". A spacetime singularity is said to occur whenever geodesic motion of a freely falling

particle under gravity suddenly pops out of existence. On the other hand the theory of "Penrose-Hawking singularity" gives the idea of the existence of a very complicated geodesic for the infalling particles. The violation of such a geodesic is considered to be the singularity. Here comes another contradiction between GR and quantum mechanics as the later one does not permit particles to occupy a space smaller than their wavelength.

The Schwarzschild solution (Named after Karl Schwarzschild) of GR, is an exact solution of the EFEs which is the most general spherically symmetric vacuum solution [32]. The Schwarzschild BH is surrounded by the spherical boundary (event horizon) under the radius which is known as Schwarzschild radius of the BH and is given by

$$r_{Sch} = \frac{2GM}{c^2} \tag{4.2}$$

The Schwarzschild metric is given as

$$ds^2 = -(1 - \frac{2GM}{r})c^2dt + (1 - \frac{2GM}{r})^{-1}dr^2 + r^2d\theta^2 + r^2sin^2\theta d\phi^2 \quad . \tag{4.3}$$

The solution of the above equation is asymptotically flat and has two singularities, at $r = 0$ and another one is at $r = \frac{2GM}{c^2}$. The approximation of Schwarzschild solution is very useful for describing the non-rotating or slowly rotating astronomical objects like stars. The Schwarzschild solution of EFE is valid only outside the gravitational object. In order to describe the gravitational field both inside and outside the gravitating body the Schwarzschild solution must be matched with some suitable interior solution at the boundary, such as the interior Schwarzschild metric.

The exterior Schwarzschild solution at $(r > r_S)$ and the interior Schwarzschild solution at $(0 \leq r < r_S)$ with singularity at $r = 0$ are completely different approaches or separate solution. These two solutions are separated by the singularity at $r = r_S$. The Schwarzschild coordinates do not provide any physical connection between the two patches. Therefore $r = r_S$ is called "coordinate singularity". It is possible to make the Schwarzschild metric regular at $r = r_S$ by using a different coordinate system and then only the extended external solution becomes relatable with the interior solution. But

still the singularity at $r = 0$ is a different case.

In the case of an interior Schwarzschild solution at $(0 \leq r < r_S)$ with singularity at $r = 0$, the solution is applicable in the interior of a non-rotating spherical astrophysical body. The density of the fluid it consists of inside the core should be constant throughout the body and at the boundary surface the pressure should be zero. We have discussed the interior Schwarzschild metric in Chapter 8 which we have used during our research to describe the interior of an non-rotating, massive and spherical neutron star in $f(T)$ modified gravity model.

4.1.2.1 The way of avoiding Coordinate Singularity of the Schwarzschild metric

The coordinate singularity of Schwarzschild metric at $r = \frac{2GM}{r}$ can be avoided by employing a different coordinate system making the metric regular at the event horizon. In order to do so, one of the popular coordinate systems has been proposed by Kruskal and Szekeres. This new coordinate system covers the entire spacetime manifold of maximally extended Schwarzschild metric (Fig. 22). Also this coordinate system should be well behaved at the point of physical singularity. In their pioneering work, they have introduced a new time coordinate τ and new spatial coordinate χ in place of t and r in Schwarzschild metric. Now the newly formed extended Schwarzschild metric with Kruskal coordinate becomes

$$ds^2 = 32\frac{G^3M^3}{c^6 r}e^{-\frac{c^2 r}{2GM}}\left(-d\tau^2 + d\chi^2\right) + r^2(d\theta^2 + \sin^2\theta d\phi^2) \quad , \tag{4.4}$$

where τ and χ are denoted as

$$\tau = \left(\frac{r}{2GM} - 1\right)^{\frac{1}{2}} exp\left\{\frac{r}{4GM}\right\}\sinh\left(\frac{t}{4GM}\right) \quad and \tag{4.5}$$

$$\chi = \left(\frac{r}{2GM} - 1\right)^{\frac{1}{2}} exp\left\{\frac{r}{4GM}\right\}\cosh\left(\frac{t}{4GM}\right) \quad . \tag{4.6}$$

The event horizon in this new coordinate system is located at $\tau = \pm\chi$ and curvature singularity is at $\tau^2 - \chi^2 = 1$.

Fig – 22

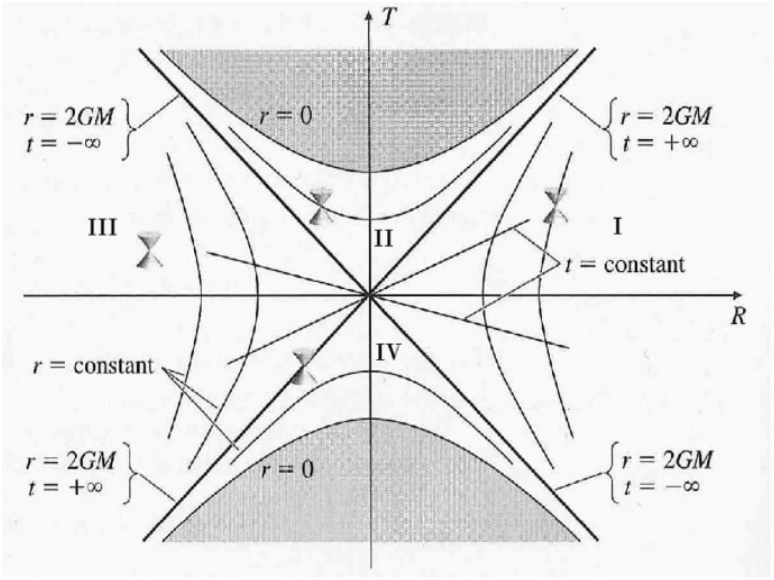

Figure 4.3: *Represents the Kruskal-Szekeres coordinates of Schwarzschild metric. Figure Credit: D. Lüst and W. Vleeshouwers,* 2019. *See text for more discussions.*

4.1.3 The concept of Black Holes: Theoretical Overview

In the year 1784, the idea of a highly massive and super dense compact object with tremendous gravitational attractive force was first proposed by English astronomer John Michell and he referred these bodies as "Dark Stars" and predicted that these non-radiative super-massive objects can only be detected through gravitational effects on nearby visible objects. At that time there was no suitable theory or evidence to prove the existence of such types of compact bodies and they also did not have any clue about how the path of light ray would be in the vicinity of these super-massive objects until the famous theory of GR is proposed by Albert Einstein. In his theory of GR he showed that the spacetime surrounding these types of objects is curved in such a way that the geodesic light travels on never leaves the surface of the star.

A black hole (BH) is a highly dense compact object which has a tremendously strong gravity and due to this gravity it curved the spacetime surrounding it in such a way that nothing including all electromagnetic waves has enough energy to escape from its gravitational pull. The GR can predict successfully the existence of it as the

deformed spacetime of a sufficient compact mass can lead to the formation of a BH. GR also gives the idea of "event horizon", the boundary of no escape surrounding the BH and according to this theory BH has not any locally detectable features. But, in contradiction, quantum field theory (QFT) predicts the radiation from the event horizon of a BH, which is popularly known as "Hawking Radiation". In 1916, K. Schwarzschild first gave the exact solution of Einstein's field equations that would characterize a BH. But, the singularity found in Schwarzschild metric at the point of Schwarzschild radius is a non-physical coordinate singularity was first showed by Sir A. Eddington in 1924 and later by G. Lemaî̂tre in 1933.

The idea of self gravitationally collapsed compact object was first established by the discovery of a rapidly rotating neutron star by Jocelyn Bell Burnell in 1967. "Cygnus X-1", a galactic X-ray source the first ever known BH (commonly accepted by the scientists) was identified by several independent researchers in 1971. At end phase of the lifecycle of the massive stars in the main sequence (See Fig. 23) are collapsed and turned into a BH of stellar mass and then it starts to grow by absorbing the mass from the surroundings. As a result of this interaction with surrounding matter, the existence of a BH can be inferred. Some super-massive BHs also can form an accretion disc surrounding them. The radio source at the center of our Milky Way galaxy is known as "Sagittarius A", and has been considered to be a super-massive BH with mass about 4.3 *million* $M_{\odot}$.

$Fig - 23$

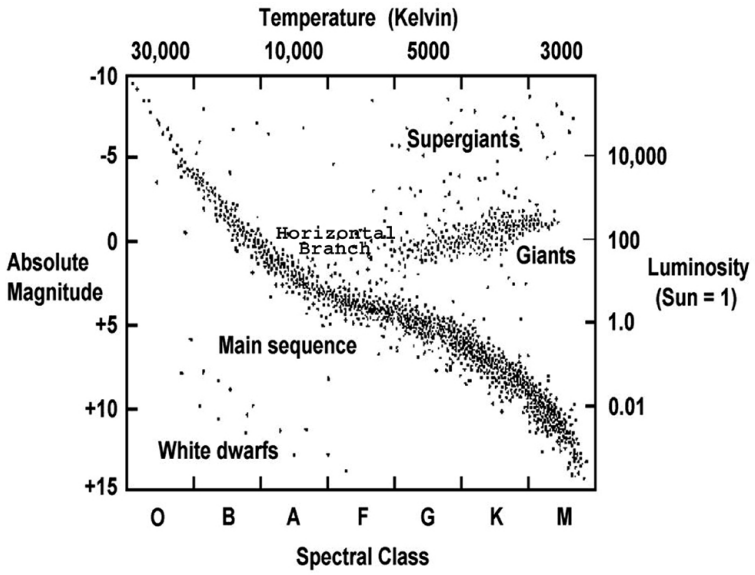

Figure 4.4: *Represents the H-R diagram of the stars. Figure Credit: CHANDRA X-ray Observatory: Educational materials (NASA).*

The discovery of pulsars established the theoretical concept of the compact stars and showed their physical relevance. After that the interest of the researchers on self gravitating collapsing astrophysical objects has increased a lot. The thermodynamic study on BHs was first formulated by Bardeen and Bekenstein along with Hawking in the early 1970s. The laws of BH thermodynamics is very crucial to describe the behavior of a BH in close analogy to the laws of thermodynamics by relating mass to energy, surface gravity to temperature. The analogy was established by the predicting effect of Hawking radiation, where using quantum cosmology Hawking showed that BHs should radiate like a black body with a temperature proportional to the surface gravity of the BH.

4.1.3.1 The Reissner-Nordström Metric

The Reissner-Nordström metric is a static solution to the Einstein-Maxwell field equations corresponding to a charged, non-rotating, spherically symmetric object. In spher-

ical coordinate system Reissner-Nordström metric is given as

$$ds^2 = -\left(1 - \frac{2m(r)}{r} + \frac{q^2}{r^2}\right) dt^2 + \frac{dr^r}{\left(1 - \frac{2m(r)}{r} + \frac{q^2}{r^2}\right)} + r^2(sin^2\theta d\phi^2 + d\theta^2) \quad , \qquad (4.7)$$

where $m(r)$ is the total mass enclosed within the boundary of the compact object with radius r at the boundary ($r = R$) and q is charged enclosed by the system.

4.1.3.2 The Tolman-Oppenheimer-Volkoff (TOV) Limit of the compact stars limiting mass

In the year 1931, S. Chandrasekhar calculated the limiting mass of an non-rotating spherical body containing electron-degenerate matter using special relativity theory and showed that above this certain limit (Chandrasekhar limit at $1.4M_\odot$) the objects is unstable [33]. It is later verified by the discovery of white dwarf and if white dwarf has a mass slightly greater than this limit, it will collapse into a more compact but stable structure as a neutron star. Again in 1939, R. Oppenheimer and his collaborators, depending on Pauli's exclusion principle, predicted about the limiting mass ($0.7M_\odot$) of a neutron star above which the neutron stars also collapsed further to form a BH [34]. But later more refined theoretical analysis has shown this analysis will be approximately 1.5 *to* 3.0 $M_\odot$, corresponding to a stellar mass of 15 *to* 20 $M_\odot$. At the same year 1996 additional work on it has given the precise limiting mass of a neutron star before collapsing into a BH is in the range of 2.2 *to* 2.9 $M_\odot$. Furthermore, the recent gravitational wave study (data from GW170817) in 2017 has refined this TOV limit in the range 2.01 *to* 2.17 $M_\odot$.

Now by solving the EFEs for a given metric, the TOV equation in GR, of any non-rotating spherically symmetric of isotropic material in gravitational equilibrium, can be written as

$$\frac{dP}{dr} = -\frac{GM\rho}{r^2}\left(1 + \frac{P}{\rho c^2}\right)\left(1 + \frac{4\pi r^3 P}{Mc^2}\right)\left(1 - \frac{2GM}{rc^2}\right)^{-1} \quad , \qquad (4.8)$$

where $\rho(r)$ and $P(r)$ are the density and pressure inside the star respectively. r denotes

the radius of the spherical object and $M(r)$ denotes the total mass within r. For a solution to the TOV equation the spherically symmetric metric becomes

$$ds^2 = -e^{A(r)}c^2dt^2 + \left(1 - \frac{2GM}{rc^2}\right)^{-1} dr^2 + r^2(d\theta^2 + \sin^2\theta d\phi^2) \quad , \tag{4.9}$$

where the metric potential $A(r)$ is given as

$$\frac{dA(r)}{dr} = -\left(\frac{2}{P + \rho c^2}\right)\frac{dP}{dr} \quad . \tag{4.10}$$

This equation fully determines the equilibrium structure of a spherically symmetric body when there is a standard EoS of the object. When the TOV equation is applied to model a bounded spherical object in vacuum, two conditions are imposed as $P(r) = 0$ and $e^{A(r)} = 1 - \frac{2GM}{c^2 r}$ at the boundary of the body and as a result the metric at the boundary becomes continuous with the vacuum solution of the EFEs, the Schwarzschild metric.

The total mass of the spherical system can be measured as

$$M_{total} = 4\pi\rho \int_0^R r^2 dr \quad , \quad \frac{dm}{dr} = 4\pi\rho r^2 \quad . \tag{4.11}$$

4.1.4 The Accelerated Expansion of the Universe

Various observational evidence (CMB, BAO etc.) has shown the accelerated phase of our Universe at present time. This actually means that the velocity of the distant galaxy at which it recedes from the observer is increasing continuously with time. It is believed that this era of the Universe started almost 5 billion years ago when the dark energy dominated era had just begun. When the EFEs have been introduced by GR theory, the reintroduction of the term cosmological constant Λ with positive value has been incorporated to encounter the effect of cosmic acceleration of the Universe by the cosmologists. This positive Λ is well considered as equivalent to the positive vacuum energy. Alternative theories also have been developed to explain the accelerated phase of the Universe by using the concept of cold dark matter along with positive Λ. This

model till now is considered to be the best standard cosmological model which is also famous as the ΛCDM model of cosmology. But this model has also faced some drawbacks as it can not properly explain the "fine tuning" problem and "cosmological coincidence" problem in cosmology.

In later time when the "Big-Bang" has been introduced by S. Hawking to explain the origin and phase evolution of the Universe, it shows the agreement with the CMB observations in 1965 [35] and supports the accelerated expansion of the Universe and become wide acceptable model. The expansion of the Universe by its confined energy can be defined by using Friedmann equation which is given as

$$H^2 = (\frac{\dot{a}}{a})^2 = \frac{8}{3}\pi G\rho - \frac{\kappa c^2}{a^2} \quad , \tag{4.12}$$

where κ denotes the curvature of the Universe with total energy density ρ and $a(t)$ is the scale factor. The Hubble parameter H in terms of critical density ρ_c of the Universe can be written as

$$H(a) = \sqrt{\frac{8}{3}\pi G\rho_c} \quad , \tag{4.13}$$

where the density parameter took the form

$$\Omega = \frac{\rho}{\rho_c} \quad . \tag{4.14}$$

4.1.4.1 The Dark Energy Domination Era of the Universe

It is hypothesized that the total energy density of our present Universe is due to the contribution of curvature (κ), matter (m), radiation (r) and the dark energy (DE). As the scale factor increases, the contribution of each term decreases except DE. So, in terms of each density parameter of these four different energy contributors, the Hubble parameter can be written as

$$H(a) = \sqrt{\Omega_\kappa a^{-2} + \Omega_m a^{-3} + \Omega_r a^{-4} + \Omega_{DE} a^{-3(1+\omega)}} \quad . \tag{4.15}$$

These various density parameters are very important to calculate the acceleration of the Universe. The evolution of the scale factor can be written as

$$\frac{\ddot{a}}{a} = -\frac{4}{3}\pi G\left(\rho + \frac{3P}{c^2}\right) \quad , \tag{4.16}$$

where the pressure P of the Universe depends on the chosen cosmological model.

Again, we also have

$$H(t) = \frac{\dot{a}(t)}{a(t)} \quad and \quad \frac{dH}{dt} = -H^2(1+q) \quad , \tag{4.17}$$

where q is the deceleration parameter which becomes negative w.r.t. the current astronomical observations and $\ddot{a}(t)$ becomes positive. It shows that ultimate $\frac{dH}{dt}$ is negative. This clearly indicates the fate of our Universe, as predicted by the scientists and its the "Big Rip". We have discussed about it according to our research based on a newly proposed cosmological model in $f(R,T)$ modified gravity in the Chapter 12.

The cosmic microwave background anisotropy gave the clear indication of the accelerated Universe. Now, there should be a theoretical explanation of those observations. This theoretical explanation can be done by two different approaches. First, one can introduce a new kind of gravity theory like $f(R)$, $f(T)$ or $f(R,T)$ theories of gravity where the extra higher order terms in the modified Friedman equations and also modified TOV equations are responsible for the accelerated Universe. The second way is to introduce some exotic matter with large negative pressure, known as DE. In order to justify the late time accelerated universe, one can choose any one of the above approaches as either taking into account dynamical dark energy in the context of standard GR or modified gravity theory without adding any exotic fluid which violates the strong energy condition as $\rho + 3P > 0$ for this kind of exotic matter.

We are in the era of dark energy dominated Universe at present situation. The WMAP probe experiment indicates the existence of DE about 68 percent at present Universe [36]. Till now cosmologists strongly believed that this DE is solely responsible for the accelerated expansion of the Universe. But the exact nature and behavior of DE is still unknown. Above all this DE behaves mysteriously in vacuum. There are many

models that have been developed in order to interpret the DE component. Amongst them are vacuum energy models [109], [38] and quintessence models [39], [40] have become very popular. But all these models cannot successfully explain the mysteries related to the "fine tuning problem" and "cosmic coincidence problem". Now in recent time research, Chaplygin gas and some of its modified versions are gaining attraction to construct various effective cosmological models [42], [43].

4.1.5 Tension in the Hubble parameter: The Propositionl of existence of Dark Matter

Two very strong evidences have been collected supporting the accelerated expansion of the Universe by the observations of high redshift of type Ia supernova [41] and visual absolute magnitude measurement of type Ia supernova at extreme luminosity [44]. Also the observations of CMB, large scale structure of the cosmos and even gravitational lensing supported the accelerating Universe. From the apparent magnitude observations we can calculate the cosmological distances and also the recession velocities of the galaxies. The relation between redshift (z) and the Hubble parameter (H) is given as

$$H(z) = -\frac{1}{1+z}\frac{dz}{dt} \quad , \tag{4.18}$$

One of the major problems in cosmology is to estimate the value of the Hubble parameter precisely. But the tension arising in the Hubble parameter because various methods applied to determine its value yield different values depending on the way of measurement. It is not possible according to the current understanding of the Universe using known physical laws. However, in the end, the Hubble parameter must be a single number. So, our universe is expanding. It is well accepted by all but scientists do not agree with the rate of expansion of the Universe. So, in this scenario, "Hubble Tension" may be the first significant indication that cosmologists may have overlooked something in the theory of origin and evolution of the Universe. Though another possibility may also have this disagreement of the value of H as may be due to some error in one or both of the estimation processes.

However, one very effective and straightforward way to determine the value of the Hubble constant is by measuring the distance of the galaxies and simultaneously measuring their recessional velocities. In this method we can get the velocity of the galaxies as a function of distance. Applying this method the value of H is estimated as $73 \pm 1\ km\ s^{-1}\ Mpc^{-1}$. The other way of measuring the value of H is by applying the method of CMB anisotropy measurement. The second method gives the precise value of H as $67.5 \pm 0.5\ km\ s^{-1}\ Mpc^{-1}$. The first one is known as "Late Time " measurement whereas the second one is denoted as "Early time" measurement. This disagreement has created a lot of excitement amongst the cosmologists as the cosmological evolution theories need to be rethought and which may lead to new discoveries.

Throughout the last two decades, it was a challenge to build a proper theoretical cosmological model which sustains observations. The presence of exotic matter (DE or quintessence or phantom energy) which is distributed homogeneously in all over the Universe is considered to explain the accelerated Universe in various models but still a best fit model is not achieved by the cosmologists. On the other hand exact EoS of these types of exotic matters are also not known precisely. The standard ΛCDM model uses an ad hoc assumption to construct it as $P + \rho = 0$ as a small change in volume dV produces $-PdV$ amount of change in energy in case of vacuum. This kind of energy is similar to the "Casimir effect" where a small suction is present where there is the formation of the virtual particles. The hidden mass problem evolved from the observations of galactic rotational curve and which can be solved by incorporating the imaginary exotic matter, popularly known as "Dark Matter" (DM)[45], [46]. The presence of DM is believed to be present at the edges(outer region) of a galaxy which causes the higher angular momentum [47].

4.1.6 Dark energy in the background of FLRW spacetime

There are various forms of DE within GR which can be used as dynamical alternatives to ΛCDM model in an attempt to solve the coincidence problem but none of the alternatives can give an idea of solving the problem related with vacuum energy. In dynamical DE models have replaced the constant $\frac{\Lambda}{8\pi G}$ by the newly proposed evolving

energy density of a DE component and the EoS is constrained by $\omega = -\frac{1}{3}$.

Again, if Λ is considered as the vacuum energy, the value of cosmological energy density becomes very small and we will get a highly fine tuned value of vacuum energy. Surprisingly, the String theory provides a tantalizing possibility of various small regions with particular small vacuum energy which exists inside the Universe. This leads to a multitude of regions that form in some sense a "multiverse", a highly speculative idea.

4.1.6.1 The Quintessence

It is possible to avoid the problems of phenomenological fluid models by constraining the effective fluid speed to unity. A scalar field ϕ with a Lagrangian becomes effective in this case. For any potential $V(\phi)$ the effective sound speed depends on V. This shows that the scalar field is non-adiabatic. The governing equations in this model can be written as

$$\rho_\phi = \frac{\dot{\phi}^2}{2} + V(\phi) \quad , \tag{4.19}$$

$$p_\phi = \frac{\dot{\phi}^2}{2} - V(\phi) \quad . \tag{4.20}$$

Now the evolution of energy conservation equation becomes

$$\ddot{\phi} + 3H\dot{\phi} + V'(\phi) = 0 \quad and \tag{4.21}$$

$$H^2 + \frac{K}{a^2} = \frac{8\pi G}{3}(\rho_r + \rho_m + \rho_\phi) \quad . \tag{4.22}$$

As already mentioned this model opens up the possibility to solve the cosmological coincidence problem but does not evade the cosmological fine tuning problem. The quintessence potential remains arbitrary unless fundamental physics selects the potential. This quintessence model gives a viable possibility and computations are straightforward. The only possibility of this model that may in future the developments of particle physics do select a candidate potential.

4.1.7 The Chaplygin Gas model: A Unique Approach towards Unification of DE and DM

On the other hand, phenomenological fluid models of DE are not so efficient. Adiabatic fluid models becomes unstable to perturbations and the adiabatic sound speed becomes imaginary for negative ω as

$$c_s^2 = \frac{\dot{P}}{\dot{\rho}} = \omega - \frac{\dot{\omega}}{3H(1+\omega)} \quad . \tag{4.23}$$

For a constant ω model, the effective sound speed must be not equal to the adiabatic speed of sound ($c^2_{s,\ eff} \neq c_s^2$), i.e., dark energy model must be non-adiabatic. Otherwise the model becomes physically unviable ($c_s^2 < 0$). The effective speed, which governs the growth of inhomogeneities in fluid, must be positive and usually sets to 1 ($c^2_{s,\ eff} = 1$).

But it is possible to avoid this constraint in an adiabatic fluid ($c^2_{s,\ eff} = c_s^2$) if $\dot{\omega}$ is sufficiently negative. This property of ω is used by the "Chaplygin gas" fluid model whose EoS is $p = -\frac{A}{\rho^\alpha}$, where A and α are constants, $0 < \alpha \leq 1$. This model provides real adiabatic sound speed.

The Chaplygin gas (CG) model is proposed recently as the candidate of unified DM and DE scenario, in which matter is considered to be a perfect fluid obeying an exotic EoS. The most significant feature of this model is that it acts as dust (pressure less fluid) like matter at an early stage and as the cosmological constant at later stages (for large values of the scale factor) which tend to accelerate the Universe. In case of simplest application the EoS of CG is taken in the form

$$p = -\frac{\beta}{\rho} \quad , \tag{4.24}$$

where β is a positive constant. This gas (CG) with the same EoS can admit a super symmetric generalization [48] and this specific property of the EoS invokes interest in String theory as well. CG is also applied successfully in Born-Infeld model whose Lagrangian becomes

$$L_{BI} = -\sqrt{B}\sqrt{1 - g^{\mu\nu}\phi_{,\mu}\phi_{,\nu}} \quad . \tag{4.25}$$

Later this EoS of CG is also modified and it took a more generalized form as generalized Chaplygin gas (GCG) and this new model is first introduces in the year 2002 [49], [50] with the EoS as

$$p = -\frac{\beta}{\rho^n} \quad , \quad 0 \leq n \leq 1 \quad . \tag{4.26}$$

Amendola in 2003 has found that the latest dada on CMB anisotropy favored the GCG model as a candidate mixture of DE and DM [51]. On the other hand the dual role GCG (as dust like matter and cosmological constant) model has been confronted quite successfully with various observations and tests like CMB peak location, $SN\ Ia$ data, gravitational lensing etc.

Another very interesting and fruitful cosmological model has been proposed by incorporating the concept of modified chaplygin gas (MCG) [52] which follows the EoS as

$$p = \alpha\rho - \frac{\beta}{\rho^n} \quad , \alpha > 0 \quad and \quad 0 \leq n \leq 1 \quad . \tag{4.27}$$

The MCG model shows the radiation dominated era with $\alpha = \frac{1}{3}$ and also the accelerated expansion era of later stage. The extended MCG model (EMCG), also has been proposed in the year 2014 [53], which have the EoS as

$$p = \sum_{1}^{r} \alpha_i \rho^i - \frac{\beta}{\rho^n} \quad , 0 < n < 1 \quad . \tag{4.28}$$

From the above EMCG EoS, the EoS of MCG can be recovered by setting $r = 1$ and also the EoS of the higher order barotropic fluid can be recovered by putting $r = 2$.

4.1.7.1 The Interacting Quintessence

One of the unified DE and DM models is the interacting quintessence model. In this approach, the quintessence and the cold DM interact with each other but not with baryonic matter or photons. This model does not violate the current constraints from the fifth force experiment as it does not interact with baryonic matter. It could lead to a new way to solve the "coincidence problem" through the coupling between DE

and DM and can explain the acceleration when $\rho_m \sim \rho_{DE}$. During the coupling, the energy conservation equations can be written as

$$\dot{\phi}\left[\ddot{\phi} + 3H\dot{\phi} + V'(\phi)\right] = Q \quad and \tag{4.29}$$

$$\dot{\rho_{dm}} + 3H\rho_{dm} = -Q \quad , \tag{4.30}$$

where rate of energy exchange due to interaction. For a given model of Q, it is possible to choice the suitable parameters to make the model consistent with the recent observational data (SNIa, BAO) on accelerating Universe.

4.1.8 The Detection of Gravitational Wave

The direct detection of gravitational waves (GW), has proved that Einstein's theoretical postulation of its existence as a consequence of GR, is absolutely correct, after a century about its prediction in 1916. On 11^{th} February 2016, the scientific collaboration of LIGO and VIRGO has declared publicly the discovery of GW signal, detected by two detectors of LIGO simultaneously [54]. This signal is named $GW150914$.

Albert Einstein described these GW as ripples in spacetime which results from his GR theory. These waves are actually the intensity of gravity that are generated by accelerated motion of gravitational masses and spread outward from the origin at the speed of light. These waves also transport energy in the form of gravitational radiation. First observational evidence of its existence was done by Hulse and Taylor by discovery of orbital decay of a system of two binary pulsars. The orbital decay is matched with the decay predicted by GR as energy lost to gravitational radiation.

In gravitational wave astronomy, the observations of GW signals give information (data) about its source such as binary star systems composed of neutron stars, white dwarfs and black holes. So, by studying GW we can infer a lot of information on those massive relativistic objects. Various detected gravitational wave spectrum with sources and detectors is shown in the Fig. 24.

Fig – 24

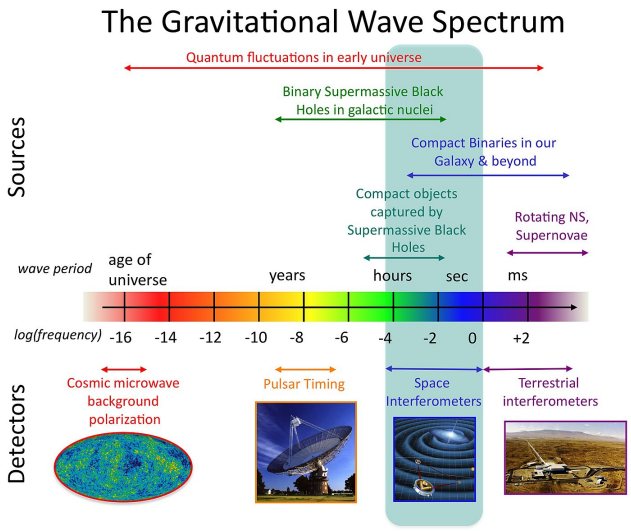

Figure 4.5: *Represents the gravitational wave spectrum with sources and detectors. Figure Credit: Goddard space flight Center (NASA).*

"Everything likes to live where it will age the most slowly, and gravity pulls it there".

—-Kip Stephen Thorne

CHAPTER 5

INTRODUCTION TO MODIFIED GRAVITY THEORIES

5.1 Teleparallel Equivalent of General Relativity: Scope of the Modified Gravity Theories

5.1.1 Theory of Modified gravity: A Brief Proposition

The progression of GR has experienced outstanding success over the decades as the underlying theory of gravity. However, the establishment of quantum mechanics in the 1920s and then quantum field theory has started to expose some of the limitations of GR. Moreover, several limitations from various astronomical observations have also focused attention on various shortcomings of GR. The Failure of GR theory not only occurs on very small scale of the physical spectrum but also on larger scales such as for galactic systems. In large scales, modifications of the standard model of particle physics [55, 56], are essential to sustain GR. This has driven us to the concept of DM that plays a crucial role in galaxies and their clusters [57, 58]. DM has shown great

impact not only in the astrophysical context but also has an important role in the cosmological context in the dynamics of the early Universe [59]. The best macroscopic version of DM is popularly known as cold dark matter (CDM). Additional corrections on the matter sector of GR are also needed to consider the very early Universe where a rapid period of inflation is enforced to explain the extremely flat and homogeneous Universe we observe at present [60]. On the other hand, modifications to the gravity sector may also explain the features of galactic rotation curves such as in the case of Starobinsky gravity [61] and conformal Weyl gravity [62]. Similarly, the accelerated expansion of the Universe [63] also requires a cosmological constant Λ [64] to adequately describe the observed expansion using GR.

So, GR can thus explain almost all phenomena provided sufficient and suitable modifications are considered in the matter sector so that we consider the widely accepted concordance model in ΛCDM plus inflation cosmology. However, the exotic nature of these particle species remains a total mystery in terms of observations despite significant theoretical advances in physics beyond the standard model of particle physics. In the same vein, it may also be the case that the standard model of particle physics does not require a significant restructuring for meeting these observational challenges and it is that the gravitational section needs further revisiting. This may take the form of extensions from GR or even modifications beyond GR that may be an alternative to its original formulation. There have been numerous proposals for new theories of gravity [65, 66] which are motivated either through phenomena or some theoretical approach, as well as for other reasons such as from quantum physics. One interesting possibility that has been gaining momentum in the literature in recent decades is that of teleparallel gravity (TG) where curvature is replaced by torsion as the mechanism by which geometric deformation produces a gravitational field. It does this by dislodging the uniquely curvature-based Levi-Civita connection with a torsion-based teleparallel connection. In fact, there are now thousands of publications related to the topic in the literature. One of the many theories that torsion-based approaches to gravity has produced is the teleparallel equivalent of general relativity (TEGR) which is dynamically equivalent to GR, meaning that they cannot be distinguished through classical

experiments.

The underlying geometry of GR is first revisited in the reference [67] and the foundational ideas behind various concepts in teleparallel gravity (TG) are put on a concrete mathematical basis. While another work [68] where the physics on which TEGR is fully fleshed out together with potential future work on quantum gravity and quantum field theory. These works again resurrect Einsteins original goal of reconciling gravity with other branches of physics [69]. TEGR continues to be studied for potential benefits as compared with GR such as in its quantum regime, and others. On the other hand, TG has since undergone a renaissance with respect to (wrt) potential modified theories of gravity. The first such modification was presented by Hayashi and Shirafuji [70] where GR was slightly modified to allow for small deviations from TEGR through a decomposition of its Lagrangian. However, the most impact suggested modification came from Ferraro and Fiorini [71] where a form of $f(T)$ gravity first appeared in the literature, and later by Linder [72]. The foundations of TG and its particular application to TEGR, $f(T)$ and some other teleparallel theories was explored in [73]. This work built on foundational work represented in the book in [67] and covered important advances on the issue of covariance in TG [74], among other topics. Another very important work is [75] where foundational aspects, such as the Poincaré gauge gravity origins of the theory, are explored but also many applications, both astrophysical and cosmology. These are very important works in the community but the literature has since drastically evolved with even more clarity on the covariant formulation of TG and its relationship to metric-affine theories being more laid out.

5.1.2 The $f(T)$ Modified Gravity: Basic Ideas and Overview

Over the last few decades, the role of torsion and its effect in gravity has been widely researched. This leads to bring gravity closer to its gauge formulation and helps to incorporate spin in a geometric illustration. In various torsional constructions, from teleparallel gravity to Einstein-Cartan, and metric-affine gauge theories, concept torsional gravity has been widely incorporated. In the paradigm the $f(T)$ gravity, where $f(T)$ is chosen as an arbitrary function of the torsion scalar T becomes very successful

in this field. Based on $f(T)$ gravity theory, various important corresponding cosmological and astrophysical applications are also there in the literature. Particularly, the search of cosmological solutions which arises from $f(T)$ gravity in different eras (both at the background and perturbation levels) along the cosmic expansion are attracting the focus of the researchers in recent times. The main advantage of this $f(T)$ gravity theory is that the equations in $f(T)$ gravity during its construction can provide a theoretical interpretation of the late-time accelerated phase of the Universe. This is an alternative way to study the cosmological constant and it can easily accommodate the regular thermal expanding history including the radiation and cold dark matter (CDM) dominated phases as well. On the other hand, if one want to trace back the very early times of our Universe then for a particular class of $f(T)$ models, a sufficiently long period of inflation can be achieved and hence can be investigated by cosmic microwave background (CMB) observations. Alternatively the Big Bang singularity can be avoided at even earlier moments due to the appearance of non-singular bounces in $f(T)$ gravity theory.

Actually GR is based on the assumption that space and time constitute a single structure assigned on Riemann's manifolds. These manifolds are the dynamical structures that reproduce the Minkowski space-time in absence of gravity. In this sense, gravity is conceived as the curvature of space-time. Any type of relativistic theory of gravity, including GR, has to match some requirements to be self-consistent. First of all, it has to reproduce the Newtonian theory in the weak-field limit, hence it has to explain the dynamics related to planets and the galactic self-gravitating structures. Further, it has to overcome various observational tests in the Solar System [76]. Moreover, by the application of any new relativistic theory of gravity to construct a self-consistent model at cosmological scales, it should reproduce the cosmological parameters such as the expansion rate, the density parameter etc. to become successful theory.

According to the various assumptions on which GR is based on, Einstein postulated that the gravitational field can also be described in terms of the metric tensor field $ds^2 = g_{\mu\nu}dx^\mu dx^\nu$, with the same signature of Minkowski metric in four dimensions. Here, the line element ds^2 is the covariant scalar related to the space-time measurements. Besides

the metric coefficients are the gravitational potentials and the spacetime is curved by the distribution of matter-energy sources according to the former Riemann's intuition. In other words, the shape of space-time is due to the distribution of mass of the astronomical bodies in space. However, GR has faced some shortcomings at ultraviolet and infrared scales. From the theoretical point of view, the shortcomings that GR is actually facing, the non-renormalizability, the presence of singularities etc. Also we don't have a self-consistent theory of quantum gravity at present. From the recent observational and experimental points of view, GR is no longer capable of explaining the galactic or extra-galactic and cosmic dynamics, unless exotic forms of matter-energy (interacting only at gravitational level) are considered. These elusive components are addressed as DM and DE and constitute up to the 95% of the total cosmological bulk of matter-energy [77].

5.1.2.1 The Concept and Importance of Torsional Field in Cosmology

One of the alternative theories of GR shows us that instead of changing the source side of the EFEs, one can search for a geometrical point of view to accommodate the missing matter-energy of the observed Universe. In order to do so, the dark sector could be addressed by incorporating further geometric invariants into the standard Hilbert-Einstein Action of GR. The effective Lagrangian of this new approach can be derived by any quantization scheme on curved space-times [66]. Torsion can be included in literature in various different forms. Generally, spin is considered to be the source of torsion. But there are several other possibilities in which torsion emerges in different contexts. In some cases a phenomenological counterpart is absent whereas in some other cases torsion arises from sources without spin as a gradient of a scalar field. Moreover, one can construct torsion tensors from the product of covariant bi-vectors and vectors, and their respective spacetime properties.

The modification of GR with torsion is strongly felt today, since several questions strictly depend on whether the spacetime connection is symmetric or not. GR is essentially a classical approach which does not consider quantum effects. However, for any theory acting at a fundamental level with gravity, these effects must be considered

strictly. In a four dimensional space-time where the torsion tensors have some peculiar properties is the first simple and straightforward generalization which tries to include the spin fields of matter into the same geometrical scheme of GR. Besides, several people think that torsion could have played some specific role in the dynamics of the early Universe and it could have yielded macroscopically observable effects today. In fact, the presence of torsion naturally gives repulsive contributions to the energy-momentum tensor so that cosmological models become singularity-free [78, 79, 80, 81]. This feature essentially depends on spin alignments of primordial particles which can be considered as the source of torsion. Again, if our Universe undergoes one or several phase transitions, there is the possibility that torsion could give rise to topological defects (e.g. torsion walls) [82, 83, 84] which today can act as intrinsic angular momenta for cosmic structures as galaxies. Furthermore, the existence of torsion in an effective energy-momentum tensor alters the spectrum of cosmological perturbations giving characteristic lengths for large-scale structures as shown in the reference [85].

Another way of classifying the torsional tensor follows the decomposition, at one point of a U_4 space-time, of the torsion tensors into three irreducible tensors w.r.t. to the Lorentz group. Moreover, one can use vectors and bi-vectors to identify their geometrical properties. It follows that the elements of the second classification are generally expressed as a "combination of elementary torsion tensors", while the "elementary torsion tensors" are generally non-irreducible. So, beside Riemannian 4-dimensional manifolds, U_4 manifolds is the first straightforward generalization which tries to include the spin fields of matter into the same geometrical scheme of GR. The paradigm is that the mass-energy is the source of curvature while the spin is the source of torsion. The Einstein-Cartan-Sciama-Kibble (ECSK) theory is one of the most serious attempts in this direction [86].

So, from above discussions the importance of torsion in any comprehensive theory of gravity that takes into account the non-gravitational counterpart of the fundamental interactions is quite clear. However, various articles have used torsion in different forms. Generally the torsion is connected to the spin density of matter but in many

examples are there where it cannot be derived from the spin matter and acquires interpretations quite different from the models with spinning fluids and particles. There are many independent torsion tensors with different properties. Torsion tensors can be constructed as the tensor product of a simple covariant bi-vector and a contravariant vector. Such objects are well understood in GR and they can be easily classified in the reference [87]. We can identify these tensors separately by calling these tensors as elementary torsion. So, torsional theories may be relevant in cosmology because of the kinematical quantities such as shear, vorticity, acceleration, expansion and their evolution equations, are modified by the presence of torsion.

5.1.2.2 Mathematical Formulation of Covariant $f(T)$ Gravity

As the spacetime manifold M be a parallelizable metric space, it is generally easy to find a trivialization $e_a = e_a^\mu \partial_\mu$ of the tangent bundle of the manifold. The dual vector basis 1-form to e_a, i.e., the tetrad is given by $h^a = h_\mu^a dx^\mu$, so that $h^a(e_b) = \delta_b^a$. We have chosen the basic teleparallel theory of gravity using torsional scalar quantity T as $f(T)$ with the tetrad formalism concept. There is nonzero torsion with no curvature in the background spacetime, which relates gravitation with tetrad and torsion. The general form of spacetime metric is taken as

$$ds^2 = g_{\mu\nu} dx^\mu dx^\nu \quad . \tag{5.1}$$

In tetrad formalism after matrix transformation to a Minkowskian, it becomes

$$ds^2 = \eta_{ij} \theta^i \theta^j \quad , \tag{5.2}$$

where η is the tangent space metric and

$$dx^\mu = e_i^\mu \theta^i \quad , \quad \theta^i = e_\mu^i dx^\mu \quad and \tag{5.3}$$

$$\eta_{ij} = diag[-1, 1, 1, 1], \quad e_i^\mu e_i^\nu = \delta_\nu^\mu \quad . \tag{5.4}$$

The given root of the metric determinant is in the form

$$\sqrt{-g} = det[e^i_\mu] = e \quad . \tag{5.5}$$

The non-vanishing Christoffel symbols are,

$$\Gamma^\alpha_{\mu\nu} = e^\alpha_i \partial_\nu e^i_\mu = -e^i_\mu \partial_\nu e^\alpha_i \quad . \tag{5.6}$$

The torsion tensor and con-torsion tensor can be written as

$$T^\alpha_{\mu\nu} = e^\alpha_i (\partial_\mu e^i_\nu - \partial_\nu e^i_\mu) \quad and \tag{5.7}$$

$$K^{\mu\nu}_\alpha = -\frac{1}{2}(T^{\mu\nu}_\alpha - T^{\nu\mu}_\alpha - T^{\mu\nu}_\alpha) \quad . \tag{5.8}$$

The super potential $S^{\mu\nu}_\alpha$ took the form

$$S^{\mu\nu}_\alpha = \frac{1}{2}(K^{\mu\nu}_\alpha + \partial^\mu_\alpha T^{\beta\nu}_\beta - \partial^\nu_\alpha T^{\beta\mu}_\beta) \quad . \tag{5.9}$$

The torsion scalar in terms of contraction of tensors becomes,

$$T = T^\alpha_{\mu\nu} S^{\mu\nu}_\alpha \quad . \tag{5.10}$$

Now TEGR takes T as its Lagrangian and the modified $f(T)$ considers an arbitrary function of T instead, i.e.,

$$S[e^i_\mu, \Phi_A] = -\frac{1}{2}\int d^4x \left[\sqrt{-g} f(T) + \sqrt{-g} L_M(\Phi_A)\right] \quad , \tag{5.11}$$

where $G = c = 1$, $L_M(\Phi_A)$ is the matter Lagrangian and $\sqrt{-g}$ is the determinant of the tetrad h^a_α. Further the variation of the above equation w.r.t. the tetrad gives the field equations as

$$\frac{2}{\sqrt{-g}}\partial_\mu \left(\sqrt{-g} S^{\alpha\mu}_\sigma e^\sigma_a f_T\right) + \frac{e^\alpha_a}{2} f = T^\alpha_\mu e^\mu_a \quad , \tag{5.12}$$

where f_T denotes $\frac{df}{dT}$ and the energy-momentum tensor T^{α}_{μ} of matter is given by

$$\frac{\delta(\sqrt{-g}L_M)}{\delta h^a_\alpha} = \sqrt{-g}T^{\alpha}_{\mu}e^{\mu}_{a} \quad . \tag{5.13}$$

We considered in our work [88] that the compact stars contain both the quintessence fields and electromagnetic field. So, Einstein equation can be taken as

$$G_{\mu\nu} = 8\pi G\left(T^{M}_{\mu\nu} + T^{q}_{\mu\nu} + T^{EM}_{\mu\nu}\right) \quad , \tag{5.14}$$

where the terms have their usual meanings. The ordinary matter energy-momentum tensor corresponding to anisotropic fluid along with anisotropic pressure becomes,

$$T^{M}_{\mu\nu} = (\rho + p_t)u_\mu u^\nu - p_t g_{\mu\nu} + (p_r - p_t)v_\mu v^\nu \quad , \tag{5.15}$$

where, u^μ is the four-velocity, v^μ is the radial four-vector and they are satisfying $u_\mu u^\nu = 1$, $v_\mu v^\nu = -1$ and $u_\mu v^\mu = 0$. Here ρ is the energy density, p_r is the radial pressure and p_t is the transverse pressure and $T^{q}_{\mu\nu}$ is the energy momentum tensor which consists of ρ_q the quintessential field energy density and state parameter ω_q $(-1 < \omega_q < -\frac{1}{3})$. The components of this tensor, require to satisfy additivity and linearity, which are given as

$$T^t_t = T^r_r = -\rho_q \quad and \quad T^\theta_\theta = T^\phi_\phi = \frac{1}{2}(3\omega_q + 1)\rho_q \quad . \tag{5.16}$$

Further, the energy-momentum tensor which represents the electromagnetic field can be written as

$$E^{EM}_{\mu\nu} = \frac{1}{4\pi}\left(g^{\delta\omega}F_{\mu\delta}F_{\omega\nu} - \frac{1}{4}g_{\mu\nu}F_{\delta\omega}F^{\mu\delta}\right) \quad , \tag{5.17}$$

where, $F_{\mu\nu}$ is Maxwell field tensor and Φ_μ is the four potential. The Maxwell's corresponding electromagnetic field equations are,

$$(\sqrt{-g}F^{\mu\nu})_{,\nu} = 4\pi J^\mu\sqrt{-g}, F_{[\mu\nu,\delta]} = 0 \quad , \tag{5.18}$$

where J^μ is the four-vector of current, satisfying all the conditions related to charge density parameter σ as, $J^\mu = \sigma u^\mu$.

In this present model we have chosen the modified $f(T)$ gravity in a simple linear form as

$$f(T) = \beta T + \beta_1 \quad , \tag{5.19}$$

where β and β_1 are integrating constants and to simplify the equation we took $\beta_1 = 0$.

We also have chosen exotic matter EoS as,

$$p_r = \frac{1}{3}(\rho - 4B_g) \quad , \tag{5.20}$$

where B_g is the Bag constant. It is a generalised approach to use the MIT bag model as it is the simplest EoS to investigate the equilibrium and stable structure of a NS. We have considered the energy density and radial pressure of the chosen anisotropic fluid in this model is connected through the relation

$$\rho = 3p_r + 4B_g \quad . \tag{5.21}$$

We have assumed the metric in spherically symmetric form to find out the interior spacetime solution (KB metric) is in the form

$$ds^2 = -e^{a(r)}dt^2 + e^{b(r)}dr^2 + r^2\left(d\theta^2 + \sin^2\theta d\phi^2\right) \quad , \quad 0 \leq \theta \leq \pi \quad , \quad 0 \leq \phi \leq 2\pi \quad , \tag{5.22}$$

where the unknown metric functions, $a(r)$ and $b(r)$ are purely radial (r varies from 0 to ∞).

Under Lorentz transformation, the above line element remains invariant and the tetrad matrix takes the form

$$[e^i_\mu] = diag\left[e^{\frac{a(r)}{2}}, e^{\frac{b(r)}{2}}, r, r\sin(\theta)\right] \quad . \tag{5.23}$$

As described by the KB metric(1975), in which the metric parameters becomes

$$a(r) = Br^2 + C \quad , \quad b(r) = Ar^2 \quad , \tag{5.24}$$

where A, B and C are the arbitrary constants, values of which can be determined by imposing physical conditions.

Now taking($G = c = 1$) the Einstein-Maxwell equations can be written as,

$$T(r) = \frac{2e^{-b}}{r}\left(a' + \frac{1}{r}\right) \quad and \tag{5.25}$$

$$T'(r) = \frac{2e^{-b}}{r}\left\{a'' + \frac{1}{r^2} - T\left(b' + \frac{1}{r}\right)\right\} \quad , \tag{5.26}$$

where, prime denotes the differentiation w.r.t. the radial coordinate r.

Therefore the Field equations corresponding to the exotic fluid (quintessence) in modified $f(T)$ gravity becomes

$$4\pi\rho + E^2 = \frac{f}{4} - \left\{T - \frac{1}{r^2} - \frac{e^{-b}}{r}(a' + b')\right\}\frac{f_T}{2} \quad , \tag{5.27}$$

$$4\pi p_r - E^2 = \left(T - \frac{1}{r^2}\right)\frac{f_T}{2} - \frac{f}{4} \quad , \tag{5.28}$$

$$4\pi p_t + E^2 = \left[\frac{T}{2} + e^{-b}\left\{\frac{a''}{2} + \left(\frac{a'}{4} + \frac{1}{2r}\right)(a' - b')\right\}\right]\frac{f_T}{2} - \frac{f}{4} \quad , \tag{5.29}$$

$$\frac{\cot\theta}{2r^2}T' f_{TT} = 0 \quad and \tag{5.30}$$

$$E(r) = \frac{1}{r}\int_o^r 4\pi r^2 \sigma e^{\frac{\lambda}{2}} dr = \frac{q(r)}{r^2} \quad , \tag{5.31}$$

where $q(r)$ is the total charge inside the sphere of radius r and E is the electric field at the surface of the compact star.

5.1.3 The $f(R,T)$ Modified gravity: A Brief Introduction

We have considered another extension of standard GR which is famous as the modified $f(R,T)$ gravity theory, where the gravitational Lagrangian is given by an arbitrary function of the Ricci scalar R and T, the trace of the energy-momentum tensor. The dependence from T may be induced by exotic imperfect fluids or quantum effects. In our model as the first step we have considered Einstein-Hilbert action in terms of $f(R,T)$ gravity as $f(R,T) = R + \alpha T$, where R is the Ricci scalar and T, the trace of energy-momentum tensor with α as the coupling parameter between matter and geometry. This helps to incorporate the minimal coupling between them. Also we have solved modified TOV equations along with the field equations. The interior space time of the spherical NS is matched to the exterior Schwarzschild line element at the surface of the star to get the model parameters.

The $f(R,T)$ gravity model depends on a source term which represents the variation of the matter stress-energy tensor w.r.t. the metric. A general expression for this source term is obtained as a function of matter Lagrangian L_M and each choice of L_M would generate a specific set of field equations. Since in the present model, the covariant divergence of the stress-energy tensor is nonzero, the motion of massive test particles is non-geodesic. The extra acceleration due to the coupling between matter and geometry is always present. The equations of motion of test particles are obtained from a variational principle which can also be used to investigate the Newtonian limit of the model and the expression of the extra acceleration is also obtained.

5.1.3.1 Mathematical Formulation of the Gravitational Field Equations of f(R, T) Gravity

In this section, we have shown how $f(R,T)$ gravity has been introduced by using integration of the Ricci scalar R, over 4 dimension, after considering Einstein-Hilbert action.

Again, in $f(R,T)$ modified gravity, modified Einstein-Hilbert action takes the form,

$$S_{EH} = \int |h| L_M d^4x + \frac{c^4}{16\pi G} \int f(R,T)|h| d^4x \quad , \tag{5.32}$$

where $|h| = det(h^a_\alpha) = \sqrt{-g}$ describes the determinant of the tetrad (h^a_α), L_M represents the matter Lagrangian and $g = det(g_{\mu\nu})$. Now, if we consider the stellar matter as perfect fluid then the energy-momentum tensor can be written as

$$T_{\mu\nu} = -\frac{2}{|h|}\frac{\delta(L_M|h|)}{\delta g^{\mu\nu}} \quad , \tag{5.33}$$

where its trace becomes

$$T = g^{\mu\nu}T_{\mu\nu} \quad . \tag{5.34}$$

The matter Lagrangian density L_M depends only on the metric tensor components $g_{\mu\nu}$ and not on its derivatives. So, we obtain

$$T_{\mu\nu} = -\frac{2}{|h|}\frac{\partial(L_M|h|)}{\partial g^{\mu\nu}} \quad . \tag{5.35}$$

Now, if we vary the Einstein-Hilbert action S_{EH} w.r.t. the metric tensor components $g^{\mu\nu}$, then we get

$$\begin{aligned} \delta S_{EH} = & \\ & \frac{1}{16\pi}\int \left[f_R(R,T)\delta R + f_T(R,T)\frac{\delta T}{\delta g^{\mu\nu}}\delta g^{\mu\nu} \right] \sqrt{-g} d^4x \\ & - \frac{1}{16\pi}\int \left[\frac{g_{\mu\nu}}{2} f(R,T)\delta g^{\mu\nu} + \frac{16\pi}{\sqrt{-g}}\frac{\delta(\sqrt{-g}L_M)}{\delta g^{\mu\nu}} \right] \sqrt{-g} d^4x \quad , \end{aligned} \tag{5.36}$$

where $f_R(R,T) = \frac{\partial f(R,T)}{\partial R}$ and $f_t(R,T) = \frac{\partial f(R,T)}{\partial T}$ respectively. Again, from the variation of the Ricci scalar gives

$$\delta R = \delta(g^{\mu\nu}R_{\mu\nu}) = R_{\mu\nu}\delta g^{\mu\nu} + g^{\mu\nu}\{\nabla_\lambda \delta\Gamma^\lambda_{\mu\nu} - \nabla_\nu \delta\Gamma^\lambda_{\mu\lambda}\} \quad , \tag{5.37}$$

where ∇_λ is the covariant derivative w.r.t. the symmetric connection Γ associated to the metric g.

Moreover, the variation of the Christoffel symbol yields

$$\delta\Gamma^{\lambda}_{\mu\nu} = \frac{g^{\lambda\alpha}}{2}\{\nabla_\mu \delta g_{\nu\alpha} + \nabla_\mu \delta g_{\alpha\mu} - \nabla_\alpha \delta g_{\mu\nu}\} \quad , \tag{5.38}$$

and again the variation of Ricci scalar provides

$$\delta R = [R_{\mu\nu}\delta g^{\mu\nu} + g_{\mu\nu}\Box\delta g^{\mu\nu} - \nabla_\mu\nabla_\nu\delta g^{\mu\nu}] \quad . \tag{5.39}$$

Therefore, for the variation of the action of the gravitational field we obtain

$$\begin{aligned}
\delta S_{EH} = & \\
& \frac{1}{16\pi}\int [f_R(R,T)R_{\mu\nu}\delta g^{\mu\nu} + f_R(R,T)g_{\mu\nu}\Box\delta g^{\mu\nu}]\sqrt{-g}d^4x \\
& - \frac{1}{16\pi}\int \left[f_R(R,T)\nabla_\mu\nabla_\nu\delta g^{\mu\nu} + f_T(R,T)\frac{\delta(g^{\alpha\beta}T_{\alpha\beta})}{\delta g^{\mu\nu}}\delta g^{\mu\nu}\right]\sqrt{-g}d^4x \\
& - \frac{1}{16\pi}\int \left[\frac{g_{\mu\nu}}{2}f(R,T)\delta g^{\mu\nu} + \frac{16\pi}{\sqrt{-g}}\frac{\delta(\sqrt{-g}L_M)}{\delta g^{\mu\nu}}\right]\sqrt{-g}d^4x \quad .
\end{aligned} \tag{5.40}$$

We can define the variation of T w.r.t. the metric tensor as

$$T_{\mu\nu} + \Theta_{\mu\nu} = \frac{\delta(g^{\alpha\beta}T_{\alpha\beta})}{\delta g^{\mu\nu}} \quad , \tag{5.41}$$

where

$$\Theta_{\mu\nu} \equiv g^{\alpha\beta}\frac{\delta T_{\alpha\beta}}{\delta g^{\mu\nu}} \quad . \tag{5.42}$$

After integrating the second and third term of the above expression of δS_{EH} partially, the field equations of the $f(R.T)$ model can be obtained as

$$f_R(R,T)R_{\mu\nu} - \frac{1}{2}f(R,T)g_{\mu\nu} + \{g_{\mu\nu}\Box - \nabla_\mu\nabla_\nu\}f_R(R,T) = 8\pi T_{\mu\nu} - f_T(R,T)T_{\mu\nu} - f_T(R,T)\Theta_{\mu\nu} \quad . \tag{5.43}$$

It is very significant to point out that the above field equation gives the field equations of $f(R)$ gravity if we chose $f(R,T) \equiv f(R)$. Again the contraction of this equation provides the relation between Ricci scalar R and the trace T of the trace-energy tensor

as

$$f_R(R,T)R + 3\Box f_R(R,T) - 2f(R,T) = 8\pi T - f_T(R,T)T - f_T(R,T)\Theta \quad , \quad \Theta = \Theta^{\mu}_{\mu} \quad , \tag{5.44}$$

where the box operation $\Box$ in terms of covariant derivative ∇_μ, is defined as $\Box = g^{\mu\nu}\nabla_\mu\nabla_\nu$ and $\Theta_{\mu\nu}$ can be obtained as

$$\Theta_{\mu\nu} = g_{\mu\nu}\nabla^{\mu} - 2T_{\mu\nu} - 2g^{\alpha\beta}\frac{\partial^2 L_M}{\partial g^{\mu\nu}\partial g^{\alpha\beta}} \quad . \tag{5.45}$$

With considering the four velocity such as $u_\mu u^\mu = 1$.

Now, eliminating the term $\Box f_R(R,T)$ between the above two equations, the gravitational field equations can be written as

$$f_R(R,T)\{R_{\mu\nu} - \frac{1}{3}Rg_{\mu\nu}\} + \frac{g_{\mu\nu}}{6}f(R,T) = 8\pi\{T_{\mu\nu} - \frac{g_{\mu\nu}}{3}T\} - f_T(R,T)\{T_{\mu\nu} - \frac{g_{\mu\nu}}{3}T\} - f_T(R,T)\{\Theta_{\mu\nu} - \frac{g_{\mu\nu}}{3}\Theta\} + \nabla_\mu\nabla_\nu f_R(R,T) \quad . \tag{5.46}$$

Again the covariant divergence of the field equation gives

$$\nabla^{\mu}\left[f_R(R,T)R_{\mu\nu} - \frac{g_{\mu\nu}}{2}f(R,T) + (g_{\mu\nu}\Box - \nabla_\mu\nabla_\nu)f_R(R,T)\right] \equiv 0 \quad , \tag{5.47}$$

where $f(R,T)$ is an arbitrary function of the Ricci scalar R and of the trace of the stress-energy tensor T, we obtain for the divergence of the stress-energy tensor $T_{\mu\nu}$ the equation

$$\nabla^{\mu}T_{\mu\nu} = \frac{f_T(R,T)}{8\pi - f_T(R,T)} \times [(T_{\mu\nu} + \Theta_{\mu\nu})\nabla^{\mu} ln f_T(R,T) + \nabla^{\mu}\Theta_{\mu\nu}] \quad . \tag{5.48}$$

Next we have considered the calculation of the tensor $\Theta_{\mu\nu}$, once the matter La-

grangian is known. So, we have

$$\frac{\delta T_{\alpha\beta}}{\delta g^{\mu\nu}} = \frac{\delta g_{\alpha\beta}}{\delta g^{\mu\nu}} L_M + g_{\alpha\beta}\frac{\partial L_M}{\partial g^{\mu\nu}} - 2\frac{\partial^2 L_M}{\partial g^{\mu\nu}\partial g^{\alpha\beta}} = \frac{\delta g_{\alpha\beta}}{\delta g^{\mu\nu}} L_M + \frac{1}{2} g_{\alpha\beta} g_{\mu\nu} L_M - \frac{1}{2} g_{\alpha\beta} T_{\mu\nu} - 2\frac{\partial^2 L_M}{\partial g^{\mu\nu}\partial g^{\alpha\beta}} \quad , \tag{5.49}$$

From the condition $g_{\alpha\sigma} g^{\sigma\beta} = \delta^{\beta}_{\alpha}$, we have

$$\frac{\delta g_{\alpha\beta}}{\delta g^{\mu\nu}} c - g_{\alpha\sigma} g_{\beta\gamma} \delta^{\alpha\gamma}_{\mu\nu} \quad , \tag{5.50}$$

where $\delta^{\alpha\gamma}_{\mu\nu}$ is the generalised Kronecker symbol. So, we have

$$\Theta_{\mu\nu} = -2T_{\mu\nu} + g_{\mu\nu} L_M - 2 g^{\alpha\beta} \frac{\partial^2 L_M}{\partial g^{\mu\nu}\partial g^{\alpha\beta}} \quad . \tag{5.51}$$

In the case of the electromagnetic field the matter Lagrangian is given by

$$L_M = -\frac{1}{16\pi} F_{\alpha\beta} F_{\gamma\sigma} g^{\alpha\gamma} g^{\beta\sigma} \quad , \tag{5.52}$$

where $F_{\alpha\beta}$ is the electromagnetic field tensor. In this case we obtain $\Theta\mu\nu = -T_{\mu\nu}$. In the case of a massless scalar field ϕ with Lagrangian $L_M = g^{\alpha\beta}\nabla_{alpha}\phi\nabla_{\beta}\phi$, we obtain $\Theta_{\mu\nu} = -T_{\mu\nu} + \frac{1}{2} T g_{\mu\nu}$. The problem of the perfect fluids, described by an energy density ρ, pressure p and four velocity u^{μ} is more complicated, since there is no unique definition of the matter Lagrangian.

However, in the present study we assume that the stress-energy tensor of the matter is given by

$$T_{\mu\nu} = (p + \rho) u_{\mu} u_{\nu} - p g_{\mu\nu} \quad , \quad L_M = -p \quad . \tag{5.53}$$

The four velocity u_{μ} hold the conditions $u_{\mu} u^{\mu} = 1$ and $u^{\mu}\nabla_{\nu} u_{\mu} = 0$ respectively. Then, with the above equation, we obtain for the variation of the stress-energy of a perfect fluid the expression

$$T_{\mu\nu} = -2T_{\mu\nu} - p g_{\mu\nu} \quad . \tag{5.54}$$

5.1.3.2 Advantages of incorporating the f(R, T) Modified Gravity

The matter and time dependent terms in the gravitational field equations play the key role of an effective cosmological constant. There is also the possibility of reconstruction of arbitrary Friedmann-Robertson-Walker cosmology by an appropriate choice of a function $f(T)$. The equations of motion corresponding to this model show the presence of an extra force acting on test particles, and the motion is generally non-geodesic. It is also possible to obtain an upper limit on the magnitude of the extra acceleration in the Solar System by using the perihelion precession of Mercury, from this modified gravity. This value of a_E, obtained from the solar system observations, is somewhat smaller than the value of the extra acceleration $a_E \approx 10^{-8} cm\ s^{-2}$, necessary to explain the DM properties, as well as the pioneer anomaly [89, 90]. However, it does not deny the possibility of the existence of some extra gravitational effects acting at both the solar system and galactic levels. Though, the assumption of a constant extra force may not be correct on larger astronomical scales.

Therefore, the predictions of the $f(R, T)$ modified gravity model could lead to some major differences, as compared to the predictions of standard GR, or other generalized gravity models, in several problems of current interest, such as cosmology, gravitational collapse or the generation of gravitational waves. The study of these phenomena may also provide some specific signatures and effects, which could distinguish and discriminate between the various gravitational models.

Part IV

UNDERSTANDING THE PRESENT ACCELERATED UNIVERSE IN THE CONTEXT OF $f(R,T)$ MODIFIED GRAVITY : CONFRONTATION WITH RECENT OBSERVATIONAL DATA

"Something deeply hidden had to be behind things".

—Albert Einstein

CHAPTER 6

COSMOLOGY IN $F(R,T)$ MODIFIED GRAVITY: PREDICTING THE FUTURE OF THE ACCELERATING UNIVERSE THROUGH CURRENT OBSERVATIONS

6.1 Cosmological Model in $f(R,T)$ Gravity Embedded in Unified Dark Energy and Dark Matter

6.1.1 Prelude

The newly proposed cosmological model deals with modified Chaplygin gas in $f(R,T) = R+\xi(T)$ gravity, where $\xi(T)$ is chosen as the linear combination of power law and logarithmic form under flat "Friedmann-Lemaitre-Robertson-Walker" space-time. It is revealed that the model is compatible with current observational data and confronts the deceleration and state parameters effectively. At large scale, the cultivated mod-

ified Chaplygin gas can reproduce the results of the standard model except assuming the prior subsistence of a cosmological constant. The model can predict the Big Rip in future infinity and can tackle the difficulties related to the fine-tuning and the coincidence problem practically.

Various observational evidence have revealed the present accelerated phase of the universe [91, 92, 93]. The standard cosmology, using Einstein gravity with normal matter, is unable to explain the above observational outcomes. Scientists are trying to adapt the predicted accelerated expansion of the universe, by incorporating modified gravity and proposing the existence of an exotic matter having an abundant amount of negative pressure acquainted with dark energy (DE). The modified Chaplygin gas (MCG hereafter) which has been considered in this present work is one of the fruitful dark energy candidate models [252, 95] with the equation of state (EoS hereafter) as $p = \left(A\rho - \frac{B}{\rho^{\psi}}\right)$, where A, B and ψ are all real constant parameters where $0 \leq \psi \leq 1$ [96, 97]. Again, if we choose $B = 0$ the perfect fluid EoS can be recovered and for $A = 0$, it is converted into generalized Chaplygin gas. Besides, MCG has been considered in our work because of its minimum small χ^2 value [95] and also it can unify both dark energy and dark matter that leads to the accelerated universe with suitable negative pressure. At large scale (later stage) its EoS is nearly equivalent to Λ (cosmological constant). MCG will also satisfy $(\rho + 3p) < 0$ because of the Friedmann equation

$$\frac{\ddot{a}}{a} = -\frac{4\pi}{3}(\rho + 3p)G \quad ; \quad \ddot{a} > 0 \quad . \tag{6.1}$$

On the other hand, the tensions in the expansion rate of the accelerated universe at present, can be well accommodated by the modified gravity theory [98, 99, 100]. The model with modified gravity theory also helps to modify the standard model alternatively in terms of dark matter [101, 102, 188]. Harko et al., have considered Einstein-Hilbert action as $f(R,T)$ where R, as the Ricci scalar and T as the trace of energy-momentum tensor [104]. Though the above mentioned model is justified due to the quantum effect as a conformal anomaly, but still the field equations have become very much complicated and due to the matter-gravity coupling, the test particle does

not follow a geodesic path. Again, a very simple form of $f(R,T)$ has been chosen by S. Chakraborty where the particles will follow the geodesic path [105]. $f(R,T)$ gravity model can also be successfully implemented to predict the accelerated universe and its fate by G. Sardar et al. [106]. Moreover, the ΛCDM model has been considered as the best fit cosmological model [107, 108]. But it can not accommodate the difficulties related to the fine-tuning and the coincidence problem [109, 110].

The motivation of this current work is to explore the effective application of MCG with $f(R,T) = R + \xi(T)$ modified gravity as a successful cosmological model during the prediction of the present accelerated universe and about its future, in the context of recent observations. This model can confront the fine-tuning problem and the coincidence problem in a practical way. At the same time, the accuracy of the support of the current choice of $\xi(T)$ in $f(R,T)$ modified gravity as a linear combination of power law and logarithmic form, under flat "Friedmann-Lemaitre-Robertson-Walker" (FLRW hereafter) space-time will also be examined with the present observational data.

6.1.2 Mathematical Construction of Basic Equations

In $f(R,T)$ modified gravity theory [104], modified Einstein-Hilbert action takes the form,

$$S_{EH} = \int \left[L_M + \frac{1}{16\pi G} \right] \sqrt{-g} d^4x \quad , \tag{6.2}$$

where $T = T_{\mu\nu} g^{\mu\nu}$ and L_M represents the perfect matter fluid Lagrangian density which gives the energy-momentum tensor as [111]

$$T_{\mu\nu} = -\frac{2}{\sqrt{-g}} \frac{\delta(\sqrt{-g} L_M)}{\delta g^{\mu\nu}} \quad , \tag{6.3}$$

and the above equation (3) can be written in a simple form if L_M depends only on $g_{\mu\nu}$, as

$$T_{\mu\nu} = g_{\mu\nu} L_M - 2 \frac{\partial L_M}{\partial g^{\mu\nu}} \quad . \tag{6.4}$$

Again, for the perfect fluid, the energy-momentum tensor took the form as

$$T_{\mu\nu} = [(p+\rho)u_\mu u_\mu - p g_{\mu\nu}] \quad with \quad L_M = -p \quad , \tag{6.5}$$

where ρ and p are the total energy density and pressure of the perfect fluid respectively, that fills the Universe.

So, in metric formalism, by using the variation w.r.t. the metric tensor, the field equations for $f(R,T)$ gravity becomes [104]

$$\frac{\partial f(R,T)}{\partial R} R_{\mu\nu} - \frac{1}{2} f(R,T) g_{\mu\nu} - [\nabla_\mu \nabla_\nu - g_{\mu\nu}\Box] \frac{\partial f(R,T)}{\partial R} = 8\pi G T_{\mu\nu} - (T_{\mu\nu} + \Theta_{\mu\nu}) \frac{\partial f(R,T)}{\partial T} \quad , \tag{6.6}$$

where the box operation $\Box$ in terms of covariant derivative ∇_μ, is defined as $\Box = g^{\mu\nu}\nabla_\mu \nabla_\nu$ and $\Theta_{\mu\nu}$ can be obtained as

$$\Theta_{\mu\nu} = \left[-2T_{\mu\nu} - 2L_M g_{\mu\nu} - 2g^{\alpha\beta} \frac{\partial^2 L_M}{\partial g^{\mu\nu} \partial g^{\alpha\beta}} \right] \quad . \tag{6.7}$$

It is very interesting that from the above equation (6), the ΛCDM model can be recovered by just replacing $f(R,T)$ as $f(R,T) = R + 2\Lambda$ with matter as dust i.e. $L_M = \rho$, where Λ is the cosmological constant. Now, for the perfect fluid, considering the restrictions on four velocity such as $u_\mu u^\mu = 1$ and $u^\mu \nabla_\nu u_\mu = 0$, the reduced form of the above equation (7) as

$$\Theta_{\mu\nu} = -\rho g_{\mu\nu} - 2T_{\mu\nu} \quad . \tag{6.8}$$

So, in this current cosmological model, we have chosen $f(R,T) = R + \xi(T)$, for which the field equation (6) took the simplifies form as [105]

$$G_{\mu\nu} = 8\pi G \left[T_{\mu\nu} - (T_{\mu\nu} + \Theta_{\mu\nu}) \xi'(T) + \frac{g_{\mu\nu}}{2} \xi(T) \right] \quad . \tag{6.9}$$

6.1.3 Incorporating Modified Chaplygin Gas in $f(R,T)$ modified gravity

As we have considered the spatially flat FLRW space-time [106], the modified Friedmann equations in terms of Hubble parameter ($H \equiv \frac{\dot{a}}{a}$) where $a(t)$ is the cosmological scale factor, can be written as

$$3H^2 = 8\pi G\left[\rho_m + (\rho_m + p_m)\xi^{'}(T) + \frac{\xi(T)}{2}\right] \quad and \tag{6.10}$$

$$3H^2 + 2\dot{H} = -8\pi G\left[p_m + \frac{\xi(T)}{2}\right] \quad . \tag{6.11}$$

Now, the above equations (10) and (11) as standard FLRW equations can be written as

$$3H^2 = 8\pi G(\rho_m + \rho_d) \quad and \tag{6.12}$$

$$3H^2 + 2\dot{H} = -8\pi G(p_m + p_d) \quad , \tag{6.13}$$

where ρ_m and p_m are the energy density and pressure of the matter respectively. Again, $\rho_d = (\rho_m + p_m)\xi^{'}(T) + \frac{\xi(T)}{2}$ and $p_d = -\frac{\xi(T)}{2}$ are the energy density and pressure respectively due to the effect of modified gravity. These terms can produce the equivalent contributions for dark fluid component.

Further, the conservation equations followed by the dark matter (DM hereafter) and dark energy (DE hereafter) respectively can be written as

$$\dot{\rho_m} + 3H(\rho_m + p_m) = 0 \quad and \tag{6.14}$$

$$\dot{\rho_d} + 3H(\rho_d + p_d) = 0 \quad . \tag{6.15}$$

Now, solving the above equation (14) we have got the energy density of the dark matter

component as

$$\rho_m = \rho_{m0}(1+z)^3 \quad as \quad p_m = 0 \quad , \tag{6.16}$$

where ρ_{m0} is a constant and $\left[z = \frac{1}{a(t)} - 1\right]$ is the cosmological redshift.

Again, considering DE in the form of MCG whose EoS is given as

$$p = \left(A\rho - \frac{B}{\rho^{\psi}}\right) \quad with \quad A,\ B \ \ are\ real\ constants \ \ and \quad 0 \leq \psi \leq 1 \quad . \tag{6.17}$$

Using the equations (15) and (17) we obtain the energy density in terms of scale factor $a(t)$ as

$$\rho_{MCG} = \left(\frac{I}{a^{3(1+\psi)(1+A)}} + \frac{B}{1+A}\right)^{\frac{1}{1+\psi}} \quad , \tag{6.18}$$

where I is the integrating constant. Now, the above equation (18) indicates that, when $a \to \infty$ i.e. at large scale the stable energy density is achievable if and only if $\psi > -1$. Further, $1 + A > 0$ and $B > 0$ corresponds to the universe dominated by DE. So, the effective EoS parameter becomes

$$\omega_{eff} = \left[A - \frac{B}{\rho_{MCG}^{1+\psi}}\right] \quad . \tag{6.19}$$

As we have considered $\xi(T)$ as the linear combination of power law and logarithmic form, the $f(R,T)$ modified gravity in our model took the form

$$f(R,T) = R + \xi_0\left[\beta_1 T^m + 2\beta_2 ln(T)\right] \quad , \tag{6.20}$$

where ξ_0, β_1, β_2 and m are arbitrary constants. Now applying the above choice and using equations (12) and (13), we can get the simplified form of ρ_d and p_d of the fluid as

$$\begin{aligned} \rho_d = & \\ & \xi_0\left[\beta_1(1-3\omega_{eff})^{m-1}\{2m(1+\omega_{eff}) + (1-3\omega_{eff})\}\rho_m^m\right] \\ & + \xi_0\left[\beta_2\left(2\frac{1+\omega_{eff}}{1-3\omega_{eff}} + ln[(1-3\omega_{eff})\rho_m]\right)\right] \quad and \end{aligned} \tag{6.21}$$

$$p_d = -\xi_0 \left[\frac{\beta_1}{2}(1-3\omega_{eff})^m \rho_m^m + \beta_2 ln\{(1-3\omega_{eff})\rho_m\}\right] \quad . \tag{6.22}$$

According to our choice in $f(R,T)$ gravity, the equation (19) took the form

$$\omega_d = -\left[\frac{(1-3\omega_{eff})ln[(1-3\omega_{eff})\rho_m]}{2(1+\omega_{eff})+(1-3\omega_{eff}+2m(1+\omega_{eff}))ln[(1-3\omega_{eff})\rho_m]}\right] \quad . \tag{6.23}$$

On the other hand, for the same choice of $f(R,T)$, the first Friedmann equation gives

$$\begin{aligned} H^2(z) =& \frac{8\pi G}{3}\left[\rho_{m0}(1+z)^3 + \xi_0\left(\beta_1(1-3\omega_d)^{m-1}[2m(1+\omega_d)+(1-3\omega_d)][\rho_{m0}(1+z)^3]^m\right)\right] \\ &+ \frac{8\pi G}{3}\left[\xi_0\left(\beta_2\left[\frac{2(1+\omega_d)}{(1-3\omega_d)} + ln[(1-3\omega_d)\rho_{m0}(1+z)^3]\right]\right)\right] \quad . \end{aligned} \tag{6.24}$$

Now, we can also define another dimensionless parameter in terms of dimensionless density parameter $\Omega_{m0} = \frac{\rho_{m0}}{H_0^2}$ as

$$E^2(z) = \left[\frac{H(z)}{H_0}\right]^2 = \left[\Omega_{m0}(1+z)^3 + \frac{\xi_0}{2}(1-3\omega_d)^{m-1}[2m(1+\omega_d)+(1-3\omega_d)][\Omega_{m0}(1+z)^3]^m\right] \quad . \tag{6.25}$$

It is very significant that the above new cosmological model reduces to ΛCDM model if we set $m = 0$ and $\beta_2 = 0$.

6.1.4 Constraining MCG and Best fit values of the EoS and Cosmological parameters : Observational Support

In the analysis, we have incorporated the present day value of H_0 to make a robust estimation of the parameters of our model and also utilizes the $H(z)$ to impose severe constraints. We have also applied the Markov Chain Monte Carlo (MCMC hereafter) code Montepython3.5 method to estimate the required cosmological parameters only [112]. This statistical analysis, through our model, implies a deep and valuable insight on the observed cosmological acceleration and also reveals the nature and role of DE

in the present expansion of the Universe. During analysis we have used the data sets (Pantheon [113], BAO (BOSS DR12 [114], SMALLZ-2014 [115]) and HST [116]) and have imposed a PLANK18 [117] prior.

The study of Type Ia supernova (SNIa hereafter) is one of the most efficient methods of studying the DE dominated accelerated expansion of the Universe [118, 119]. Here to find the constraints on the MCG parameters we have used the above mentioned dada sets. The best fit values of the parameters, tabulated in the Table 1. are obtained by considering minimum value of the χ^2 function of μ (distance modulus) of the dada set [95]. The data set also gives the required parameters of our proposed model as tabulated in the Table 2. In this work we have only measured the essential free parameters required for analysis the present situation from cosmological model. In this model in $f(R,T)$ gravity, we have considered the values of a few base parameters as $m = [-2, 2]$, $\beta_1 = 3.1$ and $\beta_2 = 0.2$. We have also chosen baryon density $100\omega_b = [1.9, 2.5]$; cold dark matter (cdm) density $\omega_{cdm} = [0.0, 0.145]$; Hubble parameter $H_0 = [60, 80]$ $km\ s^{-1}\ Mpc^{-1}$ and $\omega_{d0} = [-0.33, 0.33]$, in flat space-time prior.

Table 1.

EoS parameters of MCG	ψ	A	B	χ^2_{min}
Best	$0.57234^{+0.276}_{-0.217}$	$-0.17123^{+0.185}_{-0.189}$	$0.54435^{+0.215}_{-0.231}$	1031.82316
Fit	$0.56347^{+0.277}_{-0.218}$	$-0.16754^{+0.172}_{-0.188}$	$0.54287^{+0.214}_{-0.231}$	1031.82316
Values	$0.55481^{+0.276}_{-0.217}$	$-0.16086^{+0.168}_{-0.189}$	$0.54375^{+0.215}_{-0.231}$	1031.82316

Table 6.1: Best fit values of the MCG parameters of the present model using data set (SNIa) with 1σ confidence

The Hubble parameter and deceleration parameter in terms of cosmological redshift z can be expressed as

$$H(z) = -\frac{1}{1+z}\frac{dz}{dt} \quad , \tag{6.26}$$

where $\frac{dz}{dt}$ can be inferred as in the reference [120] and

$$q(z) = -\frac{\ddot{a}a}{\dot{a}^2} = -\left(1 + \frac{\dot{H}}{H}^2\right) \quad . \tag{6.27}$$

Table 2.

Sl NO.	EoS parameters	Best fit Values	$Mean \pm \sigma$
1	$100\omega_b$	2.251	$2.2483^{+0.0512}_{-0.0512}$
2	ω_{cdm}	0.11803	$0.1179^{+0.0021}_{-0.0021}$
3	H_0	73.01	$72.683^{+0.1681}_{-0.1683}$
4	Ω_{d0}	0.745	$0.7382^{+0.0135}_{-0.0123}$
5	Ω_{m0}	0.2675	$0.2665^{+0.0122}_{-0.0132}$
6	χ^2_{min}	1031.8232	

Table 6.2: MCMC result of the cosmological model parameters using data set (SNIa) with 1σ confidence.

6.1.5 Graphical Interpretations and Comparison of the model with ΛCDM Model

$Fig-25$

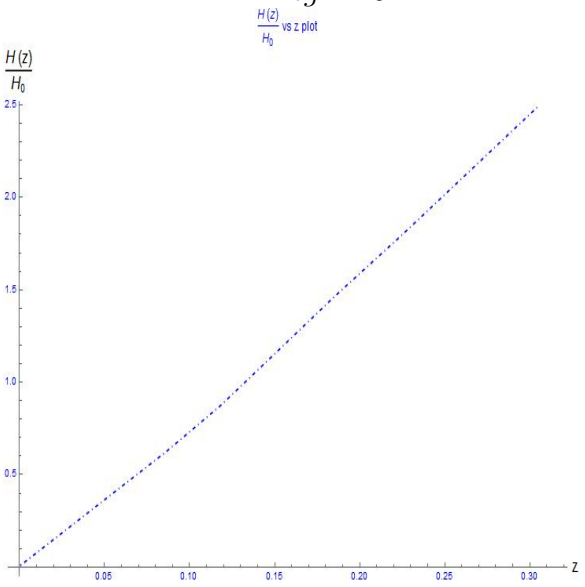

$Fig-26$

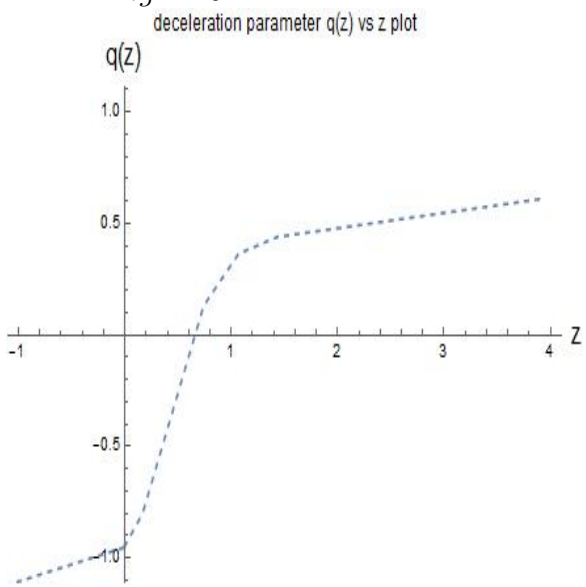

Figure 6.1: *Represents the variation of the Hubble parameter $H(z)$ as a function of cosmological redshift z.*

Figure 6.2: *Represent the variation of the deceleration parameter $q(z)$ with respect to the redshift z.*

Now, we can estimate the values of ρ_{d0} and ξ_0 using the above tables as $\rho_{d0} = 3902.01$ and $\xi_0 = 1632$.

We have also compared our model with the ΛCDM model, in order to check the suitability and viability of it by analysing Akaike Information criterion (AIC) [121, 122] and Bayesian Information Criterion (BIC) [123, 124]. Generally, the best fit data is shown by the lower values of AIC and BIC corresponds to the specific model. The values are tabulated in Table 3.

Table 3.

Sl NO.	Cosmological Model	AIC	BIC	ΔAIC	ΔBIC
1	Present	1043.814	1074.012	-2.066	8.282
2	ΛCDM	1045.88	1065.73	0	0

Table 6.3: The values for AIC and BIC for present cosmological model and ΛCDM model

6.1.6 Brief Discussions and Conclusion

In the context of various cosmological models of the present accelerated universe, till now we have seen that mainly two types of approaches have been preferred. In order to justify the late time accelerated universe, one can choose any one of the following approaches as either taking into account dynamical dark energy in the context of standard GR or modified gravity theory without adding any exotic fluid. But till now, no such a highly acceptable cosmological model has been confirmed and the hunt for the perfect model continues. Though, the ΛCDM model has a few drawbacks, it has been considered to be the most effective cosmological model at present time. So, it is very clear that these several cosmological models of present time by using any one of the above approaches can never be accepted over ΛCDM model. So, it is obvious that any one of the above approaches is not enough to reach our goal. In this scenario, cosmologists are trying to construct a best fit cosmological model to demonstrate the present observational data. In this situation, we have constructed a new cosmological model by combining the two approaches and have found that it gives a better result to observational data.

We have done the detailed study of our newly proposed cosmological model which is found to be preferable in the context of present observational universe. It can give good predictions at the present situation for both state Ω_{d0} and deceleration parameter $q(z)$. At large scale ω_d will converge slowly and MCG has no future singularity. The stability of this model does not depend on MCG EoS parameter B. Moreover, the difficulties related to fine tuning and coincidence problem can also be solved as $z \to -1$.

Now, using the calculated best fit values of the cosmological parameters we have plotted a few most important cosmological parameters of our model and the figures are given as Fig 25 and Fig 26. The present model becomes very interesting as we can look into the universe at $z < 0$ and can predict about its future in a practical way. The Figure 26 is very crucial as well as important. It shows that from our model, we have got $q(z) \to -1$ as $z \to -1$. So, from these observations we can conclude that the universe will continue its accelerating phase and go beyond the phantom region [125]. Further, we can predict about the Big Rip in the future as $z \to -1$.

According to the AIC analysis, our model gives a very good observational support for the considered data sets. Interestingly, as ΔAIC has become negative also, it clearly depicts that maximum possibility of our present cosmological model is higher than ΛCDM model. However, considering both AIC and BIC values, we can say that our model can give the best observational support w.r.t. the considered data sets.

Part V

COSMOLOGICAL EVOLUTION OF A CHARGED ROTATING BLACK HOLE UNDER DARK ENERGY DOMINATED UNIVERSE

"Black holes ain't as black as they are painted. They are not the eternal prisons they were once thought. Things can get out of a black hole, both to the outside, and possibly to another universe. So if you feel you are in a black hole, don't give up. There's a way out".

—Stephen Hawking

CHAPTER 7

BLACK HOLES UNDER DARK ENERGY AFFECTED UNIVERSE

7.1 Stability and Quantum Phase Transition of the Charged Rotating Black Hole Embedded in Quintessence Field

7.1.1 Prelude

Immediate local impacts of cosmic acceleration upon a rapidly rotating black hole are very interesting in recent studies. In this article, the stability of a rapidly rotating black hole and the minimum value of the ratio between the black hole's angular momentum to it's mass which ensures the stability, are investigated simultaneously. Also, two modern forms of uncertainty relations are proposed by enhancing the usual Heisenberg algebra with superior terms, in order to supervise on thermodynamic properties of the rotating black hole. An asymptotically flat Kiselev black hole solution, cultivated by quintessence field is chosen for this purpose. The local shifts in space-time geometry next to the rotating black hole can be resolved from a modified metric, occupying the

surrounding space-time of the black hole. The angular momentum of a rotating black hole depends on the rate of change in acquiring mass by it. On the other hand, at the same time, due to the effect of the quintessence field, there exists repulsive gravitational force inside the black hole. So, there is an uncertainty in the position of Innermost Stable Circular Orbit as well as radius of the rotating black hole. This uncertainty is also investigated in our work. Relying on two new forms of uncertainty principle, the modified thermodynamic variables like black hole's Hawking temperature, heat-capacity, entropy at the black hole's event horizon etc are computed under rotation. Quantum corrections of black hole's Hawking temperature, entropy, free-energy etc are also explored. Further, quantum corrected heat capacity of the rotating black hole is studied and also thermal stability is inquired. The existence of transitions of phase in case of a rapidly rotating black hole are also found out. Again, quantum corrected entropy of black hole contains logarithmic terms and their effects on thermal stability of the rotating black hole are also discussed. Modifications in the mass-temperature, specific heat etc of a rotating black hole are also presented according to the modified extension parameters.

Black holes (BHs hereafter) are the simplest among the families of compact stars [126, 301, 128]. Einstein's general relativity (GR hereafter), where a central singularity and some inner horizons such as Cauchy horizons, Innermost Stable Circular Orbit (ISCO) etc are intertwined by an event horizon, can be used to treat these objects. Quantum fluid studies [129] also uncover the fact that they even can radiate, named as Hawking radiation. Vacuum perturbations, which generate virtual pairs of particles, are the origin of this BH radiation. At one time, tidal forces draw them aloof, one falls in and the other escapes away giving this radiation. This idea leads us to consider the BHs as thermodynamic systems. In physics, BH thermodynamics is the area of study that seeks to reconcile the laws of thermodynamics with the existence of the BH event horizon. Also, a BH may stop to evaporate and then it may become stable at the quantum ground state. Thermodynamics and related topics are emergent ways to culture BH physics. Holographic principles [130] assists us to describe surface quantities to the BH thermodynamics. BH entropy and temperature are holographically

concerned to the horizon area and surface gravity respectively. The surface gravity of a BH comes into play only when the BH is in equilibrium, i.e., stationary [131]. But in our study, we choose rotating BH. BH parameters like mass, charges, angular momenta etc are thermodynamic variables of the first law. One of the best ways to look into what happened to the BH at the quantum scale is to study the thermal fluctuations [132, 133]. We get the knowledge about the microscopic origin of entropy from it. As a matter of fact, it is statistical fluctuation that may be illustrated as the quantum corrections. We need a theory of quantum gravity for practicing this type of quantum corrections in a strong gravitational system. It can be done via some quantum theories of gravity like string theory or loop quantum gravity. Meanwhile, it is found that leading order corrections to the BH entropy may be logarithmic [134, 135, 136]. It is actually an important term when the BH's size is small. Consequently, it can be considered to test the quantum gravity [137, 138, 139]. Such thermal fluctuations can be considered as small perturbations around the equilibrium temperature of the BH. The logarithmic correction effect on a BTZ BH [140], is observed to find thermal fluctuations which can modify the stability of BH. Logarithmic term corrected thermodynamics of Horava-Lifshitz BH [141] is also studied where extension to higher order corrections are included with inverse of entropy. These corrections are very important in order to calculate micro-canonical entropy of a BHs like Schwarzschild and BTZ [142, 143]. Newly, an exponential term, has been raised to correct the entropy of a BH. These exponential corrections in BH entropy may arise in any quantum theory of gravity but it is negligible for a large horizon radius, while it is important when the BH sizes become small. Since before, no thermodynamic analysis of a rotating BH has been done with exponential entropy corrections. In this article, it has been done for Kiselev BH [144].

At present, from different astronomical observations, we are already aware about the late time cosmic acceleration of our universe [**?**, 315]. It is also assumed that the cause of this type of cosmic acceleration is caused due to the existence of a mysterious exotic matter with negative pressure and novel behaviour, well known as dark energy or quintessence. Also, it is taken as an assumption that this weird exotic matter is

distributed all over the universe like a homogeneous fluid. Quintessence is taken as a real form of energy which is distinct from any normal matter or radiation or even dark matter. In the case of symmetric BH metric, the effect of the quintessence field is incorporated by Kiselev. Various thermodynamic quantities are resolved for different values of quintessence state parameter, ω_q where $-\frac{1}{3} > \omega_q > -1$ and $\omega_q = \frac{p_q}{\rho_q}$ [147, 148]. Phase transitions and thermodynamics in rotating Kiselev BH have been studied using first order approximation of event horizon in order to study the thermodynamic mode for all values of dark energy EoS. Thermodynamic relations for Kiselev and dilation BHs are also investigated later. The instability of a large rotating BH surrounded by quintessence has been also studied in the reference [149]. Previous thermodynamic study on modified gravity BH also discloses the fact of instability for BHs as there is a shift further from Einstein's GR model [150]. Stephen Hawking, in early 1970's applied the theory of GR in order to bring out his famous horizon area theorem, according to which the entire horizon area in a clasped system bearing BHs never decreases [151]. It can merely enhance or remain the same. A few days later, Jacob Bekenstein observed the semblance between the area theorem and entropy, i.e., also entropy of a closed system never decays. It was remarked by Bekenstein that, in reality, BH's area is an exposure of its entropy [152]. This entropy required the BH temperature as a direct conformity of radiation from the BH. Later Hawking, himself, in the year 1975, confirmed that a BH can radiate by applying a quantum-mechanical method. Hawking radiation is ejected with more competency if the tidal forces are strong enough near the BH horizon. We already know that the temperature of a BH is inversely proportional to the mass of the BH. This implies that higher the temperature of a BH, smaller its mass.

In fact, Snyder has given the primary concept of smallest measurable fundamental length much earlier [153, 154]. This model was very interesting as it sustained the full Poincaré invariance. This model of Snyder does not get any extra attention at that time but some recent approaches to the development of quantum gravity theory, like string theory [155] showed the irresistible requirement of measuring smallest measurable fundamental length. Now, in different cosmological researches we can observe many

reuses of this model on behalf of modified Heisenberg algebra [156, 157]. There also exists an anti-Snyder model. Again, quantum field studies have shown us the creation of quantum particle which may cross the event horizon of the BH via quantum tunnelling which results Hawking temperature and entropy of the BH. This tunnelling probability may also increased by incorporating the GUP [158, 159, 160]. In the reference [161], using the effect of GUP, quantum corrections of Hawking temperature and entropy of a Schwarzschild BH has been investigated. Quantum aspects of BH entropy have been studied in the references [162, 163]. Logarithmic corrections of entropy was studied by the authors in [164]. Various types of BHs using GUP approach also have been studied. T. Kanazawa et al. have studied noncommutative Schwarzschild BH using GUP [165]. G. Lambiase and F. Scardigli have studied Lorentz violation using GUP [166]. Further, Kerr-Newman solution and energy in teleparallel equivalent of Einstein's theory has been also investigated by G. G. L. Nashed [167].

So far, the stability of a slowly rotating BH, like Kerr BH, has been found out and researchers have shown that the ratio between BH's angular momentum to it's mass must be much less than 1 for these cases. But the stability of a rapidly rotating BH, has not been revealed yet. Also, the researchers are not able to determine, to ensure the stability of a BH, how small the ratio of angular momentum to the BH mass has to be. Several researches have been going on this field. Kiselev metric is a simple spherically symmetric BH solution which can be modified into other types of BH solutions by changing the values of the parameters like, ω_q and σ_q. An asymptotically flat Kiselev BH solution cultivated by quintessence field is chosen for our model. In this work, we mainly inspect the various conditions for stability of a rapidly rotating BH and quantum fluctuations of various parameters of the BH. We have also studied the ratio of angular momentum to the BH mass in case of rapidly rotating BHs and tried to point out minimum value of the ratio. At the same time, we have also investigated the fluctuations in thermodynamic parameters of a rotating BH, embedded in quintessential field under the background of cosmic acceleration of the present universe, due to its rapid rotation. Thermodynamic behaviour of a rotating BH is actually observed in terms of different parameters like radius of event horizon, mass of the BH, Hawking temper-

ature, thermal heat capacity at the event horizon, entropy, surface gravity and also the rate of emission etc. After that, we have also supervised the quantum corrections of these thermodynamic parameters using modified Heisenberg uncertainty principle. The anisotropic nature and the presence of repulsive gravitational force inside the BH are observed. At the same time, phase transitions and thermal stability of the BH are also analysed under the presence of both quintessence and modified uncertainty relations for a fast rotating charged Kiselev BH.

7.1.2 Construction of Basic Mathematical Equations for Rapidly Rotating Black Hole under Quintessence Filed

We know that the value of quintessence state parameter ω_q should remain in the range of $-\frac{1}{3} > \omega_q > -1$. In order to comprehend the effect of quintessence field in the neighbouring space-time geometry of a BH, it is necessary to construct a generalized form of exact spherically symmetric solution. For this purpose, Einstein's equations satisfying BHs enclosed by quintessential matters with the energy-momentum tensor has been considered. According to this tensor which obeys the additivity and linearity conditions, the metric derived by Kiselev, can be expressed as,

$$ds^2 = -f(r)dt^2 + \frac{dr^2}{f(r)} + r^2(d\theta^2 + \sin^2\theta d\phi^2) \quad , \quad 0 \leq \theta \leq \pi \quad and \quad 0 \leq \phi \leq 2\pi \quad , \tag{7.1}$$

with

$$f(r) = 1 - \frac{2M}{r} + \frac{Q^2}{r} - \frac{\sigma_q}{r^{(3\omega_q+1)}} \quad , \tag{7.2}$$

where M, r, and Q are the mass, radius of event horizon and charge of the BH, σ_q and ω_q are normalized quintessence parameter and exotic matter equation of state parameter around the BH respectively. The value of σ_q is of the order of 10^{-4}. The small value of σ_q will not affect ω_q so much and the impact of ω_q will be visible clearly from our present investigation. On the other hand, if we can make the contribution of last two terms in the above equation (12) negligibly small, then for very small values of those parameters σ_q and Q, the function $f(r)$ resembles to Schwarzschild metric.

For a little increase in the value of σ_q, $f(r)$ decreases slightly but as r increases, $f(r)$ increases initially and reaches to a maximum. But for further increment of r, $f(r)$ decreases slowly. In various research works the parameter σ_q is chosen in the range of 10^{-2} to 10^{-4}. Again in some study on BHs with GUP approach also σ_q is chosen as in case of our model.

The relation between the energy density of quintessence field ρ_q and ω_q is given as

$$8\pi G\rho_q = -3\omega_q \frac{1}{r^2}\left(\frac{r_q}{r}\right)^{(3\omega_q+1)} \quad , \tag{7.3}$$

where the parameter, r_q has the dimension of length. It is the length at which gravitational field evolved by the quintessence grows strong. So, it is very clear that the quintessence field can be portrayed by two parameters, r_q and ω_q.

From the above equation (12), we can say that at, $r = 0$ there exists a curvature singularity. Now, $f(r) = 0$ gives radius of BH event horizon as,

$$r_h = \frac{1}{2\sigma_q}\left(1 \pm \sqrt{(1 - 8M\sigma_q)}\right) \quad . \tag{7.4}$$

The above equation (14) shows us that the event horizon exists only when $M < \frac{1}{8\sigma_q}$. The mass of the BH for event horizon can be expressed as,

$$M = \frac{r_h}{2}(1 - r_h\sigma_q) \quad . \tag{7.5}$$

We can calculate the temperature of the BH at the event horizon using the equation,

$$T_h = \frac{1}{4\pi r_h}(1 - 2r_h\sigma_q) \quad . \tag{7.6}$$

As, $T = \frac{\kappa}{2\pi}$, the surface gravity of a BH at the event horizon can be expressed as,

$$\kappa_h = \frac{1}{2r_h}(1 - 2r_h\sigma_q) \tag{7.7}$$

Now, equating the equation (16) with the equation (5) and using the equation (15), we

acquire the expression of entropy at the BH event horizon as,

$$S_h = \pi(r_h)^2 \quad , \tag{7.8}$$

which is expected from equation (3) and it is a direct evidence of the relation between area and entropy of BHs. This entropy is known as the zeroth entropy of a BH and it is denoted by S_0. From the expressions of BH mass and temperature at the event horizon of a BH as from the above equations (15) and (16), we can compute the specific heat of the BH as,

$$C_h = -2\pi r_h(1 - 2r_h\sigma_q) \quad . \tag{7.9}$$

Hence, it is obvious that for a BH to be thermodynamically stable if $r_h > \frac{1}{2\sigma_q}$. We also can verify the thermodynamical stability of a BH by using the condition, which states that, negative value of the specific heat can make the BH unstable and if the specific heat blows up, that is the significance of a second order phase transition for the BH. The rate of emission of a BH, in terms of photon which is known as BH radiation becomes,

$$\frac{dM}{dt} \propto T_h^2 \quad , \tag{7.10}$$

where t is the time of occurrence of this emission. So, the rate of emission can be expressed as,

$$\frac{dM}{dt} \propto \frac{1}{16\pi^2 r_h^2}(1 + 4\sigma_q^2 r_h^2 - 4\sigma_q r_h) \quad . \tag{7.11}$$

7.1.3 Incorporation of Generalized and Extended Heisenberg Uncertainty Principle : A Quantum Approach

The uncertainty principle always get a novel attention in quantum physics. It is widely accepted to be a fundamental limit on the measurement precisions of incompatible observable. In the microphysics state, in quantum mechanics, Heisenberg uncertainty principle in generalised form can be written as

$$\Delta x \Delta p \geq \hbar \left(1 - \frac{\alpha L_P}{\hbar}\Delta p + \beta \Delta p^2\right) \quad , \tag{7.12}$$

where the parameter β is linked with the deformation parameter $\theta^{\mu\nu}$, which is a byproduct of noncommutative geometry. The current bounds on β works good for the $(2,0)$ ranked tensor. Violation of Lorentz invariance is also linked with the deformation parameter β of GUP approached study. GUP studied from the point of baryon asymmetry, also denotes the values of β. Again in the above equation, L_P is the Plank's length as already given in equation (8) and α is the dimensionless positive parameter with upper bound of the order of 10^{31}. For our work, by using extended Heisenberg uncertainty principal, we have chosen $\beta = \frac{\alpha^2 L_P^2}{\hbar^2}$.

So, the quadratic form of the above equation (22) can be written as,

$$\Delta p \geq \hbar \left(1 + \frac{\alpha^2 L_P^2}{\hbar^2} \Delta p^2\right) \quad . \tag{7.13}$$

The equation (22) can also be written as,

$$\Delta p \geq \frac{\hbar \Delta x}{2\alpha^2 L_P^2} \left(1 - \sqrt{1 - \frac{4\alpha^2 L_P^2}{\Delta x^2}}\right) \quad . \tag{7.14}$$

From the early work of Snyder, where he used the idea of noncommutative geometry to avoid the divergence in quantum field theory. In his work, he took the equations as

$$[X_\mu, P_\nu] = i\hbar(\eta_{\mu\nu} + \theta P_\mu P_\nu) \quad , \tag{7.15}$$

and

$$[X_\mu, X_\nu] = i\hbar\theta J_{\mu\nu} \quad , \quad [P_\mu, P_\nu] = 0 \quad , \tag{7.16}$$

where $\eta_{\mu\nu}$ is the metric tensor and given by $[\eta_{\mu\nu}] = \text{diag}[-1\ 1\ 1\ 1]$. Here, the deformation parameter, θ is taken as, $\theta \propto L_P^2$. Here, $J_{\mu\nu} = x_\mu p_\nu - x_\nu p_\mu$ with space-time indices μ and ν generates Lorentz transformations2. From the above equations (25) and (26) we can say that when $\theta > 0$ the Snyder model gives a discrete spatial and continuous time spectrum whereas $\theta < 0$ gives just the opposite case, i.e., continuous spatial and discrete time spectrum. This opposite case is known as anti-Snyder model.

Now, according to the modified Snyder model

$$[X, P] = i\hbar\sqrt{(1 + \alpha P^2)} \quad , \tag{7.17}$$

where $\alpha = \frac{\alpha_o}{M_p c^2} = \frac{\alpha_o L_P}{\hbar}$. M_p and L_P are the Planck mass and Planck length respectively. From equation (27) it is clear that $\alpha \to 0$ gives back the ordinary Heisenberg algebra. The position and momentum operators, in the momentum space can be represented as

$$P = p \quad , \qquad X = i\hbar\sqrt{(1 + \alpha p^2)}\frac{\delta}{\delta p} \quad . \tag{7.18}$$

Again using the binomial expansion, expanding the above equation (27) with respect to deformation parameter α, we get

$$[X, P] = i\hbar\left(1 + \frac{\alpha}{2}P^2 - \frac{\alpha^2}{8}P^4 + \frac{\alpha^3}{16}P^6 - .....\right) \quad . \tag{7.19}$$

The equations (27) and (29) gives the uncertainty relation after considering the average values, in the modified form as,

$$\begin{aligned}
(\Delta X)(\Delta P) &\geq \tfrac{\hbar}{2}\left\langle\left(\sqrt{(1 + \alpha p^2)}\right)\right\rangle \quad , \\
&\geq \tfrac{\hbar}{2}\left\langle\left(1 + \tfrac{\alpha}{2}P^2 - \tfrac{\alpha^2}{8}P^4 + ...\right)\right\rangle \quad , \\
&\geq \tfrac{\hbar}{2}\left(1 + \tfrac{\alpha}{2}\langle P^2\rangle - \tfrac{\alpha^2}{8}\langle P^4\rangle + ...\right) \quad , \\
&\geq \tfrac{\hbar}{2}\left(1 + \tfrac{\alpha}{2}\left[(\Delta P)^2 + \langle P\rangle^2\right] - \tfrac{\alpha^2}{8}\left[(\Delta P)^2 + \langle P\rangle^2\right] + ...\right) \quad ,
\end{aligned}$$

where we have applied the property, $\langle P^{2n}\rangle \geq \langle P^2\rangle^n$ and after using the above derivation of the modified uncertainty relation, the first order α gives,

$$(\Delta X)(\Delta P) \geq \frac{\hbar}{2}\sqrt{1 + \alpha\left[(\Delta P)^2 + \langle P\rangle^2\right]} \quad , \tag{7.20}$$

which is our required equation to find out the uncertainty in position. So, the utmost smallest uncertainty in position X becomes

$$(\Delta X) \simeq \hbar\sqrt{\frac{\alpha}{2}} \quad . \tag{7.21}$$

In the similar process, we also can obtain the required equation of finding out the

uncertainty in momentum as well. For this purpose, we took the relation between position X and momentum P as

$$[X, P] = i\hbar\sqrt{(1 + \beta X^2)} \quad , \tag{7.22}$$

where, $\beta = \frac{1}{l_H^2}$ with anti de-Sitter radius l_H^2. The position and momentum operators, in the position representation can be represented as,

$$X = x \quad , \quad P = \frac{\hbar}{i}\sqrt{(1 + \beta x^2)}\frac{\delta}{\delta x} \quad . \tag{7.23}$$

Again using the binomial expansion, expanding the above equation (32) with respect to deformation parameter β, we get

$$[X, P] = i\hbar\left(1 + \frac{\beta}{2}X^2 - \frac{\beta^2}{8}X^4 + \frac{\beta^3}{16}X^6 - .....\right) \quad . \tag{7.24}$$

Now, we use the equations (32) and (34) and also the property, $\langle X^{2n}\rangle \geq \langle X^2\rangle^n$ and after using the same above derivation like the equation (30), we can derive the modified uncertainty relation for first order β as,

$$(\Delta X)(\Delta P) \geq \frac{\hbar}{2}\sqrt{1 + \beta\left[(\Delta X)^2 + \langle X\rangle^2\right]} \quad , \tag{7.25}$$

which is our required equation to find out the uncertainty in momentum. So, the utmost smallest uncertainty in momentum P becomes,

$$(\Delta P) \simeq \hbar\sqrt{\frac{\beta}{2}} \quad . \tag{7.26}$$

7.1.4 Quantum corrections of Thermodynamic Parameters of the Rotating Black Hole Surrounded by Quintessence

For any type of thermal agitation effect, the fluctuations in energy can be written as

$$(\Delta E) = \frac{3}{2}K_B T \quad , \tag{7.27}$$

where K_B is the Boltzmann constant and T is the temperature. Using the above equation (36) we can derive the expression of temperature of any massless quantum particle near BH horizon with mass M as

$$T = \frac{c\Delta P}{K_B} \quad , \tag{7.28}$$

where c is the velocity of light and $\Delta P = \frac{\Delta E}{c}$. We can also derive the expression of radius of event horizon of a rotating Kiselev BH by using the same equation like equation (15) as

$$r = \frac{2G}{c^2}\left[\frac{r_h}{2}(1 - r_h\sigma_q)\right] \quad . \tag{7.29}$$

Here, we can see that, due to rotation of the BH and effect of quintessential field at the same time, there is a variation of mass of the BH. These effects are incorporated also. Now, using equation (39) and (15) we can also define the radius of the Kiselev BH at the event horizon at $(r = r_h)$ as,

$$(\Delta X) = 2\pi r_h = 2\pi\frac{G}{c^2}\left[r_h(1 - r_h\sigma_q)\right] \quad . \tag{7.30}$$

We employ the equations (38) and (40) in the equation (35) and find

$$\left(2\pi\frac{G}{c^2}\left[r_h(1 - r_h\sigma_q)\right]\right)(K_BT) \geq \frac{\hbar c}{2}\sqrt{1 + \beta\left(2\pi\frac{G}{c^2}\left[r_h(1 - r_h\sigma_q)\right]\right)^2} \quad . \tag{7.31}$$

This is the quadratic equation using which we can get the idea of mass-temperature relationship of a BH. Using this equation it is also possible to find out the uncertainty in momentum of the BH.

Now, as we know for a rotating BH, its angular momentum J can be expressed as,

$$J = \frac{M^2Ga}{c} \quad , \tag{7.32}$$

where a is the spin parameter of the rotating BH. The value of a lies in between maximum and minimum spin value of a BH, i.e., $0 \leq a \leq 1$. We use the angular momentum of a BH instead of ordinary momentum and using equation (38), again we

also can derive the expression of temperature of any massless quantum particle near a rotating BH horizon with mass M as,

$$T \approx \frac{c}{K_B}\left(\frac{M^2Ga}{c}\right) \quad with\ \Delta(p) = p \quad and \quad \Delta(X) = x \quad . \tag{7.33}$$

The above equation gives the mass-temperature relationship of a rotating BH with the spin parameter a with high approximation and neglecting higher order terms. Without approximation using equations (30), (35)and (40)the above equation (43) can be written as $(\Delta X)(K_BT) = (2\pi r_h)\,(K_BT) = \frac{\hbar c}{2}\sqrt{1+\beta(\Delta X)^2}$.

We now employ the equation (40) and (43) in the equation (35) in order to find out the uncertainty in the momentum of a rotating BH and can derive the equation as,

$$\left(2\pi\frac{G}{c^2}\left[r_h(1-r_h\sigma_q)\right]\right)\left(\frac{M^2Ga}{c}\right) \simeq \frac{\hbar c}{2}\sqrt{1+\beta\left(2\pi\frac{G}{c^2}\left[r_h(1-r_h\sigma_q)\right]\right)^2} \quad . \tag{7.34}$$

Now, we can also derive the equation which can give the uncertainty in position of the Innermost Stable Circular Orbit of a spinning BH by using the equations (30), (40) and (42), which gives,

$$\left(2\pi\frac{G}{c^2}\left[r_h(1-r_h\sigma_q)\right]\right)\left(\frac{M^2Ga}{c}\right) = \frac{\hbar c}{2}\sqrt{1+\alpha\left(\frac{M^2Ga}{c}\right)^2} \quad . \tag{7.35}$$

From the above equation, we also can say that, for a spinning BH, its angular momentum is conserved but not constant as when the angular momentum changes, it should be counterbalanced by the changing the position of the event horizon. As a consequence of this fact the position of ISCO also changes depending on the spin of a BH.

Here we assume the uncertainty in position (ΔX) for events near the event horizon of a rotating BH. Now, using the equations (16), (29) and (30) we can obtain the quantum corrected Hawking temperature, T_Q of a rotating BH as,

$$T_Q = T_h\left[\frac{\hbar c}{2}\sqrt{1+\alpha\left(\frac{M^2Ga}{c}\right)^2}\right]^{-1} \quad . \tag{7.36}$$

The above equation gives value of temperature depending on the quintessence field effect on the BH along with the spinning effect of the BH.

The expression for the quantum corrected entropy for the rotating BH with quintessence field effect and after using the equations (18) and (29) becomes,

$$S_Q = S_h - \pi r_h \left[\frac{\hbar c}{2} \sqrt{1 + \alpha \left(\frac{M^2 G a}{c} \right)^2} \right] \quad . \tag{7.37}$$

Above quantum corrected entropy of the rotating BH also contains the logarithmic terms and can be expressed as,

$$S_h = S_0 + \alpha ln f(S_0) + \frac{\gamma}{S_0} + \eta \exp^{g(S_0)} \quad , \tag{7.38}$$

where $S_0 = \frac{A}{4L_P^2}$. α, β and γ are some constants. Also $f(S_0)$ and $g(S_0)$ are suitable functions of uncorrected BH entropy S_0. The exponential term is negligible for large BH area, A. But its effect is important when the BH area is small, Therefore, it is considered as a quantum effect for the small BH as well as logarithmic correction. This quantum effect in our study is very much effective as the area of the event horizon shrinks when the BH rotates faster due to its spin. Now, we have used quantum corrected temperature and quantum corrected entropy in order to find the quantum corrected heat capacity and using the equations (4), (19) and (29) it can be expressed as,

$$C_Q = \frac{C_h \left[\frac{\hbar c}{2} \sqrt{1 + \alpha \left(\frac{M^2 G a}{c} \right)^2} \right]}{1 - (1 - 2 r_h \sigma_q) \left[\frac{\hbar^2 c^2}{4} \left(1 + \alpha \left(\frac{M^2 G a}{c} \right)^2 \right) \right]} \quad . \tag{7.39}$$

Physically, BH is may not be stable if it is small but for a rotating BH, when its event horizon shrinks at the same time, the effect of quintessence field comes into play and it has a important role in its stability. As the BH turns to big, there is a phase transition of the BH from first order to second order. In this way a large BH goes to the stable state and the specific heat becomes infinity.

The expression of quantum corrected Helmholtz free energy comes from using the

equations (15), (47) and (49) and it is gives as,

$$F_Q = M - T_Q S_Q = M - \left(T_h \left[\frac{\hbar c}{2} \sqrt{1 + \alpha \left(\frac{M^2 G a}{c} \right)^2} \right]^{-1} \right) \left(S_h - \pi r_h \left[\frac{\hbar c}{2} \sqrt{1 + \alpha \left(\frac{M^2 G a}{c} \right)^2} \right] \right) \quad . \tag{7.40}$$

Now, finally we can obtain the quantum corrected rate of emission given as,

$$\frac{dM}{dt} \propto \frac{1}{16\pi^2 r_h^2} (1 + 4 r_h^2 \sigma_q^2) \left(\frac{\hbar c}{2} \sqrt{1 + \alpha \left(\frac{M^2 G a}{c} \right)^2} \right)^{-2} \quad . \tag{7.41}$$

The absolute smallest uncertainty in momentum which is derived in the equation (36), gives the idea of lower bound value of the BH temperature. Using the equation (38) along with equation (36) we can derive the lower bound temperature of the BH as,

$$T_L = \frac{\hbar c}{K_B} \sqrt{\frac{\beta}{2}} \quad . \tag{7.42}$$

Now, the quadratic mass-temperature equation (41) has a solution like,

$$M(T_Q) = M(T_h) \left[1 - \frac{1}{2} \frac{T_L^2}{T^2} \right]^{-\frac{1}{2}} \quad , \tag{7.43}$$

where $M(T_h) = \frac{\hbar c^3}{8\pi G K_B T}$. From he above mass-temperature function we can say that for $T_L = 0$, it will back to its ordinary form. Now, using binomial expansion, the equation (53) can be expanded as,

$$M(T_Q) = M(T_h) \left[1 + \frac{1}{4} \frac{T_L^2}{T^2} + ... \right] \quad . \tag{7.44}$$

We also observe that, using the equation (51), the specific heat of a BH can be expressed as,

$$C(T_Q) = c^2 \frac{dM}{dT} = c^2 \frac{1}{16\pi^2 r_h^2} (1 + 4 r_h^2 \sigma_q^2) \left(\frac{\hbar c}{2} \sqrt{1 + \alpha \left(\frac{M^2 G a}{c} \right)^2} \right)^{-2} \quad . \tag{7.45}$$

By substituting equation (53) in the above equation, we obtain

$$C(T_Q) = C(T_h)\left[1 - \frac{1}{2}\frac{T_L^2}{T^2}\right]^{-\frac{3}{2}} \quad , \tag{7.46}$$

where $C(T_h) = -\frac{\hbar c^5}{8\pi G K_B T^2}$. We can also expand the above equation (56) as,

$$C(T_Q) = C(T_h)\left[1 + \frac{3}{4}\frac{T_L^2}{T^2} + ...\right] \quad . \tag{7.47}$$

Now employing the equation (53) in order to find the entropy of a BH as,

$$S(T_Q) = S(T_h)\frac{\hbar c^5}{4\pi G K_B T_L^2}\left[1 - \frac{1}{2}\frac{T_L^2}{T^2}\right]^{-\frac{1}{2}} \quad , \tag{7.48}$$

where $S(T_h) = \frac{\hbar c^5}{16\pi G K_B T^2}$. We also can expand the above equation (58) as,

$$S(T_Q) = S(T_h)\left[1 + \frac{4T^2}{T_L^2} + ...\right] \quad . \tag{7.49}$$

7.1.5 Graphical Interpretations and Observational Support

Now, in order to investigate the nature and various properties exhibited by the charged and rotating Kiselev BH, we have plotted all the derived and quantum corrected important parameters with respect to radius of event horizon, r_h and spin, a. In all the plots, we have chosen the finite mass M and very low value (almost negligible) of charge, Q of the BH. The spin parameter a and the angular momentum, J of the BH is chosen in a fashion so that the $\frac{J}{M}$ ratio becomes minimum and in our investigation the ratio becomes near 0.5.

At the beginning, we have plotted the variations of quantum corrected Hawking temperature T_Q, derived by using extended HUP, with respect to the radius r_h and spin parameter a, for different values of quintessence parameter of the rotating Kiselev BH, respectively in figures $27a - 27c$. We have chosen the value of α very small as, $\alpha = 0.5$ and the value of $\sigma_q = 10^{-4}$ and $J = 0.01$. Here, we follow the existence of points of inflection when the spin of the BH is not so fast. As spin grows high, chances

of obtaining such a point becomes less. The temperature is overall decreasing with the increase of radius of event horizon or the spin parameter both. At the same time, interestingly we have observed that, at low value of quintessence field, the temperature falls rapidly but as the quintessence field increases, the fall in temperature becomes slower.

$Fig-27a$ $Fig-27b$ $Fig-28c$

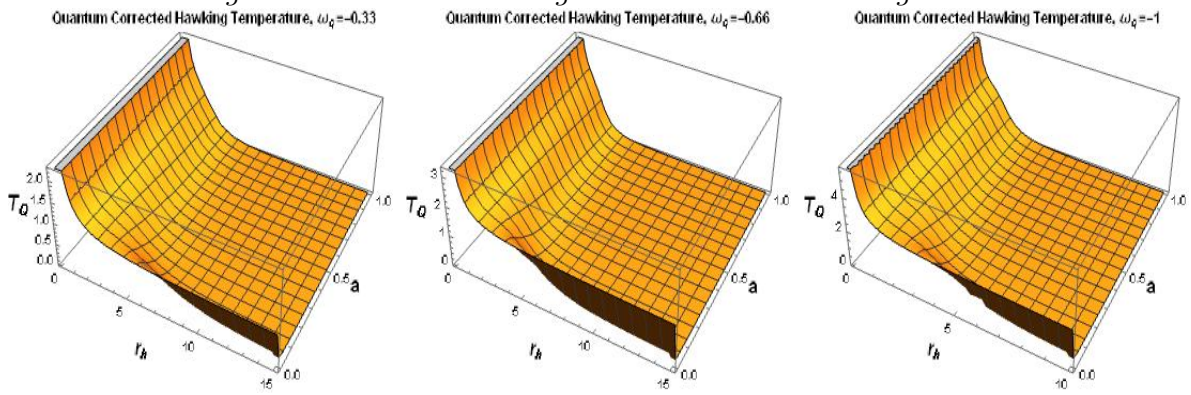

Figure 7.1: *Represent the variations of Hawking Temperature, T_Q with respect to r_h and a for $\omega_q = -0.33$.*

Figure 7.2: *Represent the variations of Hawking Temperature, T_Q with respect to r_h and a for $\omega_q = -0.66$.*

Figure 7.3: *Represent the variations of Hawking Temperature, T_Q with respect to r_h and a for $\omega_q = -1$.*

After that, we have plotted the variations of quantum corrected entropy S_Q, derived by using extended HUP, with respect to the radius r_h and spin parameter a, for different values of quintessence parameter of the rotating Kiselev BH, respectively in figures $28a - 28c$. Here also, we have taken the same value of α, σ_q and J as chosen above. The variation of entropy has shown a very strange nature. From these plots, entropy is found to increase first and then decrease and approaches to zero as radius of event horizon decreases and quintessence field increases.

Next, we have plotted the variations of quantum corrected heat-capacity C_Q, derived by using extended HUP, with respect to the radius r_h and spin parameter a, for different values of quintessence parameter of the rotating Kiselev BH, respectively in figures $29a - 29c$. We have kept the value of α very small as, $\alpha = 0.5$ and the value of

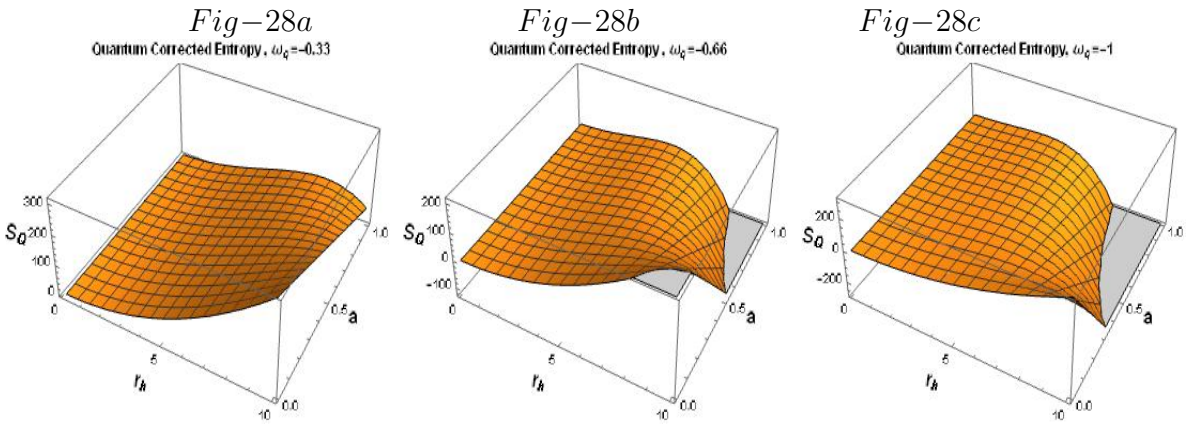

Figure 7.4: *Represent the variations entropy,* S_Q *with respect to* r_h *and a for* $\omega_q = -0.33$.

Figure 7.5: *Represent the variations of entropy,* S_Q *with respect to* r_h *and a for* $\omega_q = -0.66$.

Figure 7.6: *Represent the variations of entropy,* S_Q *with respect to* r_h *and a for* $\omega_q = -1$.

$\sigma_q = 10^{-4}$ and $J = 0.01$. These plots arises very interesting outcomes. However, heat capacity is seen to decrease first and then through an infinite jump it becomes positive. Then it again decreases to a value asymptotically equal to zero. This indicates that the considered type of BH's were in stable condition when they were not too big. Through a second kind of phase transition it turns to be stable one. Again, as the quintessence field increases, the phase transition becomes prominent with the decrease in the value of the radius of the event horizon, as it approaches zero.

Now, we have plotted the variations of quantum corrected Helmholtz free energy F_Q, derived by using extended HUP, with respect to the radius r_h and spin parameter a, for different values of quintessence parameter of the rotating Kiselev BH, respectively in the figures $30a - 30c$. We have chosen the value of α very small as, $\alpha = 0.5$ and the value of $\sigma_q = 10^{-4}$ and $J = 0.01$. A more interesting thing is found when the free energy is seen to have a cuspidal type of double points as it is plotted.

We have also plotted the variations of quantum corrected rate of emission $\frac{dM}{dt}$, derived by using extended HUP, with respect to the radius r_h and spin parameter a, for different values of quintessence parameter of the rotating Kiselev BH, respectively

$Fig-29a$ $Fig-29b$ $Fig-29c$

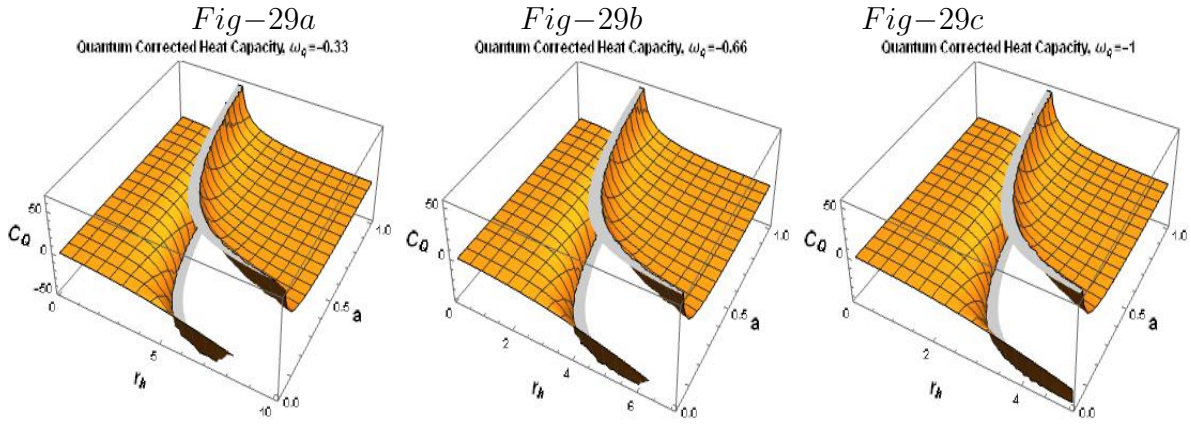

Figure 7.7: *Represent the variations of heat-capacity, C_Q with respect to r_h and a for $\omega_q = -0.33$.*

Figure 7.8: *Represent the variations of heat-capacity, C_Q with respect to r_h and a for $\omega_q = -0.66$.*

Figure 7.9: *Represent the variations of heat-capacity, C_Q with respect to r_h and a for $\omega_q = -1$.*

$Fig-30a$ $Fig-30b$ $Fig-30c$

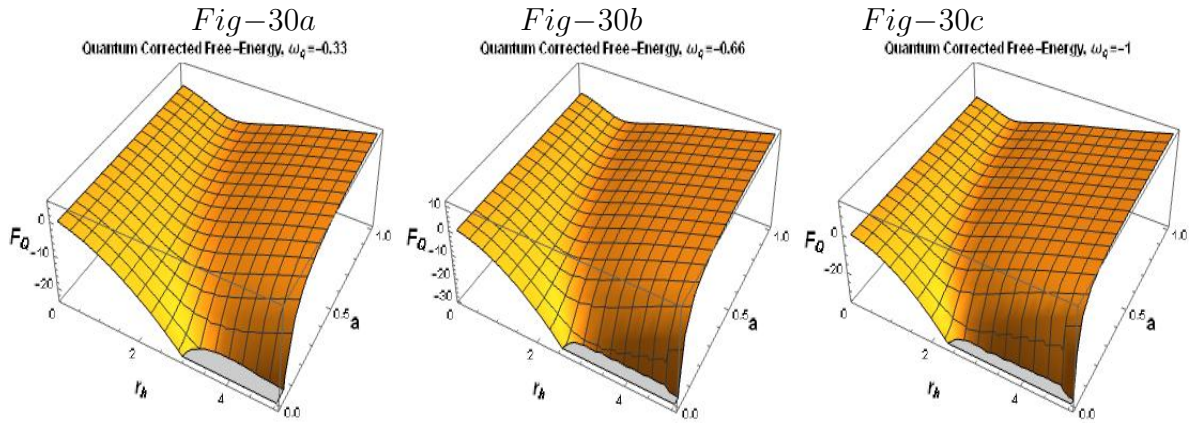

Figure 7.10: *Represent the variations of Helmholtz free energy, F_Q with respect to r_h and a for $\omega_q = -0.33$.*

Figure 7.11: *Represent the variations of Helmholtz free energy, F_Q with respect to r_h and a for $\omega_q = -0.66$.*

Figure 7.12: *Represent the variations of Helmholtz free energy, F_Q with respect to r_h and a for $\omega_q = -1$.*

in figures $31a - 31c$. We have chosen the value of α very small as, $\alpha = 0.5$ and the value of $\sigma_q = 10^{-4}$ and $J = 0.01$. The change in mass changing rate is found to be a

increasing function of the radius of event horizon.

$Fig-31a$ $Fig-31b$ $Fig-31c$

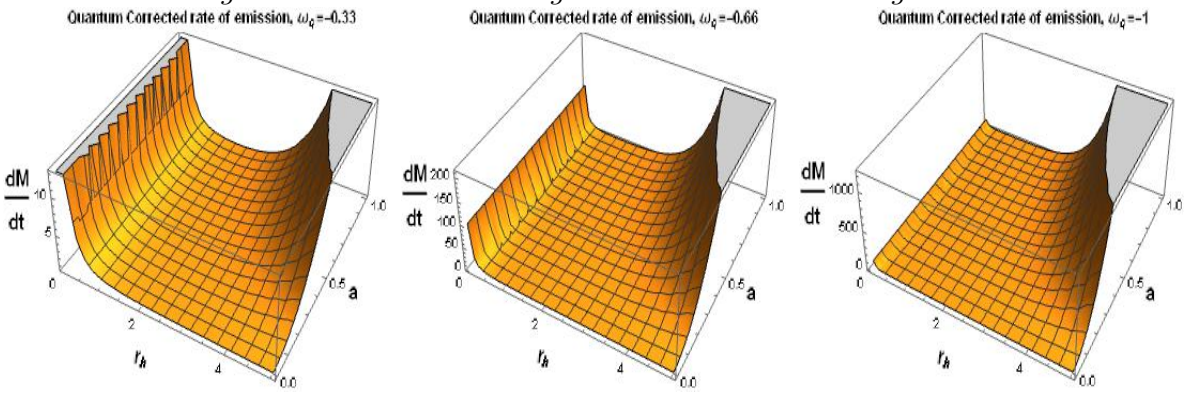

Figure 7.13: *Represent the variations of quantum corrected rate of emission,* $\frac{dM}{dt}$ *with respect to* r_h *and a for* $\omega_q = -0.33$.

Figure 7.14: *Represent the variations of quantum corrected rate of emission,* $\frac{dM}{dt}$ *with respect to* r_h *and a for* $\omega_q = -0.66$.

Figure 7.15: *Represent the variations of quantum corrected rate of emission,* $\frac{dM}{dt}$ *with respect to* r_h *and a for* $\omega_q = -1$.

We have also shown the variation of quantum corrected Hawking temperature T_Q, Entropy, S_Q, heat capacity, C_Q and Helmholtz free energy, F_Q, respectively with respect to the mass, M and charge, Q of the BH in the figures $32 - 35$. We have chosen the value of BH's angular momentum J as $J = 0.01$. These plots indicates very interesting facts of the Kiselev BH.

At last, we have plotted the variations of quantum corrected Helmholtz free energy F_Q with quantum corrected Hawking temperature T_Q, derived by using extended HUP, using quintessence parameter ω_q and spin parameter a of the rotating Kiselev BH, respectively in the figure 36. We have chosen the value of α very small as, $\alpha = 0.5$ and the value of $\sigma_q = 10^{-4}$. This plot also yield a fascinating outcome as no double point is found in the variation of the above mentioned parameters.

$Fig-32$

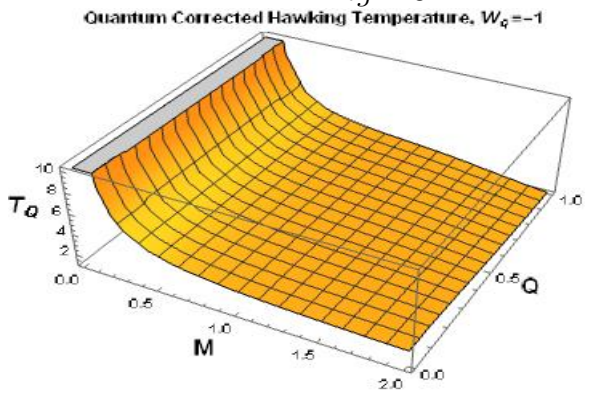

$Fig-33$

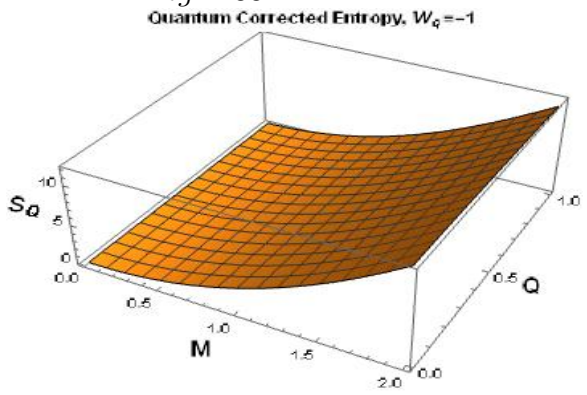

Figure 7.16: *Represent the variations of quantum corrected Hawking Temperature,* T_Q *with respect to* M *and* Q *for* $\omega_q = -1$.

Figure 7.17: *Represent the variations of quantum corrected entropy,* S_Q *with respect to* M *and* Q *for* $\omega_q = -1$.

$Fig-34$

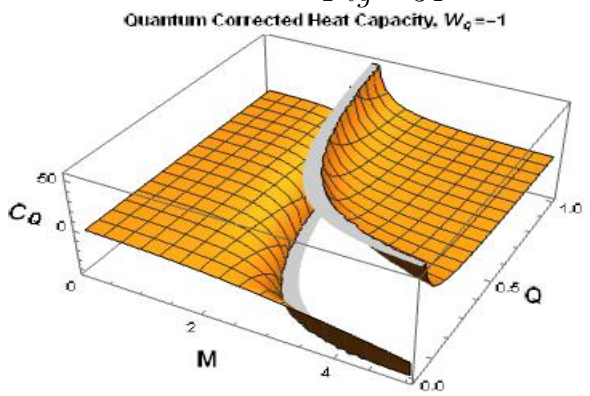

$Fig-35$

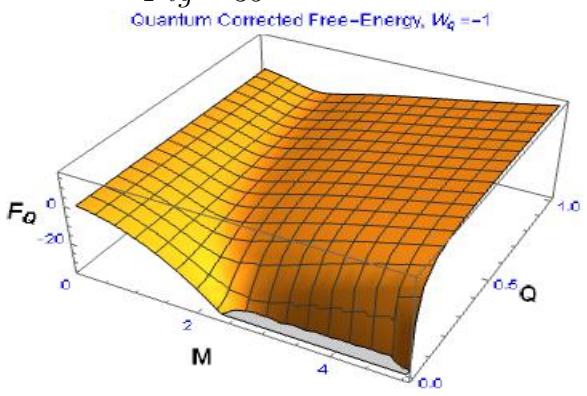

Figure 7.18: *Represent the variations of quantum corrected heat-capacity,* C_Q *with respect to* M *and* Q *for* $\omega_q = -1$.

Figure 7.19: *Represent the variations of quantum corrected Helmholtz free energy* F_Q*, with respect to* M *and* Q *for* $\omega_q = -1$.

7.1.6 Brief Discussions and Conclusion

From our investigation of this special type of BH, we have got very interesting outcomes which will motivate to study it further in future. We know that, BHs can evaporate with time by radiating heat through the process of quantum tunnelling. So, the stability of the BH depends on this tunnelling phenomenon also. This tunnelling effect can

$Fig - 36$

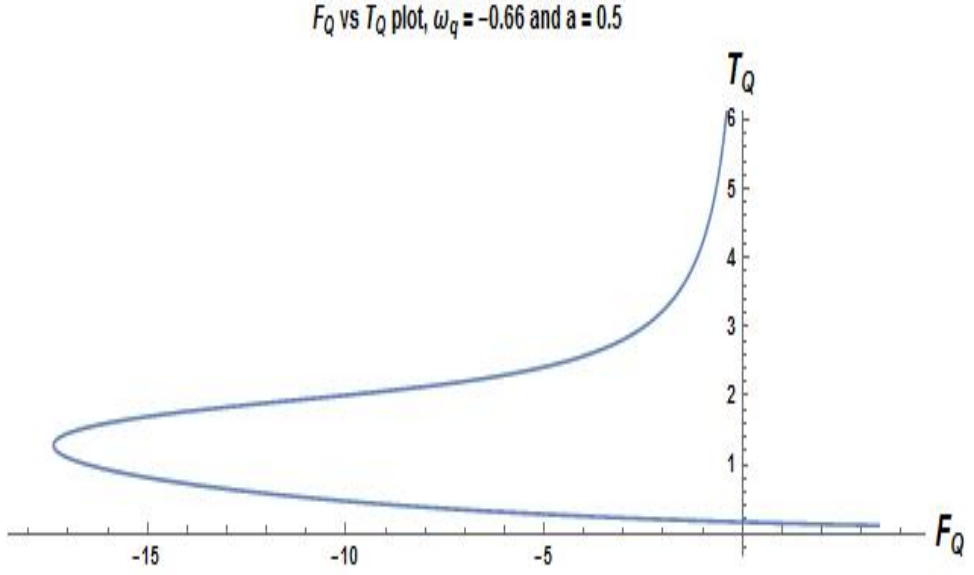

Figure 7.20: *Represent the variations of* F_Q *vs* T_Q*, for* $\omega_q = -0.66$ *and* $J = 0.01$.

be measured from the variation of Hawking temperature and entropy of a BH. In our work, we have measured the variation of quantum corrected Hawking temperature with respect to the spin, mass and charge of the BH and got very interesting result. The Hawking temperature decreases rapidly with the increase of spin and mass of the BH but the rate of fall of temperature decreases with time as the quintessence field comes into play. As the effect of quintessence field increases, the repulsive gravitational force inside the BH also increases and in turn dark matter distribution increases. Due to this effect of quintessence field, the fall of Hawking temperature becomes slower, i.e, the rate of tunnelling decreases as well as the stability of the BH with time increases. So, from this result we can conclude that, a low mass, charged and rotating BH has got its stability in space with time. The quintessence field plays a very crucial role on the stability of the BH.

Again, the variation of quantum corrected entropy shows a peculiar nature. The entropy does not depend on charge of the BH, when its mass is low. But, interestingly, it increases with the increase in mass. For large mass, if we increase the charge, entropy decreases and approaches to zero. In our work, from these plots, entropy is found to increase first and then decrease and approaches to zero as radius of event

horizon decreases and quintessence field increases. This is quite obvious and reveals an attractive information about this BH. As, we already know that, as the area of BH increases, the entropy also increases. But, due to the simultaneous effect of increasing quintessence field and the mass of the BH, the radius of event horizon and the spin of the BH decreases which turns entropy to decrease with time. This result also indicates the stability of the BH with time. Besides, if we keep the mass of the BH constant, then for a certain limit, the BH behaves as a natural system containing charge, i.e, irreversible process and if we cross the limit, the BH behaves like irreversible system. But, we have also got the fact that, the entropy increases with increases in mass and charge simultaneously which is in good understanding with the entropy of any natural system.

The plots of variation of quantum corrected heat capacity with respect to mass, charge, spin and radius of event horizon, arises very interesting outcomes. However, heat capacity is seen to decrease first and then through an infinite jump it becomes positive. Then it again decreases to a value asymptotically equal to zero. This indicates that the considered type of BH's were in stable condition when they were not too big. Through a second kind of phase transition it turns to be stable one. we also can observe that, when mass is low the heat capacity does not depend on charge of the BH. But, as we increase the mass, the heat capacity decreases and approaches to negative value. This signifies that, BH is unstable when it's mass is large. At the same time if we increase the mass and charge simultaneously, we got the second order phase transition. Again, as the quintessence field increases, the phase transition becomes prominent with the decrease in the value of the radius of the event horizon, as it approaches zero.

In the plots of variation of quantum corrected Helmholtz free energy, we have found that, if the charge of the BH is low then, this quantity becomes constant with the variation of mass. But for increasing value of charge, Helmholtz free energy increases with increase of mass of the BH. If we increase charge of the BH, keeping it's mass constant, Helmholtz free energy stars increasing slowly. From the variation of rate of emission of the BH, we observe that, under the quintessence field effect the rate of emission decreases with the increase in quintessence field.

So, after a lot of observations and discussions on the variation of various crucial parameters of a charged rotating BH, finally, we can say that, in this article, we have cultivated a special kind of BH using modified Heisenberg algebra. A charged rotating Kiselev BH, embedded in quintessence field has been chosen for this purpose. Various important thermodynamic parameters have been investigated in order to study the BH's stability and its behaviour under the present situation of the universe. We have also find out the minimum ratio of $\frac{J}{M}$, which is required for the stability. Quantum corrections of those parameters have also been done. Their variation with the radius of event horizon, spin, mass, charge and quintessence field shows different aspects of our study. The effect of quintessence field on those parameters and as well as the nature of the BH is a very crucial and interesting part of our investigation. We have got very promising graphs. Results from graphical analysis show that the chosen BH behaves not so much differently from other types of BH's but still possesses some unique properties and nature. These uncommon properties are very much interesting for the future study and investigation on these types of BH's. The phase transitions play a crucial role in the thermal stability of this kind of BH. Application of extended Heisenberg principle shows that BH temperature decreases on a long term but the specific heat signifies that the BH may turn from unstable to stable through a second order phase transition. Studies of free energy does not show any double point if it varies with temperature. Furthermore, in case of our study, we got that in case of this type of BH the ratio between angular momentum to the mass of the BH lies near 0.5, as the minimum value for the stability. So, a rotating and charged BH, under the effect of quintessence field has also got its stability by the variation of its mass, charge, spin and radius of event horizon.

Part VI

STRUCTURAL EVOLUTION OF THE NEUTRON STARS THROUGH DARK ENERGY DOMINATED UNIVERSE : INVESTIGATING THE EQUATION OF STATE AND THE PROPERTIES IN MODIFIED GRAVITY

"It is a profound and necessary truth that the deep things in science are not found because they are useful; they are found because it was possible to find them".

—Julius Robert Oppenheimer

CHAPTER 8

ANISOTROPIC NEUTRON STARS IN $F(T)$ MODIFIED GRAVITY

8.1 Equation of State and Stability of Charged Compact Stars in $f(T)$ Modified Gravity under Krori-Barua Spacetime

8.1.1 Prelude

This present work mainly focuses on modeling the charged compact stars and investigating their properties in the framework of $f(T)$ modified gravity, under the accelerated phase of the universe. In this study we have introduced the modified gravity and dark matter to culture the evolution of the charged neutron stars by considering the present situation. True knowledge and proper study on the macroscopic parameters of the compact stars are very much needed to realize the microscopic properties and behavior of the core nuclear matter at very high density and pressure. The existence of modified Chaplygin gas as an exotic fluid inside the core of these stars in $f(T)$ gravity plays a very important role inside the stars. We have found out that, exotic fluid has

a great impact on the equation of state of the core nuclear matter and even on the stability of the compact stars. Pressure anisotropy reduces the tidal deformability of the charged stars in an appreciable amount and helps to get a more compact structure. But surprisingly, the compact stars are still able to maintain their spherically stable and equilibrium configuration. Further, we can put constraints on several macroscopic parameters of the compact stars and can investigate their evolution from our present investigation.

In this decade mainly, search on compact stars has achieved a great height due to NICER data release on neutron stars [168, 169]. Again, the binary star merger event is the main source of detecting gravitational waves (GW hereafter). This discovery of GW by LIGO/VIRGO [170, 171], is path breaking and has given enthusiasm to the scientists for further study on the compact stars in various ways. A lot of research is going on but still a generalized equation of state (EoS hereafter) of the core nuclear matter of the compact stars at very high density and pressure is not found out [172, 293]. Scientists are trying to explain the accelerated phase of the universe by using the modified gravity and incorporating the existence of dark matter with large negative pressure, known as dark energy [184]. The discovery of gravitational waves and some highly massive compact stars, has given the opportunity to culture the effect of dark matter as well as the equation of state of the core nuclear matter of the compact stars simultaneously. A rigorous investigation on the star macroscopic parameters like its mass, radius etc. is needed to understand the actual EoS of the core nuclear matter. A variety of assumptions are taken into account in order to get the proper EoS by maintaining spherical configuration of the star [174, 175]. The recent discovery of GW and few highly massive neutron stars [176, 296, 178, 298] have imposed some constraints on its EoS and as well as its several macroscopic parameters. Recent studies suggest the presence of pressure anisotropy inside the compact stars [180, 223] but exact reason behind its origin and also its impact on the compact stars, under further investigation. At this present time we are well aware about the accelerated phase of the universe [182, 183]. Under the accelerated phase of the universe, the compact stars contain which type of matter is also under debate. In this situation, general relativity (GR

hereafter) theory has faced a few difficulties to give a proper explanation on these types of highly massive and relativistic compact objects. Moreover GR theory can not accommodate the tension in the Hubble Constant under the accelerated phase of the universe. In order to solve the problems raised in the case of treating the compact objects applying GR, various alternative theories come into play [185, 186, 187, 188]. Nowadays modified gravity theories instead of GR have gotten very much attention in this regard because they can successfully handle the massive relativistic compact objects by incorporating the dark energy [189, 190, 359, 192, 193].

The investigation on the charged compact objects using GR, have been studied for a long time [272, 200, 201]. Study on the stability of charged fluid spheres using Einstein-Maxwell field equations has become a good model for charged compact objects like black holes (BH hereafter), strange quark stars etc [202, 207]. So, many methods are there to study the amount of significant residual charge in compact stars [204, 205]. Equilibrium and stability of charged strange quark stars with charged perfect fluid, has been studied in the reference [279]. In the reference [207], EoS of spherically charged compact objects have been modeled by considering a Gaussian distribution of electric charge at the star's surface. In the reference [383], the charged compact stars in $f(R)$ gravity have been investigated. Stellar models on charged compact stars using $f(G)$ gravity also have been studied in the reference [384]. Biswas et al., have studied anisotropic strange stars in $f(R,T)$ gravity [210]. On the other hand, several investigations on the modified $f(T)$ teleparallel gravity theories and symmetries in teleparallel cosmology have been done in the references [212, 213]. In the references [211], analysis of cosmological perturbations in the background of $f(T)$ gravity have been studied. Again, different types of black hole (BH hereafter) solutions using gravitational waves in $f(T)$ gravity along with their stability, curvature and thermodynamic analysis have been also investigated in the references [214, 215].

In this present work, our main aim is to get a realistic and generalized EoS of the core nuclear matter of the charged compact stars and to investigate its properties and structural evolution through the accelerated universe. We have also investigated the origin and role of anisotropy on the compact stars. We have done our work under $f(T)$

gravity because of its dominance over GR to handle the compact stars. At the same time, modified gravity can also accommodate the tensions in the present accelerated phase of expansion of the universe. Under this situation how compact objects are able to maintain their spherically stable structure is also a surprising fact to study. Here, we have chosen, $f(T) = T + \alpha T^2$, where T denotes torsional scalar and α as a regulatory parameter. We also have chosen the presence of modified Chaplygin gas (MCG hereafter) as an exotic fluid inside the star along with normal matter. This will help us to study the anisotropy rigorously and also the impact of it on the stable structure of the star. We can even study the role of dark matter inside the charged compact star. In the references [192, 193], it is shown why the negative value of α is not taken and discusses the effectiveness of the positive value of α. We have also taken small positive α in units of $\frac{G^2 M_\odot^2}{c^4}$ [190, 193]. We have done further investigations on the compact stars here as an extension of our previous works.

8.1.2 Construction of Basic Mathematical Equations in $f(T)$ Gravity : The Stellar Equations under Spherical Symmetry

8.1.2.1 Incorporation of Modified Chaplygin Gas as Perfect Fluid

In the previous Chapter 5, the basic mathematical formulation of covariant $f(T)$ gravity has been discussed in detail. Here we have just shown the formulation of a few basic equations for the construction of this present model. The torsional scalar T, for the spherically symmetric structure of the compact stars is given as

$$T = \frac{2}{r^2} e^{-B} \left(e^{\frac{B}{2}} - 1\right) \left(e^{\frac{B}{2}} - 1 - rA'\right) \quad . \tag{8.1}$$

EoS of the chosen anisotropic fluid is given as

$$p(r)_{MCG} = \left(\varphi\rho - \frac{\psi}{\rho^\zeta}\right) \quad , \quad \zeta = 1 \;\; and \;\; \varphi \neq -1 \quad , \tag{8.2}$$

where φ, ψ and ζ are free parameters and energy density is denoted by ρ. The effective energy-momentum tensor $\tilde{\tau}_{\mu\nu}$, analogous to the $f(T)$ fluid, becomes

$$\tilde{\tau}_{\mu\nu} = \frac{1}{2}(f_T T - f)g_{\mu\nu} - 2S^{\sigma}_{\mu\nu}\partial_{\sigma} + (1 - f_T)G_{\mu\nu} \quad . \tag{8.3}$$

The above equation (3), in the form of an anisotropic fluid, effectively can be written as

$$\tilde{\tau}_{\mu\nu} = [(\rho + p_t)u_\mu u^\nu - p_t g_{\mu\nu} + (p_r - p_t)v_\mu v^\nu] \quad , \tag{8.4}$$

where u^μ and v^μ denotes four velocity and space like four vector respectively. They also follows, $u_\mu u^\nu = 1$, $v_\mu v^\nu = -1$ and $u_\mu v^\mu = 0$. Besides, radial pressure and the transverse pressure is denoted by p_r and p_t respectively.

8.1.2.2 Stellar Equations with Krori-Barua Metric Potentials and Modified TOV Equation

Here, spherically symmetric interior space-time metric is chosen as

$$ds^2 = -e^{A(r)}dt^2 + e^{B(r)}dr^2 + r^2 d\Omega^2 \quad , \tag{8.5}$$

where the metric functions, $A(r)$ and $B(r)$ are dependent on radius r and $d\Omega^2 = sin^2\theta d\phi^2 + d\theta^2$. For this investigation, we have chosen

$$A(r) = br^x + cr^y \quad and \quad B(r) = ar^z \quad . \tag{8.6}$$

Now, applying proper boundary conditions and taking suitable values of x, y and z, values arbitrary model parameters a, b and c can be found out.

Again, from the above metric, modified Tolman-Oppenheimer-Volkoff (TOV hereafter) equations took the form

$$\frac{dp_r}{dr} = -\frac{(\rho + p_r)}{r\{r - 2m(r)\}}\left[m + 4\pi r^3 p_r\right] + \frac{2}{r}\left[p_t - p_r\right] \tag{8.7}$$

and

$$\frac{dm(r)}{dr} = 4\pi r^2 \rho \quad , \tag{8.8}$$

where $m(r)$ is the enclosed mass within the radius r of the compact star. Now for the above metric, the proper tetrad is given as

$$[e^a_\alpha] = diag\left[e^{\frac{A(r)}{2}}, e^{\frac{B(r)}{2}} sin\theta cos\phi, -rsin\theta sin\phi, rsin\theta\right] \quad . \tag{8.9}$$

So, the effective density, radial and transverse pressure, of the above equation (4) can be written as

$$\begin{aligned}\rho =& \frac{\alpha}{2} f + \frac{2\psi}{r^2} e^{-B}\left[\left(e^{\frac{B}{2}} - 1\right)(2 + rA')\psi(1+\varphi) + rB'\right] f_T \\ &+ \left[\frac{2\alpha^2}{r(1+\varphi)} e^{-B}\left(e^{\frac{B}{2}} - 1\right)\right] T' f_{TT} + \left[\frac{\psi(1+\varphi)}{4r^2} e^{-B}\left(e^B - 1 + rB'\right)\right] \quad ,\end{aligned} \tag{8.10}$$

$$\begin{aligned}p_r =& -\frac{\alpha}{2} f - \left[\frac{\psi(1+\varphi)^2}{4r^2} e^{-B}\left(1 - e^B + rA'\right)\right] \\ &- \frac{2\alpha^2}{r(1+\varphi)} e^{-B}\left[2\left(e^{\frac{B}{2}} - 1\right) + \psi\left(e^{\frac{B}{2}} - 2\right) rA'\right] f_T \quad , \quad and\end{aligned} \tag{8.11}$$

$$\begin{aligned}p_t =& -\frac{\alpha}{2} f + \frac{\psi}{4r^2} e^{-B}\left[4 - 8e^{\frac{B}{2}} + 4e^B - 2\varphi\left(e^{\frac{B}{2}} - 3\right) rA'\right] f_T \\ &+ \frac{\psi}{4r^2} e^{-B}\left[\psi(1+\varphi) r^2 A'^2 - rB'(2 + rA') + 2\psi r^2 A''\right] f_T \\ &- \left[\frac{\alpha^2}{r(1+\varphi)} e^{-B}\left(2e^{\frac{B}{2}} - 2 - rA'\right)\right] T' f_{TT} - \\ &\left[\frac{\psi(1+\varphi)^2}{4r} e^{-B}\left(2A' + rA'^2 - B'(2 + rA') + 2rA''\right)\right] \quad .\end{aligned} \tag{8.12}$$

8.1.2.3 Determination of Model Parameters : Application of Matching Conditions at the Boundary

During our work, we have already chosen the spherical symmetric metric, describing the interior space-time of the NSs. Now, in order to find out the metric coefficients $A(r)$, and $B(r)$, in terms of some arbitrary free model parameters a, b and c, we have to

match this interior space-time metric with the exterior space-time Reissner-Nordström metric, given as

$$ds^2 = -\left(1 - \frac{2m(r)}{r} + \frac{q^2}{r^2}\right) dt^2 + \frac{dr^r}{\left(1 - \frac{2m(r)}{r} + \frac{q^2}{r^2}\right)} + r^2(sin^2\theta d\phi^2 + d\theta^2) \quad , \quad (8.13)$$

where $m(r)$ is the total mass enclosed within the boundary of the NSs with radius $r = R$ at the boundary. Now, as we know the at the boundary surface of the NSs, the various space-time variables, g_{rr}, g_{tt} and $g_{tt,r}$ are continuous between these two space-time metrics. So, after applying matching conditions at $r = R$, the boundary surface where $g_{tt}^- = g_{tt}^+$ and $g_{rr}^- = g_{rr}^+$, gives the below constraints as

$$A(r) = \left(1 - \frac{2m(r)}{r} + \frac{q^2}{r^2}\right) = e^{br^x + cr^y} \quad and \quad (8.14)$$

$$B(r) = \left(1 - \frac{2m(r)}{r} + \frac{q^2}{r^2}\right) = e^{-ar^z} \quad . \quad (8.15)$$

After solving the equations (13) and (14) we obtain the model parameters as

$$a = -\frac{1}{r^z} ln \left(1 - \frac{2m(r)}{r} + \frac{q^2}{r^2}\right) \quad , \quad (8.16)$$

$$b = -\frac{1}{r^{x(x-y)}} \left[-yln \left(1 - \frac{2m(r)}{r} + \frac{q^2}{r^2}\right) + (\frac{2m(r)}{r} - 2\frac{q^2}{r^2}) \left(1 - \frac{2m(r)}{r} + \frac{q^2}{r^2}\right)^{-1}\right] \quad and \quad (8.17)$$

$$c = \frac{1}{r^{y(x-y)}} \left[xln \left(1 - \frac{2m(r)}{r}\right) + (\frac{2m(r)}{r} - 2\frac{q^2}{r^2}) \left(1 - \frac{2m(r)}{r} + \frac{q^2}{r^2}\right)^{-1}\right] \quad . \quad (8.18)$$

So, by considering the known values of $m(r)$ and r from different observations on various charged compact stars, we can easily find out the values of required model parameters for suitable values of x, y and z.

8.1.3 Proposed Model : Physical Analysis

The study on the evolution of the compact stars has gotten very much attention during the present decade because of their strange variations and nature and not only that but also the proper study of their core nuclear matter with a generalized and realistic EoS can give a strong proof of the reason behind the present accelerating universe. At the same time in this situation their stability is also a matter of interest. Various compact star models show the existence of anisotropy and charge inside the core of the compact stars but the reason and their effect on the nature and stability of those stars are under further investigation. These are actually investigated in this present work. Our previous works also have given some focus on this matter.

For our study here we have considered three compact stars with different mass, given in Table 1 [196, 197, 198]. Some useful rations have been calculated and tabulated in Table 2. We already got enough observational evidence of our accelerating phase of the universe. The presence of dark matter as an external fluid which has large negative pressure is able to define this present situation. So, we have taken its presence inside the core of the star as MCG. In this new work we have also considered a small positive value of α and also investigated how it affects the compact stars. In this present work, to focus on other observations more, we have chosen only one suitable set of values of x, y and z to find out the model parameters A, B and C in Table 3.

Table 1.

Sl. No.	Compact Stars	$M_{obs}(M_\odot)$	$r_{obs}(km)$	$M(M_\odot)$	$r(km)$
1	SAX J1808.4-3658	0.88 ± 0.12	8.90 ± 1.20	0.88	8.90
2	PSR J0437-4715	1.44 ± 0.12	10.01 ± 1.20	1.44	10.01
3	PSR J2215+5135	2.27 ± 0.16	13.01 ± 1.21	2.27	13.01

Table 8.1: List of charged Compact stars

Now, using the above values of model parameters we can calculate the values of

Table 2.

Sl. No.	Compact Stars	Mass $M(M_\odot)$	Radius r(km)	$\frac{M}{r}$	$\frac{q^2}{r^2}$
1	SAX J1808.4-3658	0.88	8.90	0.265748	1.245848×10^{-7}
2	PSR J0437-4715	1.44	10.01	0.325423	1.325871×10^{-7}
3	PSR J2215+5135	2.27	13.01	0.427273	1.483513×10^{-7}

Table 8.2: Values of Mass (M), Radius (r), $\frac{M}{r}$ and $\frac{q^2}{r^2}$ of different compact stars

Table 3.

Sl No.	Compact stars	$a\ (km^{-2})$	$b\ (km^{-2})$	$c\ (km^{-2})$
1	SAX J1808.4-3658	0.0001325462316	0.000032782622	-0.005467291562
2	PSR J0437-4715	0.0001568237142	0.000039670705	-0.005721587423
3	PSR J2215+5135	0.0001821536478	0.000046231587	-0.006823541285

Table 8.3: Values of the model parameters a, b and c for $x = 4$, $y = 2$ and $z = 3$.

interior density, radial pressure and transverse pressure of those charged compact stars. The values are tabulated in below table.

Table 4.

Sl No.	Compact stars	$\rho_{MCG}\ (gm\ cm^{-3})$	$p_r\ (dyne\ cm^{-2})$	$p_t\ (dyne\ cm^{-2})$
1	SAX J1808.4-3658	$1.4823642563 \times 10^{15}$	$-1.3541287456 \times 10^{35}$	$1.7824736542 \times 10^{36}$
2	PSR J0437-4715	$1.5752389427 \times 10^{15}$	$-1.5142783268 \times 10^{35}$	$1.5438745234 \times 10^{36}$
3	PSR J2215+5135	$2.4012536891 \times 10^{15}$	$-1.6147365891 \times 10^{35}$	$1.7523874562 \times 10^{36}$

Table 8.4: Calculated values of ρ_{MCG}, p_r and p_t of Compact stars using Table 3.

8.1.3.1 Verification of the Energy Conditions

Now from the above table 4., we can verify that different energy conditions (SEC, NEC and WEC) are obeyed or not by the charged compact stars. If all the required energy conditions are verified by those stars, we can say that our model is perfectly suitable for the study of those types of stars.

From our investigational result we have got that,

$$\rho + p_r + 2p_t + \frac{E^2}{4\pi} \geq 0 \qquad : SEC \tag{8.19}$$

$$\rho + \frac{E^2}{8\pi} \geq 0 \qquad : NEC \tag{8.20}$$

$$\rho + p_t + \frac{E^2}{4\pi} \geq 0 \qquad : WEC \tag{8.21}$$

The above result shows that all the energy conditions are strictly followed by the charged compact stars in $f(T)$ gravity. So, our model in modified gravity is absolutely applicable for charged compact objects also.

8.1.3.2 Charge Distribution and The Electromagnetic Filed Equations

In modified gravity, the electromagnetic energy momentum tensor took the form [193, 265]

$$E^{EM}_{\mu\nu} = \frac{1}{4\pi}\left(g^{\delta\omega}F_{\mu\delta}F_{\omega\nu} - \frac{1}{4}g_{\mu\nu}F_{\delta\omega}F^{\mu\delta}\right) \quad , \tag{8.22}$$

where, $F_{\mu\nu}$ is the antisymmetric Maxwell field tensor and $\Phi(r)$ is the four potential. Now, we can write

$$F_{\mu\nu} = \frac{\partial\Phi_\nu}{\partial x^\mu} - \frac{\partial\Phi_\mu}{\partial x^\nu} \quad , \tag{8.23}$$

which satisfies the Maxwell equations,

$$F^{\mu\nu}_{\nu} = -4\pi j^\mu \quad and \tag{8.24}$$

$$F_{\mu\nu;B} + F_{\nu B;\mu} + F_{B\mu;\nu} = 0 \quad , \tag{8.25}$$

where j^μ is defied as the four-current vector.

So, from the equation (23), we can get the electric field as

$$F^{01} = -e^{\frac{B+\nu}{2}}\frac{q(r)}{r^2} \quad , \tag{8.26}$$

where $q(r)$ is the net charged enclosed by the sphere of radius r and defined as

$$q(r) = 4\pi \int_0^r \rho_e e^{\frac{B}{2}} r^2 dr \quad , \tag{8.27}$$

where ρ_e is the proper charge density. Now, the electric field E^2 in $f(T)$ modified gravity can be obtained as

$$E^2 = \frac{1}{2}\left(A - 3B - \frac{2}{r^2}\right) e^{-Ar^2}\alpha + \frac{\alpha}{r^2} - 8\pi\frac{\psi}{r^2}e^{-B} \quad . \tag{8.28}$$

For a practical and physically accepted model E^2 should be zero at $r = 0$. Its variation is shown in the graphical plot section of this article which becomes very interesting to study.

8.1.3.3 Computation of Tidal Deformability

All these charged compact stars are in a binary system. So, their evolution is quite interesting to study. Now,in equilibrium, if an external tidal field, E_{ij} acts on the compact stars, for their spherical shape, a quadruple moment, Q_{ij} is developed and can be described as [180, 223]

$$Q_{ij} = -\Lambda E_{ij} \quad , \tag{8.29}$$

where Λ is the tidal deformability, given as [180]

$$\Lambda = -\frac{2r^5}{3G}\kappa \quad , \tag{8.30}$$

where κ is called the tidal love number which is given by

$$\kappa = \frac{8}{5}\tau u^5 \left[2u[4(y+1)u^4 + (6y-4)u^3 + (26-22y)u^2 + 3(5y-8)u - 3y + 6] - 3\tau log\left(\frac{1}{1-2u}\right)\right]^{-1} \tag{8.31}$$

where u is given as $u = \frac{1}{r}m(r)$, $\tau = (1-2u)^2\left[2u(y-1) - y + 2\right]$ and y, is denoted as $y \equiv y(r)\mid_{r=R}$. It can be determined by solving the differential equations, applying

$y(0) = 2$ and which is given as

$$r\frac{d}{dr}y(r) + y^2(r) + y(r)e^{B(r)}\left[1 + 4\pi r^2(p_r - \rho)\right] + r^2Q(r) = 0 \quad , \tag{8.32}$$

where the quantity $Q(r)$ can be written as

$$Q(r) = 4\pi e^{B(r)}\left[5\rho + 9p_r + \frac{(p_r + \rho)}{\frac{dp}{d\rho}}\right] - \frac{6}{r^2}e^{B(r)} - A'^2(r) \quad . \tag{8.33}$$

So, by calculating, $m(r)$, (r), P_r and (ρ), using model parameters and then solving modified TOV equation with the above differential equation simultaneously, we can find out the tidal deformability and tidal love number of those charged compact stars.

8.1.3.4 Required Mass-Radius Relation with Compactness Factor

From our model, we can calculate the effective mass of the charged compact stars in modified $f(T)$ gravity as

$$\begin{aligned} m(r) =& 4\pi\int_0^R \rho R^2 dR \\ &= 4\pi\int_0^R \left[\frac{\alpha}{2}f + \frac{2\psi}{r^2}e^{-B}\left[\left(e^{\frac{B}{2}} - 1\right)(2 + rA')\psi(1 + \varphi) + rB'\right]f_T\right]R^2 dR \\ &+ 4\pi\int_0^R \left[\frac{2\alpha^2}{r(1+\varphi)}e^{-B}\left(e^{\frac{B}{2}} - 1\right)\right]T' f_{TT} + \left[\frac{\psi(1+\varphi)}{4r^2}e^{-B}\left(e^B - 1 + rB'\right)\right]R^2 dR \quad . \end{aligned} \tag{8.34}$$

The compactness factor u of compact objects, can be written as

$$\begin{aligned} u(r) =& \frac{1}{R}m(R) \\ &= 4\pi\int_0^R \left[\frac{\alpha}{2}f + \frac{2\psi}{r^2}e^{-B}\left[\left(e^{\frac{B}{2}} - 1\right)(2 + rA')\psi(1 + \varphi) + rB'\right]f_T\right]R dR \\ &+ 4\pi\int_0^R \left[\frac{2\alpha^2}{r(1+\varphi)}e^{-B}\left(e^{\frac{B}{2}} - 1\right)\right]T' f_{TT} + \left[\frac{\psi(1+\varphi)}{4r^2}e^{-B}\left(e^B - 1 + rB'\right)\right]R dR \quad . \end{aligned} \tag{8.35}$$

Now, incorporating those above equations, the radius of those charged compact stars with exotic fluid inside can also be measured using our model in modified gravity.

8.1.3.5 Finding The Stability : The Effect of Anisotropy

Form our previous works, we have got that $p_t > p_r$ for compact stars. This difference in pressure, produces a anisotropic force at the interior of the charged compact stars and in turn produces repulsive gravitational force, acting outward. This anisotropy has a significant effect on the compactness as well as the stability of those compact objects. The presence of exotic fluid (MCG) at the core of the NSs, increases this anisotropic factor, leads to more compact structure. We can measure the anisotropic factor Δ, from our model as

$$\Delta = \frac{2}{R}\left[p_t - p_r\right] \quad , \quad \Delta > 0 \quad . \tag{8.36}$$

We also have got a positive anisotropy, acting at the interior of the charged compact objects and we have also investigated it's effect on other parameters of the charged compact stars. This investigation will help us study the evolution of charged compact objects more.

For relativistic adiabatic index Γ, plays crucial role on compact stars stability [193]. Various observations reveals that, $\Gamma > \frac{4}{3}$ is the required condition for any stable NS. In case of achieving stability, $f(T)$ gravity plays a very important roll as well as MCG (exotic fluid) [192, 193]. We have got the proof that, due to the presence of MCG, inside the NSs core, the small positive value of α is sufficient to make a stable and equilibrium structure of the massive NSs in present accelerated phase of the universe. Now, from this present work, we can measure Γ as

$$\Gamma = \left[\frac{p_r + \rho}{p_r}\right]\frac{\partial p_r}{\partial \rho} \quad . \tag{8.37}$$

Again, from various observations [195, 196], the sound's speed V_s, through the core nuclear matter of a stable NSs, must be like $0 \leq V_s^2 \leq 1$ with high pressure of the order of $10^{36} dyne\ cm^{-2}$ and high density about $10^{15} dyne\ cm^{-3}$ at the interior. Now, during our investigation, due to the presence of MCG inside the core and with the effect of

positive α, V_s becomes

$$V_s = \sqrt{\frac{\partial p_r}{\partial \rho}} \quad . \tag{8.38}$$

So, it is very interesting to see that, condition of stability is also satisfied by our model in $f(t)$ gravity by the charged compact stars. Even from our this work, we can show that

$$\left[V_{st}^2 - V_{sr}^2\right] \leq 1 \quad , \quad and \quad V_{sr} > V_{st} \quad . \tag{8.39}$$

where V_{st} and V_{sr} are the speed of sound in transverse direction and radial direction respectively at the interior of the charged compact stars. Also in our model, no causality condition is violated with spherically symmetric configuration of the compact stars. This makes our present model more relevant and effectively realistic.

8.1.3.6 Calculation of Surface Redshift : Determination of The Equilibrium

In this present investigation we also have checked the surface redshift of the charged compact stars in order to investigate their stability. The surface redshift function is denoted as $Z(r)_s$ [197, 198], can also be measured as

$$Z_s(r) = \frac{1}{\sqrt{\left[1 - \frac{m(r)}{r}\right]}} - 1 \quad . \tag{8.40}$$

Astronomical observations reveals that, $Z_s(r) \leq 5$ to ensure stable equilibrium configuration of the NSs. We also have got same type of results. The value of $Z_s(r)$ in $f(T)$ gravity along with the presence of MCG and anisotropic pressure at the core of the NSs, strongly and clearly suggests that in this model the star has also got stable equilibrium configuration with a new realistic EoS.

Table 5.

Sl No.	Compact stars	$Mass\ from\ Model\ (M_{\odot})$	$radius\ from\ model\ r\ (km)$
1	SAX J1808.4-3658	1.172461	10.564217
2	PSR J0437-4715	1.584725	11.285364
3	PSR J2215+5135	2.495372	11.985473

Table 8.5: Calculated values of Mass and radius from the model using Table 3. and Table 4.

Table 6.

Sl No.	Compact stars	$\triangle$	Z_s	Γ
1	SAX J1808.4-3658	0.00021	0.1560296	7.1202351
2	PSR J0437-4715	0.00038	0.2041023	16.230165
3	PSR J2215+5135	0.00058	0.2380231	25.812583

Table 8.6: Calculated values anisotropic factor $\triangle$, surface redshift Z_s and adiabatic index Γ from model using Table 3. and Table 4.

8.1.4 Graphical Interpretations of the Obtained Results : Observational Support

Here, we have discussed the variation of different parameters of charged compact stars through graphical plots from our model. The Fig 37 shows the variation of transverse pressure p_t at the interior of the charged compact stars with high nuclear density. It is very clear that the transverse pressure reduces as the radius of the star starts increasing, i.e, as we go towards the surface of the charged compact star from its core, transverse pressure starts decreasing and becomes almost zero at the surface of the star. Now, the Fig 38 gives the variation of radial pressure p_r with the radius of the star. Radial pressure is also a decreasing function of r of the compact star. It decreases sharply as we increase the radius of the star and becomes zero at the surface. The Fig 39 shows the variation of the core density of the stars with radius with high pressure at the interior. It also shows a similar nature like transverse pressure. Density inside the core is tremendously high but as we go towards the surface of the star it starts decreasing and becomes almost zero at the star's surface. The plot in the Fig 40 is very important as well as crucial for our investigation on charged compact stars. The

variation of sound speed through the core nuclear matter of the charged compact stars is very interesting to study because it indicates the star's stable region at the interior. From our plot, we have found that at the interior of the charged compact star, sound speed does not violate any causality condition. So we can say that the stars are in stable condition with huge pressure and density at the core.

The plots in Fig 41 and Fig 42 are very important plots for the investigation of compact objects. The Fig 41 indicates the mass-radius relationship of the chosen charged compact stars of our model. From this plot we can get a clear idea about the mass and radius of the charged compact objects and the plot also depicts the proof of the calculated mass and radius of this work using our model in $f(T)$ gravity. We can also get the idea about minimum radius and maximum attainable mass by any charged compact stars from these plots. The Fig 42 shows the impact of anisotropic factor on the mass-radius relation of charged compact stars. It also shows that, if anisotropy increases, the stars also get a more compact structure. The Fig 43 is very important for our investigation also. It shows that, as the density of the exotic fluid increases, the pressure anisotropy at the interior of the charged compact stars also increases. The plot in Fig 44 shows the variation of adiabatic index of the star with its radius, as a function of anisotropic factor. The adiabatic index is an increasing function of the radius of the star. But as anisotropy of the star increases, the adiabatic index decreases. This indicates that, upto a certain limit, the star can increase its compactness and stability. Fig 45 shows the variation of surface redshift of the compact stars with radius as a function of anisotropy. The Fig 46 gives the idea of variation of tidal deformability of the charged compact stars.

The plot of the electric field as a function of the radius of the charged compact stars at a very high core nuclear density in Fig 47 has become very interesting for this model. The plot shows that the function E^2 is positive entirely inside the compact charged sphere. Moreover, it is monotonic increasing upto about 7.5km inside the stars with high pressure and density; then it starts decreasing monotonically.

$Fig - 37$

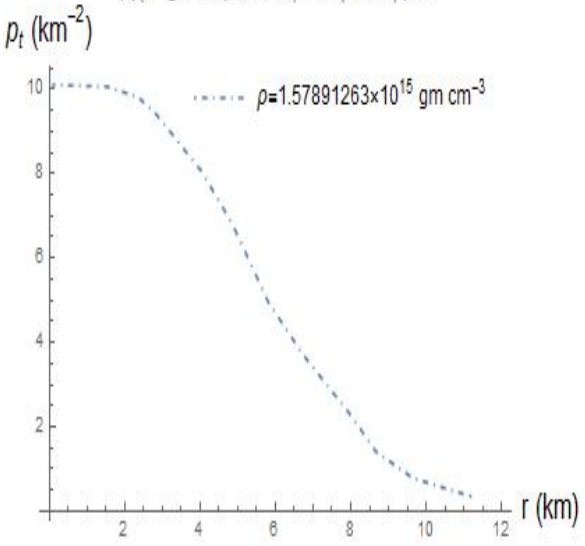

$Fig - 38$

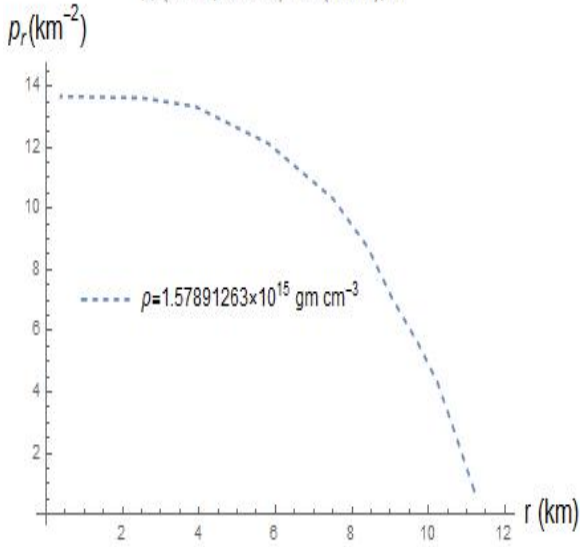

Figure 8.1: *Represents the variation of tangential(transverse) pressure* $p_t(dyne\ cm^{-2})$ *with radius* $r(km)$ *at high core density of charged compact stars.*

Figure 8.2: *Represents the variation of radial pressure* $p_r(dyne\ cm^{-2})$ *with radius* $r(km)$ *at high core density of charged compact stars.*

$Fig - 39$

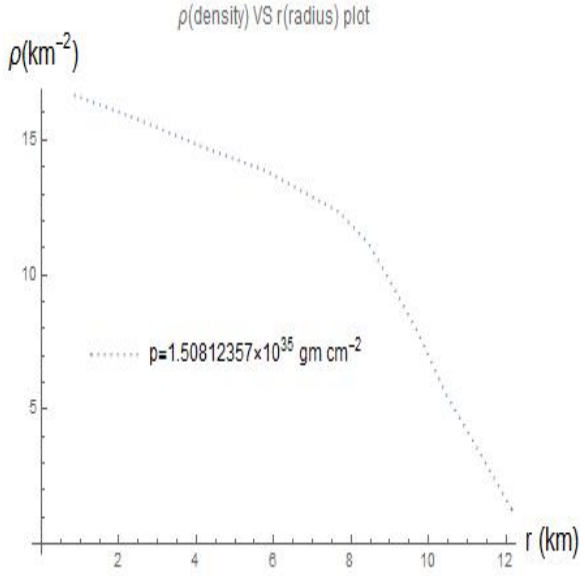

$Fig - 40$

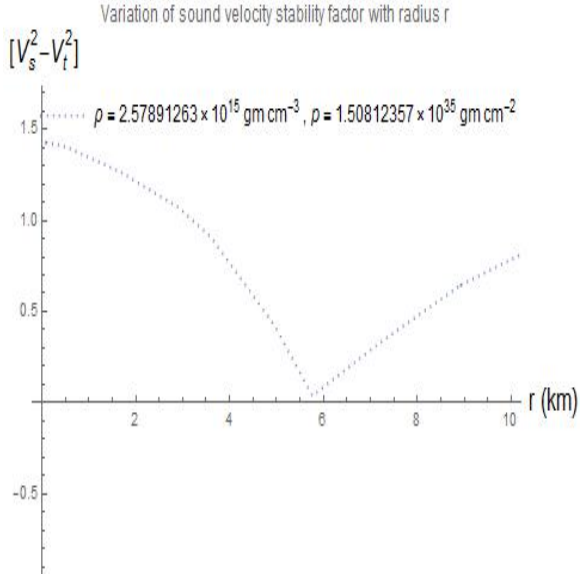

Figure 8.3: *Represents the variation of core density* $\rho(dyne\ cm^{-3})$ *with radius* $r(km)$ *at high pressure of charged compact stars.*

Figure 8.4: *Represents the variation of sound speed* V_S *with radius* $r(km)$ *at high core density and pressure of charged compact stars.*

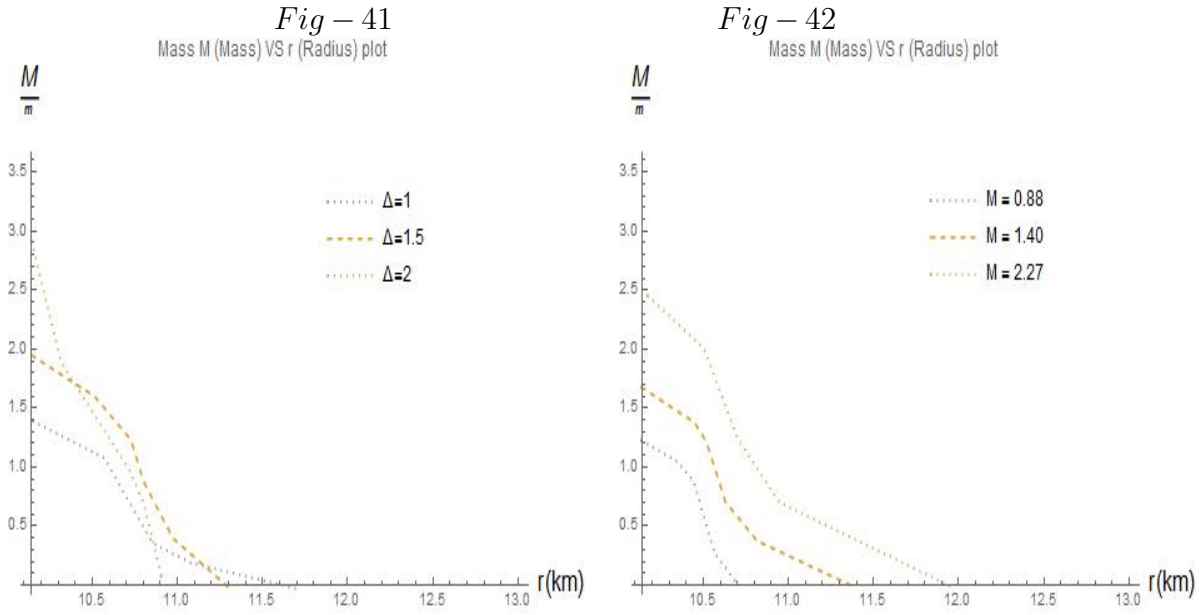

Figure 8.5: *Represents the variation of mass $M(M_{\odot})$ with radius $r(km)$ at high pressure and density of different charged compact stars.*

Figure 8.6: *Represents the variation of mass $M(M_{\odot})$ with radius $r(km)$ at high core density and pressure, as a function of anisotropic factor $\triangle$ of charged compact stars.*

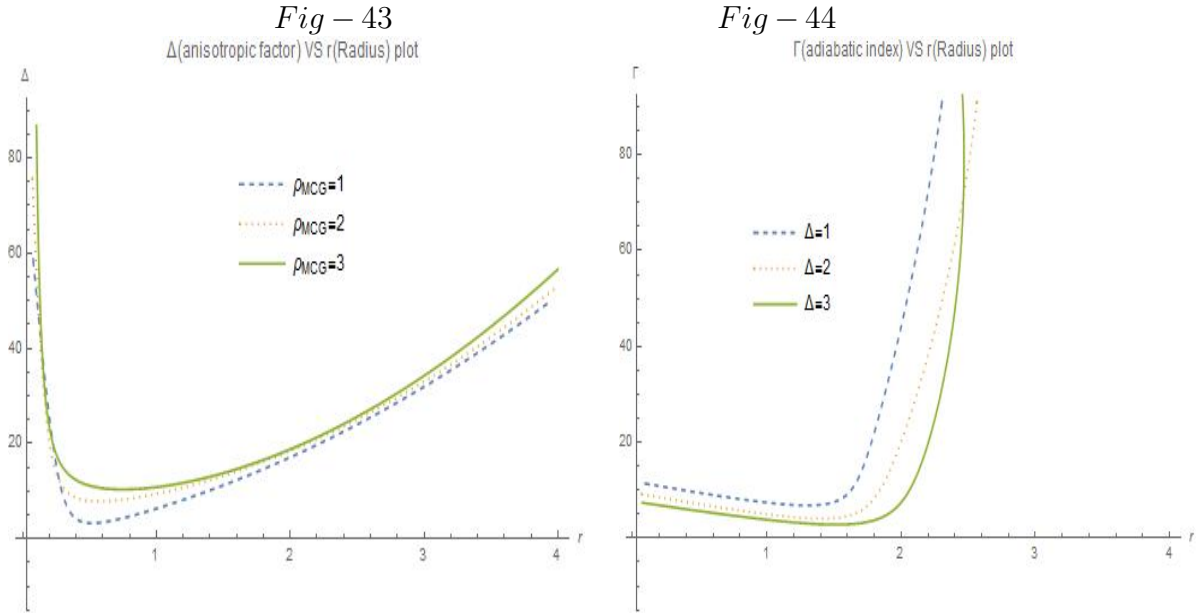

Figure 8.7: *Represents the variation of anisotropic factor $\triangle$ with radius $r(km)$ as a function of exotic fluid density $\rho_M CG$, of different charged compact stars.*

Figure 8.8: *Represents the variation adiabatic index Γ with radius $r(km)$ as a function of anisotropic factor $\triangle$ of charged compact stars.*

$Fig-45$

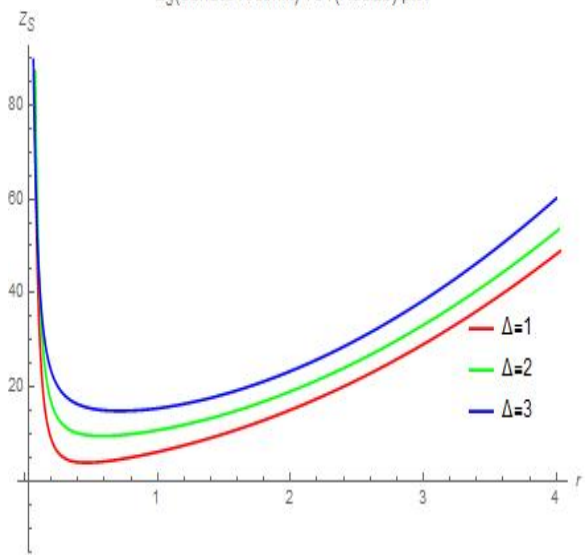

$Fig-46$

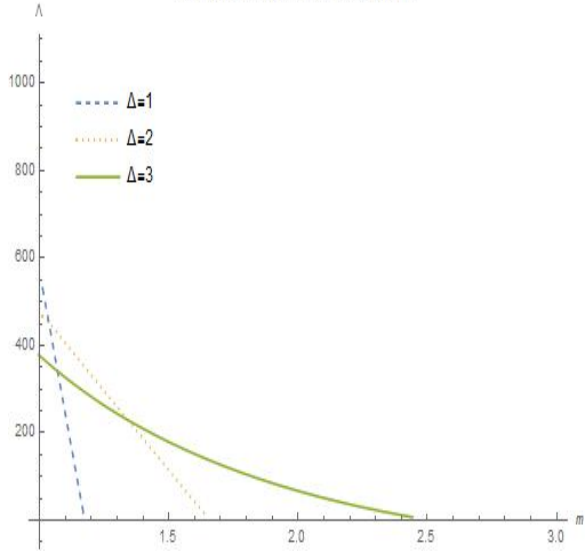

Figure 8.9: *Represents the variation of surface redshift Z_S with radius $r(km)$ as a function of anisotropic factor $\triangle$, of different charged compact stars.*

Figure 8.10: *Represents the variation tidal deformability Λ with mass $M(M_\odot)$ as a function of anisotropic factor $\triangle$ of charged compact stars.*

$Fig-47$

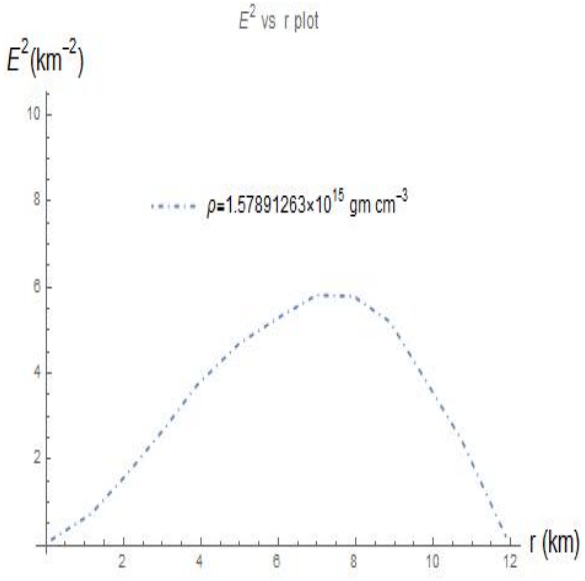

Figure 8.11: *Represents the nature of the electric field as a function of radius r of the charged compact stars at a very high core density.*

8.1.5 Brief Discussions and Conclusion

This present work with charged compact stars, by using our model in $f(T)$ gravity has become very interesting in the context of recent astronomical observations on compact stars through the accelerated phase of the universe. Our investigation on the impacts of dark matter inside the core of the charged compact stars reveals various unknown facts of the charged compact stars. From this present work we have got a clear idea about the evolution of charged compact stars with the present situation of the universe. The crucial role of modified gravity in explaining the evolution of the compact objects is also established. Variations of different crucial parameters of the charged compact stars from the graph plots depict their true evolving nature under cosmic acceleration. The compact stars we have chosen for our study, have their companion star in the binary system. So, investigation on them is very crucial and important also. We have found a generalized and realistic EoS for the charged compact objects. At the same time we have also investigated their evolution and the reason behind their compact stable configuration maintaining mechanism through the accelerated universe, successfully.

Here, we have constructed a realistic model of charged NSs in the framework of $f(T)$ modified gravity by introducing a very simple and effective quadratic form of $f(T)$, as $f(T) = T + \alpha T^2$. Nowadays, this type of compact star model, using modified gravity, is very popular to study the curvature based gravity. Early time cosmic inflation can also be described by introducing the quadratic terms of the torsional scalar. These make our current model more reasonable in the extreme gravitational environment within the neutron stars and also help to study the gravity in such a regime. This model may also explain the existence of super-massive NSs. In this case of charged compact stars, $f(T)$ gravity plays a very crucial role to maintain their spherically stable and equilibrium configuration. If we see the variations of density and both types of pressures, it is very clear that effective density and pressure of the anisotropic $f(T)$ fluid exhibits sharp transitions with positive α. When the modification term α becomes positive, the EoS of the compact stars obeys the casual limit and the central density respects causality. On the other hand, an effective $f(T)$ fluid with positive α supports more

matter contained inside the star compared to GR and the star gets a more compact structure with stability. Moreover, due to the effects of pressure anisotropy of the effective $f(T)$ fluid, stellar mass may increase by lowering central density. Again, in this model when $\alpha = 0$, $f_T = 1$ and $f_T - f = 0$. It can be checked easily from equation (3) that $\tilde{\tau}_{\mu\nu} = 0$ and the Einstein tensor reduces to the Einstein equation in GR. In this case only our model is identical to the GR and standard results can be recovered. For $\alpha > 0$, in case of GR with a very low positive value of α, the NSs can contain less stellar matter with a given radius and the $M - R$ curves become quite close to the GR curves. But as α becomes more positive, the model moves away from the standard gravity case. In case of GR as there exists nuclear degeneracy pressure which leads to a maximum stellar mass limit. But, in case of $f(T)$ modified gravity this stellar mass limit may be conquered with the effects of radial and transverse pressure of the effective $f(T)$ fluid with small positive value of α. However, there still exists the upper bound of the stellar mass due to the causality conditions. This new and interesting feature of $f(T)$ modified gravity is capable of accommodating various observations on the NSs that are far beyond GR predictions.

From this investigation we have found that, as the density of the exotic fluid as a dark matter increases at the interior of the charged compact stars, their anisotropy increases. This increase in anisotropy helps the stars to get more compact structure. But at the same time repulsive gravitational force, which acts outward direction, comes into play and helps the star to be in stable condition. The graphical plots depict that, as the density of MCG increases, the anisotropic factor also increases. This anisotropy plays a crucial role inside the stars and its impact on various other parameters and their variation as a function of it, clearly reveals the role of dark matter in case of charged compact stars. The mass-radius relationship is very interesting here. We are able to get the idea that the maximum attainable mass by any charged compact star is about $3.1M_{\odot}$ and minimum radius should be about 10.5km. Again the tidal deformability has also played a very important role in case of them because of their binary companion stars. From our investigation we can see that the tidal deformability of the charged compact stars, containing dark matter, must be in the range of $375 \leq \Lambda \leq 550$. As

the anisotropy increases, the tidal deformability of the compact stars decreases in a noticeable amount. We have also estimated the electric charge which has a crucial effect on the compact structure of the stars. The surface electric field produced by this charge distribution is about 10^{22} V/m.

So, conclusively, we can say that our present model can successfully explain the nature and stable spherical configuration of the charged compact stars. It also reveals the impacts of dark matter on them. The evolution of the charged compact stars under the accelerated phase of the universe is investigated rigorously and discussed clearly. The result we have got using our model, is absolutely comparable with other astronomical observations on charged compact stars. This makes our model more realistic and viable.

"Look at the sky. We are not alone. The whole Universe is friendly to us and conspires only to give the best to those who dream and work".

—A. P. J. Abdul Kalam

CHAPTER 9

CHARGED X-RAY BINARIES IN $F(T)$ MODIFIED GRAVITY

9.1 Confrontation of $f(T)$ Modified Gravity with Charged X-ray Binaries Embedded in modified Chaplygin gas under Tolman-Kuchowicz Spacetime

9.1.1 Prelude

Significant deviations of the properties of spacetime surrounding the neutron stars (NSs) can be predicted by using modifications of general relativity theory (GR). Amongst them, $f(T)$ modified gravity theory, with T as the torsional scalar, is considered to be an effective neutral extension of GR. In this study, singularity free modeling of the massive and charged relativistic compact binary objects $X5$ and $X7$, in the framework of $f(T) = T + \xi T^2$ modified gravity using Tolman-Kuchowicz (TK) metric potentials, have been focused on. The modified Chaplygin Gas (MCG) equation of state (EoS) as perfect fluid has been utilized to describe the core stellar matter. The interior space-

time of the compact stars is matched with exterior Reissner-Nordström spacetime at the boundary to derive the unknown constants of the model. We have obtained an exact singularity-free analytical solution, for anisotropic perfect-fluid spheres under hydrostatic equilibrium, which holds the stability criteria in the background of $f(T)$ modified gravity with small positive parameter ξ. Mass-radius relation has been acquired for this realistic model of charged compact stars. Further, we have also evaluated few important properties such as energy density, compactness factor, sound velocities, effective pressures, tidal deformability, relativistic adiabatic index, surface-redshift etc. of the charged NSs, to check the physical validity of the current model. Interestingly, it is revealed that all the derived outcomes of this model became compatible and agreed with astronomical observations, which shows the viability of the present model within $f(T)$ modified gravity.

Binary neutron stars (NSs hereafter) in the galaxy have always offered unique insight to the astrophysical study of the end stages of stellar evolution as well as the physics of matter under extreme physical environment. It has given us the opportunity to explore the properties and behavior of the core nuclear matter of the NSs and to find out its exact equation of state (EoS hereafter). In recent time, one of the most promising physical event of generation of the gravitational wave has occurred due to the inspiral and coalescence of two NSs. The event, $GW170817$ of binary neutron star mergers have imposed constraints on several parameters related to the NSs [216]. Proper understanding of different macroscopic properties like mass, radii, tidal deformability etc of the NSs are required to realize and understand the astrophysics behind them and needless to say, rigorous study is very much needed.

Several researches have shown the existence of the anisotropy inside the compact objects [217, 230, 231]. Proper modeling of the massive NSs is very much necessary to understand the properties of these stars and their core nuclear matter also. The utmost effect of the interactions between relativistic nucleons on the pressure anisotropy due to strong magnetic field at high nuclear density have been explored in the reference [218]. Also, at high nuclear density, phase transitions inside the core and the reduction of pressure along the radial direction (outward) have been examined [219, 220].

In case of the binary NS system, tidal deformability actually indicates the pre-merging stages of the two massive stars and as well as their phase evolution [221]. In the reference [222], how tidal deformability of a binary NS system affects the tidal EoS of the NSs and how tidal love number is related with the binary mass ratio, have been examined. So, investigations on the mass-radius relation and tidal deformability of the binary NSs become very important [223]. Flanagan and Hinderer have shown how tidal deformability, Λ and tidal love number, κ depend on the EoS of the stelar matter and also found out the early phase evolution of them [224]. Again, in several investigations, the tidal deformability Λ has been calculated for the NSs with mass about 1.4 $M_{\odot}$ by considering linear expansion of $\Lambda(m)$ [225]. Again, it is also difficult to construct the exact EoS of the nuclear matter by observing the gravitational waves only in GR. The inclusion of tidal deformability parameters with the modified theory of gravity, rather than GR, may be more useful to understand the exact properties and behavior of the nuclear matter inside the stars [226]. Tidal love number shows the deformability in a body due to an external tidal force acting on the body. This quantity gives the data about the core structure of the merging stars. The tidal love number can also be calculated from gravitational waves [227]. Tidal deformability of black holes (BH hereafter) in alternative theories of gravity has been studied in the reference [228, 229].

In recent times, application of various modified theories in gravity in order to study the massive compact stars has become very interesting and significant. One will get a more generalized theory of gravity by implying $f(T)$ modified gravity [230, 231]. General relativity (GR hereafter) has faced some difficulties to explain these types of massive relativistic compact objects [232, 233]. Modified theories of gravity are quite more suitable than GR for these types of stars [303]. Quantum corrections of GR Lagrangian have become very famous in this field where Einstein-Hilbert action has been modified by the Ricci scalar function, R [233]. The I-love-Q relations were studied for the first time for binary NSs which became very crucial to study about the properties of relativistic massive compact objects [235, 236]. The EoS of the core nuclear matter of the massive NSs have been explored successfully in $f(R)$ modified gravity theories

of gravity [237, 238]. Several models of anisotropic compact stars in alternative gravity theories have been investigated in the references [239, 240, 241]. MCG plays a very important role in incorporating dark energy (DE) in the study of such types of compact objects under cosmic acceleration [242, 243]. $f(T)$ theories of gravity also provide the possible explanation of accelerated expansion of the universe and help to incorporate the dark energy (DE hereafter) [250, 352]. The $M-R$ relationship with proper EoS and precise measurement of the mass and radius of the massive NSs are very important at high densities under cosmic acceleration where effect of DM can also be examined [252, 253].

In case of massive relativistic compact stars, the corrections corresponding to high energy can be studied in terms of higher orders of the torsional scalar in $f(T)$ gravity, with a nonlinear function of T [244, 359]. The $f(T)$ modified gravity is different from the GR theory because of its Lagrangian as the function f has nonlinear terms. This shows that $f(T)$ gravity may possess new features and open up new angles to explore the spacetime geometry. Mainly, in $f(T)$ gravity, field equations are of second order of derivatives. In various formulations of $f(T)$ gravity at early stages the frame dependent nature has produced some complications in the study before finding a good tetrad [296, 303]. This problem is solved by covariant formulation of the teleparallel gravity which allows the researchers to pursue difficult problems like spherically symmetric configurations in $f(T)$ gravity. Again, the existence of massive relativistic compact stars can be proved by considering a priori assumed metric with regularity of the matter in $f(T)$ gravity. Furthermore, several types of compact star solutions in $f(T)$ gravity have been investigated rigorously using this approach. A correlation between the stellar structure and the spacetime metric can be established if the stellar matter is approximated by perfect fluid with conservation of energy. The EoS of the interior matter is very much essential to the inner structure of the compact stars. The relation between core matter density and core pressure is required for closing the system of differential equations. Compact stars with polytropic EoS have been studied in the reference. Recent observations indicate the existence of massive NSs with the mass close or beyond GR prediction [291]. Moreover, this modified $f(T)$ gravity model also

becomes effective to turn away finite-time future singularities and to reduce Hubble tension [268, 269, 270].

In the context of GR theory, the charged compact stars have been investigated for a long period. The field equations can be used as an anisotropic system where electric field intensity follows the anisotropy factor. These models have given us the opportunity to investigate and understand the stability of a charged spherical system. Various mechanisms have been introduced to account for the existence of residual charge in the compact stars. Various solutions of the Einstein-Maxwell field equations have been discovered to describe the models of charged compact objects [272, 280, 276]. Properties of the ultra-compact stars with dark matter have been studied by Kiczek and Rogatko [278]. In the reference [117], stability and hydrostatic equilibrium of charged strange quark stars with charged perfect fluid, against a radial perturbation has been investigated. Compact star models with strange matter using MIT bag model EoS and gaussian distribution of the surface charge have been investigated in the references [279, 280].

The existence of massive NSs may also be explained by applying the modified gravity theories like $f(T)$ gravity theory as studied in this current model. In this current model, we want to investigate the realistic model of charged and massive binary NSs. Our aim is to obtain the numerical stellar structure and find out the possible impact of modifications of $f(T)$ gravity. We have chosen a simple but realistic model in which the quadratic terms of torsional scalar T can relate to the early time cosmic acceleration. The EoS of the stable and cold matter at very high densities that exceeds the saturation density of the nuclear matter can be well examined by the binary NSs neutron rich matter at extreme conditions. The $M-R$ relationship can be determined by this EoS. So, precise measurement of the mass and radius of the massive NSs are very important at high densities. The compact stars which have thermal radiation from the surface and have low magnetic fields ($\ll 10^{10}G$) are mainly chosen for the study because temperature distributions at their surface are not affected by the magnetic field. They have also possessed other unique properties. This is why the low mass X-ray binaries are very important for investigations on the EoS of the compact objects. In this study,

for our investigation we have also chosen two X-ray binary compact stars $X5$ and $X7$ because they have highest flux towards the Earth and various studies on them have put some constraints on the values of their mass and radius [258, 259, 260, 261, 262]. Our main motivation for this work is to study the various crucial properties of the charged compact stars and to investigate its evolution under cosmic acceleration. At the same time the effect of anisotropy on these properties have also been investigated. As we already know that GR can not describe the EoS of these types of super massive relativistic objects properly.

Again, several investigations have pointed out the presence of anisotropy inside the NSs despite their symmetrical stable configuration. In this current study, we have incorporated the $f(T)$ modified gravity, which can accommodate the cosmic acceleration effectively in order to get an effective EoS of the core nuclear matter. Moreover, cosmologists are trying to explain the accelerated phase of the universe by choosing the existence of dark matter with large negative pressure, known as dark energy. So, in this model we have also incorporated the existence of modified Chaplygin gas inside the core of the massive NSs. We have chosen $f(T) = T + \xi T^2$, where T is the torsional scalar and ξ is a free regulatory parameter. This model also helps us to study the impacts of dark energy on these super massive NSs. In our previous work [230, 231], we have shown why the negative value of ξ is not chosen and also have discussed the effectiveness of the positive value of it. Throughout our present work, we have chosen small positive value of ξ in the unit of $\frac{G^2 M_\odot^2}{c^4}$ [232].

9.1.2 Construction of Basic Mathematical Equations in f(T) Gravity : The Stellar Equations under Spherical Symmetry

9.1.2.1 Mathematical Formulation of covariant f(T) Gravity

Generally the space time metric is taken as

$$g = g_{\alpha\beta} dx^\alpha dx^\beta \quad . \tag{9.1}$$

Again the tangent space metric in tetrad formalism takes the form after transformation as

$$\eta = \eta_{ab} h^a h^b \quad . \tag{9.2}$$

So, we get that, spacetime metric, g and the tangent space metric η is related as

$$g_{\alpha\beta} = h^a_\alpha \; h^b_\beta \; \eta_{ab} \quad and \quad \eta_{ab} = g_{\alpha\beta} e^\alpha_a e^\beta_b \quad . \tag{9.3}$$

where $\eta_{ab} = diag(-1, +1, +1, +1)$ and tetrad is given by $h^a = h^a_\mu \; dx^\mu$, so that $h^a \; (e_b) = \delta^a_b$. Now, considering componentwise and considering formalism of proper tetrad, the torsion tensor can be written as [38]

$$T^\alpha_{\beta\gamma} = e^\alpha_a \left(\partial_\beta h^a_\gamma - \partial_\gamma h^a_\beta \right) = \Gamma^\alpha_{\mu\nu} \quad , \tag{9.4}$$

where $\Gamma^\alpha_{\mu\nu}$ is denoted as the non-vanishing Christoffel symbol. So, the torsion scalar with contraction of tensor can be written as,

$$T = T^\alpha_{\beta\gamma} S^{\beta\gamma}_\alpha \quad , \tag{9.5}$$

where taking into account the super potential, $S^{\beta\gamma}_\alpha$ took the form as

$$S^{\beta\gamma}_\alpha = \frac{1}{4} \left(T^{\beta\gamma}_\alpha + T^{\gamma\beta}_\alpha - T^{\beta\gamma}_\alpha \right) + \frac{1}{2} \left(\delta^\beta_\alpha T^{\lambda\gamma}_\lambda - \delta^\gamma_\alpha T^{\lambda\beta}_\lambda \right) \quad . \tag{9.6}$$

Now, Considering torsional scalar T as its Lagrangian and the $f(T)$ gravity as an arbitrary function of T with tetrad determinant $\sqrt{g}$, we can write

$$S[e^a_\alpha, \phi_A] = -\frac{1}{2} \int |h| f(T) d^4x + \int |h| L_M(\phi_A) d^4x \quad , \tag{9.7}$$

where $|h| = \sqrt{g}$ and $L_M(\phi_A)$ is the Lagrangian of the matter.

Now we got the field equation from the above equation (7) w. r. t. the tetrad as

$$\frac{2}{|h|} \partial_\beta \left(|h| f_T S^{\alpha\beta}_\sigma e^\sigma_a \right) + \frac{f}{2} e^\alpha_a = \tau^\alpha_\beta e^\beta_a \quad , \tag{9.8}$$

where f_T is given by $\frac{df}{dT}$ and matter related energy-momentum tensor τ^{α}_{β} is given as

$$|h|\tau^{\alpha}_{\beta}e^{\beta}_{a} = \frac{\delta(|h|L_M)}{\delta(h^{a}_{\alpha})} \quad . \tag{9.9}$$

Now, using equation (8) and extracting $G_{\mu\nu}$, we get

$$G_{\mu\nu} \simeq \tilde{\tau}_{\mu\nu} \quad . \tag{9.10}$$

So, the matter related effective energy-momentum tensor $\tilde{\tau}_{\mu\nu}$, analogous to the anisotropic $f(T)$ fluid, becomes

$$T^{Matter}_{\mu\nu} = \tilde{\tau}_{\mu\nu} = [(\rho + p_t)u_\mu u^\nu - p_t g_{\mu\nu} + (p_r - p_t)v_\mu v^\nu] \quad , \tag{9.11}$$

where u^μ and v^μ denotes four velocity and radial space like four vector respectively. They also follows that, $u_\mu u^\nu = 1$, $v_\mu v^\nu = -1$ and $u_\mu v^\mu = 0$. Besides ρ denotes the energy density and on the other hand, p_r and p_t denote the radial pressure and the transverse pressure respectively.

9.1.2.2 Incorporation of Modified Chaplygin gas with electromagnetic field in f(T) gravity

Now, as per our model, Einstein's field equation in terms of matter, MCG and electromagnetic (EM hereafter) field, can be written as

$$G_{\mu\nu} = 8\pi G\left(T^{Matter}_{\mu\nu} + T^{MCG}_{\mu\nu} + T^{EM}_{\mu\nu}\right) \quad , \tag{9.12}$$

where $T^{MCG}_{\mu\nu}$ denotes the energy-momentum tensor related with MCG, which is present inside the core of the super massive NSs as anisotropic perfect fluid and whose EoS is chosen in our model as

$$p(r)_{MCG} = \left(\varphi\rho - \frac{\psi}{\rho^{\zeta}}\right) \quad , \quad \zeta = 1, \quad \varphi \neq -1 \quad and \quad \psi > 0 \quad , \tag{9.13}$$

where φ, ψ and ζ are all free parameters and ρ is the energy density.

The energy momentum tensor related to EM filed becomes

$$E^{EM}_{\mu\nu} = \frac{1}{4\pi}\left(g^{\delta\omega}F_{\mu\delta}F_{\omega\nu} - \frac{1}{4}g_{\mu\nu}F_{\delta\omega}F^{\mu\delta}\right) \quad , \tag{9.14}$$

where the field tensor of Maxwell given by $F_{\mu\nu} = (\Phi_{\nu,\mu} - \Phi_{\mu,\nu})$. So, Maxwell's EM field equations become

$$(\sqrt{g}F^{\mu\nu})_{,\nu} = 4\pi J^{\mu}\sqrt{g} \quad and \quad F_{[\mu\nu,\delta]} = 0 \quad , \tag{9.15}$$

where J^{μ} denotes four vector of current and satisfy the relation with charge density σ that $J^{\mu} = \sigma u^{\mu}$. Now by using equation (14), the expression for the electric field becomes

$$F^{01} = -e^{\frac{B(r)+A(r)}{2}}\left[\frac{q(r)}{r^2}\right] \quad , \tag{9.16}$$

where $q(r)$ denotes the net charge inside the sphere of radius r with proper charge density ρ_e and can be obtained as

$$q(r) = 4\pi\int_0^r \rho_e e^{\frac{B(r)}{2}} r^2 dr \quad . \tag{9.17}$$

9.1.2.3 Stellar Equations with Tolman-Kuchowicz Metric Potentials and Modified TOV Equation

Here, the static spherically symmetric interior space-time metric is chosen as

$$ds^2 = -e^{A(r)}dt^2 + e^{B(r)}dr^2 + r^2 d\Omega^2 \quad , \tag{9.18}$$

where the unknown metric potentials, $A(r)$ and $B(r)$ are purely radial and $d\Omega^2 = sin^2\theta d\phi^2 + d\theta^2$. The range of r is from 0 to ∞ and $0 \leq \theta \leq \pi$, $0 \leq \phi \leq 2\pi$.

As our main aim is to get a singularity free and physically reasonable model of the charged compact star, for our study, we have chosen the following Tolman-Kuchowicz ansatz [254, 379] as

$$e^{B(r)} = 1 + ar^2 + br^4 \quad and \quad e^{A(r)} = C^2 e^{Dr^2} \quad , \tag{9.19}$$

where a, b, C and D are constants.

Several researchers have already used this above approach successfully for modelling compact objects in GR as well in modified gravity. Anisotropic spheres in $f(R,G)$ modified gravity have been investigated by Javed et al. [281]. Model of Quark star in massive Brans-Dicke gravity have been studied by Majid and Sharif [382]. Charged compact stars in $f(R)$ gravity have been studied in the reference [381]. Stellar model with charge in $f(G)$ modified gravity have been obtained by Naz and Shamir [381]. The model of anisotropic strange star in the framework of $f(R,T)$ modified gravity have been investigated in the reference [286]. Bhar et al. have been obtained a compact star model by using modified EBG gravity [287].

Now, using this matter distribution and from the above space-time metric, the Tolman-Oppenheimer-Volkov (TOV hereafter) equations can be written in modified form as

$$\frac{dp_r}{dr} = -\frac{(\rho+p_r)}{r(r-2m(r))}\left(m+4\pi r^3 p_r\right)+\frac{2}{r}(p_t-p_r)+\frac{\xi}{(2+4\pi)}[\frac{d\rho}{dr}+\frac{dp_r}{dr}+2\frac{dp_t}{dr}] \quad and \tag{9.20}$$

$$\frac{dm(r)}{dr} = 4\pi r^2\rho \quad , \tag{9.21}$$

where $m(r)$ is the enclosed mass within the radius r. Now for the above metric, the proper tetrad [41-43] is chosen as

$$[e^a_\alpha] = diag\left[e^{\frac{A(r)}{2}}, e^{\frac{B(r)}{2}} sin\theta cos\phi, -r sin\theta sin\phi, r sin\theta\right] \quad . \tag{9.22}$$

So, the torsional scalar T, for the above metric is given by

$$T = \frac{2}{r^2}e^{-B(r)}\left(e^{\frac{B(r)}{2}}-1\right)\left(e^{\frac{B(r)}{2}}-1-rA'(r)\right) \quad . \tag{9.23}$$

Again, in our model we have chosen the modified gravity in the form of $f(T)$ as

$$f(T) = T+\xi T^2 \quad and \quad \xi > 0 \quad , \tag{9.24}$$

where ξ is a small positive constant and for $\xi \to 0$ generates the GR field equations.

Now, for the line element of the spherical metric of equation (18), the field equations in modified gravity becomes

$$8\pi\rho^{EG} + \frac{q^2}{r^4} = \frac{e^{-B}}{r}B^{'}(r) + \frac{1}{r^2}(1 - e^{-B(r)}) \quad , \tag{9.25}$$

$$8\pi p_r^{EG} - \frac{q^2}{r^4} = \frac{1}{r^2}(e^{-B(r)} - 1) + \frac{A^{'}(r)}{r}e^{-B(r)} \quad and \tag{9.26}$$

$$8\pi p_t^{EG} + \frac{q^2}{r^4} = \frac{1}{4}e^{-B^(r)} + [2A^{''}(r) + A'^2 - B'(r)A'(r) + \frac{1}{r}(A'(r) - B'(r))] \quad , \tag{9.27}$$

where the quantities ρ^{EG}, p_r^{EG} and p_t^{EG} are the density, radial pressure and transverse pressure in Einstein Gravity respectively and can be written as

$$\rho^{EG} = \rho + \frac{\xi}{8\pi}(\rho - p_r - 2p_t) \quad , \tag{9.28}$$

$$p_r^{EG} = p_r + \frac{\xi}{8\pi}(\rho + 3p_r + 2p_t) \quad and \tag{9.29}$$

$$p_t^{EG} = p_t + \frac{\xi}{8\pi}(\rho + p_r + 4p_t) \quad . \tag{9.30}$$

Our main focus is to find out the solutions of the system, governed by the equations (24) to (26), which entirely specify the behaviour of the interior of the X-ray binaries. ρ, p_r and p_t are the density, radial pressure and tangential pressure in modified $f(T)$ gravity respectively. The differentiation w.r.t. r is denoted by prime.

The quantity $q(r)$ in terms of the electric filed $E(r)$ can be written as

$$E(r) = \frac{q(r)}{r^2} \quad . \tag{9.31}$$

9.1.3 Proposed Model in $f(T)$ Modified Gravity

9.1.3.1 Determination of the Parameters related to the Neutron Stars

Now, employing the metric coefficients as chosen in the equation (19), in the equations (24) to (26), we have obtained the following sets of equations as

$$8\pi\rho^{EG} + \frac{q^2}{r^4} = \frac{3a + (a^2 + 5b)r^2 + 2abr^4 + b^2r^6}{\tau^2} \quad , \tag{9.32}$$

$$8\pi\rho^{EG} - \frac{q^2}{r^4} = -\frac{a - 2D + br^2}{\tau} \quad and \tag{9.33}$$

$$8\pi\rho^{EG} + \frac{q^2}{r^4} = \frac{1}{\tau^2}[-a + 2D + (D(a + D) - 2b)r^2 + aD^2r^4 + bD^2r^6] \quad , \tag{9.34}$$

where τ is the function of r and is given by

$$\tau = (1 + ar^2 + br^4) \quad . \tag{9.35}$$

In this model, for the study of the effect of anisotropy, we have considered MCG and its Eos is given by equation (13). Now using the equation (13), we have solved the equations (31) to (33) and obtained the expressions of ρ^{EG}, p_r^{EG} and p_t^{EG} in Einstein Gravity. Then applied these expressions in the equations (27) to (29) and solved them in order to get the values of these quantities in $f(T)$ modified gravity for our investigation.

So, according to our current model, the effective components, i.e, effective density, radial and transverse pressure of the X-ray binaries respectively in $f(T)$ modified gravity, can be written as

$$\begin{aligned}\rho =& \frac{\xi}{2}f + \frac{2\psi}{r^2}\left[(2b + aD)\left(2 + r(a + b)\right)\psi(1 + \varphi) + r(2b + D)\right]\frac{f_T}{\tau} \\ &+ \frac{1}{\tau^2}\left[\frac{2\xi^2}{r(1 + \varphi)}(bD)\left(a + D + (2b + aD)\right)\right]T' f_{TT} \\ &+ \left[\frac{\psi(1 + \varphi)}{4r^2}(a + D)\left(b - 1 + r^2D\right)\right] \quad ,\end{aligned} \tag{9.36}$$

$$
\begin{aligned}
p_r =& -\frac{\xi}{2}f - \left[\frac{\psi(1+\varphi)^2}{4r^2}\left(1-(a+D)+r^2(2b+aD)\right)\right] \\
& - \frac{2\xi^2}{r(1+\varphi)}\left[2\left(a+b+2D\right)+\psi\left(a+b\right)br^4\right]\frac{f_T}{\tau} \quad and
\end{aligned}
\tag{9.37}
$$

$$
\begin{aligned}
p_t =& -\frac{\xi}{2}f + \frac{\psi}{4r^2}\left[4(a+b+(2b+aD)r)+4aD-2\varphi\left(b+D-2a\right)\right]\frac{f_T}{\tau} \\
& + \frac{\psi}{4r^2}\left[\psi(1+\varphi)r^2 - r(a+b)\left(2+r(b+D)\right)\right]\frac{f_T}{\tau} \\
& - \left[\frac{\xi^2}{r(1+\varphi)}\left(2e^{\frac{B}{2}}-2-r^4(b+aD)\right)\right]T' f_{TT} \\
& - \frac{1}{\tau^2}\left[\frac{\psi(1+\varphi)^2}{4r}\left(2a+rb-D(2+rb)+2r^2(a+D-1)\right)\right] \quad .
\end{aligned}
\tag{9.38}
$$

Now, the anisotropic factor in $f(T)$ modified gravity is obtained as

$$
\begin{aligned}
\Delta =& \frac{1}{3\xi+4\pi}\left[8\psi(\xi+2\pi)\right] \\
& + \frac{1}{3\xi+4\pi}\left[\frac{\varphi}{\tau^2(\xi+4\pi)}\{(2D-5a)\xi+8\psi(D-a)\pi+\{aD(\xi+4\pi)-2b(5\xi+8\pi)\}r^2\}\right] \\
& + \frac{1}{3\xi+4\pi}\frac{1}{\tau(\xi+4\pi)}\left[\{2D(2\pi-\xi)-a(\xi+4\pi)-(b-D^2)(\xi+4\pi)r^2\}\right] \quad .
\end{aligned}
\tag{9.39}
$$

Again the electric field E^2 in modified gravity is obtained as

$$
\begin{aligned}
E^2 =& \frac{1}{(3\xi+4\pi)}\left[-4\psi(\xi+2\pi)(\xi+4\pi)\right] \\
& + \frac{1}{(3\xi+4\pi)}\left[\frac{1}{\tau}\{2a(1+\psi)\varphi(\xi+2\pi)-2D(\xi+3\pi)+(D^2\xi+2b(\xi+2\pi))r^2\}\right] \\
& + \frac{1}{(3\xi+4\pi)}\left[\frac{1}{\tau^2}\left(2D\xi+2b(\xi+2\pi)r^2+a\psi(\xi+2\pi+D\xi r^2)\right)\right] \quad .
\end{aligned}
\tag{9.40}
$$

For the physically viable model, it is required that $E^2(r=0)=0$. We have estimated from our current model, the surface electric filed of the charged compact star $X7$ is of the order of 10^{22} (V/m). The Fig. 53 shows the variation of the electric field with

radius of the charged compact objects.

So, the energy density, radial pressure, transverse pressure, anisotropic factor and the electric field in the $f(T)$ modified gravity background have been successfully obtained.

9.1.3.2 Finding the Constants of the Proposed Model

Now, in order to find the constants used in TK metric potentials, we have to match smoothly the interior spacetime metric to the exterior spacetime at the boundary ($r = R$) of the compact stars.

During our work, we have already chosen the spherical symmetric metric, describing the interior space-time of the NSs. Now, in order to find out the metric coefficients as given in the equation (19), we have matched this interior spacetime metric with the exterior Reissner-Nordström metric [256, 257], given as

$$ds^2 = -\left(1 - \frac{2m(r)}{r} + \frac{q^2}{r^2}\right) dt^2 + \frac{dr^2}{\left(1 - \frac{2m(r)}{r} + \frac{q^2}{r^2}\right)} + r^2(sin^2\theta d\phi^2 + d\theta^2) \quad , \quad 0 \leq \theta \leq \pi, \quad 0 \leq \phi \leq 2\pi \quad . \tag{9.41}$$

where $m(r)$ is the total mass enclosed within the boundary of the NSs with radius $r = R$ at the boundary. Now, as we know the at the boundary surface of the NSs, the various space-time variables, g_{rr}, g_{tt} and $g_{tt,r}$ are continuous between these two spacetime metrics. So, after applying matching conditions at the boundary surface ($g_{tt}^{-} = g_{tt}^{+}$ and ($g_{rr}^{-} = g_{rr}^{+}$), we have got the below constraints as

$$\left(1 - \frac{M}{R} + \frac{q^2}{R^2}\right) = C^2 e^{DR^2} \quad , \tag{9.42}$$

$$\left(1 - \frac{M}{R} + \frac{q^2}{R^2}\right) = (1 + aR^2 + bR^4)^{-1} \quad and \tag{9.43}$$

$$\frac{M}{R} - \frac{q^2}{R^2} = DR^2 C^2 e^{DR^2} \quad , \tag{9.44}$$

where $m(r = R) = M$ is the total mass within the boundary of the compact star.

So, in order to calculate the model constants of our present work, we have solved the equations (41) and (43) by applying the condition $p_r(r = R) = 0$ and hence we have obtained

$$a = \frac{1}{R^2(\xi + 2\pi)(1 + 3\chi^2)} \left[-2(\xi + 2\pi) + (\xi + 2\pi)(2 + DR^2)\chi + 6D\pi R^2\chi^2\right] \quad , \quad (9.45)$$

$$b = -\frac{-1 - aR^2 + \chi}{R^4} \quad , \quad (9.46)$$

$$C = e^{-\frac{DR^2}{2}}\chi^{-\frac{1}{2}} \quad and \quad (9.47)$$

$$D = \frac{\chi}{R^2}[\frac{M}{R} - \frac{q^2}{R^2}] \quad , \quad (9.48)$$

where $\chi = \left(1 - 2\frac{M}{R} + \frac{q^2}{R^2}\right)^{-1}$.

As the radial pressure vanishes at the boundary surface of the compact stars, it gives the expression of the surface density of the compact star as

$$\rho_s = \psi + \frac{3\varphi(a + D + (2b + aD)R^2 + bDR^4)}{4(\xi + 4\pi)\tau_R^2} \quad . \quad (9.49)$$

Now, it is clear that, by considering the known values of $m(r)$ and r from different observations on various massive binary NSs, we can easily find out the required model parameters and then substituting these values we can measure all the required quantities related to the binary NSs. we have chosen two binary compact stars $X5$ by assuming $M = 1.4M_\odot$ with $R = 9.6\ km$ and $X7$ by assuming $M = 1.4M_\odot$ with $R = 11.1\ km$ for our study and also assumed $q = 0.0085$ in case of our model [262].

9.1.4 Physical Analysis of the Proposed Model

9.1.4.1 Nature of the Tolman-Kuchowicz metric potentials at the Boundary Surface

In case of this current model, for the asymptotically flat spacetime, the metric potentials $A(r)$ and $B(r)$ does not tend to zero as $r \to \infty$. We have also taken the spacetime signature as (-,+,+,+). Here, $e^{A(r)} = C^2 e^{Dr^2}$ and $e^{B(r)} = (1 + ar^2 + br^4)$. This implies, $e^{A(r)} \mid_{r=0} = e^C > 0$ and $e^{B(r)} \mid_{r=0} = 1$. Furthermore, we can also have, $(e^{A(r)})' = 2rDe^{C+Dr^2}$ and $(e^{B(r)})' = 2are^{Ar^2}$. This behaviour of the metric potentials has given us the opportunity to match the inner spacetime to the exterior spacetime smoothly at the boundary ($r = R$) of the compact stars. This helps to get the constant parameters of our current model. It is also clear that in the interval $(0, R)$, metric potentials are behaving well.

The matching conditions of the metric potentials $e^{A(r)}$ and $e^{B(r)}$ are shown in Fig. 10 and Fig. 11. These plots clearly indicate the smooth matching of the metric potentials at the boundary of the charged compact stars. This also depicts the physical validity of the model using Tolman-Kuchowicz ansatz.

9.1.4.2 Finding the Cental Density and Pressure a function of ξ

In this $f(T)$ modified gravity, the main thermodynamic variables of the compact stars remains almost unaltered but they must obey some criteria. Now, at the centre of the compact stars we have obtained by using Equations (35) to (37)

$$\rho_c = \frac{3\varphi(a+D) + \psi(\xi + 4\pi)}{4(\xi + 4\pi)} \quad and \tag{9.50}$$

$$p_c = -\psi + \frac{\varphi(a+D)}{(\xi + 4\pi)} \quad , \tag{9.51}$$

where ρ_c and p_c are the central density and central pressure of the compact stars respectively. We can also find the corresponding quantities in GR by setting $\xi = 0$. Various important parameters related to the compact stars as obtained from our model is tabulated in Table 3 for the charged binary compact star $X7$. Table 1 [262] and Table

2 gives some important parameters about the chosen binary compact stars as for our model.

Table 1.

Sl. No.	Compact Stars	$M_{obs}(M_\odot)$	$r_{obs}(km)$	$M(M_\odot)$	$r(km)$
1	X5	1.42 ± 0.15	$9.60^{+0.9}_{-1.1}$	1.40	9.60
2	X7	1.41 ± 0.10	$11.1^{+0.8}_{-0.7}$	1.40	11.0

Table 9.1: Charged binary compact stars

Table 2.

Sl. No.	Compact Stars	Mass $M(M_\odot)$	Radius r(km)	$\frac{M}{r}$	$\frac{q^2}{r^2}$
1	X5	1.4	9.60	0.248367	1.251836×10^{-7}
2	X7	1.4	11.0	0.150768	1.182354×10^{-7}

Table 9.2: Mass (M), Radius (r), $\frac{M}{r}$ and $\frac{q^2}{r^2}$ of the charged compact stars

Table 3.

Sl. No.	ξ	p_c $(dyne\ cm^{-2})$	ρ_s $(gm\ cm^{-3})$	ρ_c $(gm\ cm^{-3})$
1	0.00	2.680565×10^{34}	2.354871×10^{15}	2.513483×10^{15}
2	0.08	2.714562×10^{34}	2.424823×10^{15}	2.657281×10^{15}
3	0.16	2.807213×10^{34}	2.584721×10^{15}	2.710628×10^{15}
4	0.24	2.893482×10^{34}	2.672342×10^{15}	2.775691×10^{15}
5	0.32	2.956718×10^{34}	2.852387×10^{15}	2.912348×10^{15}

Table 9.3: Calculated values of p_c, ρ_s and ρ_c of $X7$ for different values of ξ from the model

The variation of radial pressure, transverse pressure and central density are shown in Fig. 48, Fig. 49 and Fig. 50 respectively. The plots depicts that all these parameters obey all the required physical conditions of the realistic compact stars.

9.1.4.3 Observational Constraints

We have also plotted the variations of core matter density (ρ), radial pressure (p_r), transverse pressure (p_t) etc. w.r.t. the radius of the compact stars which are shown in graphical analysis section. The profiles show that all these parameters are positive inside the boundary of the compact star i.e., for $r \in (0, R)$. These above quantities are all monotonically decreasing functions of r. The radial pressure becomes zero at the boundary surface but the transverse pressure and matter density remains positive at the boundary of the compact star.

The central pressure becomes non-negative inside the fluid sphere depicts the physical acceptance of the current model i.e., $p_c > 0$. Again, the Zeldovich condition [388], $\frac{p_c}{\rho_c} < 1$ is fully satisfied by our model when ψ is positive only. Moreover applying this must satisfy condition for any physically accepted compact star model we also have obtained the valid range of ξ as $0 \leq \xi \leq 0.5$. This is why we have also not considered negative values of ξ in this current model. The measured values of core density of the charged compact stars, clearly indicated that the central fluid possess anisotropic form.

9.1.4.4 Verification of Causality Condition

We know that, in order to fulfill the criteria of a physically viable and realistic model, it is essential to satisfy the causality condition and hydrostatic equilibrium by the compact star model. To satisfy the causality condition, the sound velocity must be less than the velocity of light, everywhere at the interior of the object. In case of our model, radial sound velocity V_r and transverse sound velocity V_t both maintain causality i.e., $(V_r^2\ ,\ V_t^2) < 1$. Again, according to Le Chatelier's condition, $(V_r^2\ ,\ V_t^2) > 0$. These two conditions implies that $\mid V_r^2 - V_t^2 \mid < 1$, which is also plotted for different values of ξ.

For any realistic compact star, the "cracking" condition of Herrera [387] must be obeyed for ensuring stability of the object under small radial perturbations. This condition is also satisfied by the anisotropic and charged compact stars in our model. Investigation proved that in the potentially stable region of the anisotropic compact

stars, the radial velocity of sound crosses the transverse velocity of sound [386]. So, we have obtained

$$-1 \leq (V_t^2 - V_r^2) \leq 0 \quad for\ potentially\ stable\ region \quad and \tag{9.52}$$

$$0 < (V_t^2 - V_r^2) \leq 1 \quad for\ potentially\ unstable\ region \quad . \tag{9.53}$$

We have obtained from our current model

$$V_r^2 = \frac{dp_r}{d\rho} = \frac{1}{3} \quad and \tag{9.54}$$

$$V_t^2 = \frac{dp_t}{d\rho} \approx \frac{2}{3} \quad . \tag{9.55}$$

It is also confirmed from our model that the speed of sound in transverse direction is greater than that of in radial direction. So, it is conclusive to say that the causality condition is not violated in case of our model. From all the above conditions and measured values it is clear that various stability conditions under spherical configuration have been fully satisfied by the massive charged NSs under the present situation of the universe. This makes our present model more relevant and effectively realistic. The plots in Fig. 54 and Fig. 55, are indicating the variations and limits of the sound velocities in different directions respectively, whereas the Fig. 56 indicates the variation of stability factor at the interior of the charged binary compact stars.

9.1.4.5 Tidal Deformability and Tidal Love Number

Now, as we know that the equilibrium condition of NSs get tidally deformed due to the presence of an external tidal field, E_{ij}. At the same time due to the spherical symmetric structure, the NSs will develop a quadruple moment, Q_{ij} [224]. The relation between these two quantities can be described as

$$Q_{ij} = -\Lambda E_{ij} \quad , \tag{9.56}$$

where Λ is the tidal deformability, given as [224]

$$\Lambda = -\frac{2r^5}{3G}\kappa \quad , \tag{9.57}$$

where κ is called the tidal love number which is given as

$$\kappa = \frac{8}{5}\tau_M u^5 \left[2u[4(y+1)u^4 + (6y-4)u^3 + (26-22y)u^2 + 3(5y-8)u - 3y + 6] - 3\tau_M log\left(\frac{1}{1-2u}\right)\right] \tag{9.58}$$

where u is the compactness factor of the NS [263], is given as $u = \frac{1}{r}m(r)$, $\tau_M = (1-2u)^2\left[2u(y-1) - y + 2\right]$ and the quantity y, is defined as $y \equiv y(r)\mid_{r=R}$ and can be determined by solving the differential equation numerically, with the initial condition $y(0) = 2$ and which is given as

$$r\frac{d}{dr}y(r) + y^2(r) + y(r)e^{B(r)}\left[1 + 4\pi r^2(p_r - \rho)\right] + r^2Q(r) = 0 \quad , \tag{9.59}$$

where the quantity $Q(r)$ is given as

$$Q(r) = 4\pi e^{B(r)}\left[5\rho + 9p_r + \frac{(p_r+\rho)}{\frac{dp}{d\rho}}\right] - \frac{6}{r^2}e^{B(r)} - A'^2(r) \quad . \tag{9.60}$$

So, for spherically symmetric NSs, by calculating it's mass $m(r)$, radius (r), radial pressure (P_r), energy density (ρ) by using the metric coefficients (or model parameters) and then solving the modified TOV equation and the above differential equation (58) simultaneously, we can find out the tidal deformability and tidal love number of the massive NSs. The dimensionless effective tidal deformability is given by

$$\tilde{\Lambda} = \frac{1}{m^5(r)}\Lambda \quad . \tag{9.61}$$

Again, in case of binary NSs merger, the dimensionless tidal deformability which can be measured by detecting the gravitational wave, is given by

$$\tilde{\Lambda} = \frac{16}{13}\left[\frac{(1+12q)\Lambda_1}{(1+q)^5} + \frac{q^4(12+q)\Lambda_2}{(1+q)^5}\right] \quad with \quad 0 < q(m) \leq 1 \quad , \tag{9.62}$$

where Λ_1 and Λ_2 are the tidal deformability of the two different stars in the binary system respectively and the quantity $q(m) = \frac{m_2}{m_1}$ is the mass ratio of the binary system of two NSs with mass m_1 and m_2 respectively and $m_1 \geq m_2$. The variation of $\tilde{\Lambda}$ with mass of the compact star as a function of anisotropy is shown in the Fig. 65.

On the other hand a specific mass combination in case of a binary NS system is called chirp mass, M_c and given as

$$M_c = \frac{(m_1 m_2)^{\frac{3}{5}}}{(m_1 + m_2)^{\frac{1}{5}}} = m_1 \frac{q^{\frac{3}{5}}}{(1+q)^{\frac{1}{5}}} \quad . \tag{9.63}$$

The variations of the tidal love number and tidal deformability with mass as a function of anisotropy factor in Fig. 51 and Fig. 52 respectively. These plots depict the effect of anisotropy on these quantities of the binary charged compact stars as well as on their stability. It is evident that the presence of anisotropy at the core of these types of binary compact objects reduces the tidal deformable force in a significant amount as compared to other non-anisotropic stars, predicted by GR. This is how these anisotropic compact stars get more stability and get a more compact structure than the stars without anisotropy. Due to the effect of anisotropy. These stars also can acquire more mass as compared to their GR counterparts.

9.1.4.6 Verification of the Energy Conditions

Current proposed model of the charged compact stars will satisfy the weak energy conditions (WEC), the strong energy condition (SEC), null energy condition (NEC) and the dominant energy condition (DEC) if at each and every point inside the stellar interior, the following inequalities holds :

$$\rho + p_r \geq 0 \quad , \quad \rho + p_t + \frac{E^2}{4\pi} \geq 0 \quad , \quad \rho + \frac{E^2}{8\pi} \geq 0, \quad WEC. \tag{9.64}$$

$$\rho + p_r \geq 0 \quad , \quad \rho + p_t + \frac{E^2}{4\pi} \geq 0 \quad , \quad \rho + p_r + 2p_t + \frac{E^2}{4\pi} \geq 0, \quad SEC. \tag{9.65}$$

$$\rho + p_r \geq 0 \quad , \quad \rho + p_t + \frac{E^2}{4\pi} \geq 0, \quad NEC. \tag{9.66}$$

$$\rho - p_t \geq 0 \quad , \quad \rho + \frac{E^2}{8\pi} \geq 0 \quad , \quad \rho - p_r + \frac{E^2}{4\pi} \geq 0 \quad DEC. \tag{9.67}$$

In our study all the above mentioned energy conditions are satisfied and indicates the physical viability of the present model.

9.1.4.7 Mass-Radius Relationship and Compactness Factor

Now, we have obtained the effective mass of the charged massive NSs in $f(T)$ gravity as

$$\begin{aligned} m(r) =& 4\pi \int_0^R \rho R^2 dR \\ &= 4\pi \int_0^R \left[\frac{\xi}{2} f + \frac{2\psi}{r^2} \left[(2b + aD)\left(2 + r(a+b)\right)\psi(1+\varphi) + r(2b+D) \right] \frac{f_T}{\tau} \right] R^2 dR \\ &+ 4\pi \int_0^R \frac{1}{\tau^2} \left[\frac{2\xi^2}{r(1+\varphi)} (bD)\{a + D + (2b + aD)\} \right] T' f_{TT} \\ &+ 4\pi \int_0^R \left[\frac{\psi(1+\varphi)}{4r^2} (a+D)\{b - 1 + r^2 D\} \right] R^2 dR \quad . \end{aligned} \tag{9.68}$$

So, the effective mass of those super massive NSs using our model from the above equation (39). On the other hand, compactness factor of NSs in our work, can be written as

$$\begin{aligned} u(r) =& \frac{1}{r} m(r) \\ &= 4\pi \int_0^R \left[\frac{\xi}{2} f + \frac{2\psi}{r^2} \left[(2b + aD)\left(2 + r(a+b)\right)\psi(1+\varphi) + r(2b+D) \right] \frac{f_T}{\tau} \right] R dR \\ &+ 4\pi \int_0^R \frac{1}{\tau^2} \left[\frac{2\xi^2}{r(1+\varphi)} (bD)\{a + D + (2b + aD)\} \right] T' f_{TT} \\ &+ 4\pi \int_0^R \left[\frac{\psi(1+\varphi)}{4r^2} (a+D)\{b - 1 + r^2 D\} \right] R dR \quad . \end{aligned} \tag{9.69}$$

Now, using equations (67) and (68), we can also measure the radius of those super massive charged NSs from our model. The calculated value of the mass and radius of the two stars are tabulated below. The mass vs radius plot is absolutely interesting for our investigation. Besides we have also plotted the variation of the compactness factor of the charged NSs with radius of the stars and further investigated the effect of anisotropy on this parameter. The outcome which is very amusing, we have discussed later. The Fig. 60 shows the most important $M - R$ relation of the charged compact stars. We can also predict about the maximum possible mass of the $X7$ (Yellow line) and $X5$(green line) and lowest possible radius of these two charged binary compact stars.

For our model, as $m(r) \to 0$ as $r \to 0$. So, we can say that the mass function is regular at the centre. We have also measured the compactness of the charged NSs which lies in between 10^{-1} to $\frac{1}{4}$ which obeys the Buchdahl limit [290]. The plot in the Fig. 61 indicates the same. Further, it shows that, the compactness of the charged binary compact stars increases as anisotropy at the interior of the star increases.

Table 4.

Sl No.	Compact stars	$Mass\ (M_\odot)$	$Obtained\ (M_\odot)$	$radius\ r\ (km)$	$Obtained\ r\ (km)$
1	X5	1.40	1.11258	9.60	11.58723
2	X7	1.40	1.12083	11.0	11.73241

Table 9.4: Calculated values of Mass and radius from the model with $\xi = 0.45$

9.1.4.8 Anisotropic Nature

Interestingly, in our present work, we have got that pressure in radial direction (p_r) is different from the pressure in the transverse direction (p_t), inside the core of the massive charged NSs and actually $p_t > p_r$. This pressure difference inside the core of a NSs, produces anisotropic repulsive force which is acting outward direction and have a great impact on the stability of the compact stars. We can measure the anisotropic

force factor in this present work as $(\Delta^{'})$, at the core of massive NSs and given as

$$\Delta^{'} = \frac{2}{R}\left[p_t - p_r\right] \quad and \quad \Delta^{'} > 0 \quad . \tag{9.70}$$

So, this model shows a positive anisotropy is acting inside the core and we also have investigated its effect on several other crucial parameters of the massive NSs. The origin of this anisotropy is the presence of MCG (as an exotic fluid at the core) inside the NSs and as it increases, the star becomes more and more compact but still finds its stable equilibrium avoiding the collapse. This is the very interesting nature of the NSs which we have discussed later. Several plots in the graphical analysis section show the effect of the anisotropy on various parameters of the charged compact stars. Besides the Fig. 63 shows the variation of anisotropy factor itself against the radius of the star at high core density.

9.1.4.9 Relativistic Adiabatic Index and The Stability

For relativistic compact objects, adiabatic index Γ, plays a important role on it's stability. The value of Γ as if $\Gamma > \frac{4}{3}$ the NSs has got it's stability. In this case of achieving stability $f(T)$ gravity plays a very important roll as well as MCG. We have got the proof that, due to the presence of MCG, inside the NSs core, the small positive value of ξ is sufficient to make a stable and equilibrium structure of the massive NSs in the present accelerated phase of the universe. The relativistic adiabatic index can be measured as

$$\Gamma = \left[\frac{p_r + \rho}{p_r}\right]\frac{dp_r}{d\rho} \quad . \tag{9.71}$$

The above expression depicts that the adiabatic index depends on $\frac{\rho}{p_r}$ ratio. We have also plotted its variation against r inside the stellar interior for different values of ξ. The value of Γ of the charged NSs, we have obtained from this model also confirms the stability of the charged compact object under spherical configuration. The plot in the Fig. 62 depicts the same.

9.1.4.10 Surface Redshift and Equilibrium

The surface redshift function $Z_s(r)$ [48, 49] of the massive NSs can also be measured by using the equation as

$$Z_s(r) = \frac{1}{\sqrt{\left[1 - \frac{m(r)}{r}\right]}} - 1 \quad . \tag{9.72}$$

As a part of our investigation, we have also checked the surface redshift parameter $Z_s(r)$ for the massive NSs and got a very interesting outcome. Astronomical observations suggests that for NSs, it should be like $Z_s(r) \leq 5$ to ensure stable equilibrium configuration. We also have same type of results. The value of $Z_s(r)$ in $f(T)$ gravity along with the presence of MCG and anisotropic pressure at the core of the NSs, strongly and clearly suggests that in this model the star has also got stable equilibrium configuration with a new realistic EoS. The Fig. 64 shows the variation of $Z_s(r)$ with radius as a function of ξ.

Table 5.

Sl No.	Compact stars	Δ'	$Z_s(r)$	Γ
1	X5	0.00022	0.181462	5.120231
2	X7	0.00037	0.170413	5.230165

Table 9.5: Calculated values anisotropic force Δ', surface redshift $Z_s(r)$ and adiabatic index Γ from the model with $\xi = 0.45$

Table 6.

Sl No.	Compact stars	$\frac{V_r^2}{c^2}$	$\frac{V_t^2}{c^2}$	$DEC(dyne\ cm^{-2})$
1	X5	0.198753	0.108141	2.687234×10^{34}
2	X7	0.208121	0.112582	2.784235×10^{34}

Table 9.6: Calculated values of $\frac{V_r^2}{c^2}$, $\frac{V_t^2}{c^2}$ and $DEC(dyne\ cm^{-2})$ from the model with $\xi = 0.45$ at the center of the charged compact objects

9.1.4.11 Equilibrium of the Spherical Configuration of the Neutron Stars under Various Force

Now in order to ensure the viability of this current model in modified gravity, we shall examine the validity of the TOV equation. For this, we will assume that the charged NSs, $X7$ and $X7$ are under equilibrium under different forces acting on the system. There are four different forces acting on the present system, namely : the hydrostatic force F_h, the gravitational force F_g, anisotropic force F_a and finally newly introduced force related to modified gravity F_m.

In this investigation, we have figured out the explicit form of these forces as follows :

$$F_h = -\frac{dp_r}{dr} \quad , \tag{9.73}$$

$$F_g = -\frac{A^{'}(r)}{2}(\rho + p_r) \quad , \tag{9.74}$$

$$F_a = \frac{2}{r}(p_t - p_r) \quad and \tag{9.75}$$

$$F_m = -\frac{\xi}{8\pi + 2\xi}(\rho^{'} + 2p_t^{'} + p_r^{'}) \quad . \tag{9.76}$$

The TOV equation in modified gravity can be written as in equation (20). Now the equation can be written as

$$F_h + F_g + F_a + F_m = 0 \quad . \tag{9.77}$$

Now, the NS $X7$ is in a hydrodynamic equilibrium as the total forces verify the equation (20). The plots of all the forces depicts that the negative gravitational force compensates the positive forces to get a stable equilibrium. So, our model successfully achieved the physical conditions of a charged and anisotropic compact star in stable equilibrium under modified gravity. This can be also verified by the Fig in the graphical section. It assured that the hydrodynamic stability holds true for the anisotropic and

charged binary NSs $X5$ and $X7$. The Fig. 59 confirms the same.

9.1.5 Graphical Analysis : Observational Support

From our present model and investigations, through graphical plots variations of different parameters, of the charged NSs have shown. Plots have given some outstanding outcomes which are very much interesting in the context of various astronomical observations. These variations also have made our chosen model entirely reliable and physically acceptable.

The Fig. 48, shows the variation of radial pressure, p_r with radius, r of the charged NSs. The variation shows that it has a step-like soft phase transition inside the core matter of the NSs at the distance, almost half of its radius ($r \simeq 5.56\ km$). The radial pressure has its highest value at the center of the star and it decreases towards the boundary of the star and at the boundary vanishes. The transverse pressure, p_t in Fig. 49 also has shown the variation in the same fashion but it does not vanish at the boundary of the star ($r = R \simeq 11.65\ km$) but has some positive value when it reaches the surface of the star. The core energy density, ρ also varies in the same pattern like p_t as in the Fig. 50. This type of nature of the radial pressure, transverse pressure and energy density, inside the charged NSs is also supported by several other investigations on them and has given birth to the core and crust concept of NSs [230]. This concept is also clearly reflected by our model. We can see a phase transition at the point almost middle at the interior of the charged NSs which helps to identify separately the core and crust region of the star at high pressure and temperature clearly. Now we have got very interesting results from the variation in the graphical plots between the tidal love number and tidal deformability of the charged NSs with their mass in Fig. 51 and Fig 52 respectively, as a function of anisotropy. The variation shows that, as the anisotropy inside the star increases, its compactness increases which in turn reduces the tidal love number as well as tidal deformability. So, if anisotropy increases inside the star, its tidal love number and tidal deformability both will decrease. So, it is clear that anisotropy has a very crucial effect on the stability and equilibrium of the charged binary compact stars. These plots reveal the utmost impact of anisotropy on

these parameters. As anisotropy increases, the tidal deformability of compact stars decreases in a noticeable amount. The Fig. 53 gives the variation of the electric field as a function of the radius of the charged compact stars at high central density. The plots in Fig. 54 and Fig 55 respectively are very crucial variations for our model as they have shown that in case of our model no causality condition is violated. The Fig. 56 shows the variation of the stability factor with radius of the compact stars. This plot is very important because it shows the potentially stable or unstable region inside the charged compact stars.

The plots in Fig. 57 and Fig. 58 have given the most attractive and crucial plot of our model. These plots show that how the chosen metric potentials, as in our model, match smoothly at the boundary surface of the charged binary compact stars. The matching of the interior and exterior metric potentials reveals the successful applications of spacetime in case of this investigation. On the other hand the Fig. 59 also supports our modified gravity model by showing the stable equilibrium of the present model of the charged compact stars. The most important plot of the $M - R$ relation of these stars is shown in the Fig. 60. The variation in this plot clearly reveals the value of mass and radius of these NSs. The nature of the curves and values of this parameter as shown by the curves are consistent with other astronomical observations on the charged NSs through gravitational wave study. In the Fig. 61, Fig. 62, Fig. 63 and Fig. 64, gives the variation of different crucial parameters related to the charged binary NSs like compactness factor, Adiabatic index, anisotropic factor and surface redshift etc. respectively. Here in the Fig. 65, we have plotted the dimensionless tidal parameter of the NSs as a function of the mass of the star. One can easily get the value of the parameter by studying binary neutron star systems or by the study of gravitational waves.

9.1.6 Final Remarks

In this investigation we have successfully developed a singularity free model of charged binary compact stars $X5$ and $X7$ within the framework of $f(T)$ modified gravity with the presence of an electric field. We have also successfully incorporated the physically

$Fig - 48$

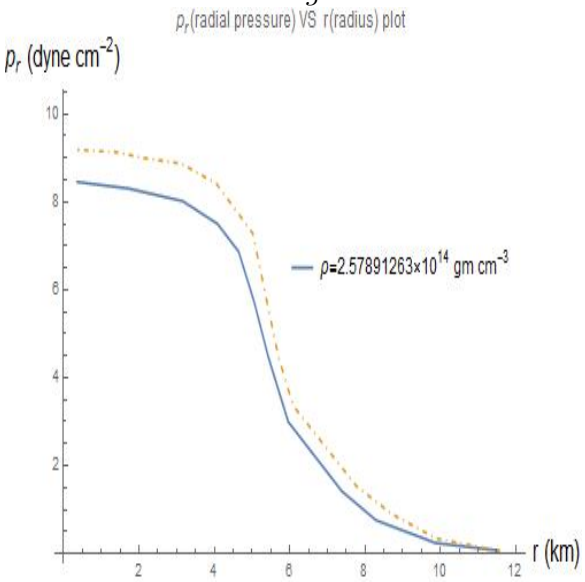

$Fig - 49$

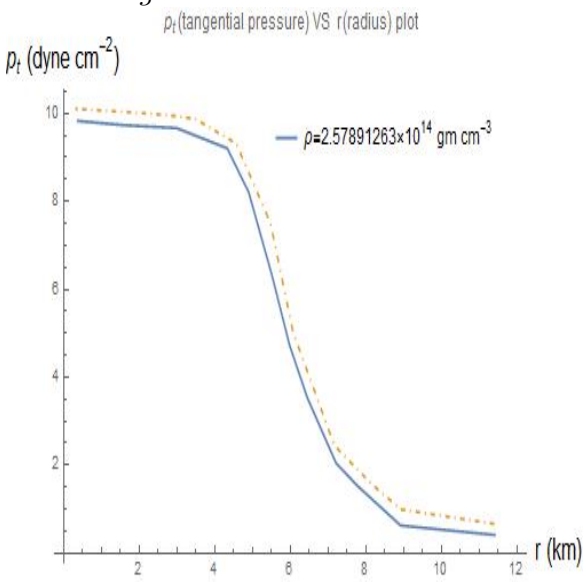

Figure 9.1: *Represents the variation of radial pressure $p_r[dyne\ cm^{-2}]$ with radius $r[km]$ for a high value of central density and for small positive value of ξ.*

Figure 9.2: *Represents the variation of transverse pressure $p_t[dyne\ cm^{-2}]$ with radius $r[km]$ for a high value of central density and for small positive value of ξ.*

$Fig - 50$

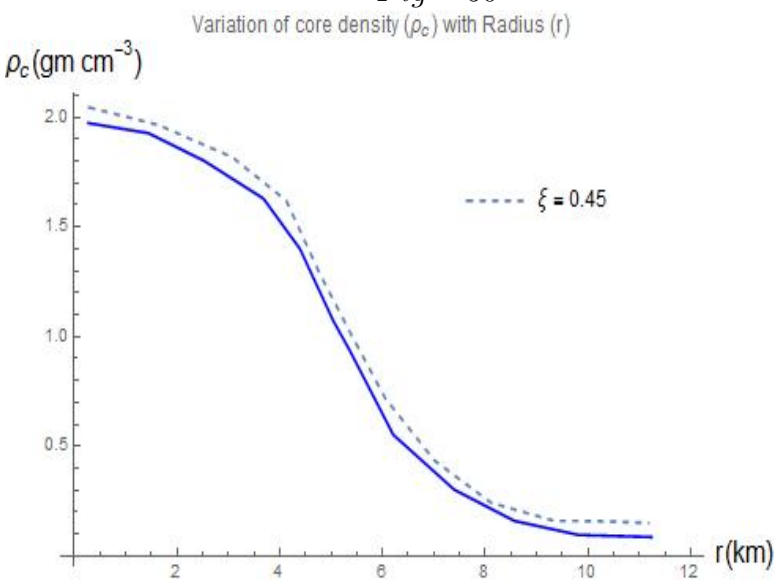

Figure 9.3: *Represents the variation of core density ρ $[dyne\ cm^{-3}]$ with radius r $[km]$ for small positive value of ξ of the massive charged NSs.*

$Fig - 51$

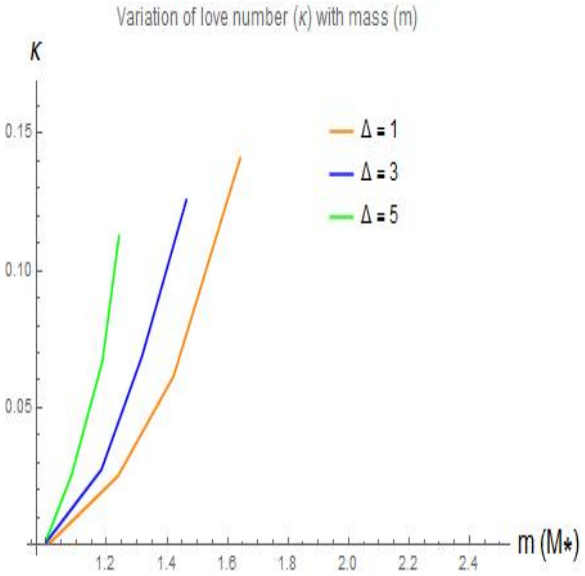

$Fig - 52$

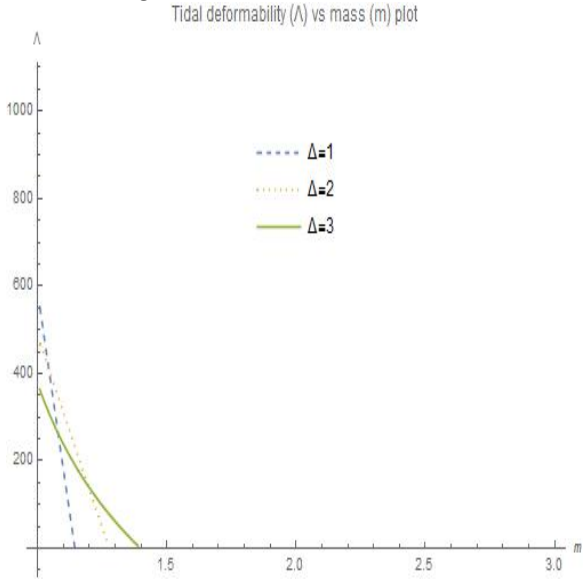

Figure 9.4: *Tidal love number κ for different values of anisotropic parameter Δ with small positive value of ξ are plotted as a function of mass of the charged NS X7.*

Figure 9.5: *Tidal deformability Λ for different values of anisotropic parameter Δ with small positive value of ξ are plotted as a function of mass of the charged NS X7.*

$Fig - 53$

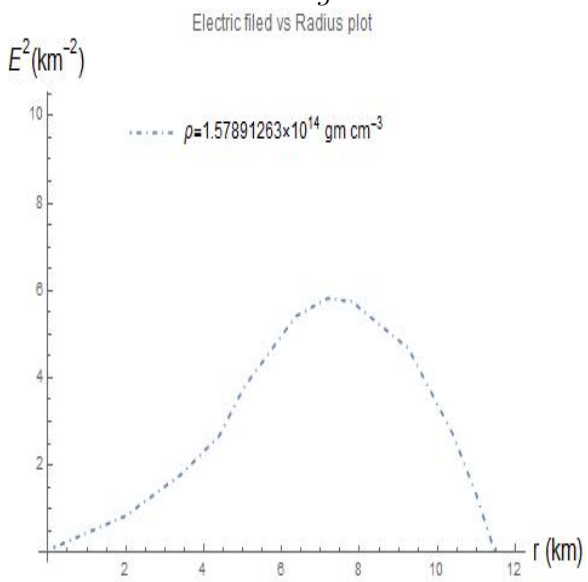

Figure 9.6: *The variation of the electric field of the charged NSs with small positive value of ξ at high core density.*

$Fig-54$

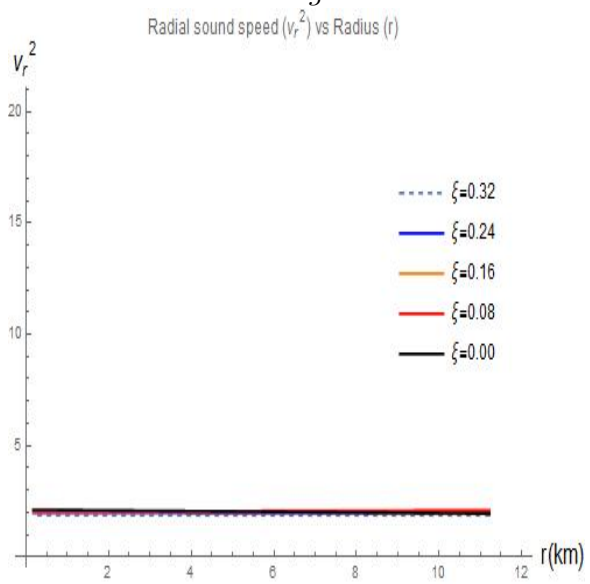

$Fig-55$

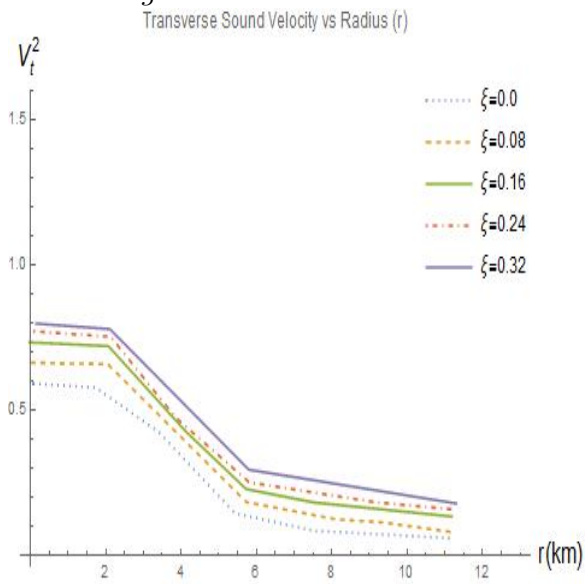

Figure 9.7: *Represents the variation of square of the radial sound velocity V_r^2 with radius $r[km]$ for a high value of central density and for different small positive values of ξ.*

Figure 9.8: *Represents the variation of square of the transverse sound velocity V_t^2 against radius $r[km]$ for a high value of central density and for different small positive values of ξ.*

$Fig-56$

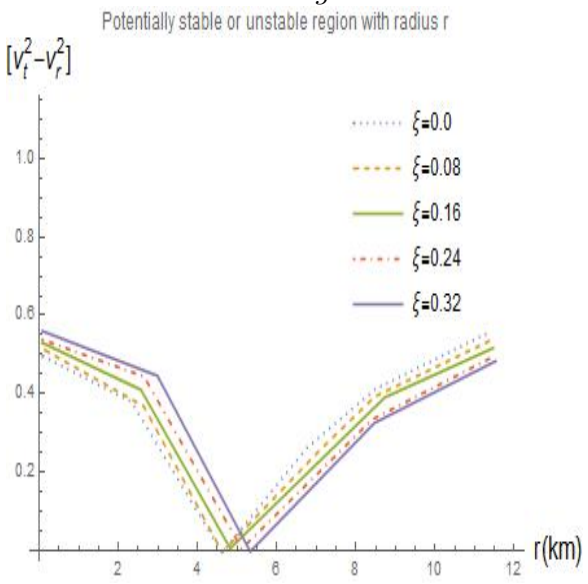

Figure 9.9: *The variation of the stability factor $\mid V_t^2 - V_r^2 \mid$ of the charged NSs with different small positive values of ξ at high core density.*

$Fig - 57$

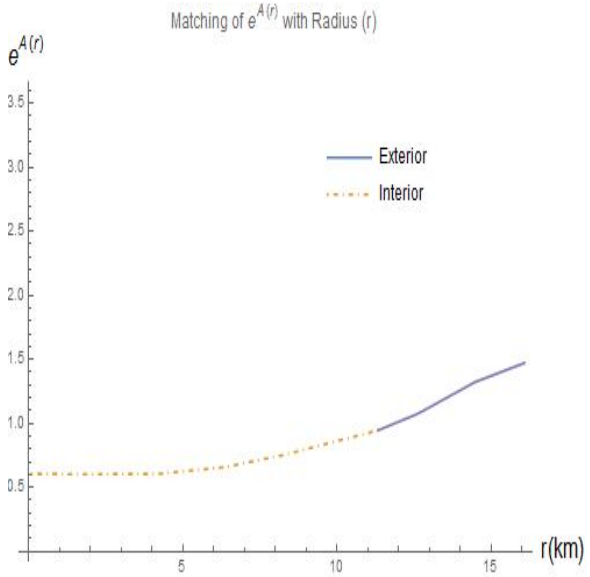

$Fig - 58$

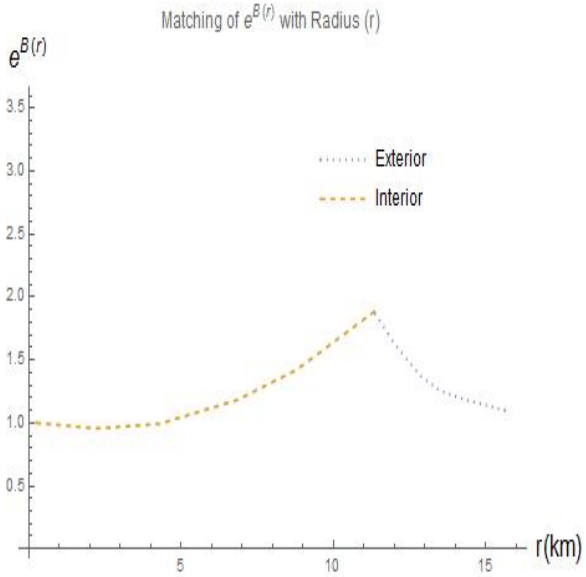

Figure 9.10: *Represents the matching condition of the metric potential* $e^{A(r)}$ *against radius* $r[km]$ *for the charged compact star* $X7$.

Figure 9.11: *Represents the matching condition of the metric potential* $e^{B(r)}$ *against radius* $r(km)$ *for the charged compact star* $X7$.

$Fig - 59$

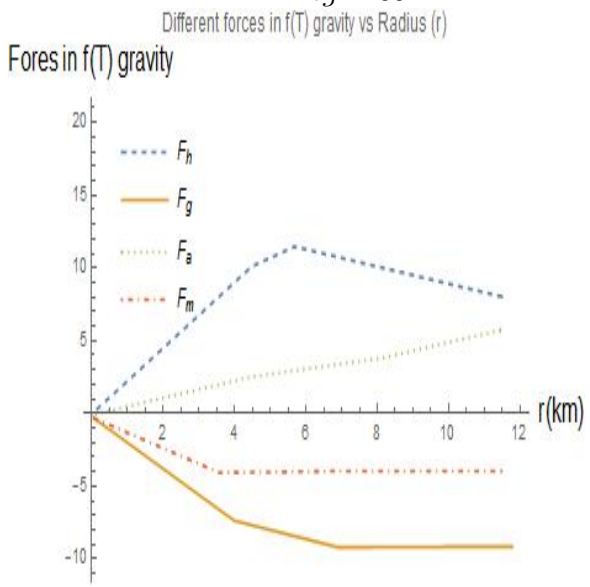

Figure 9.12: *The various forces of the amended TOV equation given by Eq.* (20) *of the charged compact stars* $X5$ *and* $X7$.

$Fig-60$ $Fig-61$

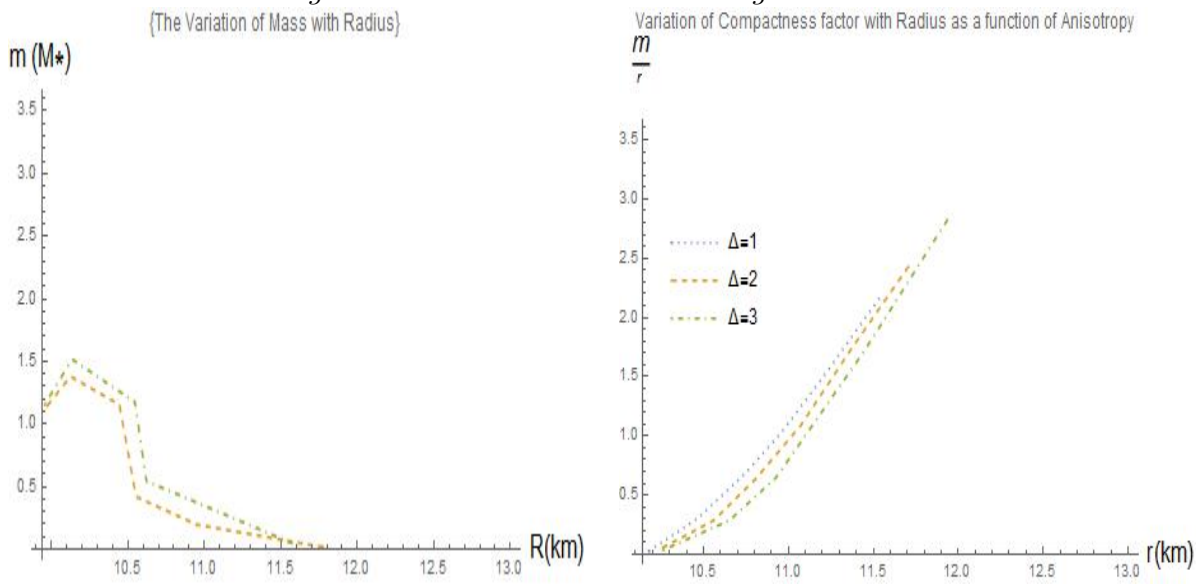

Figure 9.13: *Represents the $M-R$ relation for the charged compact stars.*

Figure 9.14: *Represents the variation of compactness factor for the charged compact stars as a function of anisotropy Δ.*

$Fig-62$ $Fig-63$

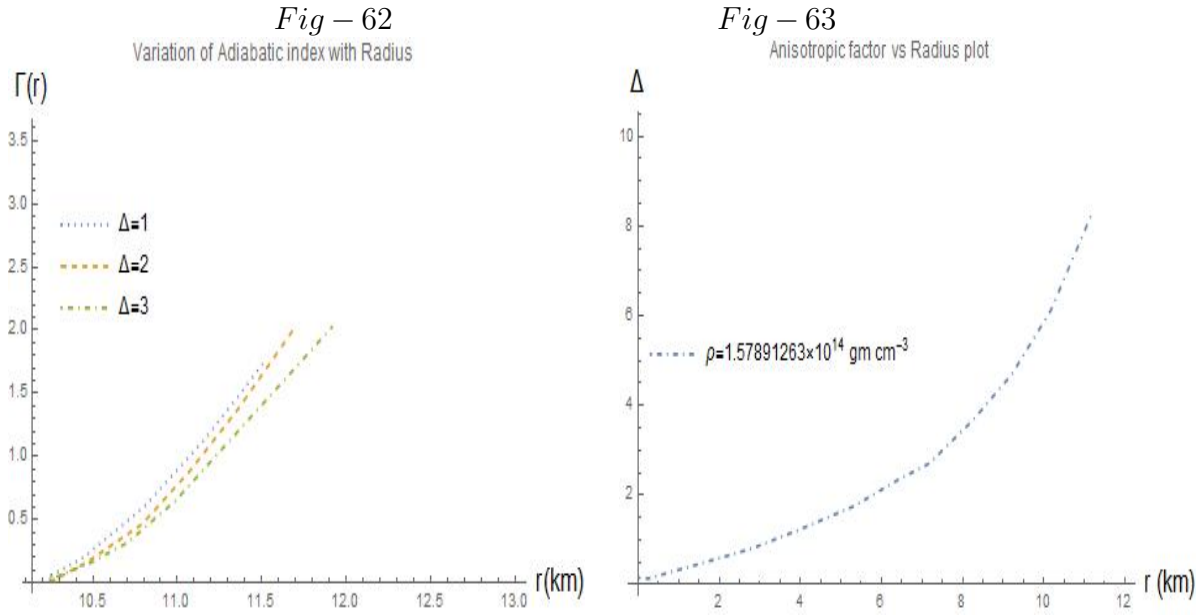

Figure 9.15: *Represents the variation of adiabatic index $\Gamma(r)$ with radius $r(km)$ for the charged compact stars as a function of Δ.*

Figure 9.16: *Represents the variation of anisotropy factor Δ with radius $r(km)$for the charged compact stars at very high central density.*

$Fig - 64$

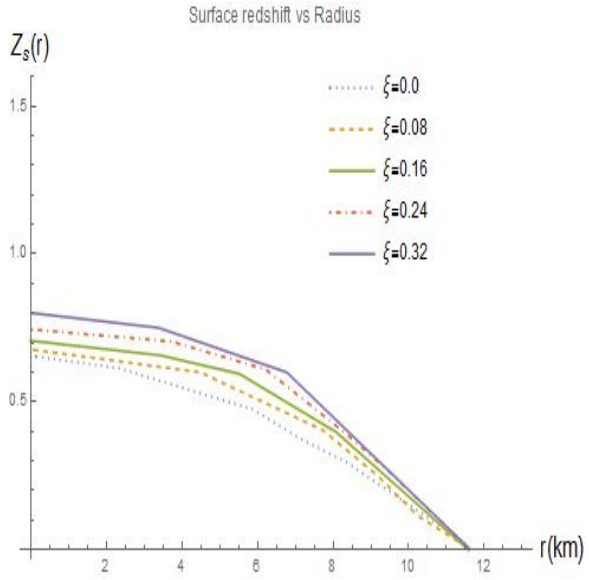

Figure 9.17: *Represents the variation of surface redshift $Z_s(r)$ against radius $r(km)$ for the charged compact stars as a function of ξ.*

$Fig - 65$

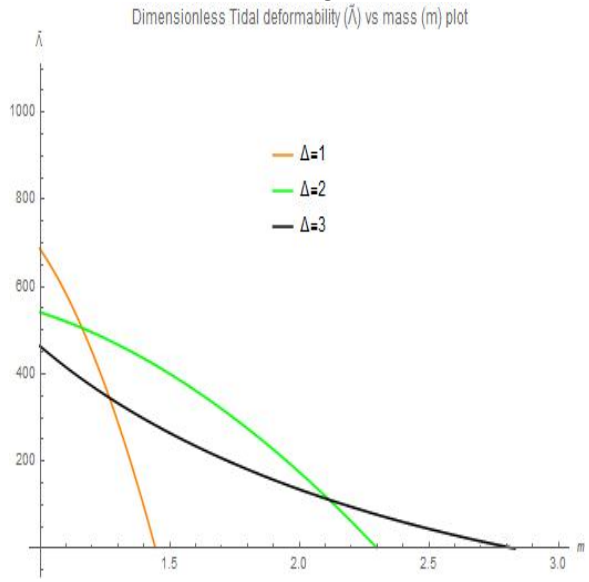

Figure 9.18: *Represents the variation of dimensionless tidal deformability $\tilde{\Lambda}$ with mass $m(M_\odot)$ for massive charged NSs as a function of Δ for small positive value of ξ.*

reasonable Tolman-Kuchowicz (TK) ansatz for the metric potentials which have shown smooth matching at the stellar boundary obeying all the required physical conditions of a singularity free model. Instead of considering an ad hoc equation of state $p+\rho = 0$, we have introduced MCG EoS, exists as perfect fluid inside the core of the stars to examine the impact of dark energy on the EoS of these types of stars and study their evolution through accelerated expansion of the Universe. We have solved the system governing equations using MCG EoS quite successfully as the system produces a stable and spherically equilibrium configuration. Moreover, the behavior of various parameters related to the charged compact stars we have obtained in this model, obeying all the observational constraints and almost similar to the other astronomical observations. This current model has been subjected to rigorous stability, regularity and causality tests which reveals the crucial role of charge, anisotropy and ξ on the compact stars in modified gravity. We have also tested the modified TOV equations by plotting various forces produced from it which affects the stability and equilibrium of the total star system. We have fixed the free constants which arise from the integration of the field equations of our model successfully, by applying the proper boundary conditions.

In this investigation we also have successfully investigated the effect of anisotropy on tidal deformability, mass-radius relation, adiabatic index, surface redshift etc. of the charged, anisotropic binary NSs along with phase transitions at the interior. We have got a clear idea about mass and radius of massive NSs using our model. Furthermore, we have got a very realistic and generalized EoS of the core nuclear matter using $f(T)$ modified gravity accompanied by modified TOV equations. The result is beyond GR predicted values and can avoid different cosmological issues during the present time accelerated universe. From our investigation we also have got the clear picture on the core-crust concept of the charged compact stars. Phase transitions of density and both the pressure at the core-crust interface (at the distance half of the radius) are very interesting and have a great impact on the stable compact structure of the massive binary stars. Even, we are able to give a strong proof on the presence of anisotropic fluid and its impact, inside the core. The role of anisotropy on the behavior and nature of the compact stars is also revealed. Due to the presence of anisotropy at the interior,

a repulsive force appears which acts outward from the center. This repulsive force plays a crucial role to maintain the stability of the star. The very promising results on $X5$ and $X7$, in the context of recent astronomical observations, which we have got from our present model are very much consistent with other astronomical observations as well. This makes our model more realistic and acceptable.

From the mass-radius relationship, we have got some interesting evidence. It is clear from the plot that, for the NS $X5$ (yellow dotted line) with mass about $1.11M_{\odot}$ have the maximum radius around 11.6 km whereas the NS $X7$ (green dotted line) has the mass $1.12M_{\odot}$ with the radius around 11.8 km. Again, we can also predict the maximum possible mass and lowest possible radius of both these stars. They both can possess a maximum mass of around $1.45M_{\odot}$ with a radius about 10.2 km. So, this result has given us a proper understanding about the massive charged binary NSs. At the same time, variation in tidal deformability also reveals some interesting facts on these types of stars. We have found that, for anisotropic charged NSs with mass around $1.15M_{\odot}$, the maximum tidal deformability is around 550 but as anisotropy increases, tidal deformability stars decreasing and becomes around 350, giving the star more stable structure but more compactness with mass about $1.42M_{\odot}$. This observation is very important to explain the stability and equilibrium condition of the charged binary NSs. Fig. 65 also reflects the fact of imposing constraints for the value of dimensionless tidal deformability, through gravitational wave observations. So, it is very clear that binary charged NSs in modified gravity can acquire more mass but still are able to maintain their stable equilibrium configuration by decreasing its tidal deformability.

So, briefly we can say, what we have got from our investigation, we have obtained a singularity free model of the charged anisotropic compact stars. We can even focus on the origin and immediate effect of anisotropy on the nature and properties of NSs which are just remarkable and under further investigation. Interestingly, the presence of exotic fluid at the core of the compact stars and its role is also very crucial indeed. The presence of MCG is the main reason behind the production of anisotropy at the core, which makes the star more compact but at the same time stable. The stable compact structure of the binary charged NSs in $f(T)$ modified gravity with the direct

impact of MCG on the mass-radius relationship and tidal deformability is crucial and as well as attractive for further research on binary anisotropic NSs. The required EoS of the core nuclear matter of the NSs from our model is more realistic and generalized in the sense that we have got it with a very small positive value of ξ and simultaneous presence of exotic fluid at the core as dark matter. Setting ξ as zero we can also recover the GR results. This is how $f(T)$ gravity plays a very important role in case of the compact stars. Due to the presence of positive anisotropy inside, repulsive gravitational force also comes into play and it has a great impact on the stability of the charged compact stars in such a dense condition with high pressure.

After this above detail and clear discussions of our investigation, we can conclude that this present working model is very interesting, realistic as well as self sufficient to describe all possible nature and behavior of the charged NSs in a lucid way. It helps to understand the binary compact stars in a more generalized manner with a realistic EoS of the core nuclear matter. Moreover the compatibility of the results we have got, with other observational results, reflects the importance and viability of the present model in the background of $f(T)$ modified gravity.

"Look up at the stars and not down at your feet. Try to make sense of what you see, and wonder about what makes the Universe exist. Be curious".

—Stephen Hawking

CHAPTER 10

ANISOTROPIC NEUTRON STARS IN $F(R,T)$ MODIFIED GRAVITY

10.1 The Effect of Anisotropy on Massive Neutron stars in $f(R,T)$ Modified Gravity under Krori-Barua Space-Time

10.1.1 Prelude

In this present study, our main focus is to investigate, specially the mass-radius relation and several important properties of massive neutron stars to realize the nature, behavior and evolution of these kinds of compact objects through present time. Also, we want to understand the equation of state of the core nuclear matter precisely with their stable equilibrium configuration. We have chosen a few massive binary pulsars and investigated on maximum attainable mass and lowest possible radius of them. We have considered Einstein-Hilbert action as $f(R,T) = R + \alpha T$, where R is the Ricci scalar and T, the trace of energy-momentum tensor with α as the coupling parameter and also used modified TOV equations. The interior space time of the spherical neutron star is

matched to the exterior Schwarzschild line element at the surface of the star. The $M-R$ curve has given the maximum allowable mass is about $3.51M_{\odot}$ with lowest possible radius of around 10.5 km for the massive compact stars under stable equilibrium. We have got a clear picture of structural evolution of massive neutron stars through accelerating space-time and can put some constraints on several quantities related to them. It is depicted from our present investigation that all the derived outcomes are compatible with physically adopted regimes which reveals the viability of our current model in the context of $f(R,T)$ modified gravity.

The discovery of compact binary coalescence, by LIGO/VIRGO scientific collaboration has created a lot of enthusiasm amongst the researchers [291, 293, 292, 294]. Neutron stars (NSs hereafter) actually provides a extraordinary environment to look into the matter at extremely high density. It has also given the opportunity to study the massive relativistic objects in strong gravitational fields. The study on the exact equation of state (EoS hereafter) of compact objects and their evolution through the accelerated expansion of the universe are also matters of immense interest in this decade. Recent observations of X-ray also provide the opportunity to determine the mass and radii of NSs along with gravitational waves. The main aim of the NISER mission is to study on millisecond pulsars and to determine their mass and radii as well as EoS. So far, scientists are able to determine the mass of few pulsars which leads to $M = (1.97 \pm 0.04\ M_{\odot})$ for PSR $J1614-2230$, PSR $J0348+0432$ has $M = (2.01 \pm 0.04\ M_{\odot})$ and the other one is PSR $J0740+6620$, with $M = (2.14 \pm 0.1\ M_{\odot})$ [295, 296, 297]. Very recently, Romani. et. al., have found the mass of PSR $J0952-0607$ as $M = 2.35 \pm 0.17 M_{\odot}$ [298]. Now, from the above observations, it is very clear that a stiff equation of state is very much needed in order to describe the high mass of these anisotropic compact stars under strong gravity [299, 300, 301]. There are many alternative solutions to the field equations of GR, for fluid spheres under spherical symmetry. Whereas Krori-Barua(KB) [342] solutions are very famous for modelling realistic NSs as its metric satisfies the physical requirements of a real star. This alternative KB metric can be applied in order to describe the geometry of space-time. Researchers also get the opportunity to explore its implications

and applications in understanding the gravity precisely. However, various observational evidence have unlocked the accelerated expansion of the universe at present [302, 303, 304]. Scientists are in the conflict of choosing the proper gravity theory as well as the matter contained. Normal matter with Einstein's gravity theory cannot assist the above observational results. It suggests that the general relativity (GR hereafter) theory must be modified in order to explain this phenomena [305, 306, 307, 309]. Researchers have been trying to explain the accelerated universe using the presence of dark energy [310, 349, 351]. Modified gravity theory is able to accommodate the tension in the present expansion rate of the present accelerated universe in a natural way. This theory can also modify the standard cosmological model alternatively through dark matter [313, 372, 315]. The significant deviation of the space-time around the massive NSs can be well predicted by the modified $f(R,T)$ gravity theory as a neutral extension of GR. Generally, the positive dimensionless coupling parameter α of this modified gravity theory predicts the massive and larger size of the compact stars compared to GR theory. It is because of a new force resulting due to the matter-geometry coupling [341].

Harko et al. [316], have proposed $f(R,T)$ gravity as a generalized and arbitrary function of $f(R)$ gravity theory in order to establish a coupling between geometry and matter with T, as the trace of the energy-momentum tensor. The role of the matter part in the lagrangian of gravity is justified due to the quantum effect as a conformal anomaly. Indeed, the linear model of modified gravity as $f(R,T) = R + \alpha T$, is a very simple and most cultured model with a minimal matter-gravity coupling with various cosmological aspects [317, 318, 319, 320]. Interestingly, the very important property of this model is that, we get $R = 0$ outside the compact star and as a result of that the exterior spacetime can still be explained by using the Schwarzschild exterior solution. Further, the anisotropic sector of the compact stars can also be investigated by using this $f(R,T)$ modified gravity model governed by the term $\theta_{\mu\nu}$ [321, 374, 375, 324]. Besides, the results of Einstein's gravity theory can also be recovered by making α zero in $f(R,T)$ gravity theory [385, 329, 376, 331]. Furthermore, this very interesting $f(R,T)$ gravity, is one type of generalization of $f(R)$ gravity which has become very significant

and gained a lot of attention in recent times. In various cosmological investigations on massive relativistic objects, the generalised matter-curvature coupling become significant by using $f(R,T)$ gravity [332, 333]. Solutions to relativistic compact stars have been also studied in $f(R,T)$ gravity [334, 356]. A few hypothetical models of quark stars with their properties have been also studied in $f(R,T)$ gravity [336, 337, 338, 339]. Beyond GR, the anisotropic space-time is very much relevant to the modified theories of gravity. Several investigations in modified gravity theories are going to allow the anisotropic contributions to the gravitational field by modifying Einstein's field equations. Researchers can test and examine the implications of anisotropic space-time by studying this anisotropic space-time.

For a few decades, scientists have been studying the EoS of equilibrated charge-neutral matter and its inter-connections with the properties of the NSs. The massive compact stars provide very important insights into the nature and behavior of the matter under extreme conditions of strong magnetic fields and intense gravitational fields. Proper knowledge and understanding of compact star properties may constrain the nature of the EoS at supra-saturation densities. The study of the properties and evolution in modified gravity is very much important in the context of recent astronomical observations. The binary star merger event is the main source of detecting gravitational waves (GW hereafter) also. The investigation on the mass-radius relations of the massive NSs through a modification of the Tolman-Oppenheimer-Volkoff (TOV hereafter) equations induced by extended $f(R,T)$ gravity theory has become very interesting at present time. In this present work, we have taken a linear and analytical extension of $f(R,T)$ and investigated the impacts of the parameter α to the internal structure of the compact objects. We have also solved the modified TOV equations for a uniform density inside the core of the NSs. We have investigated the structural evolution of the compact stars through this present working model in the background of $f(R,T)$ modified gravity.

10.1.2 Construction of Basic Mathematical Equations in $f(R,T)$ Gravity : The Stellar Equations under Spherical Symmetry

10.1.2.1 Mathematical Formulation of $f(R,T)$ Gravity

Basic mathematical construction of $f(R,T)$ gravity has been discussed in detail in the Chapter 5. Here we have incorporated only few basic equations required to construct this current model. In this section, we have supervised, in a nutshell, the methodology used to obtain our main results by incorporating the $f(R,T)$ extended gravity formalism after considering the spherical symmetry of the NSs. In this section, we have shown how $f(R,T)$ gravity has been introduced by using integration of the Ricci scalar R, over 4 dimension, after considering Einstein-Hilbert action.

The relation between spacetime metric, $g_{\mu\nu}$ and the tangent space metric η is given by

$$g_{\mu\nu} = h^a_\mu \; h^b_\nu \; \eta_{ab} \quad , \tag{10.1}$$

where $\eta_{ab} = diag(-1,+1,+1,+1)$ and the tetrad is given by $h^a = h^a_\mu \; dx^\mu$, so that $h^a \; (e_b) = \delta^a_b$.

Again, in $f(R,T)$ modified gravity, modified Einstein-Hilbert action takes the form,

$$S_{EH} = \int |h| L_M d^4x + \frac{c^4}{16\pi G} \int f(R,T)|h| d^4x \quad , \tag{10.2}$$

where $|h| = det(h^a_\alpha) = \sqrt{-g}$ describes the determinant of the tetrad (h^a_α), L_M represents the perfect matter fluid Lagrangian and $g = det(g_{\mu\nu})$. Now, if we consider the stellar matter as perfect fluid then we can assume the energy-momentum tensor as

$$T_{\mu\nu} = [(p+\rho)\, u_\mu u_\nu - p g_{\mu\nu}] \quad , \tag{10.3}$$

where $T_{\mu\nu}$ can be defined as

$$T_{\mu\nu} = -\frac{2}{|h|} \frac{\partial (L_M |h|)}{\partial g^{\mu\nu}} \quad . \tag{10.4}$$

So, in metric formalism, by using the variation w.r.t. the metric tensor, the equations (6) and (8) gives the field equation in $f(R,T)$ gravity as

$$\frac{\partial f_R(R,T)}{\partial R}R_{\mu\nu}-\frac{1}{2}f(R,T)g_{\mu\nu}-[\nabla_\mu\nabla_\nu-g_{\mu\nu}\Box]\frac{\partial f_R(R,T)}{\partial R}=E_{\mu\nu}+T_{\mu\nu}-T_{\mu\nu}f_T(R,T)-f_T(R,T)\Theta_{\mu\nu} \quad , \tag{10.5}$$

where $f_R(R,T)=\frac{\partial f(R,T)}{\partial R}$ and $f_t(R,T)=\frac{\partial f(R,T)}{\partial T}$ and $E_{\mu\nu}$ is the energy momentum tensor related with the electromagnetic field of the NSs. Here, the box operation $\Box$ in terms of covariant derivative ∇_μ, is defined as $\Box=g^{\mu\nu}\nabla_\mu\nabla_\nu$ and $\Theta_{\mu\nu}$ can be obtained as

$$\Theta_{\mu\nu}=g_{\mu\nu}\nabla^\mu-2T_{\mu\nu}-2g^{\alpha\beta}\frac{\partial^2 L_M}{\partial g^{\mu\nu}\partial g^{\alpha\beta}} \quad . \tag{10.6}$$

With considering the four velocity such as $u_\mu u^\mu=1$ and equations (8) and (9) gives the reduced form of the above equation (10) as

$$\Theta_{\mu\nu}=-\rho g_{\mu\nu}-2T_{\mu\nu} \quad ,if\ we\ take,\ L_M=\rho\ and\ \frac{\partial^2 L_M}{\partial g^{\mu\nu}\partial g^{\alpha\beta}}=0 \quad . \tag{10.7}$$

Now, using the equations (6) and (7), we get the effective energy-momentum tensor in $f(R,T)$ modified gravity as

$$T_{\mu\nu}=\left[T_{\mu\nu}f_T+\frac{1}{2}\left(f-Rf_R\right)g_{\mu\nu}-\rho g_{\mu\nu}f_T-\left(g_{\mu\nu}\Box-\nabla_\mu\nabla_\mu\right)f_R\right] \quad . \tag{10.8}$$

10.1.2.2 Field Equations in Krori-Barua Space-Time

In this work, we have chosen the spherically symmetric metric as

$$ds^2=-e^{a(r)}dt^2+e^{b(r)}dr^2+r^2d\Omega^2 \quad , \tag{10.9}$$

where the unknown metric functions, $a(r)$ and $b(r)$ are purely radial and $d\Omega^2=sin^2\theta d\phi^2+d\theta^2$. Here, for our purpose, we have chosen the metric potentials in terms of Krori-Barua (KB) Ansatz [342] as

$$a(r)=Br^x+Cr^y \quad and \quad b(r)=Ar^z \quad , \tag{10.10}$$

where under properly chosen physical conditions and taking worthy values of these arbitrary constants x, y and z, we can easily find out the values of the model parameters A, B and C of this present work. For the specific values of $x = 2$ and $y = z = 3$, the unknown radial functions $a(r)$ and $b(r)$ reduce to the forms in which anisotropic quintessence star has been investigated in the reference [336].

Again, we have also chosen the realistic $f(R,T)$ gravity as some separate arbitrary functions of R and T respectively as

$$f(R,T) = f_1(R) + f_2(T) = R + \alpha T \quad as \; f_1(R) = R \quad and \quad f_2(T) = \alpha T \quad , \tag{10.11}$$

in order to investigate the coupling between matter and curvature of space-time simultaneously where α is the coupling constant.

In this modified gravity formalism, the field equations along the line element of the spherically symmetric metric can be written as [337]

$$4\pi p - \alpha\left(\rho - 3p\right) = \frac{1}{2}e^{-b(r)/2}\left[\frac{a^{''}}{2} + \frac{a^{'2}}{4} - \frac{a^{'}b^{'}}{4} + \frac{a^{'} - b^{'}}{2r}\right] \quad , \tag{10.12}$$

$$4\pi\rho + \alpha\left(3\rho - p\right) = \left[\frac{1 - e^{-b(r)}}{r^2} + \frac{b^{'}(r)e^{-b(r)}}{r}\right] \quad and \tag{10.13}$$

$$4\pi p - \alpha\left(\rho - 3p\right) = \left[\frac{e^{-b(r)} - 1}{r^2} + \frac{b^{'}(r)e^{-b(r)}}{r}\right] \quad . \tag{10.14}$$

where prime ($'$) represents the derivative w.r.t. r.

Now, the matter density ρ and the radial pressure p becomes

$$\rho = e^{-b(r)/2}\left[\left(\frac{a^{''}}{2} + \frac{a^{'2}}{4} - \frac{a^{'}b^{'}}{4} + \frac{a^{'}}{r}\right)f_R + \left(\frac{b^{'}}{2} - \frac{2}{r}\right)f_R^{'} - e^{b(r)/2}\frac{1}{2}f - f_R^{''}\right] \quad and \tag{10.15}$$

$$p = \frac{e^{-b(r)/2}}{1 + f_T}\left[\left(\frac{b(r)^{'}}{r} - \frac{a^{''}}{2} - \frac{a^{'2}}{4} + \frac{a^{'}b^{'}}{4}\right)f_R + \left(\frac{b^{'}}{2} - \frac{2}{r}\right)f_R^{'} - \frac{e^{b(r)/2}}{2}\left(\rho f_T - \frac{f}{2}\right)\right] \quad . \tag{10.16}$$

So, in $f(R,T)$ gravity, the field equations can be written as

$$\rho = \frac{2}{(1+\alpha)}\left[\left(\frac{2+5\alpha}{1+\alpha}\right)\kappa_1 - \alpha\kappa_2 + 2\alpha\kappa_3\right] \quad , \tag{10.17}$$

$$p_r = \frac{-2}{(1+\alpha)}\left[\left(\frac{2\alpha}{1+\alpha}\right)\kappa_1 - (2+3\alpha)\kappa_2 + 2\alpha\kappa_3\right] \quad and \tag{10.18}$$

$$p_t = \frac{-2}{(1+\alpha)}\left[\left(\frac{\alpha}{1+\alpha}\right)\kappa_1 + \alpha\kappa_2 - 2(1+\alpha)\kappa_3\right] \quad , \tag{10.19}$$

where κ_1, κ_2 and κ_3 are given as

$$\kappa_1 = \alpha e^{-b(r)/2}\left[\left(\frac{a''}{2} + \frac{a'^2}{4} - \frac{a'b'}{4} + \frac{a'}{r}\right)f_{1R} + \left(\frac{b'}{2} - \frac{2}{r}\right)f'_{1R} - e^{b(r)/2}\frac{1}{2}f_1 - f''_{1R}\right] \quad , \tag{10.20}$$

$$\kappa_2 = \frac{\alpha}{1+\alpha}e^{-b(r)/2}\left[\left(-\frac{a''}{2} - \frac{a'^2}{4} + \frac{a'b'}{4} + \frac{b'}{r}\right)f_{1R} + \left(\frac{a'}{2} - \frac{2}{r}\right)f'_{1R} + e^{b(r)/2}\frac{1}{2}f_1 - f''_{1R}\right] \quad and \tag{10.21}$$

$$\kappa_3 = \frac{\alpha}{1+\alpha}e^{-b(r)/2}\left[\left(-\frac{a'}{2r} - \frac{1}{r^2} - \frac{e^{-b(r)/2}}{r^2} + \frac{b'}{2r}\right)f_{1R} + \left(-\frac{b'}{2} + \frac{a'}{2} + \frac{1}{r}\right)f'_{1R} - e^{b(r)/2}\frac{1}{2}f_1 + f''_{1R}\right] \quad . \tag{10.22}$$

10.1.3 Proposed Model in $f(R,T)$ Gravity

10.1.3.1 Finding the Constants of the Proposed Model: Application of Matching Conditions at the Boundary

The exterior solution of modified $f(R,T)$ gravity is the Schwarzschild solution as the vacuum solutions of GR theory and modified $f(R,T)$ gravity are equivalent [340]. We have chosen the exterior space-time metric for the NSs as Schwarzschild metric as

$$ds^2 = -\left(1 - \frac{2M}{r}\right)dt^2 + \frac{1}{\left(1 - \frac{2M}{r}\right)}dr^2 + r^2(sin^2\theta d\phi^2 + d\theta^2) \quad , \tag{10.23}$$

where M is the total mass of the NS within it's boundary ($r = R$) and r is it's radius. So, at the boundary surface of the NSs, between the exterior and interior metrics, the space-time variables like g_{tt}, g_{rr} and $g_{tt,r}$ are continuous, i.e, $g_{rr}^{-} = g_{rr}^{+}$ *and* $g_{tt}^{-} = g_{tt}^{+}$ and yield the below constraints as

$$\left(1 - \frac{2M}{R}\right) = e^{BR^x + CR^y} \quad and \tag{10.24}$$

$$\left(1 - \frac{2M}{R}\right) = e^{-AR^z} \quad . \tag{10.25}$$

For our investigation we have already chosen the interior static spherically symmetric metric as given by equation (13) and the unknown metric function in terms of some arbitrary constants A, B, and C of our model as given by equation (14). The values of these constant can be found out by using some observational data of compact stars and applying matching conditions simultaneously under suitable boundary conditions. The interior solution should behave as regular and as a result the energy-density, radial and tangential pressures of the fluid which is under consideration must be non-singular inside the core of the compact stars. It should behave regularly everywhere inside the star.

Further, physical quantities as mentioned above, should have maximum values at the stars center. The quantities will behave in a decreasing manner towards the surface boundary of the star. Also the density, radial and tangential pressure all should be positive in the range ($0 < r < R$). At the surface of the star, radial pressure p_r must be zero, i.e, $(p_r \mid_{r=R}) = 0$. But On the other hand, the tangential pressure p_t does not essentially have to be zero at stars surface. All the above considered matching conditions at the boundary are strictly obeyed by the massive NSs which are chosen in this model. The verification of the result has been indicated in the graphical plots in the Fig 1 to Fig 4.

So, in order to get the values of our model parameters, we have solved the above equations (27) and (28) by considering all the above boundary conditions and obtained

$$A = -\frac{1}{R^z} ln\left(1 - \frac{2M}{R}\right) \quad , \tag{10.26}$$

$$B = -\frac{1}{R^{x(x-y)}}\left[-yln\left(1 - \frac{2M}{R}\right) + \frac{2M}{R}\left(1 - \frac{2M}{R}\right)^{-1}\right] \quad and \tag{10.27}$$

$$C = \frac{1}{R^{y(x-y)}}\left[xln\left(1 - \frac{2M}{R}\right) + \frac{2M}{R}\left(1 - \frac{2M}{R}\right)^{-1}\right] \quad . \tag{10.28}$$

Now, the values of A, B and C can be calculated by putting the values of M and R from various observations. Then we are able to find out the values of different crucial parameters of our model related with the super massive NSs.

10.1.3.2 Determination of the Parameters related to the Neutron Stars

In terms of these chosen arbitrary constants, the solutions of the equations $(17) - (19)$ can be written as

$$\begin{aligned}\rho =& \frac{2\alpha e^{-Ar^z/2}}{(1+\alpha)(1+2\alpha)}\left[\left(2\tau(1+\alpha)(3B - ABr^x + B^2r^2) + 4A\alpha + \frac{2\alpha}{r^2}(e^{Ar^z/2} - 1)\right) f_{1R}\right] \\ &+ \frac{2\alpha e^{-Ar^z/2}}{(1+\alpha)(1+2\alpha)}\left[\left((2+3\alpha)(Ar - \frac{2}{r}) + 3\alpha Br\right) f'_{1R} - (2+3\alpha) f''_{1R} - f_1(1+\alpha)e^{Ar^z/2}\right] \quad ,\end{aligned} \tag{10.29}$$

$$\begin{aligned}p_r =& \frac{2\alpha e^{-Ar^z/2}}{(1+\alpha)(1+2\alpha)}\left[e^{Ar^z/2}2(1+\alpha)f_1 - \alpha f''_{1R} + \left(\alpha Ar^z + Br(2+\alpha) + \frac{(2+3\alpha)}{r}\right) f'_{1R}\right] \\ &- \frac{2\alpha e^{-Ar^z/2}}{(1+\alpha)(1+2\alpha)}\left[\left(2\tau(1+\alpha)\left(B - 2A - ABr^x + B^2r^2\right) + \frac{2\alpha}{r^2}\left(e^{Ar^z/2} - 1\right)\right) f_{1R}\right] \quad and\end{aligned} \tag{10.30}$$

$$\begin{aligned}p_t =& \Theta\left[e^{Ar^z/2}2(1+2\alpha)f_1 + (2+3\alpha)f''_{1R} - \left(2\tau\alpha\left(Ar(2+3\alpha)\right) - Br(2+\alpha) - \frac{1}{r}(1+\alpha)\right) f'_{1R}\right] \\ &- \Theta\left[A - Br^x(1+2\alpha) - \frac{1}{r^2}(1+\alpha)\left(1 - e^{Ar^z/2}\right) f_{1R}\right] \quad ,\end{aligned} \tag{10.31}$$

where $\tau = (xBr^x + yCr^y + zAr^z)$ and $\Theta = \frac{2\alpha e^{-Ar^z/2}}{(1+\alpha)(1+2\alpha)}$.

10.1.4 Physical Analysis

In this article, for our investigation, we have chosen the $f(R,T)$ modified gravity formalism to study the super massive NSs and as well as for obtaining the maximum allowable mass by any binary NS in stable condition. Very recent discovery of Todd. A. Thompson et. al., shows that they have found a compact object of about $3.3M_{\odot}$ which indicates the low mass black hole or ultra massive NS [45]. On the other hand, TOV limit in GR predicts the maximum allowable mass by any NS is about $3M_{\odot}$ [46], but GR has some shortcomings in case of study of these super massive relativistic compact objects. Few study on $f(R)$ modified gravity agrees with the GR predicted value whereas some other studies on $f(T)$ modified gravity theories has shown that the upper bound of the stellar mass of NSs may be about $3.2M_{\odot}$ [47, 48].

So, in this context, we can say that the study of massive stellar compact objects on the basis of these modified gravity theories alone, has arisen some controversial issues. More investigations are needed to get the upper bound of maximum attainable mass by the NSs. For this types of investigation NSs in binary systems are very important. So, to avoid such type of controversy and getting a reliable compact structure of ultra massive NSs we have chosen $f(R,T)$ modified gravity formalism where, Ricci scalar (R) and trace of energy-momentum tensor (T) has a coupling between them which plays a crucial role in explaining the massive compact stars quite successfully through the coupling between matter and curvature [62-64]. This formalism also provides us a viable study on the structural evolution of the massive compact stellar objects with the present evolution of the universe.

10.1.4.1 Observational Constraints

In case of our present model of the massive NSs in the framework of $f(R,T)$ modified gravity, various properties of the massive stars are under different observational constraints. To get a spherically stable equilibrium condition, these constraints plays a very crucial role. At the present time of the accelerated universe the study of the evolu-

tion of the massive compact stars is very significant as well as important. The density, tangential pressure and radial pressure should be positive i.e., $\rho(0 < \frac{r}{R} < 1) > 0$, $p_r(0 < \frac{r}{R} < 1) > 0$ and $p_t(0 < \frac{r}{R} < 1) > 0$. At the boundary $(r = R)$ of the stars radial pressure must be zero but tangential pressure is not necessary to be zero. These conditions are well verified for the massive NSs in our model as shown in Fig. 66 to 71. The interior solutions of the stars must have a regular, non-singular pattern at the core. The derived values of the density, radial pressure and tangential pressure of the compact stars from our model shows that our current model supports that core of the stars contains neutrons. Moreover, the value of the core energy density exhibits that the fluid has an anisotropic form.

Again, the anisotropic parameter, Δ, should be zero at the centre of the star i.e., $p_r(r = 0) = p_t(r = 0)$. Also Δ should be increasing at the surface of the stars. So, it implies that the anisotropic force should be zero at the core. These conditions are also verified by our model as shown in the Fig. 13. $\Delta(r > 0) > 0$ is very crucial and important as we have exhibited by our model. This condition makes the anisotropic force repulsive in nature, allowing more mass with larger size of the compact stars. Furthermore, gravitational red-shift must have a finite value at the interior and should be positive. It decreases along the surface of the star from the core i.e., $Z_s(r) > 0$. This condition is also fulfilled by the massive NSs as shown in the Fig. 75.

10.1.4.2 Calculation of the Model Parameters

Here, for our investigation, we have chosen a few super massive NSs with their mass and radius which are tabulated in Table 1 [297, 298, 326, 367, 385]. Also we have chosen three different sets of suitable values of x, y and z respectively in order to find the values of model parameters A, B and C, which are tabulated in Tables $2-4$ respectively. It will also help us to get an idea about the most suitable sets of the values of these parameters which we can use later for better results and investigations. The values of the model parameters will help us to find the numerical values of different important parameters related to the massive NSs.

Table 1.

Sl. No.	Neutron Star	$M_{obs}(M_\odot)$	$R_{obs}(km)$	$M(M_\odot)$	$R(km)$
1	PSR J0740+6620	2.08 ± 0.17	12.39 ± 1.5	2.08	12.39
2	PSR J1748-2446ad	2.10 ± 0.08	12.01 ± 1.2	2.10	12.01
3	4U1820-30	2.25 ± 0.12	10.01 ± 1.2	2.25	10.01
4	PSR J2215+5135	2.27 ± 0.15	13.01 ± 1.2	2.27	13.01
5	PSR J0952-0607	2.35 ± 0.17	10.01 ± 1.5	2.35	10.01

Table 10.1: List of few super massive NSs with mass (M) and radius (R)

Table 2.

Sl No.	Neutron Star	$A(km^{-2})$	$B(km^{-2})$	$C(km^{-2})$
1	PSR J0740+6620	0.0066151473	0.0048603446	-0.0001302372
2	PSR J1748-2446ad	0.0061887028	0.0033291857	-0.0001408375
3	4U1820-30	0.0053639625	0.0022327764	-0.0002513014
4	PSR J2215+5135	0.0042313125	0.0020167795	-0.0003540742
5	PSR J0952-0607	0.0038645644	0.0011646550	-0.0005214305

Table 10.2: Values of the parameters A, B and C by choosing $x = 2$, $y = 3$ and $z = 4$

Table 3.

Sl No.	Neutron Star	$A(km^{-2})$	$B(km^{-2})$	$C(km^{-2})$
1	PSR J0740+6620	0.0062851472	0.0047034232	-0.0000132503
2	PSR J1748-2446ad	0.005968733	0.0033180185	-0.0000148045
3	4U1820-30	0.0042396045	0.0028107761	-0.0000262071
4	PSR J2215+5135	0.0036813024	0.0022670954	-0.0000307417
5	PSR J0952-0607	0.0024560461	0.0018460523	-0.0000549014

Table 10.3: Values of the parameters A, B and C by choosing $x = 3$, $y = 4$ and $z = 2$

10.1.4.3 Calculation of Various Parameters related to the Neutron Stars as a Function of α

So, from the above tables $2 - 4$, we got the values of our model parameters using equations $(29) - (31)$ and incorporating the several suitable value sets of x. y and z.

Table 4.

Sl No.	Neutron Star	$A(km^{-2})$	$B(km^{-2})$	$C(km^{-2})$
1	PSR J0740+6620	0.0068823574	0.0042356041	-0.000158235
2	PSR J1748-2446ad	0.0053821548	0.0039621583	-0.000260344
3	4U1820-30	0.0045232846	0.0025648723	-0.000362371
4	PSR J2215+5135	0.0036805241	0.0019635874	-0.000467741
5	PSR J0952-0607	0.0024564061	0.0015123872	-0.000579214

Table 10.4: Values of the parameters A, B and C by choosing $x = 4$, $y = 2$ and $z = 3$

Now, we have applied these values of model parameters in the equations $(23) - (25)$ and got the various values of different crucial parameters of the NSs. During this calculation of NS parameters we also varies the value of α, which is important to incorporate the effect of coupling between momentum and curvature on those parameters. By this coupling effect we can also able to investigate the present time evolution of the NSs by minute observations of the changes of these parameters. These values are tabulated in the following Tables $5 - 13$. We have taken the sets of values of model parameters from respective Tables $2 - 4$ and used them for different values of α, in order to find out those important parameters of those super massive NSs.

Table5.

Sl No.	Neutron star	ρ $(gm\ cm^{-3})$	p_r $(dyne\ cm^{-2})$	p_t $(dyne\ cm^{-2})$
1	PSR J0740+6620	$2.5652389743 \times 10^{15}$	$1.7546238723 \times 10^{35}$	$2.2321547823 \times 10^{36}$
2	PSR J1748-2446ad	$2.3654872313 \times 10^{15}$	$1.6485012180 \times 10^{35}$	$2.2080254189 \times 10^{36}$
3	4U1820-30	$2.2832460021 \times 10^{15}$	$1.4375874236 \times 10^{35}$	$2.1658745624 \times 10^{36}$
4	PSR J2215+5135	$2.2153232581 \times 10^{15}$	$1.3263548736 \times 10^{35}$	$2.1045325621 \times 10^{36}$
5	PSR J0952-0607	$2.1700984321 \times 10^{15}$	$1.2352584763 \times 10^{35}$	$2.0223589456 \times 10^{36}$

Table 10.5: For $\alpha = 1.0$, values of ρ, p_r and p_t of various massive NSs using Table 2.

Table 6.

Sl No.	Neutron star	ρ $(gm\ cm^{-3})$	p_r $(dyne\ cm^{-2})$	p_t $(dyne\ cm^{-2})$
1	PSR J0740+6620	$2.3473594682 \times 10^{15}$	$1.6233774282 \times 10^{35}$	$2.2015698452 \times 10^{36}$
2	PSR J1748-2446ad	$2.2116820362 \times 10^{14}$	$1.5397258923 \times 10^{35}$	$2.1524808721 \times 10^{36}$
3	4U1820-30	$2.2005412675 \times 10^{14}$	$1.4462356238 \times 10^{35}$	$2.1084217912 \times 10^{36}$
4	PSR J2215+5135	$2.1914563257 \times 10^{14}$	$1.3605846012 \times 10^{35}$	$2.0508542348 \times 10^{36}$
5	PSR J0952-0607	$2.1645650891 \times 10^{14}$	$1.2253015825 \times 10^{35}$	$2.0014225453 \times 10^{36}$

Table 10.6: For $\alpha = 0.5$, values of ρ, p_r and p_t of various massive NSs using Table 2.

Table 7.

Sl No.	Neutron star	ρ $(gm\ cm^{-3})$	p_r $(dyne\ cm^{-2})$	p_t $(dyne\ cm^{-2})$
1	PSR J0740+6620	$2.2265897434 \times 10^{14}$	$1.5625894756 \times 10^{35}$	$1.8922354126 \times 10^{36}$
2	PSR J1748-2446ad	$2.1956482356 \times 10^{14}$	$1.4875216584 \times 10^{35}$	$1.7825413789 \times 10^{36}$
3	4U1820-30	$2.0123589647 \times 10^{14}$	$1.3612548635 \times 10^{35}$	$1.5874369521 \times 10^{36}$
4	PSR J2215+5135	$1.8745132158 \times 10^{14}$	$1.2954862136 \times 10^{35}$	$1.3612549756 \times 10^{36}$
5	PSR J0952-0607	$1.7895264135 \times 10^{14}$	$1.1854723654 \times 10^{35}$	$1.2456238923 \times 10^{36}$

Table 10.7: For $\alpha = 0.1$, values of ρ, p_r and p_t of various massive NSs using Table 2.

Table 8.

Sl No.	Neutron star	ρ $(gm\ cm^{-3})$	p_r $(dyne\ cm^{-2})$	p_t $(dyne\ cm^{-2})$
1	PSR J0740+6620	$2.4723238974 \times 10^{15}$	$1.6854231978 \times 10^{35}$	$2.2056489232 \times 10^{36}$
2	PSR J1748-2446ad	$2.3234548723 \times 10^{15}$	$1.5236482594 \times 10^{35}$	$2.1462588022 \times 10^{36}$
3	4U1820-30	$2.2452384721 \times 10^{15}$	$1.4425682392 \times 10^{35}$	$2.0945267858 \times 10^{36}$
4	PSR J2215+5135	$2.1923654784 \times 10^{15}$	$1.3623145678 \times 10^{35}$	$2.0123548934 \times 10^{36}$
5	PSR J0952-0607	$2.1256728314 \times 10^{15}$	$1.2825641238 \times 10^{35}$	$2.0023546782 \times 10^{36}$

Table 10.8: For $\alpha = 1.0$, values of ρ, p_r and p_t of various massive NSs using Table 3.

Table 9.

Sl No.	Neutron star	ρ $(gm\ cm^{-3})$	p_r $(dyne\ cm^{-2})$	p_t $(dyne\ cm^{-2})$
1	PSR J0740+6620	$2.3254123892 \times 10^{15}$	$1.5752469872 \times 10^{35}$	$2.1645298412 \times 10^{36}$
2	PSR J1748-2446ad	$2.2425836916 \times 10^{14}$	$1.5256487295 \times 10^{35}$	$2.1224808721 \times 10^{36}$
3	4U1820-30	$2.1805413214 \times 10^{14}$	$1.4645821354 \times 10^{35}$	$2.0984217912 \times 10^{36}$
4	PSR J2215+5135	$2.1214542575 \times 10^{14}$	$1.3845123697 \times 10^{35}$	$2.0298562334 \times 10^{36}$
5	PSR J0952-0607	$2.0723546829 \times 10^{14}$	$1.3205423981 \times 10^{35}$	$2.0009225459 \times 10^{36}$

Table 10.9: For $\alpha = 0.5$, values of ρ, p_r and p_t of various massive NSs using Table 3.

Table 10.

Sl No.	Neutron star	ρ $(gm\ cm^{-3})$	p_r $(dyne\ cm^{-2})$	p_t $(dyne\ cm^{-2})$
1	PSR J0740+6620	$2.1674523197 \times 10^{14}$	$1.5025843564 \times 10^{35}$	$1.8856423924 \times 10^{36}$
2	PSR J1748-2446ad	$2.1185469723 \times 10^{14}$	$1.4472162354 \times 10^{35}$	$1.8225415628 \times 10^{36}$
3	4U1820-30	$2.0745236894 \times 10^{14}$	$1.3812358635 \times 10^{35}$	$1.7764343251 \times 10^{36}$
4	PSR J2215+5135	$1.8456789231 \times 10^{14}$	$1.3285412356 \times 10^{35}$	$1.6458461254 \times 10^{36}$
5	PSR J0952-0607	$1.7552689742 \times 10^{14}$	$1.2754391556 \times 10^{35}$	$1.5823546879 \times 10^{36}$

Table 10.10: For $\alpha = 0.1$, values of ρ, p_r and p_t of various massive NSs using Table 3.

Table 11.

Sl No.	Neutron star	ρ $(gm\ cm^{-3})$	p_r $(dyne\ cm^{-2})$	p_t $(dyne\ cm^{-2})$
1	PSR J0740+6620	$2.5423254612 \times 10^{15}$	$1.5523648127 \times 10^{35}$	$2.2154238524 \times 10^{36}$
2	PSR J1748-2446ad	$2.4712543678 \times 10^{15}$	$1.4852346185 \times 10^{35}$	$2.1621546625 \times 10^{36}$
3	4U1820-30	$2.3645213879 \times 10^{15}$	$1.3654127824 \times 10^{35}$	$2.0745241368 \times 10^{36}$
4	PSR J2215+5135	$2.2745136527 \times 10^{15}$	$1.2845178963 \times 10^{35}$	$2.0015486375 \times 10^{36}$
5	PSR J0952-0607	$2.1854236942 \times 10^{15}$	$1.1745236892 \times 10^{35}$	$2.0018953678 \times 10^{36}$

Table 10.11: For $\alpha = 1.0$, values of ρ, p_r and p_t of various massive NSs using Table 4.

Table 12.

Sl No.	Neutron star	ρ $(gm\ cm^{-3})$	p_r $(dyne\ cm^{-2})$	p_t $(dyne\ cm^{-2})$
1	PSR J0740+6620	$2.4652489753 \times 10^{15}$	$1.5352547683 \times 10^{35}$	$2.1821548735 \times 10^{36}$
2	PSR J1748-2446ad	$2.3854823596 \times 10^{14}$	$1.4875231456 \times 10^{35}$	$2.1125468972 \times 10^{36}$
3	4U1820-30	$2.2645892356 \times 10^{14}$	$1.4187452364 \times 10^{35}$	$2.0531256476 \times 10^{36}$
4	PSR J2215+5135	$2.2085697456 \times 10^{14}$	$1.3345827691 \times 10^{35}$	$2.0054123875 \times 10^{36}$
5	PSR J0952-0607	$2.1256789425 \times 10^{14}$	$1.2745823612 \times 10^{35}$	$2.0007254873 \times 10^{36}$

Table 10.12: For $\alpha = 0.5$, values of ρ, p_r and p_t of various massive NSs using Table 4.

Table 13.

Sl No.	Neutron star	ρ $(gm\ cm^{-3})$	p_r $(dyne\ cm^{-2})$	p_t $(dyne\ cm^{-2})$
1	PSR J0740+6620	$2.3685412356 \times 10^{14}$	$1.4925487326 \times 10^{35}$	$1.8042568343 \times 10^{36}$
2	PSR J1748-2446ad	$2.2754123856 \times 10^{14}$	$1.4354827912 \times 10^{35}$	$1.7156897252 \times 10^{36}$
3	4U1820-30	$2.2164528783 \times 10^{14}$	$1.3612458793 \times 10^{35}$	$1.6423561871 \times 10^{36}$
4	PSR J2215+5135	$1.8923623575 \times 10^{14}$	$1.2945782356 \times 10^{35}$	$1.5712489325 \times 10^{36}$
5	PSR J0952-0607	$1.6825413684 \times 10^{14}$	$1.2245872369 \times 10^{35}$	$1.4824961374 \times 10^{36}$

Table 10.13: For $\alpha = 0.1$, values of ρ, p_r and p_t of various massive NSs using Table 4.

10.1.4.4 Verification of the Energy Conditions

The energy conditions, which arises due to the restrictions on energy-momentum tensor $T_{\mu\nu}$, can be generalised to $f(R,T)$ modified gravity theory beyond GR. The conditions

put limits on various properties of the compact stars based on geometric properties. In $f(R,T)$ gravity, in terms of energy-momentum tensor, the energy conditions can be expressed as $T_{\mu\nu} = diag(-\rho, p_r, p_t, p_t)$.

From various astronomical observations, it is expected that, the distribution of mass inside the core of those super massive NSs must obey all energy inequalities. From the above tables we already got the values of critical density ρ, radial pressure p_r and tangential pressure p_t of those super massive NSs inside the core. In this condition it is very easy to verify that, under critical pressure and density inside the core those compact objects obey all energy conditions or not. From our present model we have got that

$$(\rho - p_r - 2p_t) \geq 0 \quad , \quad (\rho + p_r) \geq 0 \quad and \quad (\rho + p_t) \geq 0 \quad : SEC \tag{10.32}$$

So, from the above equation we can say that, the strong energy condition (SEC) is fulfilled by the super massive NSs. Now, we have checked other energy conditions [54] named as null energy (NEC), weak energy (WEC) and dominant energy condition (DEC) as

$$(\rho + p_t) \geq 0 \quad and \quad (\rho + p_r) \geq 0 \quad : NEC \tag{10.33}$$

$$(\rho + p_t) > 0 \quad , \quad \rho \geq 0 \quad and \quad (\rho + p_r) > 0 \quad : WEC \tag{10.34}$$

$$(\rho - p_r) \geq 0 \quad , \quad \rho \geq 0 \quad and \quad (\rho - p_t) \geq 0 \quad : DEC \tag{10.35}$$

So, from the above equations (32) to (35), we can say that, in our present model, all the required energy conditions are satisfied by these super massive NSs in $f(R,T)$ gravity.

10.1.4.5 Anisotropic nature and Analysis of stability

Interestingly, we have seen that inside the super massive NSs, the pressure in radial direction somehow varies differently from the pressure in the tangential direction. The

tangential pressure is higher than the radial pressure. Due to this pressure difference inside, anisotropic force comes into play which in turn produces the repulsive gravitational force, acting outward direction inside the core of these massive NSs. We can calculate the anisotropic force F_a in terms of anisotropic parameter Δ, inside the super massive NSs as

$$F_a = \frac{2}{r}(p_t - p_r) \quad . \tag{10.36}$$

From our model we have got that, anisotropic pressure is always positive inside the core of these super massive NSs i.e., $\Delta > 0$. This also implies that, $p_t > p_r$. This condition is also verified by the massive compact stars in our model.

Now, we have discussed about the most essential condition of these highly massive NSs, under present situation of the universe, which is the stability of these stars. The relativistic adiabatic index Γ, is the measure of stability for the compact stars. We have got the values of the variation of the adiabatic index inside the core of the NSs from our model, which exhibits their stability [55, 56]. If the value of Γ is such that, $\Gamma > \frac{4}{3}$, then the NSs are under stability. The relativistic adiabatic index can be measured as

$$\Gamma = \left(\frac{p+\rho}{p}\right)\frac{\partial p_r}{\partial \rho} \quad . \tag{10.37}$$

In this model we have also measured the variation of Γ with the radius of the NSs for different values of α. The values of Γ are tabulated in below Table 14.

Table 14.

Sl. No.	Neutron Star	Γ for $\alpha = 1.0$	Γ for $\alpha = 0.5$	Γ for $\alpha = 0.1$
1	PSR J0740+6620	22.25413	21.34652	19.15723
2	PSR J1748-2446ad	25.85642	23.24735	22.25841
3	4U1820-30	27.52183	26.32746	24.63217
4	PSR J2215+5135	31.13267	28.12463	26.52143
5	PSR J0952-0607	33.72314	30.87452	28.42315

Table 10.14: Values of adiabatic index (Γ) for various super massive NSs, using Table4.

Again, we know that the speed of sound v_s inside the stellar region must be positive

and be less or equal to the speed of light, i.e., $0 \leq v_s^2 \leq 1$ and they should decrease towards the boundary. Now, v_s at the core of the massive NSs can be measured as

$$v_s = \sqrt{\frac{\partial p}{\partial \rho}} \quad . \tag{10.38}$$

This condition for the speed of sound is also satisfied in our model. Besides we also can able to show from our model that,

$$\left(v_{st}^2 - v_{sr}^2\right) \leq 1 \quad . \tag{10.39}$$

So, it is very clear from all the above conditions which are fully satisfied by the massive NSs in case of our investigation in $f(R,T)$ gravity model, they all got their stability under present situation. It is also verified from our model that, the speed of sound in transverse direction is less than the speed of sound in radial direction. In our model, we have also measured the variation of the sound speed through the core material with the radius of the massive NSs. The massive compact stars structure also fulfilled the causality conditions. The radial and tangential sound speeds are given as

$$v_r^2 = \frac{dp_r}{d\rho} \approx \frac{1}{3} \quad and \tag{10.40}$$

$$v_t^2 = \frac{dp_t}{d\rho} \quad . \tag{10.41}$$

10.1.4.6 Surface Redshift and Equilibrium

We can also measure the surface redshift function $Z(r)_s$ [60, 61] of the massive NSs by using the equation as

$$Z_s(r) = \frac{1}{\sqrt{\left(1 - \frac{m(r)}{r}\right)}} - 1 \quad . \tag{10.42}$$

In our present investigation, we have measured the variation of surface redshift with the radius of the compact star for different massive NSs and not only that we have also

measure the variation of $Z_s(r)$ for different values of coupling parameter α, which gives a very interesting result. Various astronomical observations suggests that the value of surface redshift for massive NSs should be ≤ 5 in order to ensure stable equilibrium [59, 60]. We also got the same type of result. The values of $Z_s(r)$ are tabulated in below Table 15.

Table 15.

Sl. No.	Neutron Star	$Z_s(r)\ for\ \alpha = 1.0$	$Z_s(r)\ for\ \alpha = 0.5$	$Z_s(r)\ for\ \alpha = 0.1$
1	PSR J0740+6620	0.786413	0.665431	0.584587
2	PSR J1748-2446ad	0.656781	0.625891	0.552345
3	4U1820-30	0.525846	0.486235	0.425236
4	PSR J2215+5135	0.428934	0.385284	0.324278
5	PSR J0952-0607	0.382473	0.348547	0.277425

Table 10.15: Values of Surface redshift $Z_s(r)$ for various super massive NSs, using Table 4.

10.1.4.7 Modified TOV Equations and Mass-Radius Relation with Compactness Factor

Generally, the TOV equation predicts the upper bound to the mass of a NSs in GR theory. At the same time it is more applicable for the cold and non-rotating NSs. This equation also predicts about hydrostatic equilibrium of those compact stars containing isotropic fluid distribution inside them [61]. On the other hand various astronomical observations suggests that GR is not suitable for massive relativistic objects. So, as we take the $f(R,T)$ modified gravity formalism and rotating NSs for our investigation, this equation should also be modified accordingly. We also consider a coupling between momentum and curvature which plays a crucial roll on attaining a maximum mass by the NSs before collapsing into a black hole. It is very interesting from the result of our study that the upper bound of mass for NSs has been changed from TOV predicted value. At the same time $f(R,T)$ theory overcomes the shortcomings of GR theory quite successfully. In our investigation, in $f(R,T)$ extended gravity formalism, the

generalised TOV equation takes the form

$$-\frac{a'(r)}{2}(p+\rho)-\frac{\partial p}{\partial \rho}=\frac{\alpha}{2(\alpha+4\pi)}(p'-\rho') \quad . \tag{10.43}$$

The above equation gives a very interesting outcomes of our investigation. The effective mass of the super massive compact stars in our model, in $f(R,T)$ gravity becomes

$$\begin{aligned} M(R) =&4\pi\int_0^R \rho_R R^2 dR \\ &= 4\pi\int_0^R \Theta\left[\left(2\tau(1+\alpha)(3B-ABr^x+B^2r^2)+4A\alpha+\frac{2\alpha}{r^2}(e^{Ar^z/2}-1)\right)f_{1R}\right]R^2dR \\ &+4\pi\int_0^R \Theta\left[\left((2+3\alpha)(Ar-\frac{2}{r})+3\alpha Br\right)f'_{1R}-(2+3\alpha)f''_{1R}-f_1(1+\alpha)e^{Ar^z/2}\right]R^2dR \quad . \end{aligned} \tag{10.44}$$

We can measure the effective mass of those super massive NSs using our model from the above equation (47). The measured values of mass from our model of those massive stars are tabulated below. Again the compactification factor of those massive compact stars using our model, can be written as [325]

$$\begin{aligned} u(R) =&\frac{1}{R}M(R) \\ &= 4\pi\int_0^R \Theta\left[\left(2\tau(1+\alpha)(3B-ABr^x+B^2r^2)+4A\alpha+\frac{2\alpha}{r^2}(e^{Ar^z/2}-1)\right)f_{1R}\right]RdR \\ &+4\pi\int_0^R \Theta\left[\left((2+3\alpha)(Ar-\frac{2}{r})+3\alpha Br\right)f'_{1R}-(2+3\alpha)f''_{1R}-f_1(1+\alpha)e^{Ar^z/2}\right]RdR \quad . \end{aligned} \tag{10.45}$$

Now, using the above equations (47) and (48), we can also measure the radius of those super massive NSs from our model. The measured values of the mass and radius from our model of those massive NSs are tabulated in below Tables 16 − 18. From the measured values of these two important parameters, we can clearly observe the effect of coupling parameter α minutely. It is very interesting to notice the momentum-curvature coupling has a great effect on acquiring a high mass by the stars and as well as on their stability.

Table 16.

Sl. No.	Neutron Star	$M(M_\odot)$	$R(km)$	$M(M_\odot)$ from model	$R(km)$ from model
1	PSR J0740+6620	2.08	12.39	2.12561	12.38036
2	PSR J1748-2446ad	2.10	12.01	2.16274	12.35537
3	4U1820-30	2.25	10.01	2.28523	12.31764
4	PSR J2215+5135	2.27	13.01	2.30842	12.30574
5	PSR J0952-0607	2.35	10.01	2.37547	12.26971

Table 10.16: For $\alpha = 0.1$, Values of mass (M) and radius (R) of super massive NSs from the model, using Table 4.

Table 17.

Sl. No.	Neutron Star	$M(M_\odot)$	$R(km)$	$M(M_\odot)$ from model	$R(km)$ from model
1	PSR J0740+6620	2.08	12.39	2.25461	11.89368
2	PSR J1748-2446ad	2.10	12.01	2.28748	11.87537
3	4U1820-30	2.25	10.01	2.37523	11.85376
4	PSR J2215+5135	2.27	13.01	2.42842	11.82574
5	PSR J0952-0607	2.35	10.01	2.57547	11.80297

Table 10.17: For $\alpha = 0.5$, Values of mass (M) and radius (R) of super massive NSs from the model, using Table 4.

Table 18.

Sl. No.	Neutron Star	$M(M_\odot)$	$R(km)$	$M(M_\odot)$ from model	$R(km)$ from model
1	PSR J0740+6620	2.08	12.39	2.89461	10.60768
2	PSR J1748-2446ad	2.10	12.01	3.28748	10.57753
3	4U1820-30	2.25	10.01	3.37523	10.53917
4	PSR J2215+5135	2.27	13.01	3.42842	10.52748
5	PSR J0952-0607	2.35	10.01	3.51547	10.50829

Table 10.18: For $\alpha = 1.0$, Values of mass (M) and radius (R) of super massive NSs from the model, using Table 4.

10.1.5 Graphical Analysis : Observational Support

Now, in this section, we have plotted variations of several crucial measured parameters, of those super massive NSs, using our model. Each graph depicts several important and interesting facts on their variations. We have also varied the momentum-curvature coupling parameter α with the NSs parameters and graphs shows the evolution of those parameters through the present universe. So, from these graphical variations we can get the idea of structural evolution of the massive compact stellar objects.

Fig. 66 shows the variation of radial pressure of those different massive NSs with their radius. As more massive the NS, it's radial pressure is also higher than the others. We can see that the radial pressure is a perfectly decreasing function of radius of the star. This means as the radius of the NS begins to increase, the pressure starts decreasing towards the surface of the star from the core, which depicts that at the core of the NSs the pressure becomes very high but as we go towards the surface from the core, the pressure decreases and becomes zero at the surface. Again, Fig. 67 is very important and interesting. It shows the direct effect of momentum-curvature coupling on the radial pressure of the stars. It is clear from three different values of coupling parameter that, as matter-curvature coupling increases, the radius of the star begins to decrease and the "pressure curves" becomes more stiffer than the previous. It indicates that, as the coupling increases, the stars shrinks in size and getting more compact structure. At the same time the rate of decreasing of radial pressure increases inside the core of the NSs, i.e., the radial pressure falls more rapidly inside as it shrinks more and more in size due to increase in the space-time curvature around it. Now, Fig. 68 and Fig. 69 have shown the variation of tangential pressure of the massive compact stars. These curves also have same type of nature. But at the boundary transverse pressure almost vanishes but never becomes zero.

Fig. 70 gives the variation of core density of the different massive NSs with it's radius. As massive a NS is, its density is also higher than others. The density also a decreasing function of radius but the "density curves" are not so stiff like "pressure curves". Inside the core, the density is very high as well as pressure but as we go

towards the surface of the star from the core, the radius increases and core density starts decreasing slowly. At the surface of the NSs, it almost vanishes but never becomes zero. Now, the Fig. 71 shows the variation of core density of the massive NSs with the momentum-curvature coupling parameter α. As the coupling increases, the star stars to shrink in radius and at the same time core density also decreases in a slow rate from core to surface.

We know the redshift of these compact objects are always a function of the radius of that object. Here also we have plotted the variation of surface redshift of various NSs according to their different mass in Fig. 72 It is very clear from the plots that the surface redshift is monotonically decreasing function of the radius of the star. At the same time, it is also clear that, if the mass of the NS is high, the redshift is also high for that particular NS respect to others. The Fig 73, shows the variation of the surface redshift with momentum-curvature coupling parameter α. It is very interesting to show that, as the coupling increases, the mass of the stars also increases while the radius decreases and in this situation surface redshift increases. These two plots also depicts that the massive NSs are in stable equilibrium also under this critical situation.

The plots in the Fig 74 and Fig 75, are very crucial parameter plots for the massive NSs. They shows the variation of sound speed and adiabatic index with radius of the star respectively for different values of α. Both plots describes the stability of the massive NSs and tells about the future evolution of the star. The velocity of sound speed inside the core of the star through the stellar matter always obey the causality conditions, under extreme conditions of pressure, density and temperature. On the other hand the variation in adiabatic index indicates that stability of the massive NSs under such critical conditions with the present situation of the universe.

At last, we have plotted the most important and significant curve of our working model as the curve between the mass and radius of the super massive NSs. These curves not only explains the mass-radius constraints observed in the compact binary coalescence, $GW190814$ event but also explains the maximum attainable mass by any massive NS. From these curves we can get the clear indication about the upper bound of the mass as well as the lowest radius of the star at the same time. Again, as we

varies the momentum-curvature coupling parameter during the plot of $M-R$ curves, it is also very interesting to find that the coupling has a crucial effect on gaining mass by the NSs and also on increasing the space-time curvature around the NSs. The Fig. 76 shows the variation of mass with radius for different compact stars with different values of α. It is very clear that as we start increasing the value of the coupling parameter, the mass of the NSs starts increasing whereas the radius stars decreasing. For the maximum value of α, the "mass-radius" curve has got it's peak value of mass and the lowest possible value of the radius at that point of peak mass. This is upto the point where the massive NSs are still in stable equilibrium. From the mass-radius plot, it is clear that the massive NSs in a mass range in between $2.0-2.5M_{\odot}$ will be in the radius range of $12.0-12.5$ km. On the other hand, the massive NSs in a mass range in between $2.5-3.0M_{\odot}$ will be in the radius range of $11.8-12.0$ km. Again, the massive NSs which have mass almost $3.1M_{\odot}$ or above, will must have radius not less than 10.5 km under stability. Fig. 77 has shown the variation of the compactness parameter of the massive NSs with radius for different values of α. As α increases the compactness also increases.

The Fig. 78 represents the variation of the anisotropic factor of the compact stars with their radius as a function of the coupling parameter α. as the anisotropic force inside the massive compact stars increases their, compactness increases and allowing them to consume more mass. So, with positive coupling parameter in $f(R,T)$ gravity theory, the compact stars still have the ability to accommodate higher mass while satisfying the stability conditions.

10.1.6 Brief Discussions and Conclusion

In this work, we have effectively modeled the massive compact stars in the framework of $f(R,T)$ modified gravity. From our investigation, we are able to give some focus on the upper bound of the attainable mass and lowest possible radius by any super massive NSs. We have mainly chosen some of super massive NSs in a binary system to study their evolution under accelerated expansion of the universe. We have chosen the binary system NSs because they possesses all the required properties for our study.

$Fig-66$

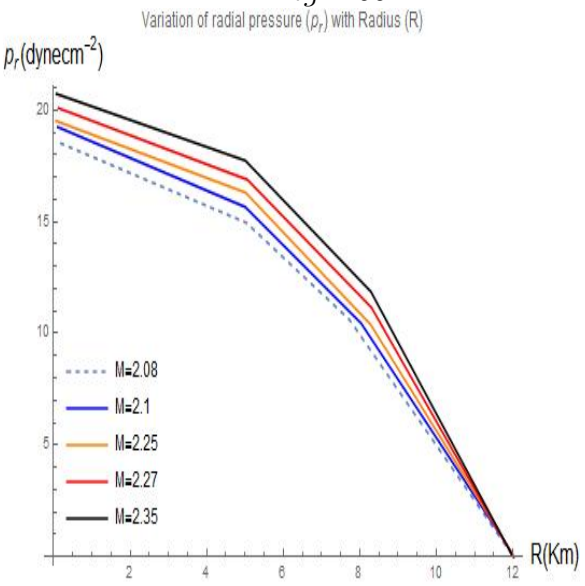

$Fig-67$

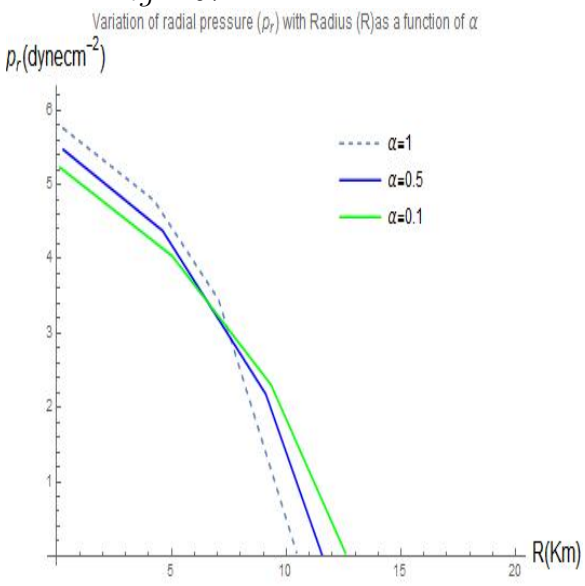

Figure 10.1: *Represents the variation of radial pressure p_r with radius $R(km)$ for different super massive NSs.*

Figure 10.2: *Represents the variation of radial pressure p_r with radius $R(km)$ of the NSs as a function of the coupling parameter α.*

$Fig-68$

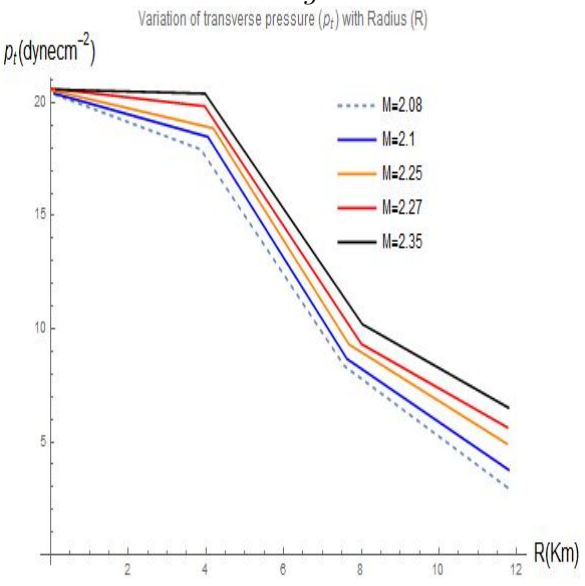

$Fig-69$

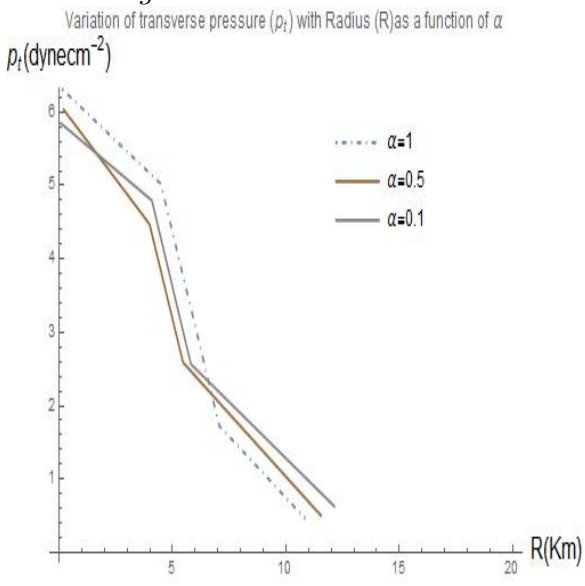

Figure 10.3: *Represents the variation of transverse pressure p_t with radius $R(km)$ for different super massive NSs.*

Figure 10.4: *Represents the variation of transverse pressure p_t with radius $R(km)$ of the NSs as a function of the coupling parameter α.*

$Fig-70$

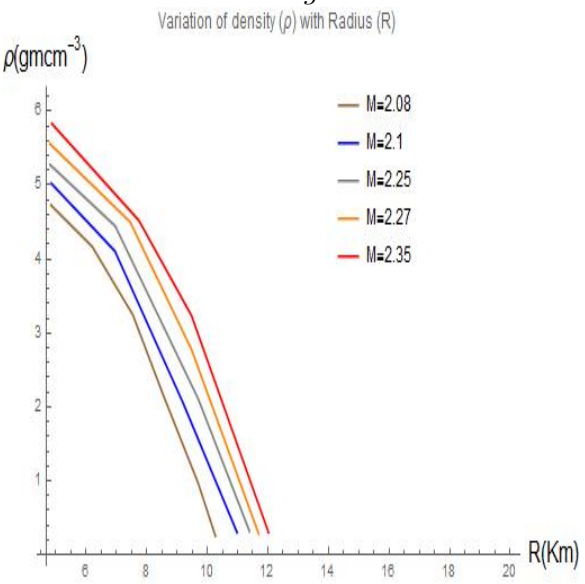

$Fig-71$

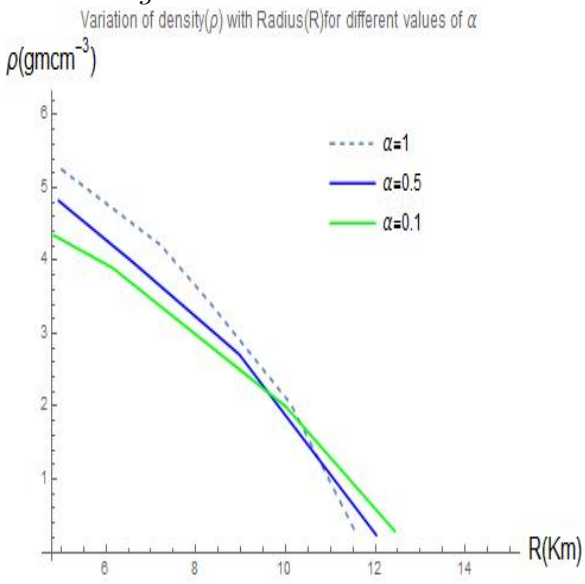

Figure 10.5: *Represents the variation of core density ρ with radius $R(km)$ for different super massive NSs.*

Figure 10.6: *Represents the variation of core density ρ with radius $R(km)$ for different values of coupling parameter α.*

$Fig-72$

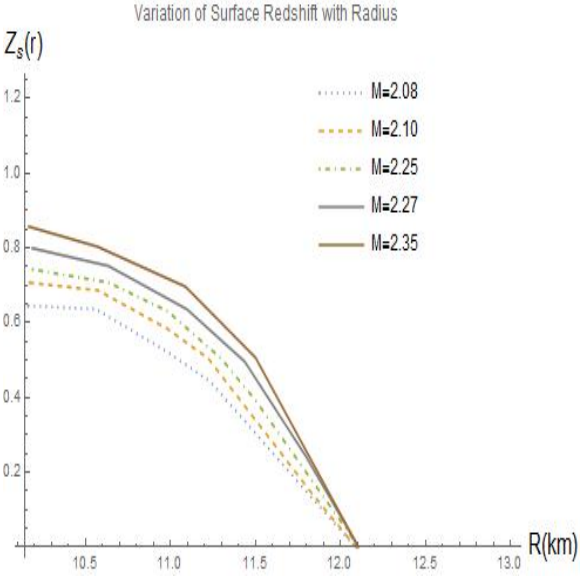

$Fig-73$

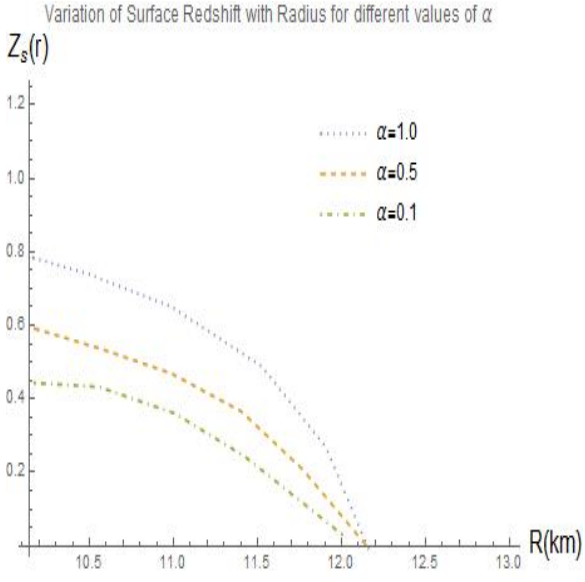

Figure 10.7: *Represents the variation of surface redshift $Z_s(r)$ with radius $r(km)$ for different super massive NSs.*

Figure 10.8: *Represents the variation of surface redshift $Z_s(r)$ as a function of α.*

$Fig-74$

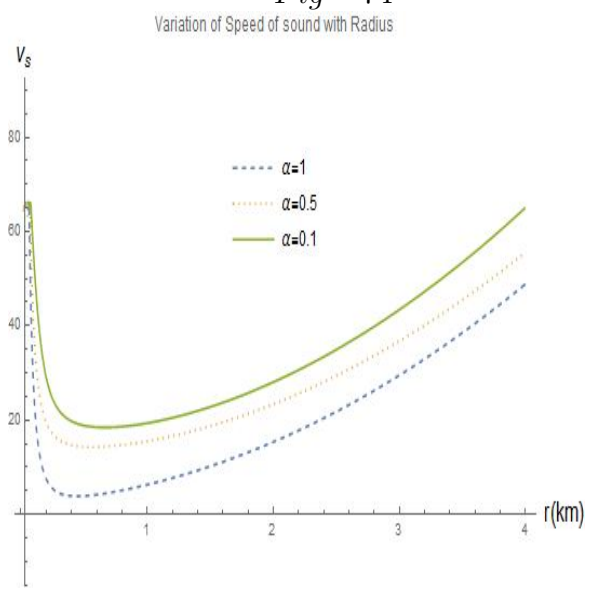

$Fig-75$

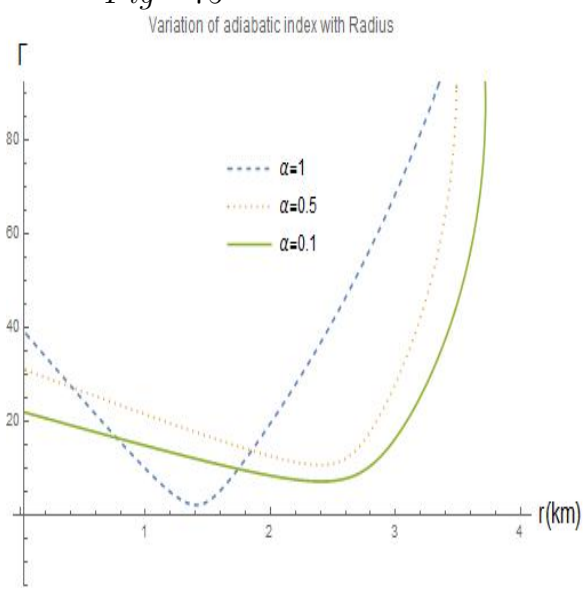

Figure 10.9: *Represents the variation of sound speed v_s with radius (r) for different super massive NSs and for different values of α.*

Figure 10.10: *Represents the variation of adiabatic index Γ with radius (r) for different super massive NSs and for different values of α.*

$Fig-76$

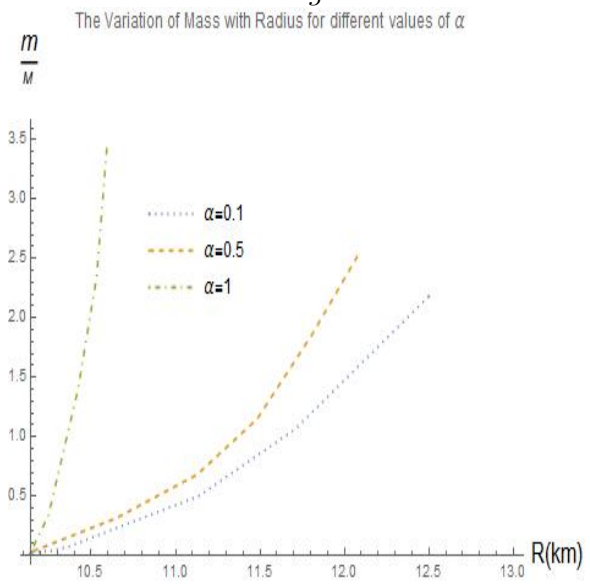

$Fig-77$

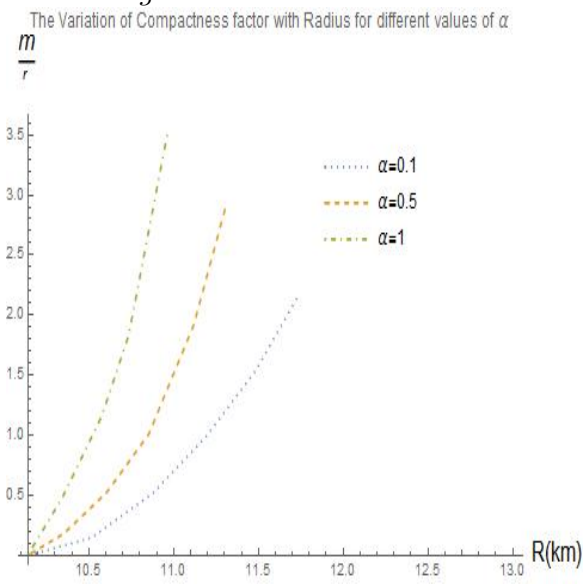

Figure 10.11: *Represents the variation of mass $M(r)$ with radius R for different super massive NSs and for different values of α.*

Figure 10.12: *Represents the variation of compactness factor $\frac{M(r)}{r}$ with radius R for different super massive NSs as a function of α.*

$Fig - 78$

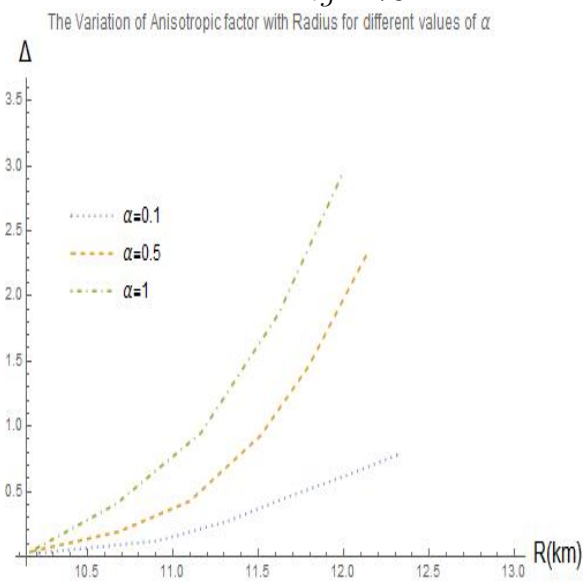

Figure 10.13: *Represents the variation of anisotropic factor Δ of the massive compact stars with radius R with higher positive values of coupling parameter α.*

Even the existence of very strong gravitational field around the stars allow researchers to examine GR, doppler effects, production of gravitational waves, tidal deformability etc. of the compact stars. There is also mass transfer between the stars what would lead us to investigate the structural evolution of the massive compact stars. Moreover, we can get proper understanding about the exact EoS of the core nuclear matter of those stars. This model of massive compact stars in $f(R,T)$ gravity has been subjected to strict regularity, stability and causality tests. It depicts the decisive role of coupling between momentum and curvature of space-time. The free constants which arises due to the integration of the field equations in our model, becomes fixed through the application of the boundary conditions. The contribution of the modified gravity upon the compact stars is revealed by the plots of various physical properties of the stars for various values of the coupling constant. The results of our model is very interesting and agrees with the other astronomical observations [65], which make our model realistic and viable.

The mass-radius relationship curve clearly shows that the super massive pulsars which have mass around $2.3M_{\odot}$, must have radius of about 12.3 km and they must

be in their stable equilibrium. Again, the super massive NS which have mass around $2.7M_{\odot}$, must have radius around 11.8 km under stability. This outcome undoubtedly explains all the observed facts and mass-radius constraints during the gravitational wave detection event. Now, if we look at the case where the coupling parameter with it's highest value as $\alpha = 1.0$, the mass of the super massive NSs has also got it's peak value as around $3.51M_{\odot}$, with stability and lowest possible radius about 10.5 km. In this critical conditions also they have managed to be in equilibrium. We have also found that, the coupling constant actually lowers the density and pressure (in both directions) at the interior of the compact stars and their is a increase in the mass of the star and its compactness. The presence of anisotropy at the interior, leads to higher values of surface redshift of the stars. The radial pressure and density bears a linear relationship which is also clear from our assumption and $f(R,T)$ stars have the ability to acquire more mass as compared to their GR counterparts. From our result we can also exhibit that $\Delta(r > 0) > 0$ which implies that $p_t > p_r$. This condition is very much crucial because of this repulsive anisotropic force comes into play inside the massive NSs and as a result of this force larger size of NSs are allowed compared to an isotropic fluid.

So, in brief, with positive coupling parameter in $f(R,T)$ gravity theory, the compact stars still have the ability to accommodate higher mass while satisfying the stability conditions. We can conclude that, for massive NSs under spherically stable equilibrium and highest possible space-time curvature, can attain maximum mass of around $3.51M_{\odot}$ and lowest possible radius around 10.5 km.

"The Universe is vast and mysterious, and it is our privilege to uncover its secrets".

—Subrahmanyam Chandrasekhar

CHAPTER 11

ISOLATED NEUTRON STARS IN $F(R,T)$ MODIFIED GRAVITY

11.1 Impacts of $f(R,T)$ Modified Gravity on the Isolated Neutron Stars Embedded in Modified Chaplygin Gas under Tolman-Kuchowicz Spacetime

11.1.1 Prelude

Our main motive is to model and study the mass-radius relation of the specific isolated compact star $RXJ1856.5-3754$ in the background of the accelerated universe. We have also focused on achieving the equation of state of the core nuclear matter under stable equilibrium in $f(R,T)$ modified gravity using Tolman-Kuchowicz metric potentials. We have taken Einstein-Hilbert action with $f(R,T) = R+2\xi T$, where R denotes the Ricci scalar, T is the trace of energy-momentum tensor and ξ is coupling parameter. We have numerically solved modified Tolman-Oppenheimer-Volkoff equations by considering the presence of modified Chaplygin gas (MCG hereafter) inside the star and also solved the

field equations. We have got an explicit scenario of the structural evolution of neutron stars through accelerating space-time. Interestingly, from our model and investigations, all the derived outcomes have become compatible with physically adopted regimes which reveals the physical viability of our current model.

Observations regarding the recessional speed of Type Ia supernova, fluctuation categories in the density of the visible baryonic matter and many others ensured us to believe regarding late time cosmic acceleration [343, 344, 345]. Conventional matter with Einsteins gravity theory cannot accommodate above accelerated expansion. As a consequence, modifications of either or both the sides of Einsteins field equations were very much required [346, 347, 348]. Cosmologists have been trying to illustrate the accelerated universe by using the presence of dark matter (DM hereafter) [349, 350, 351]. Existence of modified Chaplygin gas (MCG hereafter) is chosen as a DM candidate to work at the core of a compact star.

General relativity (GR hereafter) is not singularity free while discussion of relativistic compact objects is carried over. There are so many physically inspired modifications in GR, which can compute effective deviations in the features of space-time that surrounds a neutron star (NS hereafter). Amongst these modified theories, $f(R,T)$ modified gravity theory with R as Ricci scalar and T as traces of energy-momentum tensor can accommodate the tension in the Hubble constant during the present accelerated situation [352, 353, 354]. Besides using $f(R,T)$ gravity theory we can investigate the coupling between the matter and geometry of spacetime of an evolving compact object [356, 357, 358]. Again by using the term $\theta_{\mu\nu}$ in this modified gravity theory, we can also study the anisotropic sector of the compact objects [359, 360, 361, 362]. Outside the compact star, $f(R,T) = R+2\xi T$ gravity possess a vanishing curvature R. Here ξ is a coupling constant. So, the exterior spacetime of the star can be treated by using the Schwarzschild exterior solution. Einstein's gravity theory can be reproduced at the terminal case to let the coupling constant, ξ be zero [363, 364, 365, 366].

Recently in the context of $f(R,T)$ modified theory of gravity, several anisotropic charged and uncharged NS models are also proposed to examine the stability of the spherical compact objects [367, 368, 369]. The stable and static structural config-

uration of the compact objects in $f(R,T)$ modified gravity have been explored by Pretel et al. Bianchi type I (LRSBI) cosmological models with the presence of bulk viscous fluid, under local rotational symmetry has been constructed by Mahanta in modified $f(R,T)$ gravity. Moreover, Singh et al. have inquired the particle formation under $f(R,T)$ gravity, by using flat Friedmann-Lemaitre-Robertson-Walker (FLRW hereafter) metric and simultaneous presence of MCG [356]. Houndjo et al. have made an experiment to reconstruct the Little Rip cosmological model in $f(R,T)$ modified gravity and reproduced the present phase of the universe without Big Rip . However, Santos and Frest have proposed a violation of causality condition in $f(R,T)$ modified gravity [360]. Static wormholes under spherical symmetry in modified $f(R,T)$ gravity have been explored by Zubair et al. Also isotropic Tolman VII solution in $f(R,T)$ gravity using gravitational decoupling method has been inspected by Azmat and Zubair. The relevance of $f(R, Matter)$ theories in cosmology that directly coupled with the curvature and the matter, with the universal coupling has been also examined in various investigations [373].

Under the present cosmic acceleration, the study on the nature and behavioral changes of an isolated compact star and how the core nuclear matter equation of state (EoS hereafter) has evolved, has become a very promising topic of research in recent years. In this current investigation we have chosen a very interesting and mysterious isolated compact star $RXJ1856.5-3754$ for our study [375, 376]. Here, we have obtained an exact analytical solution of the isolated NSs by considering them as a anisotropic fluid spheres in hydrostatic equilibrium under $f(R,T)$ modified gravity. We have also incorporated the positive dimensionless coupling parameter ξ by taking into account the linear form of modified gravity as $f(R,T) = R+2\xi T$. In general, with the positive coupling parameter, the theory can predict a more compact and higher mass star than what is predicted by GR [381, 383, 386].

We actually want to build a realistic model of compact stars and to investigate its properties and EoS of the core nuclear matter in the background of modified $f(R,T)$ gravity. In this model we also have investigated how the dimensionless coupling parameter ξ affects the internal structure of the isolated NSs. In this current model, the

modified Tolman-Oppenheimer-Volkoff (TOV hereafter) system of equations are solved numerically to find out the uniform density profile of the stars. At the same time, we have also examined the effects of the extra anisotropic force and the force due to modified gravity that are originated from this theory. Furthermore, in the case of this type of modified theories of gravity, anisotropic spacetime is very much relevant, in such a study beyond GR. Investigating the space-time along with anisotropy, scientists can test and refine the understandings on gravity and can also explore their implications as well as effective observational signature.

One of the nearby and brightest young NS is $RXJ1856.5-3754$ with a very strong gravitational field. Interestingly, $RXJ1856.5-3754$ has not exhibited any indication of activity such as variability or pulsations like other younger isolated NSs or binary NSs. General relativistic studies on this star have shown that it possessed a mass about $0.9M_{\odot}$ with radius almost 17 km. It is a soft X-ray pulsar and a member of a small group of radio silent (thermal radiation emitting) and isolated NSs. But investigations also suggest that it behaves as a normal radio pulsar and its surface temperature is surprisingly high. Various researches have also been done on it during the last few years to understand its mysterious behavior. It has also shown higher spin down power and non-thermal emissions with various peculiar characteristics.

Various mysterious properties of this nearby cooling star have made this star ideal for study further under cosmic acceleration in $f(R,T)$ modified gravity. One can also study the NSs thermal emission from the properties of this star. The presence of core stellar matter as anisotropic fluid (MCG) also helps us to investigate the effect of DM on this NS. The main aim of this study is to find out the properties of this particular star and study the EoS of this type of stars. Scientists have been studying the EoS of core nuclear matter and its inter-connections with the properties of the NSs for a long time. We can reveal the structural evolution of the compact stars through this present important study using our model in the framework of $f(R,T)$ modified gravity, applying Tolman-Kuchowicz (TK hereafter) metric potentials [391, 379]. These metric potentials give a singularity free solution for the compact objects with stability. Applying TK spacetime several investigations on the compact stars have been done in

the references [389, 390].

11.1.2 Construction of Basic Mathematical Equations in f(R, T) Gravity : The Stellar Equations under Spherical Symmetry

11.1.2.1 Basic Mathematical Formulation

Here, we will formulate the primary equations of $f(R,T)$ gravity by integration of the Ricci scalar R and considering Einstein-Hilbert action which in $f(R,T)$ modified gravity becomes

$$S_{EH} = \int |h| L_M d^4x + \frac{1}{2}\int f(R,T)|h| d^4x \quad , \quad 8\pi G = 1 \quad , \tag{11.1}$$

where $|h| = det(h^a_\alpha) = \sqrt{-g}$ describes the determinant of the tetrad (h^a_α), L_M represents the perfect matter fluid Lagrangian and $g = det(g_{\mu\nu})$. The energy-momentum tensor in the diagonal form can be written as

$$T^\alpha_\beta = diag(-\rho, p_r, p_t, p_t) \quad . \tag{11.2}$$

Now, if we consider the stellar matter as anisotropic perfect fluid then the energy-momentum tensor becomes

$$T_{\mu\nu} = [(p+\rho)\, u_\mu u_\nu - p g_{\mu\nu}] \quad , \tag{11.3}$$

where $T_{\mu\nu}$ can be defined as [100]

$$T_{\mu\nu} = -\frac{2}{|h|}\frac{\partial(L_M|h|)}{\partial g^{\mu\nu}} \quad . \tag{11.4}$$

So, in metric formalism, by using the variation w.r.t. the metric tensor, the equations

(1) and (3) gives the field equation under modified $f(R,T)$ gravity as

$$\frac{\partial f_R(R,T)}{\partial R}R_{\mu\nu}-\frac{1}{2}f(R,T)g_{\mu\nu}-[\nabla_\mu\nabla_\nu-g_{\mu\nu}\Box]\frac{\partial f_R(R,T)}{\partial R}=T_{\mu\nu}-T_{\mu\nu}f_T(R,T)-f_T(R,T)\Theta_{\mu\nu} \quad , \tag{11.5}$$

where $f_R(R,T)=\frac{\partial f(R,T)}{\partial R}$ and $f_T(R,T)=\frac{\partial f(R,T)}{\partial T}$. Here, the box operation,"$\Box$" (D'Alembert operator) in terms of covariant derivative ∇_μ, is defined as $\Box=g^{\mu\nu}\nabla_\mu\nabla_\nu$ and $\Theta_{\mu\nu}$ can be obtained as

$$\Theta_{\mu\nu}=g_{\mu\nu}\nabla^\mu-2T_{\mu\nu}-2g^{\alpha\beta}\frac{\partial^2 L_M}{\partial g^{\mu\nu}\partial g^{\alpha\beta}} \quad . \tag{11.6}$$

With considering the four velocity such as $u_\mu u^\mu=1$, equations (3) and (4) gives the reduced form of the above equation (5) as

$$\Theta_{\mu\nu}=-\rho g_{\mu\nu}-2T_{\mu\nu} \quad , \quad if \quad we \quad take, \quad L_M=\rho \quad and \quad \frac{\partial^2 L_M}{\partial g^{\mu\nu}\partial g^{\alpha\beta}}=0 \quad . \tag{11.7}$$

Now, using the equations (3) and (5), we get

$$T_{\mu\nu}=\left[T_{\mu\nu}f_T+\frac{1}{2}\left(f-Rf_R\right)g_{\mu\nu}-\rho g_{\mu\nu}f_T-\left(g_{\mu\nu}\Box-\nabla_\mu\nabla_\mu\right)f_R\right] \quad . \tag{11.8}$$

Again, taking the trace of the field equation (5) yields

$$Rf_R(R,T)-2f+3\Box f_R(R,T)=T_{\mu\nu} \quad . \tag{11.9}$$

The above equation (9) is a non-linear second order differential equation describing the dynamical nature of the Ricci scalar for $f(R,T)$ modified gravity. This has a different structure than the case of pure general relativistic algebraic form. The Lagrangian of $f(R,T)$ modified gravity consists of the stress-energy tensor $T_{\mu\nu}$ as a non-minimal coupling. As a byproduct, even at the region exterior to the compact object, Ricci scalar does not vanish. This clearly depicts that, the chosen energy-momentum tensor of the anisotropic perfect fluid and related EoS along with field equations in modified $f(R,T)$ gravity are far beyond the standard model of gravity and not at all constrained by general relativistic assumptions, rather contain some significant and interesting new

features of modified gravity theories.

Further, in this model in $f(R,T)$ modified gravity, energy-momentum tensor of matter is not conserved. An extra force (anisotropic force) comes into play which is repulsive in nature may effect the gravitational field of the NS beyond GR and it might be relevant at galactic scales as well.

11.1.2.2 Field Equations under Tolman-Kuchowicz Spacetime

In this work, we have chosen the spherically symmetric metric as

$$ds^2 = -e^{A(r)}dt^2 + e^{B(r)}dr^2 + r^2d\Omega^2 \quad , \tag{11.10}$$

where the unknown metric functions, $A(r)$ and $B(r)$ are purely radial (r varies from 0 to ∞) and $d\Omega^2 = sin^2\theta d\phi^2 + d\theta^2$, $0 \leq \theta \leq \pi$, $0 \leq \phi \leq 2\pi$. Here, for our purpose to get a singularity free and stable compact star model, we have chosen the metric potentials according to the Tolman-Kuchowicz ansatz as

$$e^{A(r)} = \tau(r) = 1 + ar^2 + br^4 \quad and \quad e^{B(r)} = C^2e^{Dr^2} \quad , \tag{11.11}$$

where a, b, C and D are constants (model parameters). In this present case, these metric potentials $A(r)$ and $B(r)$ does not become zero as $r \to \infty$. Earlier, it was effectively used by several researchers to construct a model of the compact stars both in GR and modified gravities [87-90]. In the framework of Tolman-Kuchowicz (TK) ansatz [391, 379], anisotropic spheres in $f(R,G)$ gravity have been explored by Javed et al. [380]. Biswas et al. have examined anisotropic strange stars in the background of $f(R,T)$ modified gravity.

Again, to incorporate matter-curvature coupling effect, we have considered the $f(R,T)$ modified gravity in the form

$$f(R,T) = R + 2\xi T \quad , \tag{11.12}$$

where ξ is the coupling constant (small and positive) and $\xi = 0$ can reproduce the GR

field equations. The term $2\xi T$ induces a time dependent coupling between matter and curvature.

The field equations under modified gravity along with the line element (10), becomes

$$8\pi\rho^{eff} + \xi(3\rho - p) = \left[\frac{B^{'}(r)}{r}e^{-B(r)} + \frac{1}{r^2}\left(1 - e^{-B(r)}\right)\right] \quad , \tag{11.13}$$

$$8\pi p_r^{eff} - \xi(\rho - 3p) = \left[\frac{A^{'}(r)}{r}e^{-B(r)} + \frac{1}{r^2}\left(e^{-B(r)} - 1\right)\right] \quad and \tag{11.14}$$

$$8\pi p_t^{eff} - \xi(\rho - 3p) = \frac{1}{4}e^{-B(r)}\left[2A''(r) + A'^2(r) - A'(r)B'(r) + \frac{2}{r}(A'(r) - B'(r))\right] \quad , \tag{11.15}$$

where prime ($'$) represents the derivative w.r.t. r. ρ^{eff}, p_r^{eff} and $8\pi p_t^{eff}$ are effective density, radial pressure and transverse pressure respectively in Einstein's gravity and can be written as

$$\rho^{eff} = \rho + \frac{\xi}{8\pi}(\rho - p_r - 2p_t) \quad , \tag{11.16}$$

$$p_r^{eff} = p_r + \frac{\xi}{8\pi}(\rho + 3p_r + 2p_t) \quad and \tag{11.17}$$

$$p_t^{eff} = p_t + \frac{\xi}{8\pi}(\rho + p_r + 4p_t) \quad . \tag{11.18}$$

Now, after taking covariant divergence of the equation (5) we have got

$$\nabla^\mu T_{\mu\nu} = \frac{f_T(R,T)}{8\pi - f_T(R,T)}\left[(T_{\mu\nu} + \Theta_{\mu\nu})\nabla^\mu ln f_T(R,T) + \nabla^\mu\Theta_{\mu\nu} - \frac{g_{\mu\nu}\nabla^\mu T}{2}\right] \quad . \tag{11.19}$$

Above equation shows that, $\nabla^\mu T_{\mu\nu} \neq 0$ if $f_T(R,T) \neq 0$ which depicts that the system will not be conserved.

Now, the modified TOV equation in $f(R,T)$ gravity becomes

$$-\frac{A^{'}(r)}{2}(\rho + p_r) - \frac{dp_r}{dr} + \frac{2}{r}(p_t - p_r) + \frac{\xi}{(2\xi + 8\pi)}\left[\frac{d\rho}{dr} + \frac{dp_r}{dr} + 2\frac{dp_t}{dr}\right] = 0 \quad , \tag{11.20}$$

where $m(r)$ is the total mass enclosed within the radius r of the NS $RXJ1856.5-3754$. Here, conservation equations of Einstein's gravity can be reconstructed by putting $\xi = 0$.

11.1.3 Proposed Model in $f(R,T)$ Modified Gravity

11.1.3.1 Obtaining Neutron Star Parameters with MCG

Now, applying the metric potentials from equation (11), in the equations (13) – (15), we obtain

$$\left[8\pi\rho^{eff} + \xi(3\rho - p)\right]\tau^2 = \left[3a + (a^2 + 5b)r^2 + 2abr^4 + b^2r^6\right] \quad , \tag{11.21}$$

$$\left[8\pi p_r^{eff} - \xi(\rho - 3p)\right]\tau = -(a - 2D + br^2) \quad and \tag{11.22}$$

$$\left[8\pi p_t^{eff} - \xi(\rho - 3p)\right]\tau^2 = \left[-a + 2D + (D(a + D) - 2b)r^2 + aD^2r^4 + bD^2r^6\right] \quad . \tag{11.23}$$

In this present model, we have taken the existence of MCG at the core of this star. The EoS of this fluid takes the form

$$p(r)_{MCG} = \varphi\rho - \frac{\psi}{\rho^{\zeta}} \quad , \quad 0 \leq \zeta \leq 1 \quad and \quad \varphi \neq -1 \quad , \tag{11.24}$$

where φ, ψ and ζ are free parameters and ρ is the energy density and $p(r)$ is the radial pressure.

Now, using equation (24), we have solved the equations (21) – (23) and got the expression of density and pressure in Einstein's gravity as

$$\rho^{eff} = \psi + \frac{3\varphi\{a + D + (2b + aD)r^2 + bDr^4\}}{16\pi\tau^2} \quad , \tag{11.25}$$

$$p_r^{eff} = -\psi + \frac{\varphi\{a + D + (2b + aD)r^2 + bDr^4\}}{16\pi\tau^2} \quad and \tag{11.26}$$

$$\begin{aligned} p_t^{eff} =& \psi + \frac{\varphi}{16\pi\tau^2}\left[-5a + 7D + \left(-2a^2 - 8b + aD + 2D^2\right)\right] r^2 \\ &+ \frac{\varphi}{16\pi\tau^2}\left[\{3bD + 2a(-2b + D^2)\}r^4 + 2b(-b + D^2)r^6\right] \quad . \end{aligned} \tag{11.27}$$

Now, we have solved the equations $(16) - (18)$ after using the expressions given in the equations $(25) - (27)$ and obtained the expressions of matter density, radial pressure and transverse pressure in $f(R,T)$ modified gravity as

$$\rho = \frac{1}{3}\left[3\psi + \frac{\varphi\,(a + D + (2b + aD)r^2 + bDr^4)}{(\xi + 4\pi)\tau^2}\right] \quad , \tag{11.28}$$

$$p_r = \left[-\psi + \frac{\varphi\,(a + D + (2b + aD)r^2 + bDr^4)}{(\xi + 4\pi)\tau^2}\right] \quad and \tag{11.29}$$

$$\begin{aligned} p_t =& \frac{1}{2(\xi + 4\pi)^2}\left[\psi(\xi + 4\pi)^2 + \frac{1}{\tau}[-D(\xi - 12\pi) - 2a(\xi + 4\pi) + 2(-b + D^2))(\xi + 4\pi)r^2\right] \\ &+ \frac{\varphi}{2(\xi + 4\pi)^2}\left[\frac{1}{\tau^2}[4D(\xi + 4\pi) - 2b(7\xi + 12\pi)r^2 + a\left(2D(\xi + 4\pi)r^2 - (7\xi + 12\pi)\right)]\right] \quad . \end{aligned} \tag{11.30}$$

So, from the above equations (29) and (30), we can easily obtain the anisotropic factor Δ of the NS, $RXJ1856.5 - 3754$ in $f(R,T)$ modified gravity as

$$\begin{aligned} \Delta =& \frac{1}{2(\xi + 4\pi)}\left[8\psi(\xi + 2\pi)\right] \\ &+ \frac{1}{2(\xi + 4\pi)}\left[\frac{1}{\tau^2(\xi + 4\pi)}\{(2D - 5a)\xi + (D - a)8\pi + \{aD(\xi + 4\pi) - 2b(5\xi + 8\pi)\}r^2\}\right] \\ &+ \frac{\varphi}{2\tau(\xi + 4\pi)^2}\left[-2D(\xi - 2\pi) - a(\xi + 4\pi) - (b - D^2)(\xi + 4\pi)r^2\right] \quad . \end{aligned} \tag{11.31}$$

So, under the modified $f(R,T)$ gravity, the density, radial pressure, transverse pressure and anisotropic factor of the isolated NS $RXJ1856.5-3754$ have been acquired successfully.

11.1.3.2 Determination of the Model Constants : Application of Matching Conditions at The Boundary

So, in order to obtain various model parameters of the TK metric potentials, we have matched the interior solution in modified $f(R,T)$ gravity to the exterior Schwarzschild space-time as the vacuum solutions at the boundary $r = R$ of the NS. In this work, we have considered the exterior Schwarzschild metric as

$$ds^2 = -\left(1-\frac{2M}{r}\right)dt^2+\frac{dr^2}{\left(1-\frac{2M}{r}\right)}+r^2(sin^2\theta d\phi^2+d\theta^2) \quad , \quad 0\leq\theta\leq\pi, \quad 0\leq\phi\leq 2\pi \quad . \tag{11.32}$$

where M is the total mass of the NS within its boundary ($r = R$). So, at the boundary surface of the NSs, between the exterior and interior metrics, the space-time variables like g_{tt}, g_{rr} and $g_{tt,r}$ are continuous, i.e, $g_{rr}^{-} = g_{rr}^{+}$ *and* $g_{tt}^{-} = g_{tt}^{+}$ and yield the relations

$$\left(1-\frac{2M}{R}\right) = C^2e^{DR^2} \quad and \tag{11.33}$$

$$\left(1-\frac{2M}{R}\right) = (1+aR^2+bR^4)^{-1} \quad . \tag{11.34}$$

For our investigation, the values of these constants a, b, C and D can be found out by using some observational data of the compact star as we have assumed for the star $RXJ1856.5-3754$ ($M = 0.9M_{\odot}, R \cong 17km$) and applying matching conditions simultaneously under suitable boundary conditions. The interior solution should behave as regular and as a result the energy-density, radial and tangential pressures of the fluid which is under consideration must be non-singular inside the core of the compact stars.

It should behave regularly everywhere inside the star. Further, physical quantities as mentioned above, should have maximum values at the stars center. The quantities will behave in a decreasing manner towards the surface boundary. Also the density,

radial pressure ((p_r) and transverse pressure ((p_t) all should be positive in the range $(0 < r < R)$. At the surface of the star, p_r must be zero, i.e, $(p_r \mid_{r=R}) = 0$.

On the other hand, the tangential pressure p_t does not essentially have to be zero at stars surface. Moreover, during our work, we have chosen the metric potentials as given in equation (16). So, we have $(e^{A(r)} \mid_{r=0}) = e^C > 0$ and $(e^{B(r)} \mid_{r=0}) = 1$.

Furthermore, $(e^{A(r)})' = 2Dre^{C+Dr^2}$ and $(e^{B(r)})' = 2Are^{Ar^2}$. These boundary conditions allows the matching of interior space-time of the NS to exterior space-time at star's surface, $(r = R\ ,\ (0 < r < R))$ smoothly and helps to get the model parameters (constants) of our present model easily as for the well behaved metric potentials in the interval $(0, R)$.

Now, after solving the above equations (33) and (34) by considering all boundary conditions we obtain

$$a = \frac{1}{R^2(\xi + 2\pi)(1 + 3N^2)}\left[-2(\xi + 2\pi) + (\xi + 2\pi)(2 + DR^2)N + 6D\pi N^2R^2\right] \quad , \tag{11.35}$$

$$b = \left[\frac{-1 - aR^2 + N}{R^4}\right] \quad , \tag{11.36}$$

$$C = e^{-\frac{DR^2}{2}}\left[N^{-\frac{1}{2}}\right] \quad and \tag{11.37}$$

$$D = \frac{N}{R^2}\left[\frac{M}{R}\right] \quad , \tag{11.38}$$

where $N = (1-2\frac{M}{R})^{-1}$. Now, the values of a, b, C and D can be calculated by employing the values of M and R from the observations of the isolated NS $RXJ1856.5 - 3754$.

11.1.4 Physical Analysis

11.1.4.1 Calculation of Neutron star Parameters

Here, we have verified both analytic and graphical resolution to examine the mathematical and physical behaviour and properties of this current model.

Now, at the boundary surface of the NS, p_r vanishes which gives the surface density of this star as

$$\rho_s = \psi + \frac{\varphi(a + D + (2b + aD)R^2 + bDR^2)}{3(\xi + 4\pi)\tau^2} \quad . \tag{11.39}$$

Again from the equations $(28) - (30)$, we have got the expression of core density ρ_c and core pressure p_c of the isolated NS in modified $f(R,T)$ gravity as

$$\rho_c = \frac{\varphi(a + D) + 3\psi(\xi + 4\pi)}{3(\xi + 4\pi)} \quad and \tag{11.40}$$

$$p_c = -\psi + \frac{\varphi(a + D)}{(\xi + 4\pi)} \quad . \tag{11.41}$$

It is notable that we can get the corresponding quantities in GR by considering $\xi = 0$. Again, we have also obtained the density and pressure gradients by differentiating the equations $(28) - (30)$ and got the result that $\rho' \mid_{r=0} = 0$, $p'_r \mid_{r=0} = 0$ and $p'_t \mid_{r=0} = 0$. We have tabulated the measure values of the surface density, central pressure and density respectively of the isolated compact star $RXJ1856.5 - 3754$ from our current model in the Table 1.

Table 1.

Sl. No.	ξ	p_c $(dyne\ cm^{-2})$	ρ_s $(gm\ cm^{-3})$	ρ_c $(gm\ cm^{-3})$
1	0.00	4.680565×10^{34}	5.354871×10^{14}	6.513483×10^{14}
2	0.08	4.714562×10^{34}	5.424823×10^{14}	6.657281×10^{14}
3	0.16	4.807213×10^{34}	5.584721×10^{14}	6.710628×10^{14}
4	0.24	4.893482×10^{34}	5.672342×10^{14}	6.775691×10^{14}
5	0.32	4.956718×10^{34}	5.852387×10^{14}	6.912348×10^{14}

Table 11.1: Values of p_c, ρ_s and ρ_c of $RXJ1856.5 - 3754$ for different values of ξ from the present model

From the above table, we can observe the values of the density and pressure at the core of the isolated NS $RXJ1856.5 - 3754$ in modified $f(R,T)$ gravity. This clearly indicates that, the main thermodynamic variables remain almost unaltered but must respect some criteria. Moreover, the derived values from this model strongly agree with other astronomical observations on anisotropic compact stars in spherically stable

equilibrium. So the star $RXJ1856.5-3754$ is also under stable equilibrium. The value of the relativistic adiabatic index Γ also indicates the same.

11.1.4.2 Observational constraints and Physically stable conditions

For any compact object, in order to maintain a stable equilibrium structure, its free parameters should follow some restrictions. This constraints the value as well as the range of various specific NS parameters. In this model, we have also obtained several constraints on the properties of the star $RXJ1856.5-3754$. The density, radial pressure and tangential pressure should be positive at the interior of the star $RXJ1856.5-3754$, i.e., $\rho(0 < \frac{r}{R} < 1) > 0$, $p_r(0 < \frac{r}{R} < 1) > 0$ and $p_t(0 < \frac{r}{R} < 1) > 0$.

The interior solutions of the star should be regular and non-singular so that energy density, radial pressure and tangential pressure of the effective anisotropic fluid must be non-singular at the interior of the NS. These parameters should be behaved as regular throughout the interior of the star. In this model, we have also verified that, $\rho(r = 0) > 0$, $p_r(r = 0) > 0$ and $p_t(r = 0) > 0$. Again at the boundary surface of the isolated compact star, the radial pressure of the anisotropic fluid must be zero, i.e., $p_r(r = R) = 0$. Though at the boundary, transverse pressure is not zero necessarily. These conditions are also verified in our present model. These are also clear from the graphical plots in the Fig. 1 to Fig. 3.

The measured core density of the isolated NS, from our current investigation, is $6.66 \times^{14}\ gm\ cm^{-3}$ which clearly reveals that the central fluid possess anisotropic form and at the same time shows the possibility of finding neutrons inside the core. The anisotropic parameter should be zero at the center of the star and it should be increasing towards the surface, i.e., $\Delta'(0 \leq \frac{r}{R} \leq 1) > 0$. This criteria has also been confirmed from our current model.

For a physically accepted model, the pressure of the isolated NS should be non-negative at the interior, i.e., $p_c > 0$. Now, from our present model, applying the Zeldivich condition [**?**], i.e., $\frac{p_c}{\rho_c} < 1$ we can get the valid range of values for the dimensionless coupling parameter ξ for the isolated compact star $RXJ1856.5 - 3754$, which becomes $0 \leq \xi \leq 0.5$. This clearly reveals that why the negative values of the

parameter ξ, which may produce from the modified TOV equation is not acceptable for a valid and physically accepted model of a isolated compact star.

11.1.4.3 Verification of different Energy Conditions

Now, we will check that our proposed model will satisfy various energy conditions, such as the null energy condition (NEC), the weak energy condition (WEC), the strong energy condition (SEC) and the dominant energy condition (DEC) or not. Subsequent inequalities must be satisfied simultaneously at every point inside the stellar model.

$$(\rho + p_t) \geq 0 \quad and \quad (\rho + p_r) \geq 0 \quad : NEC \tag{11.42}$$

$$(\rho + p_t) > 0 \quad , \quad (\rho + p_r) > 0 \quad and \quad \rho \geq 0 \quad : WEC \tag{11.43}$$

$$(\rho - p_r - 2p_t) \geq 0 \quad , \quad (\rho + p_r) \geq 0 \quad and \quad (\rho + p_t) \geq 0 \quad : SEC \tag{11.44}$$

and

$$(\rho - p_r) \geq 0 \quad , \quad (\rho - p_t) \geq 0 \quad and \quad \rho \geq 0 \quad : DEC \tag{11.45}$$

From the above expressions $(42) - (45)$ and the present investigation on the NS $RXJ1856.5 - 3754$, we can say that, in case of our present model, all the required energy conditions are satisfied in $f(R,T)$ modified gravity.

11.1.4.4 Verification of the Causality Condition

If the present model of the NS $RXJ1856.5 - 3754$ obeys the causality and hydrostatic equilibrium conditions then only our model will fulfill the physical requirements for the realistic model of the isolated compact stars. The causality condition of the model is that sound velocity everywhere inside the isolated NS must be less than the speed of light. From our model, we have obtained the expressions of square of radial velocity

v_r^2 and transverse velocity v_t^2 as

$$v_r^2 = \frac{dp_r}{d\rho} = \frac{1}{3} \quad and \tag{11.46}$$

$$v_t^2 = \frac{dp_t}{d\rho} \approx \frac{2}{3} \quad . \tag{11.47}$$

So, the causality conditions are strictly obeyed by our model as both v_r^2 *and* $v_t^2 < 1$. Again, according to the research on relativistic compact stars [51, 52], we also have got the idea of potentially stable and unstable regions of the star as

$-1 \leq (v_t^2 - v_r^2) \leq 0$: Potentially stable region ,

$0 < (v_t^2 - v_r^2) \leq 1$: Potentially unstable region .

and the above two conditions implies that $\mid (v_r^2 - v_t^2) \mid < 1$ for the star $RXJ1856.5-3754$. From this model we can also verify the "cracking" condition of Herrera, which deals with the stability of anisotropic compact stars under radial perturbation.

11.1.4.5 Anisotropic Nature Analysis

Interestingly, the radial pressure p_r varies differently from the transverse pressure p_t. Due this difference in pressure inside, anisotropic force comes into play inside the star. We can calculate the anisotropic force ($\Delta^{'}$)in modified gravity, inside the NS by using the equation (36) as

$$\begin{aligned}\Delta^{'} = \frac{2}{r}\Delta =& \frac{1}{r(\xi+4\pi)}\left[8\psi(\xi+2\pi)\right] \\ &+ \frac{1}{r(\xi+4\pi)}\left[\frac{1}{\tau^2(\xi+4\pi)}\{(2D-5a)\xi + (D-a)8\pi + \{aD(\xi+4\pi) - 2b(5\xi+8\pi)\}r^2\}\right] \\ &+ \frac{\varphi}{r\tau(\xi+4\pi)^2}\left[-2D(\xi-2\pi) - a(\xi+4\pi) - (b-D^2)(\xi+4\pi)r^2\right] \quad .\end{aligned} \tag{11.48}$$

Now, Δ may be positive or negative and in turn the force also changes. Again this force vanishes for isotropic case. From our model we have got that, anisotropic pressure is always positive inside the core of this NS i.e., $\Delta^{'} > 0$. This also implies that,

$p_t > p_r$. This is also verified for the compact star in our present model. The anisotropic parameter vanishes at the centre of the isolated NS and stars increasing towards the surface. This condition is very crucial because it supports the repulsive anisotropic force inside the core of the NS. Moreover, this force allows a more compact star than for an isotropic fluid case [377].

11.1.4.6 Relativistic Adiabatic Index and Stability

The relativistic adiabatic index (Γ), is the measure of stability for the compact stars [39-41]. It also shows the stiffness of the EoS of the star with given density. If the value of Γ is such that, $\Gamma > \frac{4}{3}$, then the NS is under stability. The relativistic adiabatic index can be measured as

$$\Gamma = \left(\frac{p_r + \rho}{p_r}\right)\frac{\partial p_r}{\partial \rho} \quad . \tag{11.49}$$

The measured values of Γ from our model, for different values of ξ for $RXJ1856.5-3754$ is tabulated in Table 2. The Fig. 9 also depicts the stability of the isolated compact star.

11.1.4.7 Equation of state

The EoS of the NS $RXJ1856.5-3754$ according to this model can be obtained by using the following relations as $p_r = \omega_r \rho$ and $p_t = \omega_t \rho$.

From the assumptions, it is clear that the linear relation exists between radial pressure and density. The tangential pressure w.r.t. density almost follows a parabolic curve.

11.1.4.8 Redshift and Equilibrium

We can also measure the surface redshift function $Z_s(r)$ [73, 74] of $RXJ1856.5-3754$ by using the equation as

$$Z_s(r) = \frac{1}{\sqrt{\left(1-\frac{m(r)}{r}\right)}} - 1 \quad . \tag{11.50}$$

In this present work, we have measured the numerical values of $Z_s(r)$ for different values of ξ, which becomes very interesting. Various astronomical observations suggests that the value of surface redshift for the compact stars should be ≤ 5 in order to ensure stable equilibrium. We also got the same type of result.

Again, the gravitational redshift of the $RXJ1856.5-3754$, according to the present model can be calculated as

$$Z_g(r) = \left[e^{\frac{A(r)}{2}} - 1\right] \Rightarrow Z_g(r) = \left[\frac{1}{C}e^{-\frac{Dr^2}{2}} - 1\right] \quad ,$$

and

$$\frac{dZ_g(r)}{dr} = 0 \text{ and } \frac{d^2Z_g(r)}{d^2r} = -\frac{D}{C} < 0, \quad \text{at the origin.}$$

So, the gravitational redshift of the star decreases monotonically with the radius of the star. The Fig. 88 also verifies this.

Table 2.

Sl. No.	ξ	Γ	$\Delta^{'}$	$Z_s(r)$
1	0.00	4.768472	0.0002385	0.187562
2	0.08	4.853914	0.0002396	0.190245
3	0.16	4.942573	0.0002541	0.194587
4	0.24	5.103587	0.0003245	0.196354
5	0.32	5.119656	0.0003387	0.197523

Table 11.2: Values of (Γ), ($\Delta^{'}$) and $Z_s(r)$ of $RXJ1856.5-3754$ for different values of ξ from the present model

11.1.4.9 Mass- radius relation with Compactness Factor

The effective mass of the compact star $RXJ1856.5-3754$ in case of our model in $f(R,T)$ gravity becomes

$$\begin{aligned}
M(r) =&4\pi\int_0^r \rho r^2 dr \\
&= \frac{r}{2}(1-\frac{1}{\tau}) + \frac{r^3}{2(\xi+4\pi)}\left[-\psi(\xi+2\pi)(\xi+4\pi)\right] \\
&+ \frac{r^3}{2(\xi+4\pi)}\left[\frac{1}{\tau}\{2a+(\xi+2\pi)-2D(\xi+3\pi)+\left(D^2\xi+2b(\xi+2\pi)\right)r^2\}\right] \\
&+ \frac{r^3}{2(\xi+4\pi)}\left[\frac{1}{\tau^2}\{2D\xi+2b(\xi+2\pi)r^2+a(\xi+2\pi+D\xi r^2)\}\right] \quad .
\end{aligned} \tag{11.51}$$

We can measure the effective mass of the isolated NS using our model from the above equation (58) and this also implies $M(r)\to 0$ as $r\to 0$, which shows the regularity of $M(r)$ at the interior.

Again, Compactness factor $u(r)$ of this compact stars, using our model can be written as

$$\begin{aligned}
u(r) =&\frac{1}{r}M(r) \\
&= \frac{1}{2}(1-\frac{1}{\tau}) + \frac{r^2}{2(\xi+4\pi)}\left[-\psi(\xi+2\pi)(\xi+4\pi)\right] \\
&+ \frac{r^2}{2(\xi+4\pi)}\left[\frac{1}{\tau}\{2a+(\xi+2\pi)-2D(\xi+3\pi)+(D^2\xi+2b(\xi+2\pi))r^2\}\right] \\
&+ \frac{r^2}{2(\xi+4\pi)}\left[\frac{1}{\tau^2}\{2D\xi+2b(\xi+2\pi)r^2+a(\xi+2\pi+D\xi r^2)\}\right] \quad .
\end{aligned} \tag{11.52}$$

For a neutron star $u(r)\in(10^{-1},\frac{1}{4})$ but if $u(r)\in(\frac{1}{4},\frac{1}{2})$, it defines an ultra compact star and a black hole is represented by $u(r)=\frac{1}{2}$ [57, 58]. According to our model, the measured compactness factor of $RXJ1856.5-3754$ lies in between the proposed upper and lower bound of the compactness factor [377] and also obey the Buchdahl limit [358]. The measured values of $u(r)$ have confirmed the verification of the inequalities of our model for the compact star in $f(R,T)$ modified gravity.

Now, using the above equations (58) and (59), we can also measure the radius of the NS $RXJ1856.5-3754$ from our model. From the measured values of these two important parameters, we can clearly observe the effect of the coupling parameter ξ minutely. It is very interesting to notice the momentum-curvature coupling has a great effect on acquiring more mass and getting a more compact structure by the star and as well as on maintaining the stability.

Table 3.

Sl. No.	ξ	$M(M_{\odot})$	$R(km)$	$u(r)$
1	0.00	1.084236	11.395424	0.095146
2	0.08	1.092537	11.254783	0.097544
3	0.16	1.101358	11.238756	0.098303
4	0.24	1.109753	11.028752	0.100635
5	0.32	1.112384	11.015428	0.100984

Table 11.3: Values of mass (M), radius (R) and $u(r)$ of $RXJ1856.5-3754$ for different values of ξ from the present model

11.1.4.10 Verification of Equilibrium condition under different forces

Now in order to ensure the viability of this current model in modified gravity, we shall examine the validity of the TOV equation [389]. For this, we will assume that the NS, $RXJ1856.5-3754$ is under hydrostatic equilibrium under different forces acting on the system. There are four different forces acting on the present system namely, the hydrostatic force F_h, the gravitational force F_g, anisotropic force F_a and newly introduced force related to modified gravity F_m. In this investigation, we have figured out the explicit form of these forces as follows:

$$F_h = -\frac{dp_r}{dr} \quad , \tag{11.53}$$

$$F_g = -\frac{A'(r)}{2}(\rho + p_r) \quad , \tag{11.54}$$

$$F_a = \frac{2}{r}(p_t - p_r) \quad and \tag{11.55}$$

$$F_m = -\frac{\xi}{8\pi + 2\xi}(\rho^{'} + 2p_t^{'} + p_r^{'}) \quad . \tag{11.56}$$

Now, the equilibrium equation can be written as

$$F_h + F_g + F_a + F_m = 0 \quad . \tag{11.57}$$

The isolated NS $RXJ1856.5-3754$ is under the hydrodynamic equilibrium because the total forces satisfy equation (20). The attractive gravitational forces compensates the repulsive anisotropic forces to get a stable equilibrium. So, our model has successfully achieved the physical conditions of an isolated and anisotropic compact star in stable equilibrium under $f(R,T)$ modified gravity. This can be also be verified by the Fig. 12 in the graphical section. It assured that the hydrodynamic stability holds true for the isolated NS $RXJ1856.5-3754$.

11.1.5 Graphical Interpretation : Observational Support

Here, we have plotted the variations of several important parameters, of the isolated NS $RXJ1856.5-3754$, which we have measured using our present model, for different values of coupling parameter ξ. Each and every graph depicts crucial facts on $RXJ1856.5-3754$. The impact of momentum-curvature coupling parameter ξ on the parameters of the compact star is also investigated and the evolution of $RXJ1856.5-3754$ under the present accelerated universe is clearly disclosed. This graphical analysis has given the clear concept of structural evolution of this compact stellar object $RXJ1856.5-3754$.

Fig 79 and Fig 80 show the variation of radial pressure and transverse pressure with the radius for different values of ξ respectively. Again, Fig 81 also shows the variation of density for different values of ξ. Both pressure and density are monotonically decreasing functions of radius of the compact star. They possess a utmost value at the core and

gradually decrease towards the surface of the compact star. The graphical variations depicts that both pressures and density are not negative at the interior. At $r = R$, $\rho > 0$ and $p_t > 0$ for different values of ξ but p_r vanishes. It is very interesting as it determines the size of the compact star. The direct impact of momentum-curvature coupling on the size of the star and also on the pressures and density are revealed. From different values of coupling parameters, it is clear that as the matter-curvature coupling increases, the radius of the star begins to decrease and the star shrinks in size and gets a more compact structure. Now, the Fig 82 and Fig 83 show the behavior of sound velocities in different directions for various values of ξ. The radial sound velocity does not depend on ξ but transverse sound velocity clearly depends on the coupling constant ξ. As the value of ξ increases, the transverse sound velocity also increases. The variation of both the sound velocities inside the compact star indicates about the fulfillment of the stability criterion at the core of the NS $RXJ1856.5-3754$. The Fig 84 represents the stability factor of the isolated compact star for different values of ξ.

The Fig 85 and Fig 86 depict the variation of compactness factor and the mass of $RXJ1856.5-3754$ with the radius of the star respectively for different values of ξ. These variations are very important in case of the study of such isolated compact stars. It helps to determine the mass-radius relation of the compact star. As the coupling constant increases the compactness of the star as well as its mass. At the same time, as $p_t > p_r$, the anisotropic force is repulsive within the boundary of the star. The repulsive contributions of anisotropic force and the contributions of coupling constant ξ helps the stabilization of the inner core of the star. In Fig 87, variations of $\Gamma(r)$ is shown as a function of ξ. $\Gamma(r)$ is monotonic increasing function of radius r and everywhere inside the star it is greater than $\frac{4}{3}$. For higher values of ξ, $\Gamma(r)$ takes higher values also. The higher values of $\Gamma(r)$ confirms the stability of the star $RXJ1856.5-3754$ from our model. The Fig 88 shows the variation of surface redshift $Z_s(r)$ of the star for different values of ξ. It is positive and have a finite value inside the star but decreases towards the stellar surface. The presence of anisotropy at the core of $RXJ1856.5-3754$ leads to higher surface redshift. The Fig 89 shows how the anisotropic factor of the star varies with the radius of the star for different values of

$Fig-79$

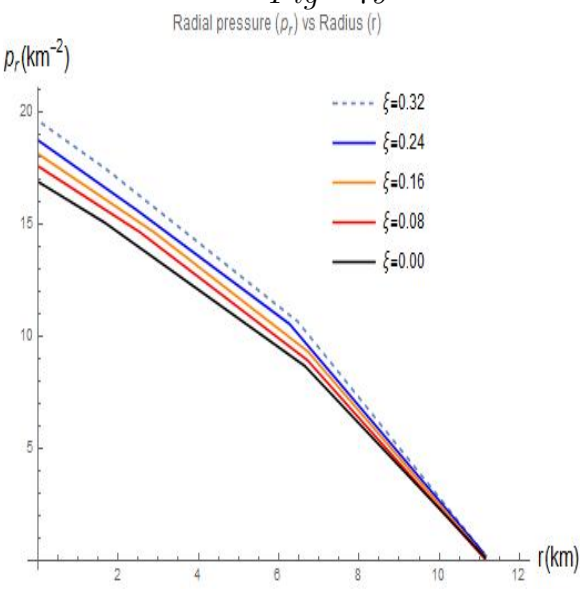

$Fig-80$

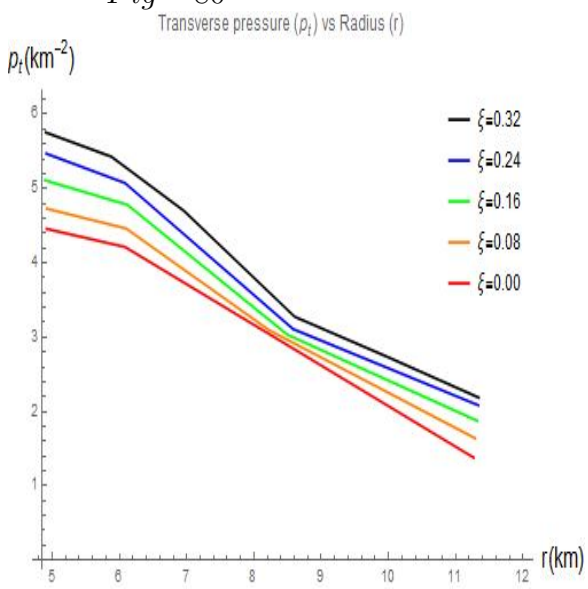

Figure 11.1: *Represents the variation of radial pressure p_r with radius r of $RXJ1856.5-3754$ for different values of ξ.*

Figure 11.2: *Represents the variation of transverse pressure p_t with radius r of $RXJ1856.5-3754$ for different values of ξ.*

ξ. From this variations we can say that the anisotropic factor increases towards the boundary of the star and has became more positive near the boundary surface which may leads to the greater stability in this region.

In Fig 90 and Fig 91, we have plotted the metric potentials $e^{B(r)}$ and $e^{A(r)}$ as a function of the radius of the isolated compact star $RXJ1856.5-3754$, respectively . We can also see the exterior space-time in both the figures. It is very clear that the metric potentials are free from the singularity and continuous at the interior of the star and also independent of the coupling parameter ξ. At the boundary, the interior and exterior metrics coincide with each other.

At last, we have plotted a very crucial and important variation of various forces of the modified TOV equation of the isolated compact star $RXJ1856.5-3754$, in the Fig 92. The figure assured the hydrodynamic stability of the present compact star model under $f(R,T)$ modified gravity. It also ensure the viability of the present model.

$Fig-81$

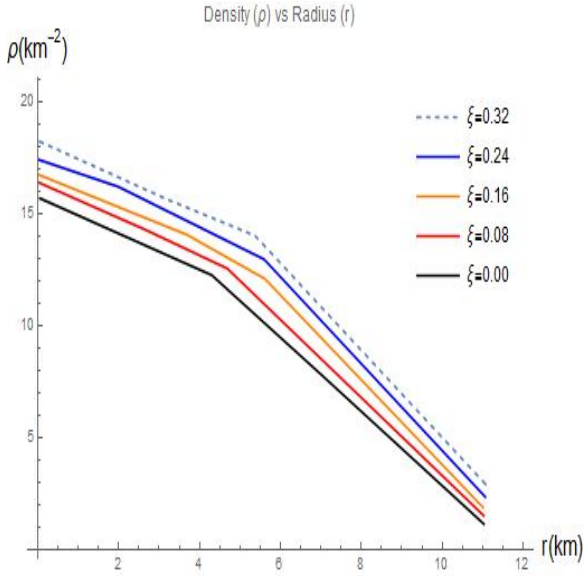

Figure 11.3: *Represents the variation of energy density ρ with radius r for different values of ξ of $RXJ1856.5-3754$.*

$Fig-82$

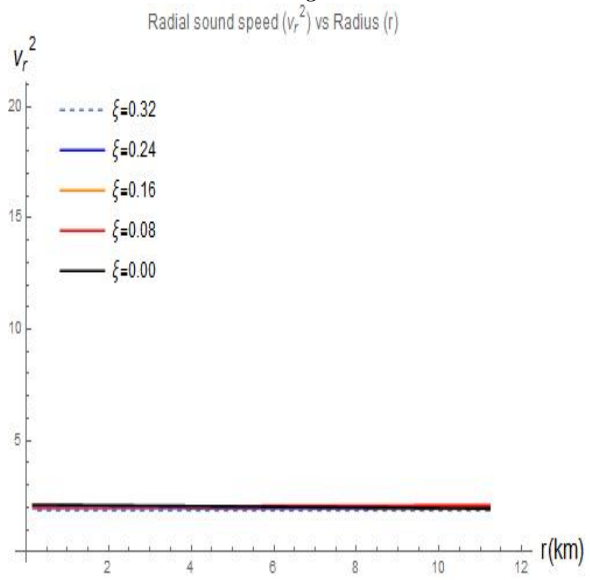

$Fig-83$

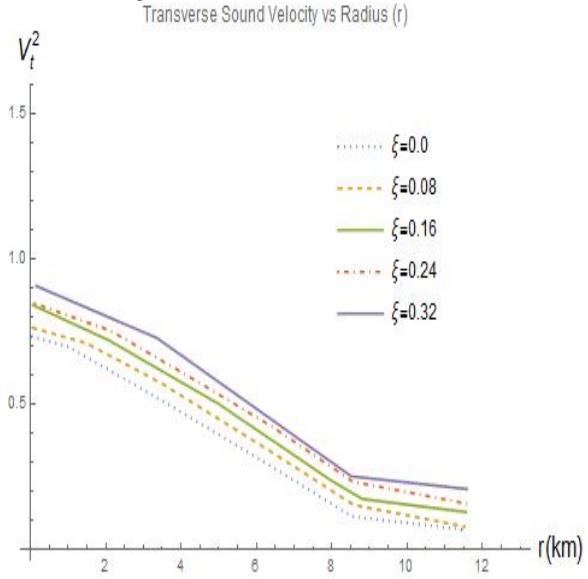

Figure 11.4: *Represents the variation of sound speed in radial direction V_r with radius r for different values of ξ of $RXJ1856.5-3754$.*

Figure 11.5: *Represents the variation of sound speed in transverse direction V_t with radius r for different values of ξ of $RXJ1856.5-3754$.*

$Fig-84$

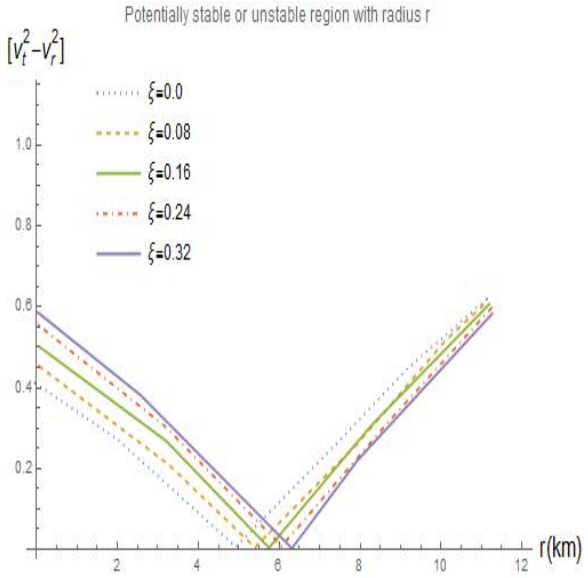

Figure 11.6: *Represents the stability factor* $(v_t^2 - v_r^2)$ *with radius* r *for different values of* ξ *of* $RXJ1856.5-3754$.

$Fig-85$

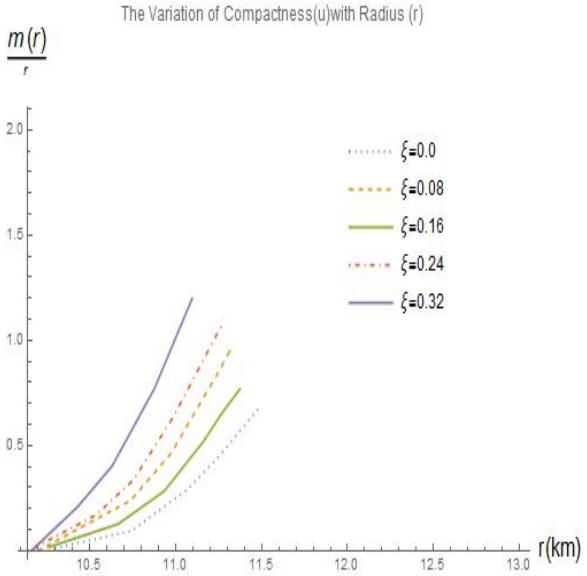

$Fig-86$

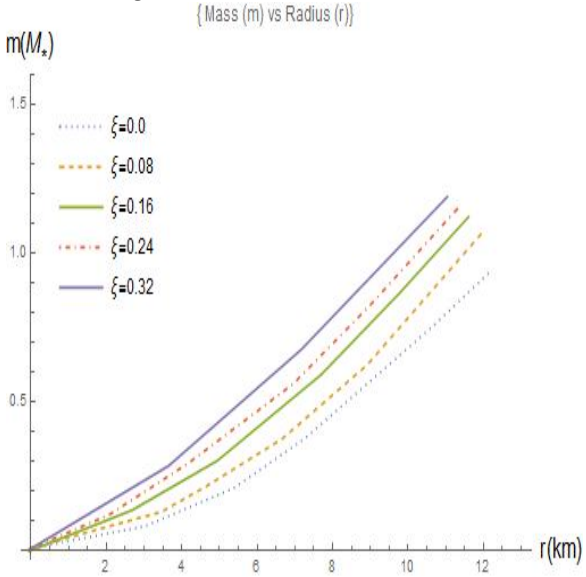

Figure 11.7: *Represents the variation of compactness factor* $u(r)$ *with radius* r *for different values of* ξ *of* $RXJ1856.5-3754$.

Figure 11.8: *Represents the variation of mass* $m(r)$ *with radius* r *for different values of* ξ *of* $RXJ1856.5-3754$.

$Fig-87$

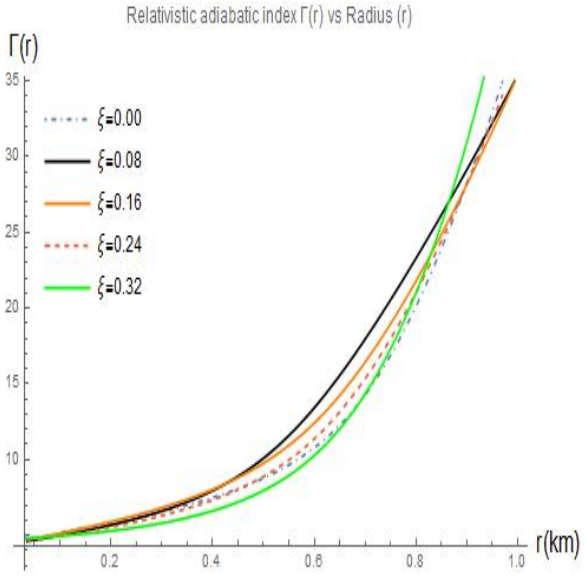

Figure 11.9: *Represents the variation of relativistic adiabatic index* $\Gamma(r)$ *with radius* r *for different values of* ξ *of* $RXJ1856.5-3754$.

$Fig-88$

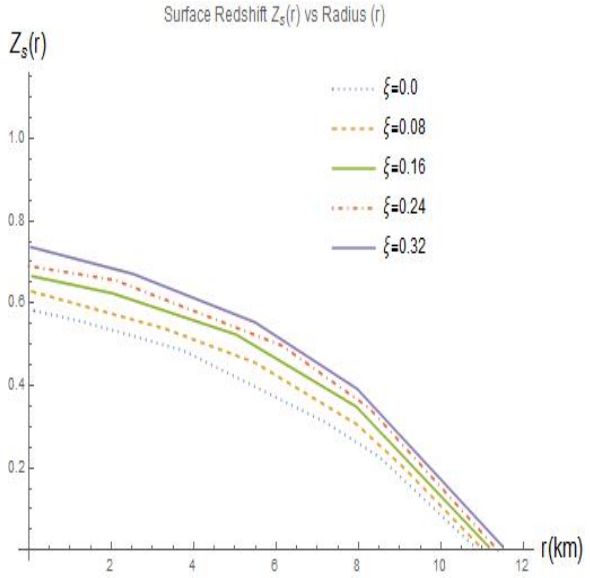

$Fig-89$

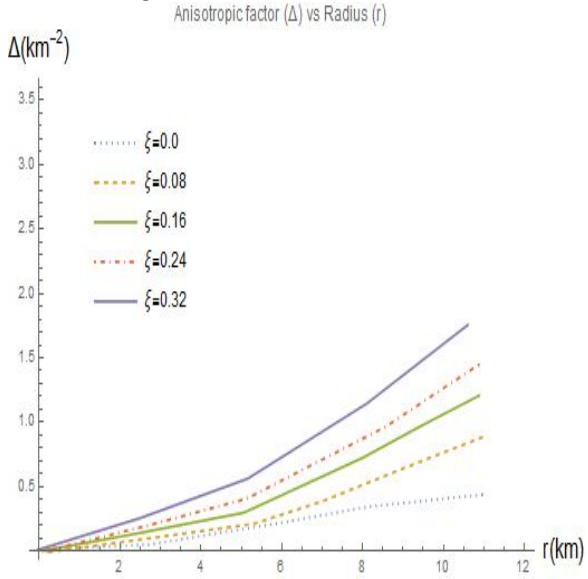

Figure 11.10: *Represents the variation of surface redshift* $Z_s(r)$ *with radius* r *for different values of* ξ *of* $RXJ1856.5-3754$.

Figure 11.11: *Represents the variation of anisotropic factor* Δ *with radius* r *for different values of* ξ *of* $RXJ1856.5-3754$.

$Fig-90$

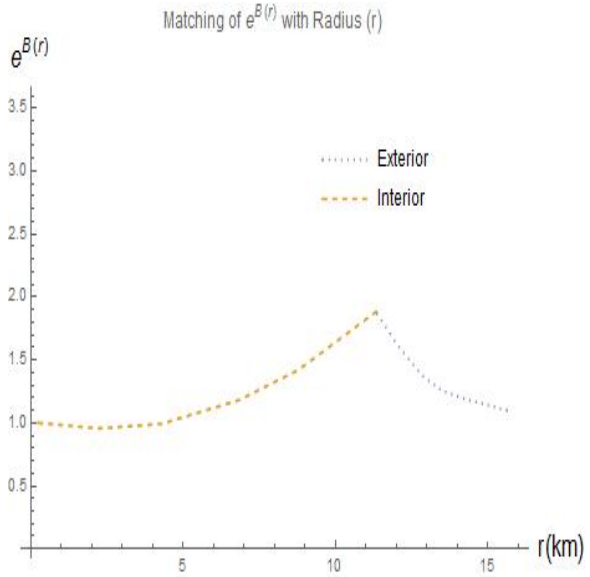

$Fig-91$

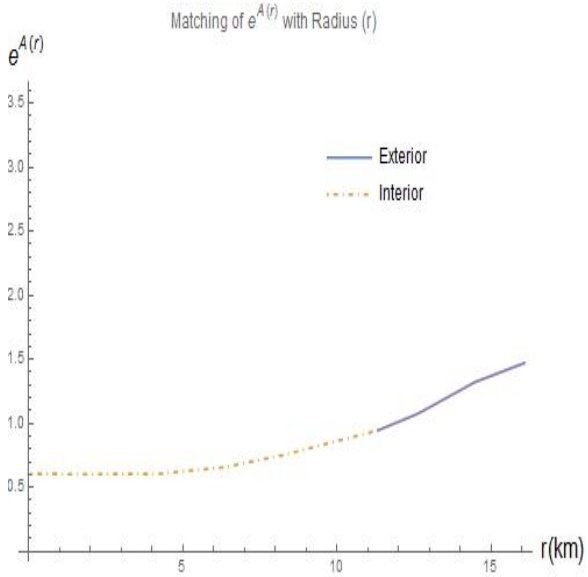

Figure 11.12: *Represents the matching condition of the metric potential* $e^{B(r)}$ *with radius* r *for the isolated compact star* $RXJ1856.5-3754$.

Figure 11.13: *Represents the matching condition of the metric potential* $e^{A(r)}$ *with radius* r *for the isolated compact star* $RXJ1856.5-3754$.

$Fig-92$

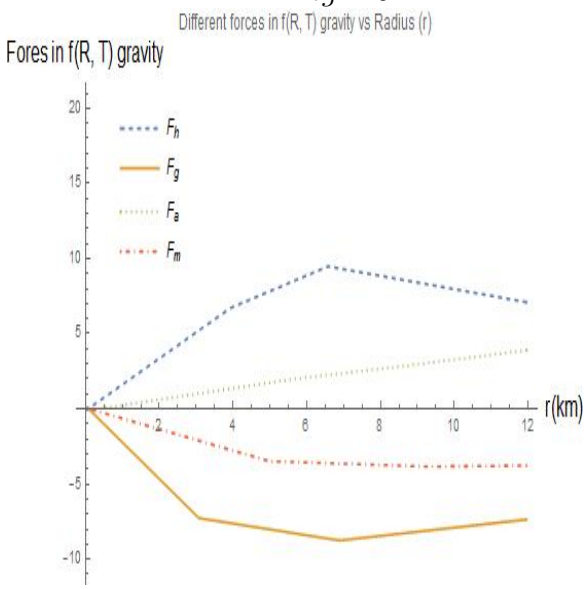

Figure 11.14: *Represents the various forces of the modified TOV equation with radius* r *for the isolated compact star* $RXJ1856.5-3754$.

11.1.6 Discussions and Conclusion

In this work, we have practically modeled the isolated compact star $RXJ1856.5-3754$ in the background of $f(R,T)$ modified gravity. We have introduced physically reasonable Tolman-Kuchowicz ansatz for the metric potentials. The metric potentials are singularity free and inside the boundary, they are continuous. Again, the metric potentials are also independent of coupling constant ξ. We have also argued the consideration of the equation of state $p+\rho=0$ by most researchers during construction of electromagnetic mass models. In lieu of choosing this type of EoS, in this present work we have adopted a modified Chaplygin gas model EoS. Our present model has been tested through rigorous regularity, stability and causality conditions which clearly revealed the impact of coupling constant ξ and anisotropic fluid (MCG). From the integration of field equations, the free constants raised are fixed by applying the proper boundary conditions. We have focused on the maximum attainable mass and radius by the isolated NS $RXJ1856.5-3754$ in modified gravity. The contribution of modified gravity on the isolated compact stars is also revealed. The outcomes of this present model agree with the various other investigations, which make our current model realistic and viable in the context of astronomical observations.

Moreover, the plausibility of the EoS of the anisotropic fluid MCG along with modified $f(R,T)$ gravity as we have chosen in our present model, is acceptable and also verified by the modified TOV equation. As all the forces that defines the modified TOV equation of a compact system, can produce a hydrodynamically equilibrium and spherically stable configuration of the isolated NS $RXJ1856.5-3754$, the viability of our model is also verified. The additional force comes into play due to matter-curvature coupling has a crucial effect to establish a stable compact structure, which is shown in the Fig 14. Further, as the metric potential at the boundary of the compact star coincides with each other, it also depicts the physical validity of the present model for the compact star $RXJ1856.5-3754$ clearly. The positive coupling parameter ξ, gives a more compact structure of a star as compared to the prediction of GR, which is also verified from different other astronomical observations. We have also got a valid range

of ξ from our study. Using Zeldivich condition [**?**], we can also discard the negative values of ξ for a physically valid compact star model.

The mass-radius curve clearly shows that $RXJ1856.5-3754$ possesses the mass around $1.11M_{\odot}$ with radius about 11.4 km under its stable equilibrium. The mass of this isolated compact star, $RXJ1856.5-3754$, increases when the value of the coupling parameter ξ increases progressively. This suggests that the star has the tendency to acquire some nearby interstellar medium through its strong gravitational field. The same trend of result was obtained by Astashenok et at. [377] in $f(R)$ gravity in case of a non-perturbative model. From our current working model we can conclude that in $f(R,T)$ gravity stars have larger masses as compared to their GR counterparts. As the matter-curvature coupling increases, the radius of the star starts decreasing and the star shrinks in size i.e., the compactness of the NS increases. The repulsive contributions of anisotropic force and the impacts of coupling constant ξ along with the new gravitational force arises due to $f(R,T)$ gravity helps the inner core of the star to stabilize. These forces creates a hydrodynamic equilibrium condition for the compact star and due to which it still manages to maintain its spherical equilibrium configuration under accelerated universe. From the graphical analysis section we already have got a clear idea about the nature and behavior of different parameters of $RXJ1856.5-3754$.

So, this current model is a singularity free model of the isolated and anisotropic NS $RXJ1856.5-3754$ in $f(R,T)$ modified gravity. The matter-curvature coupling plays a very crucial role in case of the evolution of the isolated compact stars. The results of this present working model have been analyzed graphically and analytically. The solutions of the field equations depend on the modified Chaplygin gas EoS, as it is very popular for modeling the compact stars in dark sectors by several researchers. Finally, it is also clear that by considering $\xi \to 0$, GR results in four dimensions can be recovered.

Part VII

SUMMARY AND OUTLOOK

"The highest Education is that which does not merely gives us information but that makes our life in harmony with all existence".

—-Rabindranath Tagore

CHAPTER 12

CONCLUSION AND FUTURE PROSPECTS

12.1 Final Remarks

12.1.1 Results and Discussion

12.1.1.1 Understanding Black Hole Thermodynamics under Dark Energy Dominated Universe and Evolution of the Properties of Neutron stars

In this thesis, it was my main focus to study the structural evolution of the massive compact objects (mainly various massive Neutron stars), through the accelerated phase of the Universe which is dominated by dark energy. At the same time I have also investigated the realistic EoS of the mysterious core matter of these massive relativistic compact objects through modeling the NSs in modified gravity. Various important properties of the NSs also have been studied w.r.t. the recent phase evolution of the Universe. I have also studied the thermodynamic evolution of the charged and rotating BHs using the quantum approach with the help of the Heisenberg uncertainty principle, in the dark energy regime. In this thesis, I have explored the theoretical and observational research on the structural characteristics and physical properties of the

Neutron stars.

In different chapters, we have already discussed in detail about the advantages of incorporating the modified Chaplygin gas and Quintessence field along with modified gravity for modeling the NSs. Using this unique approach we have got a more generalized way to study the properties of the NSs with a realistic EoS and also have got some unique features of the NSs as a part of our investigations. More interestingly, I am able to construct a new cosmological model in $f(R,T)$ gravity under the approach of unifying dark energy and dark matter, which can not only predict about the fate of our Universe quite successfully but also provides the value of Hubble parameter which is perfectly compatible with the observational results of recent accelerating Universe. Our investigation has proven that the massive NSs, beyond the limiting mass given by Tolman by using GR, can exists in nature and during the evolution process throughout their life they can possess more compact structure with stability.

Through the investigation we have got the clear idea of how the NSs gets a more compact structure while maintaining spherically stable and equilibrium configuration under the dark energy domination. We have shown the existence of physical anisotropy inside the compact objects and also discussed its effect on the stability of the NSs. Besides, the modified TOV equations that we have got from our model in modified gravity has shown how different forces come into play to maintain the stable equilibrium configuration of the massive NSs. On the other hand the existence of charge in the surface of the NSs creates a huge electric field at the surface of the stars but the exact effect of charge on the various properties of NSs are still under investigation. From our study, we can give the clue about the maximum attainable mass with lowest possible radius of the NSs during its evolution process. I have focused on the question: can we think of a systematic method to characterize the NS EoS by a lesser number of model independent parameters such that astrophysical surveys can be used to limit their values? This present work has demonstrated that the EoS can be well-modeled at very high nuclear density by using the concept of modified gravity as in $f(T)$ and $f(R,T)$ gravity theories. EoS with exotic matter as MCG and quintessence field required several parameters though the number of parameters can be waned by fixing the boundary

conditions between the regions of the compact stars.

So, throughout my entire research, basically I have looked for the suitable answers of some quarries related to the black holes and neutron stars. Precisely the questions are as follows :

• How do the black holes evolve through accelerated spacetime? Is it possible to investigate the thermodynamic evolution of the black hole parameters using quantum approach? How effective is the quantum approach to study the black hole evolution?

• How does the neutron star properties evolved through accelerated phase of the Universe? What is upper bound of the mass of the neutron stars? Is there any maximum mass limit for the neutron stars?

• Which theory is more suitable for studying the neutron stars over GR? What are the advantages of the modified gravity theories? How effective are these modified theories?

• Does the existence of massive neutron stars in the mass gap between $2.2-5.3M_{\odot}$ possible? If so, how can they achieve a spherically stable equilibrium configuration under such extreme conditions? How dark energy affects them?

• Is it possible to get a realistic and generalized EoS for the core matter of the neutron stars under extreme high density, pressure and temperature? Is there any new mechanism evolved inside the neutron stars which can justify the non-squeezability as its mass increases?

I have also got very strong support from various recent cosmological observations which gives potential to my entire investigations. The data from the detected gravitational wave, $GW190814$ indicates that there exists a super massive neutron star of mass about $2.68M_{\odot}$. Further the gravitational wave, $GW230529$ confirms the existence of the massive compact object in the mass gap between $2.5-4.5M_{\odot}$. Besides, from the NICER data the existence of the pulsar PSR$J0952-0607$ with mass about 2.35 ± 0.17 has been confirmed by the scientists. Even the observational data from NICER of two different pulsars PSR$J0030+0451$ and PSR$J0740+6020$ has given surprising evidence against the more squeezable nature of the neutron stars. According to NICER data, these two pulsars have almost the same size irrespective of their different mass. The

later pulsar is more massive than the former but still not more compact (squeezed) in size w.r.t. the former. This phenomenon indicates the existence of a new mechanism inside the neutron stars which I can explain from my compact star models with the presence of anisotropy and dark energy inside the core of the neutron stars.

12.1.1.2 Impacts of Modified gravity to Understand the Present Universe

At the same time our constructed cosmological model in the context of $f(R,T)$ modified gravity helps to understand the accelerated phase of the Universe profoundly through the evolution of the Hubble parameter under dark energy domination. Further, from the value of the deceleration parameter, we can even predict about the future of this accelerating Universe. Further, the study of the evolution of the thermodynamic parameters of the black holes through the quantum corrections give a deep insight on the evolution of black holes and their properties under accelerated expansion of the Universe.

12.1.1.3 Structural Characteristics of the Neutron Stars

I have considered my goal to construct a reformed framework planned to investigate the NS structure, its physical properties and the EoS of the core material it contains. Throughout the thesis, I have also tried to design a closed system with logical structure and physically viable EoS. I have started with realizing the NS structure by resolving the modified Einstein's field equations combined with the specific choice of the EoS, and closing with a minute profile of various properties of neutron stars by using modified gravity theories. In this way, I have investigated the main features of the NSs and got the results in good agreement to other equivalent and sophisticated astronomical observations. This study, the addition of further exotic equations of state considering additional properties and phase transitions are also investigated by defining the EoS through some the of pressure-density relationship or parameterizations by incorporating the presence of modified Chaplygin gas.

The properties of different types of neutron stars in various spacetime geometry for any given structural model, i.e., choice of EoS by using the different modified gravity

theories. This is concentrated into chapters 8 to 11. The structure of the NSs can be determined by the properties of its constituents, which includes electrons, protons, neutrons and also possibly other exotic particles. The central region of these compact stars is believed to be composed of strongly bounded neutrons. The outer region of the neutron stars may contain a mixture of electrons, protons and other particles. On the other hand, the EoS of the matter inside the neutron stars is a crucial parameter that determines the structure and properties of the neutron stars. The EoS actually describes the relationship between density, pressure and temperature of the matter inside the compact stars. The theoretical EoS of the neutron star matter has been constructed using a variety of models, some of which are investigated in this thesis as well including effective field theories.

The observations on the masses and radii of the NSs have provided important confinements on EoS of the core matter of the star. Mass of the NSs can be measured using pulsar timing observations and the radii can be inferred from the analysis of X-ray spectra emitted from their surfaces. Recent observations have also provided strong evidence for relatively large neutron star radii, which suggests that the EoS of the matter of the NSs may be relatively soft.

12.1.1.4 Physical Properties the Neutron Stars

Astrophysicists are very much interested about a number of properties of the neutron stars including their surface temperature, rotational properties and magnetic field strength. The surface temperature of the star is determined by the balance between the energy emitted by the star and the energy produced in its core through nuclear reactions. The magnetic field of the neutron stars can reach upto 10^{15} G. This immensely strong magnetic field can produce a lot of significant phenomena including pulsar emission, magnetic flares and particle acceleration. The rotational energy of the neutron stars can be tapped into by accreting matter from a companion star, producing X-ray emission and other observable phenomena.

12.1.2 Future Prospects

The neutron stars are fascinating and mysterious objects with unique structural characteristics and physical properties. Theoretical models and observational investigations have provided a deep and significant insight into the nature and various properties of these compact objects including their internal composition, EoS of core matter, magnetic field strength and rotational properties. These studies on NSs continue to be a vibrant area of research, with ongoing efforts to refine theoretical models and develop new observational techniques. Recent advancement of gravitational wave astronomy has opened up the new way for studying the neutron stars mergers and their aftermaths.

The investigated models in this thesis can construct a fully realistic NS with all its exotic properties and exact EoS of the core matter. These models give the idea of constructing a general and realistic EoS of the core matter. At the same time, the non-squeezable nature of the NSs with the increase in its mass, can also be justified from these models. A few general features like powerful magnetic fields as well as electric field strengths at the surface are still needed to model which can reveal the exciting observed properties of the pulsars. Rapid neutrino emission during the cooling of the neutron star may also occur due to the presence of exotic particles inside the core such as mesons at very high nuclear density. The atmosphere surrounding the neutron star is thick enough to absorb the X-rays. The higher energy photons coming from deeper layers may have the possibility to be absorbed by the atmosphere. So, to determine the surface temperature of the star through spectrum analysis is not so reliable. The observed spectra from the neutron stars which almost fits with the blackbody spectra, yield surface temperatures sometimes 2 times higher than the actual value of it. The presence of a very strong magnetic field may also have a crucial effect on the ejected X-ray spectra from the NSs.

In our Universe, accreting compact objects have offered us the unique insights into the core astrophysical ideas of the last stages of stellar evolution and to culture the physics of matter at extreme environment or physical conditions. Till now, we have discovered but not fully understood the thermonuclear flashes from the surface

and periodic pulsation in X-rays emitted by the rapidly spinning neutron stars. The mass measurement process of the neutron stars is still under question but provides the strongest evidence for the existence of black holes in the Universe. A compact star can also accrete matter from a companion star if the companion star is losing its mass in the form of a stellar wind and does not fill its Roche Lobe. The companion star should have the mass $\geq 10M_{\odot}$ in order to drive a strong stellar wind.

The NSs can be excited by a small perturbation that oscillates into a set of normal modes. Again, these normal modes can also be excited during various astrophysical processes, such as the formation of a proto-NS, collapse of a compact binary NS system. The strong oscillations can be found from the hot and differentially rotating proto-NSs. Further, if there is major rearrangements in the internal structure (during giant flares of magnetars) of the NSs or during the glitches we can also get the oscillations of excited normal modes. These coherent vibrations in turn becomes the significant source of gravitational radiation. As for examples during core collapse and bounce the consecutive compressions and expansions of the core density induces oscillations in the new-born proto-NS. During this process, the non-linear coupling between the normal modes of the proto-NS produces the GWs. The computation of these normal modes of a NS is quite complicated. It involves both perturbations of the metric around and inside the NS. Moreover, in also involves the perturbations of the variables of the core matter of the NSs.

Further, during the inspiral phase of two NSs in a binary system, NS deformation can occur by the tidal gravitational field of the companion star. Interestingly, this tidal deformability also depends on the EoS of the interior of the NS. This in turn affects the phase of the GW signal in such a way that we are able to detect it through advanced interferometers, uncovered the possibility of obtaining trace on the EoS of the NS. This leading milestone when the LIGO/Virgo detectors observed the GW signal named $GW170817$ from a the coalescence of NS-NS binary. A large number of telescopes also identified the total transient electromagnetic spectrum that strengthened the association with a NS-NS merger. This sensational event then marked the beginning of the era of multi-messenger astrophysics.

12.1.3 Conclusion

The study of neutron stars is a rapidly evolving field of research that combines theoretical modeling with astronomical observations across a range of wavelengths. Advances in our understanding of the structural characteristics and physical properties of the neutron stars will continue to be driven by a combination of theoretical and observational research. My aim is to construct a massive compact stellar object and study its physical consequences in the framework of modified gravity theories as an alternative to GR.

As an alternative to GR, the modified gravity theories play an essential role to understand the basic physics of the compact objects like the BHs and NSs. For the NSs, these theories basically switch the TOV equations and therefore various astrophysical properties are also altered. From this thesis one can easily understand the very prominent impact of anisotropy in case of NSs under extreme high pressure and density. My work reveals that presence of anisotropy causes effective changes in the main characteristics of the NSs. The evolved repulsive force, behaves against the attractive gravitational force, due to anisotropy at the core of these stars leads to achieve a more compact (high mass) but stable equilibrium configuration. The non-squeezable nature of the neutron stars with the increase in its mass, can also be justified due to the presence of anisotropy inside the neutron stars. The major finding of my research establishes the fact that the massive NSs in the lower mass gap between $2.1 - 5.3 M_{\odot}$ can exist in nature. The gravitational wave detection of two merging compact stars already predicts the massive NSs of mass about $2.68 M_{\odot}$, which is far beyond the predicted maximum mass of the NSs as $2.1 M_{\odot}$. At the same time, the generalized and realistic EoS, of the core nuclear matter of the NSs, which I have constructed during my work, provides the core matter density compatible with nuclear saturation density and a linear EoS for the massive NSs.

So, ultimately I can say that my thesis will help to understand the structural characteristics and physical properties of the neutron stars more in the background of modified gravity theories as an alternative to GR and also under the dark energy

domination phase of the Universe. Also the investigations on black holes clearly reveals their thermodynamic evolution process under accelerated Universe. This study will not only deepen our knowledge of these massive relativistic compact objects, their evolution process but also provide insights into fundamental physics and the evolution of the Universe as a whole. Further, the cosmological model in the background of the modified gravity gives the significant interpretation about the accelerated Universe and its fate.

APPENDICES

Appendix A

ABBREVIATIONS

CG.....Chaplygin gas
CMB.....Cosmic Microwave Background
GCG.....Generalised Chaplygin gas
MCG.....Modified Chaplygin gas
NS.....Neutron Star
EMCG.....Extended modified Chaplygin gas
TG.....Teleparallel Gravity
TEGR.....Teleparallel Equivalent of General Relativity
QMC.....Quantum Monte Carlo
DoF.....Degrees of Freedom
DE.....Dark Energy
DM.....Dark Matter
NGR.....New General Relativity
wrt.....with respect to
FLRW.....FriedmannLemaîtreRobertsonWalker
LHS.....Left hand side
STEGR.....Symmetric Teleparallel Equivalent of General Relativity
HDE.....Holographic Dark Energy
PlDE.....Pilgrim Dark Energy
HST.....Hubble Space Telescope
JWST.....James Web Space Telescope
CMASS.....Constant stellar MASS
MCMC.....Markov chain Monte Carlo
BINGO.....Baryon acoustic oscillation In Neutral Gas Observations
BAO.....Baryonic Acoustic Oscillations

Appendix B

CONSTANTS and VALUES

The numerical values of various constants with units, which are used during the work are tabulated in below Tables $B.1$ and $B.2$.

Table B.1 : Natural constants (in cgs unit) as used in the work.

Constant	Explanation	Applied Value
G	Gravitational constant	$6.67430 \times 10^{-8} cm^3\ g^{-1} s^{-2}$
c	Speed of light in vacuum	$2.99792 \times 10^{10} cm\ s^{-1}$
$\hbar$	Reduced Planck constant	$1.05457 \times 10^{-27} erg\ s$
m_u	Muon mass	$1.88353 \times 10^{-25} g$
m_e	Electron mass	$9.10938 \times 10^{-28} g$
m_p	Proton mass	$1.67262 \times 10^{-24} g$
m_n	Neutron mass	$1.67493 \times 10^{-24} g$
k_B	Boltzmann's constant	$1.38065 \times 10^{-16} erg K^{-1}$
σ_{SB}	Stefan-Boltzmann's constant	$5.67037 \times 10^{-5} erg\ cm^{-2} K^{-2} s^{-1}$

Table B.2 : Auxiliary constants (in cgs unit) as used in the work.

Constant	Explanation	Applied Value
ρ_{nuc}	Nuclear density	$2.80 \times 10^{14} g\ cm^{-3}$
n_0	Nuclear saturation QMC	$1.60 \times 10^{38} cm^{-3}$
$M_\odot$	Solar mass	$1.98841 \times 10^{33} g$
$R_\odot$	Solar radius	$6.9570 \times 10^{10} cm$
$R_{S\odot}$	Schwarzschild radius	$2.95325 \times 10^{5} cm$

BIBLIOGRAPHY

REFERENCES

[1] R. A. Hulse and J. H. Taylor Jr., "Discovery of a pulsar in a binary system", *Astrophys. J.* **195**, L51-L53 (1975).

[2] M. Burgay et al., "An increased estimate of the merger rate of double neutron stars from observations of a highly relativistic system", *Nature* **426**, 531-533 (2003).

[3] W. Baade and F. Zwicky, "On Super-Novae", *Proc. Nat. Acad. Sci.* **20**(5), 254-259 (1934).

[4] R. C. Tolman, "Static Solutions of Einstein's Field Equations for Spheres of Fluid", *Phys. Rev.* **55**, 364 (1939).

[5] F. Pacini, "Energy Emission from a Neutron Star", *Nature* **216**, 567-568 (1967).

[6] A. Hewish et al.,"Observation of a Rapidly Pulsating Radio Source", *Nature* **217**, 709-713 (1968).

[7] T. Gold, "Rotating Neutron stars as the Origin of the Pulsating Radio sources", *Nature* **218**, 731-732 (1968).

[8] V. Kaspi et al., "Isolated neutron stars, in Compact stellar X-ray Sources", **249**, Cambridge University Press, (2006).

[9] B. Link et al., "Pulsar glitches as probes of neutron star interiors", *Nature* **359**(6396), 616-618 (1992).

[10] R. Giacconi et al., "Evidence for X Rays From Sources Outside the Solar System", *Phys. Rev. Lett.* **9**, 439 (1962).

[11] C. Will, "The Confrontation between General Relativity and Experiment", *Living Re. Rel.* **9**, 3 (2005).

[12] A. Joyce et al., "Beyond the Cosmological Standard Model", *Phys. Rep* **568**, 1-98 (2015).

[13] C. Misner, K. Thorne and J. Wheeler, "Gravitation", 1973.

[14] E. Komatsu et al., "Seven-Year Wilkinson Microwave Anisotropy Probe (WMAP) Observations: Cosmological Interpretations", *Astrophys. J.* **192**, 18 (2011).

[15] P. Bernardis et al., "A Flat Universe from High-Resolution Maps of the Cosmic Microwave Background Radiation", *Nature* **404**, 955-959, (2000).

[16] N. Aghanim et al., "Plank 2018 results. VI. Cosmological Parameters", *Astrophys. Astron.* **A6**, 641 (2020).

[17] M. Betoule et al., "Improved cosmological constraints from a joint analysis of the SDSS-II and SNLS supernova samples ", *Astrophys. Astron.* **A22**, 568 (2014).

[18] S. Weinberg, "The cosmological constant problem", *Rev. Mod. Phys.* **61**, 1 (1989).

[19] K. Aoki et al., "Massive Graviton Geons", *Phys. Rev.* **D97**, 044005 (2018).

[20] K. Aoki and S. Mukohyama, "Massive gravitons as dark matter and gravitational waves", *Phys. Rev.* **D94**, 024001 (2016).

[21] M. Bandyopadhyay and R. Biswas, "Impacts of modified Chaplygin gas on super massive neutron stars embedded in quintessence field with $f(T)$ gravity", *Int. J. Mod. Phys. D* **32**(3), 235006 (2023).

[22] M. Bandyopadhyay and R. Biswas, "Repulsive gravitational force and quintessence field in $f(T)$ gravity: How anisotropic compact stars in strong energy condition behave", *Mod. Phys. Lett. A* **36**(7), 2150044 (2021).

[23] M. Bandyopadhyay and R. Biswas, "Nuclear Matter Equation of State and Stability of Charged Compact Stars Embedded in $f(T)$ Modified Gravity, under Cosmic Acceleration", *Int. J. Geom. Methods Mod. Phys.* (2023).

[24] M. Bandyopadhyay and R. Biswas, "Investigating the Equation of state, Stability and Mass-Radius relationship of Anisotropic and Massive Neutron Stars embedded in $f(R,T)$ modified gravity", *Int. J. Geom. Methods Mod. Phys.* (2023).

[25] M. Bandyopadhyay and R. Biswas, "Repulsive gravitational force and quintessence field in $f(T)$ gravity: How anisotropic compact stars in strong energy cndition behave", *Mod. Phys. Lett. A* **36**(7), 2150044 (2021).

[26] M. Bandyopadhyay and R. Biswas, "Impacts of $f(R,T)$ Modified gravity on Mass-Radius relation and Stability of an Isolated compact star Embedded in Modified Chaplygin Gas under Tolman-Kuchowicz Spacetime", *Eur. Phys. J. C* (2023).

[27] F. Reif, "Fundamentals of statistical and thermal physics", *McGraw-Hill*, (1965).

[28] N. K. Glendenning, "Compact stars: nuclear physics, particle physics, and general relativity", *Springer-Verlag, New York*, (2000).

[29] W. de Boer, "Grand Unification theories and supersymmetry in particle physics and cosmology", *arXiv: hep-th/9402266* **33**, 201-302 (1994).

[30] A. Einstein, "The foundation of General theory of Relativity", *Annalen der Physik* **354**, 769 (1916).

[31] R. Penrose, "The Road to Reality: a Complete Guide to the Laws of the Universe", *Knopf.* (2005).

[32] K. Schwarzschild, "Uber das Gravitationsfeld eines Massenpunktes nach der Einsteinschen Theorie", *Sitzungsberichte der KÖniglich Preussischen Akademie der Wissenschaften* **Vol. I**, 189-196 (1916).

[33] S. Chandrasekhar, "The maximum mass of ideal white dwarf", *Astrophys. J.* **74**, 81-82 (1931).

[34] M. Kilic et al., "The Lowest Mass White Dwarf", *Astrophys. J.* **660**, 2 (2007).

[35] A. A. Penzias and R. W. Wilson, "A measurement of excess antenna temperature at 4080 Me/s", *Astrophys. J.* **142**, 419-421 (1965).

[36] H. V. Pelris et al., "First Year Wilkinson Microwave anisotropy Probe (WMAP) Observations: Implications for Inflations", *Astron. J. suppl* **148**, 213 (2003).

[37] S. Weinberg, "The cosmological constant problem", *Rev. Mod. Phys.* **61**, 1 (1989).

[38] S. M. Carroll, "The Cosmological constant", *Living Rev. Rel.* **4**, 1 (2001).

[39] B. Ratra and P. J. E. Peebles, "cosmological consequences of a rolling homogenous scalar field", *Phys. Rev. D* **37**, 3406 (1988).

[40] C. Wetterich, "Cosmology and the fate of dilatation symmetry", *Nucl. Phys. B* **302**, 688 (1988).

[41] A. Riess et al., "Observational Evidence from Supernovae for Accelerating Universe and a Cosmological Constant", *Astron J.* **116**, 19-1038 (1998).

[42] A. Kamenhchik et al., "An alternative to quintessence", *Phys. Lett. B* 511, 265 (2011).

[43] V. Gorini et al., "Proceedings, 10th Marcel Grossmann Meeting on Recent Developments in Theoretical and Experimental General Relativity", *Gravitation and Relativistic Field Theories, Brazil*, (2003).

[44] S. Perlmutter et al., "Cosmology from Type Ia Supernovae", *Bull. Am. Astron. Soc.* **29**, 1351 (1999).

[45] T. Lacroix et al., "A unique probe of dark matter in the core of M87 with Event Horizon Telescope", *Physical Rev. D* **96**, 063008 (2017).

[46] A. Abramowski et al., "Constraints on an Annihilation Signal from a core of constant Dark matter Density around the Milky Way Center with H. E. S. S.", *Phys. Rev. Lett.* **114**, 081301 (2015).

[47] J. Silk and H. Bioemen, "A gamma-ray constraints on the nature of dark matter", *Astrophys. J.* **313**, L47-L51 (1987).

[48] R. Jackiw, "", *A particle Field Theorist's Lectures on Supersymmetric, Non Abelian Fluid Mechanics and d-Branes*, *A series of six lectures given at the centre de Researches Mathematiques in Montreal*, (2000).

[49] M. C. Bento, O. Bertolami and A. A. Sen, "Generalized Chaplygin gas, accelerated expansion and dark energy matter unification", *Phys. Rev. D* **66**, 043507 (2002).

[50] M. Makler et al., "Constraints on the generalized Chaplygin gas from supernovae observations", *Phys. Lett. B* **555**, 1 (2003).

[51] L. Amendola, "Coupled Quintessence", *Phys. Rev. D* **62**, 043511 (2000).

[52] H. B. Benaoum, "Accelerated Universe from Modified Chaplygin gas and Tachyonic Fluid", *Proceedings* (2002).

[53] B. Pourhassan and E. O. Kahaya, "Extended Chaplygin gas Model", *Results in Physics* **4**, 101 (2014).

[54] B. P. Abott et al., "Observation of Gravitational Waves from a Binary Black Hole Merger", *Phys. Rev. Lett.* **116**, 061102 (2016).

[55] S. L. Glashow, "Partial symmetries of weak interactions", *Nucl. Phys.* **22**, 57988 (1961).

[56] S. Weinberg, "A model of leptons", *Phys. Rev. Lett.* **19**, 12646 (1967).

[57] V. C. Rubin and Ford W. K. Ford Jr., "Rotation of the Andromeda nebula from a spectroscopic survey of emission regions", *Astrophys. J.* **159**, 379403 (1970).

[58] J. Silk et al., "Particle Dark Matter: Observations, Models and Searches", *Cambridge: Cambridge University Press*, (2010).

[59] V. Mukhanov, "Physical Foundations of Cosmology", *Cambridge: Cambridge University Press*, (2005).

[60] A. D. Linde, "A new inflationary universe scenario: a possible solution of the horizon, flatness, homogeneity, isotropy and primordial monopole problems", *Phys. Lett. B* **108**, 38993 (1982).

[61] C. A. Sporea, A. Borowiec and A. Wojnar, "Galaxy rotation curves via conformal factors", *Eur. Phys. J. C* **78**, 308 (2018).

[62] P. D. Mannheim and J. G. OBrien, "Galactic rotation curves in conformal gravity", *J. Phys.: Conf. Ser.* **437**, 012002 (2013).

[63] A. G. Riess et al., "Observational evidence from supernovae for an accelerating universe and a cosmological constant", *Astron. J.* **116**, 100938 (1998).

[64] S. Weinberg, "The cosmological constant problem", *Rev. Mod. Phys.* **61**, 123 (1989).

[65] P. Bull et al., "Beyond CDM: problems, solutions and the road ahead", *Phys. Dark Universe***12**, 569(2016).

[66] S. Capozziello and M. De Laurentis, "Extended theories of gravity", *Phys. Rep.* **509**, 167 (2011).

[67] R. Aldrovandi and J. Pereira, "An Introduction to Geometrical Physics" *Singapore: World Scientific* (1995).

[68] R. Aldrovandi and J. G. Pereira, "Teleparallel Gravity vol 173" *Dordrecht: Springer* (2013).

[69] J. W. Maluf, "The teleparallel equivalent of general relativity", *Ann. Phys. Lpz.* **525**, 33957 (2013)

.

[70] K. Hayashi and T. Shirafuji, "New general relativity", *Phys. Rev. D* **19** 352453 (1979).

[71] Ferraro R and F. Fiorini, "Modified teleparallel gravity: inflation without inflation", *Phys. Rev. D* **75** 08403 (2007).

[72] E. V. Linder, "Einsteins other gravity and the acceleration of the universe", *Phys. Rev. D* **81** 127301 (2010).

[73] M. Krššák et al., "Teleparallel theories of gravity: illuminating a fully invariant approach", *Class. Quantum Grav.* **36** 183001 (2019).

[74] M. Krššák, and E. N. Saridakis, "The covariant formulation of $f(T)$ gravity", *Class. Quantum Grav.* **33** 115009 (2016).

[75] Y. F. Cai et al., "$f(T)$ teleparallel gravity and cosmology", *Rep. Prog. Phys.* **79**, 106901 (2016).

[76] C.M. Will, "Theory and Experiment in Gravitational Physics", *Cambridge University Press, Cambridge, UK* **2nd ed.**, (1993).

[77] S. Capozziello and G. Lambiase, "Open problems in gravitational physics", *New Adv. in Physics* **7**, 13 (2013).

[78] P. Chatterjee and B. Bhattacharya, "Space-time torsion, broken Lorentz symmetry and inflation in the early universe", *Mod. Phys. Lett. A* **8**, 2249 (1993).

[79] A. J. Fennelly, J. C. Bradas and L. L. Smalley, "Inflation in Einstein-cartan Theory With Energy Momentum Tensor With Spin", *Phys. Lett. A* **129**, 195 (1988).

[80] C. Wolf, "The effect of spin generated torsion on the early universe's evolution", *Gen. Rel. Grav.* **27**, 1031 (1995).

[81] I. L. Buchbinder, S. D. Odintsov and I. L. Shapiro, "Nonsingular Cosmological Model With Torsion Induced By Vacuum Quantum Effects", *Phys. Lett. B* **162**, 92 (1985).

[82] L. C. Garcia de Andrade, "Space-time defects: Torsion walls", *Mod. Phys. Lett. A* **12**, 2005 (1997).

[83] P. S. Letelier, "Space-time defects: Torsion loops", *Class. Quant. Grav.* **12**, 2221 (1995).

[84] L. Fabbri and S. Vignolo, "A modified theory of gravity with torsion and its applications to cosmology and particle physics", *Int. J. Theor. Phys.* **51**, 3186 (2012).

[85] S. Capozziello and C. Stornaiolo, "Scalar perturbations in a cosmological model with torsion", *Nuovo Cim. B* **113**, 879 (1998).

[86] F. W. Hehl et al., "General Relativity with Spin and Torsion: Foundations and Prospects", *Rev. Mod. Phys.* **48**, 393 (1976).

[87] C. W. Misner, K. S. Thorne and J. A. Wheeler, "Gravitation", *San Francisco*, 1279p (1973).

[88] M. Bandyopadhyay and R. Biswas, "Repulsive gravitational force and quintessence field in $f(T)$ gravity: How anisotropic compact stars in strong energy condition behave", *Mod. Phys. Lett. A* **36**(7), 2150044 (2021).

[89] O. Bertolami, J. Paramos, and S. Turyshev, "In Lasers, Clocks, and Drag-Free: Technologies for Future Exploration in Space and Tests of Gravity", *edited by H. Dittus et al. (Springer-Verlag, Berlin*, pp. 2767 (2006).

[90] O. Bertolami, F. Gil Pedro, and M. Le Delliou, *Phys. Lett. B* **654**, 165 (2007).

[91] A. G. Riess et al., *Astron. J.* **607**, 665 (2004).

[92] M. Tegmark et al., *Phys. Rev. D* **69**, 103501 (2004).

[93] D. N. Spergel et al., *Astrophys. J. Suppl. Ser.* **170**, 377 (2007).

[94] S. Chakraborty et. al., *Eur. Phys. J. C* **72**, 2101 (2012).

[95] J. B. Lu et al., *High Energy Phys. Lett. B* 071, 02 (2015).

[96] H. Benaoum, *Adv. High Energy Phys.* **2012** 357802 (2012).

[97] H. Benaoum, *Universe* **8**(7), 340 (2012).

[98] S. Nojiri, S. D. Odintsov, *Phys. Lett. B* **657**, 238-245 (2007).

[99] S. Nojiri, S. D. Odintsov, *Phys. Rev. D* **77**, 026007 (2008).

[100] G. Cognalo et al., *Phys. Rev. D* **77**, 046009 (2008).

[101] T. P. Sotiriou, V. Faraoni, *Rev. Mod. Phys.* **82**, 451-497 (2010).

[102] E. Elizalde et al., *Phys. Rev. D* **83**, 086006 (2011).

[103] S. Nojiri, S. D. Odintsov, *Prog. Theor. Phys. Suppl.* **190**, 155-178 (2011).

[104] T. Harko et al., *Phys. Rev. D* **84**, 4020 (2011).

[105] S. Chakraborty, *Gen. Rel. Grav.* **45**, 2039-2052 (2013).

[106] G. Sardar et al., *Eur. Phys. J. C* **83**, 41 (2023).

[107] T. Padmanabhan, *Phys. Rep.* **380**(5-6), 235-320 (2003).

[108] P. J. E. Peebles, B. Ratra, *Rev. Mod. Phys.* **75**, 559-606 (2003).

[109] S. Weinberg, *Rev. Mod. Phys.* **61**, 1-23 (1989).

[110] F. K. Anagnostopoulos et al., Phys. Lett. B **822**, 136634 (2021).

[111] L. D. Landau, E. M. Lifschits, *The Classical Theory of Fields, Course of Theoritical Physics, vol. 2* (Pergamon Press, Oxford, 1975).

[112] T. Brinckmann, J. Lesgourgues, *Phys. Dark. Univ.* **24**, 100260 (2019).

[113] D. M. Scolnic et al., *Astrophys. J.* **859**(2), 101 (2018).

[114] S. Alam et al., *Mont. Not. R. Astron. Soc.* **470**(3), 2617-2652 (2017).

[115] A. J. Ross et al., *Mont. Not. R. Astron. Soc.* **449**(1), 835-847 (2015).

[116] A. G. Riess et al., *Astrophys. J.* **730**(2), 119 (2011).

[117] N. Aghanim et al., *Astron. Astrphys.* **641**, A6 (2020).

[118] N. c, *Astrophys. J.* **716**(1), 85 (2012).

[119] M. Betoule et al., *Astron. Astrphys.* **568**, A22 (2014).

[120] R. Jimenez, A. Loeb, *Astrophys. J.* **573**(1), 37 (2002).

[121] H. Akaike, *IEEE Trans. Autum. Control.* **19**(6), 716-723 (1974).

[122] K. P. Burnham, D. R. Anderson, *Model Selection and Multimodel Inference : A Practical Information-Theoritic approach* (Springer, New York, 2007).

[123] K. P. Burnham, D. R. Anderson, *Sociol. Methods Res.* **33**(2), 261-304 (2004).

[124] A. R. Liddle, *Mon. Not. Roy. Astron. Soc.* **377**, L74-l78 (2007).

[125] E. E. O. Ishida et al., *J. Cosmol. Astropart. Phys.* 1203, 027 (2012).

[126] J. M. Bardeen, B. Carter, S. W. Hawking, *Commun. Math. Phys.* **31**, 161 (1973).

[127] M. Bandyopadhyay, R. Biswas, *Mod. Phys. Lett. A* **36**, 7, 2150044 (2021).

[128] J. D. Bakenstein, *Phys. Rev. D* **7**, 2333 (1973).

[129] S. W. Hawking, *Nature* **30-31**, 248 (1974).

[130] D. Bak, S. J. Rey, *Clss. Quant. Grav.* **17**, L1 (2000).

[131] B. Pourhassan, K. Kokabi, *Can. J. Phys.* **96**, 262 (2018).

[132] S. Upadhyay, S. H. Hendi, S. Panahiyan, B. E. Panah, *Prog. Theor. Exper. Phys.* **093E01**, (2018).

[133] M. Dehghani, *Phys. Lett. B* **793**, 234 (2019).

[134] B. Pourhassan, H. Farahani, S. Upadhyay, *Int. J. Mod. Phys. A* **34**, 1950158 (2019).

[135] A. Dabholkar, J. Gomes, S. Murthy, **JHEP 074**, 1503 (2015).

[136] J. Sadeghi, B. Pourhassan, M. Rostami, *Phys. Rev. D* **94**, 064006 (2016).

[137] B. Pourhassan, M. Faizal, S. A. Ketabi, *Int. J. Mod. Phys. D* **27**, 1850118 (2018).

[138] B. Pourhassan, S. Chougule, S. Dey, M. Faizal, *Clss. Quant. Grav.* **37**, 135004 (2020).

[139] B. Pourhassan, M. Faizal, S. Capozziello, *Ann. Phys.* **108**, 377 (2017).

[140] S. Chougule, S. Dey, B. Pourhassan, M. Faizal, *Eur. Phys. J. C* **78**, 685 (2018).

[141] B. Pourhassan, *Eur. Phys. J. C* **79**, 740 (2019).

[142] A. Iorio, G. Lambiase, P. Pais, F. Scardigli, *Phys. Rev. D* **101**, 105002 (2020).

[143] A. Chatterjee, A. Ghosh, *Phys. Rev. Lett* **125**, 041302 (2020).

[144] V. V. Kiselev, *Class. Quantum Gravity* **20**, 1187 (2003).

[145] A. G. Riess et al., *Astron J.* **116**, 1009 (1998).

[146] M. Bandyopadhyay, R. Biswas, *Int. J. Mod. Phys. D* **32**, 3 (2023).

[147] P. J. Steinhardt, L. Wang, I. Zlatev, *Phys. Rev. D* **59**, 123504 (1999).

[148] I. Zlatev, L. Wang, P. J. Steinhardt, *Phys. Rev. Lett.* **82**, 896 (1999).

[149] A. Mandal, R. Biswas, *Astrophys. Space Sci.* **357**, 8 (2015).

[150] R. Biswas, S. Chakraborty, *Astrophys. Space Sci.* **326(1)**, 39 (2010).

[151] S. W. Hawking, *Commun. Math. Phys.* **43**, 199 (1975).

[152] R. B. Mann, S. L. Solodukhin, *Nucl. Phys. B* **523**, 293 (1998).

[153] H. S. Snyder, *Phys. Rev.* **71**, 38 (1947).

[154] H. S. Snyder, *Phys. Rev.* **72**, 68 (1947).

[155] R. Dijkgraaf, E. P. Verlinde, H. P. Verlinde, *Nucl. Phys. B* **484**, 543 (1997).

[156] H. Shabidi, W. S. Chung, *Mod. Phys. Lett. A* **35**, 2050018 (2019).

[157] K. Nouicer, *Phys. Lett. B* **646**, 63 (2007).

[158] M. Maggiore, *Phy. Lett. B* **304**, 65 (1993).

[159] F. Scardigli, *Phys. Lett. B* **452**, 39-44 (1999).

[160] R. Zhao, Y. Q. Wu, L. C. Zhang, *Class. Quant. Grav.* **20**, 4885 (2003).

[161] B. Majumder, *Gen. Rel. Grav.* **11**, 2403 (2013).

[162] H. Casini, M. Huerta, R. C. Myers, *JHEP*, **1105**, 036 (2011).

[163] M. J. Magán, D. Melnikov, M. R. O. Silva, *JHEP* **1411**, 069 (2014).

[164] R. K. Kaul, P. Majumder, Phys. Rev. Lett. **84**, 5255 (2000).

[165] T. Kanazawa, G. Lambiase, G. Vilasi, A. Yoshioka, *Eur. Phys. J. C* **79**, 95 (2019).

[166] S. Das et. al., *Phys. Lett. B* **824**, 136841 (2022).

[167] G. G. L. Nashed, *Mod. Phys. Lett. A* **22**, 1047-1056 (2007).

[168] A. Brazier et al., *Astrophys. J.* **859**, 47 (2018).

[169] G. Baym, S. Furusawa, T. Hatsuda, T. Kojo and H. Togashi, *Astrophys. J.* **885**, 42 (2019).

[170] B. P. Abbott et at., *Phys. Rev. Lett.* **121**, no. 16, 161101 (2018).

[171] B. P. Abbott et at., *Phys. Rev. X* **9**, 011001 (2019).

[172] D. Radice, A. Perego, F. Zappa and S. Bernuzzi, *Astrophys. J.* **852**, L 29 (2018).

[173] L. Rezzolla, E. R. Most and L. R. Weih, *Astrophys. J.* **852**, L 25 (2018).

[174] D. D. Doneva et al., *Phys. Rev. D* **90**, 104021 (2014).

[175] G. Pappas and T. P. Stiriou, *Phys. Rev. D* **91**, 044011 (2015).

[176] P. Demorest, T. Pennucci, S. Ransom, M. Roberts, J. Hessels, *Nature* **467**, 1081-1083 (2010).

[177] J. Antoniadis et al., *Science* **340**, 448 (2013).

[178] H. Cromartie et. al., *Nat. Astron.* **4**, 72-76 (2020).

[179] R. W. Romani, D. Kandel, A. V. Filippenko, T. G. Brink, WeiKang Zheng, *Astrophys. J. Lett* **934**, L17 (2022).

[180] T. Damour and A. Nagar, *Phys. Rev. D* **80**, 084035 (2009).

[181] T. Hinderer, *Astrophys. J.* **677**, 1216 (2008).

[182] A. G. Riess et al., *Astron. J.* **116**, 1009-1038 (1998).

[183] S. Perlmmutter et al., *Astrophys. J.* **517**, 565-586 (1999).

[184] D. N. Spergel et al., *Astrophys. J. Suppl.* **148**, 175-194 (2003).

[185] S. S. Yazadjiev et al., *arXiv: 1705.06984v1* (2017).

[186] S. S. Yazadjiev et al., *arXiv: 1501.04591v1* (2015).

[187] S. Capozziello and M. de Laurentis, *Phys. Rep.* **509**, 167 (2011).

[188] S. Nojiri and S. D. Odintsov, *Phys. Rept.* **505**, 59 (2011).

[189] Y. H. Sham, L. M. Lin and P.T. Leung, Astrophys. J. **781**, 66 (2014).

[190] G. Abbas, S. Qaisar and A. Jawad, Astrophys. Space Sci. **359**, 57 (2015).

[191] M. C. Millar et al., *Astrophys. J. Lett.* **887**, L24 (2019).

[192] M. Bandyopadhyay and R. Biswas, *Int. J. Mod. Phys. D* **32**, 3 (2023).

[193] M. Bandyopadhyay and R. Biswas, *Mod. Phys. Lett. A* **36**, 7, 2150044 (2021).

[194] H. T. Cromertie et al., *Nat. Astron.* **4**, 72 (2019).

[195] Y. N. Obukhov and G. F. Rubilar, *Phys. Rev. D* **73**, 124017 (2006).

[196] X-D. Li, I. Bombaci, J. Dey and E. P.J. van den Heuvel, *Phys. Rev. Lett.* **83**, 19 (1999).

[197] F. A. Jenet et al., *Astrophys. J.* **498**, 365-372 (1998).

[198] J. W. Broderick et al., *Mon. Not. R. Astron. Soc.* **459**(3), 2681-2689 (2016).

[199] B. V. Ivanov, *Phys. Rev. D* **65**, 104011 (2002).

[200] W. B. Bonnor, F. I. Cooperstock, *Phys. Lett. A* **139**, 442 (1989).

[201] A. L. Mehra, *J. Aust. Math. Soc.* **6**, 153 (1966).

[202] A. L. Mehra, *Gen. Relativ. Grav.* **12**, 187 (1980).

[203] R. P. Negreiros, F. Weber, M. Malheiro, V. Usov, *Phys. Rev. D* **80**, 083006 (2009).

[204] S. Ray et al., *Phys. Rev. D* **68**, 084004 (2003).

[205] B. Kiczek and M. Rogatko, *J. Cosmol. Astropart. Phhys.* **09**, 049 (2019).

[206] J. D. V. Arbañil, M. Malheiro, *Phys. Rev. D* **92**, 084009 (2015).

[207] F. Weber, M. Malheiro et al., *J. Phys. Conf. Ser.* **312**, 042018 (2011).

[208] M. F. Shamir, I. Fayyaz, *Int. J. Geom. Methods Mod. Phys.* **17**(09), 2050140 (2020).

[209] T. Naz, M. F. Shamir, *Int. J. Mod. Phys. A* **35**(09), 2050040 (2020).

[210] S. Biswas et al., *Eur. Phys. J. C* **80**(02), 175 (2020).

[211] T. Papanikolaou et al., *Eur. Phys. J. C* **83**, 31 (2023).

[212] G. Farrugia et al., *Phys. Rev. D* **97**, 124064 (2018).

[213] S. Capozziello et al., *JHEP* **1302**(039), (2013).

[214] G. G. L. Nashed, E. N. Saridakis, *Class. Quant. Grav.* **36**(13), 135005 (2019).

[215] G. G. L. Nashed, E. N. Saridakis, *J. Cosmol. Astropart. Phys.* **05**, 017 (2022).

[216] J. S. Read et al., *Phys. Rev.* **D 79**, 124033 (2009).

[217] V. Canuto, S. M. Chitre *Phys. Rev. D* **9**, 1587 (1974).

[218] L. Herrera, N. O. Santos, *Astrophys. J.* **438**, 308-313 (1997).

[219] R. F. Sawer, *Phys. Rev. Lett.* **29**, 382-385 (1972).

[220] J. B. Hartle, R.F. Sawer, D. J. Scalapino, *Astrophys. J.* **199**, 471-481 (1975).

[221] T. Binnington, E. Poisson, *Phys. Rev. D* **80**, 084018 (2009).

[222] T. Damour, A. Nagar, *Phys. Rev. D* **80**, 084035 (2009).

[223] T. Hinderer, *Astrophys. J.* **677**, 1216 (2008).

[224] *É. É.* Flanagan and T. Hinderer, *Phys. Rev. D* **77**, 021502 (2008).

[225] B. P. Abbott et at., *Phys. Rev. X* **9**, 011001 (2019).

[226] K. Yagi, N. Yunes, *Phys. Rept.* **681**, 1 (2017).

[227] M. Ruiz, S. L. Shapiro, A. Tsokaros, *Phys. Rev.* **D 97**, 021501 (2018).

[228] M. Shibata et al., *Phys. Rev.* **D 96**, 123021 (2017).

[229] V. Cardoso et al., *Phys. Rev.* **D 95**, 084014 (2017).

[230] M. Bandyopadhyay, R. Biswas, *Int. J. Mod. Phys. D* **32**, 3 (2023).

[231] M. Bandyopadhyay, R. Biswas, *Mod. Phys. Lett. A* **36**, 7, 2150044 (2021).

[232] R. H. Lin, X. N. Chen, X. H. Zhai, *Eur. Phys. J. C* **82**, 308 (2022).

[233] S. Capozziello, R. D. Agostino, O. Luongo, *Int. J. Mod. Phys. D* **509**, 167 (2019).

[234] F. J. Fattoyev, C. J. Horowitz, J. Piekarewicz and B. Reed, *Phys. Rev. C* **102**, 065805 (2020).

[235] Y. H. Sham, L. M. Lin and P.T. Leung, Astrophys. J. **781**, 66 (2014).

[236] B. Kleihaus, J. Kunz and S. Mojika, *arXiv* **1407.6884**, (2014).

[237] P. Pani, E. Berti, *Phys. Rev. D* **90**, 024025 (2014).

[238] D. D. Doneva et al., *Phys. Rev. D* **90**, 104021 (2014).

[239] G. Pappas, T. P. Stiriou, *Phys. Rev. D* **91**, 044011 (2015).

[240] A. Bauswein, O. Just, H. T. Janka, N. Stergioulas, *Astrophys. J.* **850**, L 34 (2017).

[241] B. Margalit, B. D. Metzger, *Astrophys. J.* **850**, L 19 (2017).

[242] D. Radice, A. Perego, F. Zappa, S. Bernuzzi, *Astrophys. J.* **852**, L 29 (2018).

[243] L. Rezzolla, E. R. Most, L. R. Weih, *Astrophys. J.* **852**, L 25 (2018).

[244] G. Abbas, S. Qaisar, A. Jawad, Astrophys. Space Sci. **359**, 57 (2015).

[245] M. C. Millar et al., *Astrophys. J. Lett.* **887**, L24 (2019).

[246] S. Chandrasekhar, *Astrophys. J.* **140**, 417 (1964).

[247] L. Herrera, *Phys. Lett. A* **165**, 206 (1992).

[248] P. Demorest, T. Pennucci, S. Ransom, M. Roberts and J. Hessels, *Nature* **467**, 1081-1083 (2010).

[249] J. Antoniadis et al., *Science* **340**, 448 (2013).

[250] H. Cromartie et. al., *Nat. Astron.* **4**, 72-76 (2020).

[251] R. W. Romani, D. Kandel, A. V. Filippenko, T. G. Brink and WeiKang Zheng, *Astrophys. J. Lett* **934**, L17 (2022).

[252] S. Chakraborty et. al., *Eur. Phys. J. C* **72**, 2101 (2012).

[253] B. C. Paul, P. Thakur, *J. Cosmol. Astropart. Phys. 11*, 052 (2013).

[254] R. C. Tolman, *Phys. Rev.* **55**, 364 (1939).

[255] B. Kuchowicz, *Acta Phys. Pol* **33**, 541 (1968).

[256] H. Reissner, *Ann. Phys.* **50**, 106 (1916).

[257] G. Nordström, *Proc. K. Ned. Akad. Wet* **20**, 1238 (1918).

[258] C. O. Heinke et al., *Astrophys. J* **644**, 1090 (2006).

[259] S. Guillot et al., *Astrophys. J* **722**, 7 (2013).

[260] M. Servillant et al., *MNRS* **423**, 1556 (2012).

[261] A. Y. Potekhin, *Phys. Univ.* **735**, 57 (2014).

[262] S. Bogdanov et al., *Astrophys. J.* **831**(2), 184 (2016).

[263] A. V. Astashenok et al., *JCAP* **12**, 040 (2013).

[264] M. C. Miller et al., *Astrophys. J. Lett.* **887**(1), L24 (2019).

[265] H. T. Cromertie et al., *Nature Astron.* **4**(1), 72 (2019).

[266] M. Lineres et al., *Astrophys. J.* **859**(1), 54 (2018).

[267] R. Abbott et al., *Astrophys. J. Lett.* **896**(2), L44 (2020).

[268] Y. F. Cai et al., *Astrophys. J.* **888**, 62 (2020).

[269] K. Bamba et al., *Phys. Rev. D* **85**, 104036 (2019).

[270] G. G. L. Nashed, W. El Hanafy, S. K. Ibrahim, *arXiv: 1411.3293* (2014).

[271] K. Rezazadeh et al., *JHEP* **01**, 131 (2016).

[272] B. V. Ivanov, *Phys. Rev. D* **65**, 104011 (2002).

[273] A. L. Mehra, *J. Aust. Math. Soc.* **6** 153 (1966).

[274] S. Ray et al., *Phys. Rev. D* **68**, 084004 (2003).

[275] A. L. Mehra, *Gen. Relativ. Gravit.* **12**, 187 (1980).

[276] W. B. Bonnor, F. I. Cooperstock, *Phys. Lett. A* **139**, 442 (1989).

[277] R. P. Negreiros et al., *Phys. Rev. D* **80**, 083006 (2009).

[278] B. Kiczek, M. Rogatko, *JCAP* **09**, 049 (2019).

[279] J. D. V. Abrañil, M. Malheiro, **Phys. Rev. D 92**, 084009 (2015).

[280] M. Malheiro et al., *J. Phys. Conf. Ser.* **312**, 042018 (2011).

[281] M. Javed et al., *New Astron.* **84**, 101518 (2021).

[282] A. Majid, M. Sharif, *Universe* **6**, 124 (2020).

[283] M. F. shamir, T. Naz, *Phys. Dark Univ.* **27**, 100472 (2020).

[284] M. F. Shamir, I. Fayyaz, *Int. J. Geom. Methods Mod. Phys.* **17**(09), 2050140 (2020).

[285] T. Naz, M. F. Shamir, *Int. J. Mod. Phys. A* **35**(09), 2050040 (2020).

[286] S. Biswas et al., *Eur. Phys. J. C* **80**(2), 175 (2020).

[287] P. Bhar et al., *Eur. Phys. J. C* **79**(11), 922 (2019).

[288] Y. B. Zeldovich, I. V. Navikov, *Relativistic Astrophysics.* **Vol. 1**, Stars and Relativity (University of Chikago Press, Chikago, 1971).

[289] H. Abreu et al., *Class. Quant. Grav.* **24**, 4631 (2007).

[290] H. A. Buchdahl, *Phys. Rev* **116**, 1027 (1959).

[291] R. Abbott et al., *Astrophys. J.* **896**, L44 (2020).

[292] M. Shibata, E. Zhou, K. Kiuchi, S. Fujibayashi, *Phys. Rev. D* **100**, 023015 (2019).

[293] L. Rezzolla, E. R. Most, *Astrophys. J.* **852**, L25 (2018).

[294] L. Tolos, L. Fabbietti, *Prog. Part. Nucl. Phys.* **112**, 103770 (2020).

[295] P. Demorest, T. Pennucci, S. Ransom, M. Roberts, J. Hessels, *Nature* **467**, 1081-1083 (2010).

[296] J. Antoniadis et al., *Science* **340**, 448 (2013).

[297] H. Cromartie et al., *Nat. Astron.* **4**, 72-76 (2020).

[298] R. W. Romani, D. Kandel, A. V. Filippenko, T. G. Brink, WeiKang Zheng, *Astrophys. J. Lett.* **934**, L17 (2022).

[299] A. Tsokaros, M. Ruiz, S. L. Shapiro, *Astrophys. J.* **905**, 48 (2020).

[300] E. R. Most, L. J. Papenfort, L. R. Weih, L. Rezzolla, *MNRS. Lett.* **499** , L82-L86 (2020).

[301] M. Bandyopadhyay, R. Biswas, *Mod. Phys. Lett. A* **36**, 7, 2150044 (2021).

[302] D. A. Godzieba, D. Radice, S. Bernuzzi, *Astrophys. J.* **908**, 122 (2021).

[303] F. J. Fattoyev, C. J. Horowitz, J. Piekarewicz, B. Reed, *Phys. Rev. C* **102**, 065805 (2020).

[304] R. H. Lin, X. N. Chen, X. H. Zhai, *Eur. Phys. J. C* **82**, 308 (2022).

[305] S. Capozziello, R. D. Agostino, O. Luongo, *Int. J. Mod. Phys. D* **509**, 167 (2019).

[306] A. D. Felice, S. Tsujikawa, *Living Rev. Rel.* **13**, 3(2010).

[307] J. Harada, *Phys. Rev. D* **101**, 024053 (2020).

[308] G. J. Olmo, D. R. Garcia, A. Wojnar, *Phys. Rept.* **876**, 1 (2020).

[309] G. G. L. Nashed, S. Capozziello, *Eur. Phys. J. C* **80**(10), 969 (2020).

[310] R. Ferraro, F. Fiorini, *Phys. Rev. D* **91**, 064019 (2015).

[311] C. Will, *Living Rev. Rel.* **17**, 4 (2014).

[312] E. G. Adelberger et al., *Phys. Rev. Lett.* **98**, 131104 (2007).

[313] L. Tolos, L. Fabbietti, *Prog. Part. Nucl. Phys.* **112**, 103770 (2020).

[314] D. Huterer, D. L. Shafer, *Rep. Prog. Phys.* **81**, 016901 (2018).

[315] M. Bandyopadhyay, R. Biswas, *Int. J. Mod. Phys. D* **32**, 3 (2023).

[316] T. Harko, F. S. Lobo, S. I. Nojiri, S. D. Odintsov, *Phys. Rev. D* **84**, 024020 (2011).

[317] M. Mondal et al., *Int. J. Mod. Phys. D* **30** 2150095 (2021).

[318] M. Houndjo, *Int. J. Mod. Phys. D* **21** 1250003 (2012).

[319] E. H. Baffou et al., *Astrophys. Space Sci.***356**, 173-180 (2015).

[320] P. H. R. S. Moraes, J. D. V. Arbanil, M. Malheiro, *J. Cosmol. Astropart. Phys.* **7**, 168 (2016).

[321] H. Desmond, B. Jain, J. Sakatein, *Phys. Rev. D* **100**, 043537 (2019).

[322] G. Abbas et al., *Astrophys. Space Sci.* **357** 158 (2015).

[323] I. Bombaci, *Astron. Astrophys.* **305**, 871 (1996).

[324] S. Hansraj, A. Banerjee, *Phys. Rev. D* **97**, 104020 (2018).

[325] A. V. Astashenoka, S. Capozziello, S. D. Odinstov, *Phys. Lett. B* **742**, 160 (2015).

[326] A. de la Cruz-Dombriz et al., *arXiv: 1207.2663* (2012).

[327] P. Kaaret et al., *Astrophys. J. Lett.* **520**, L37 (1999).

[328] M. Linares, T. Sahabaz, J. Casares, *Astrophys. J.* **859**(1), 54 (2018).

[329] P. H. R. S. Moraes, *Astrophys. Space Sci.* **352**, 273 (2014).

[330] H. Shabani, M. Farhoudi, *Phys. Rev. D* **90**, 044031 (2014).

[331] P. H. R. S. Moraes, *Eur. Phys. J. C* **75**, 168 (2015).

[332] T. B. Goncalves, J. L. Rosa, F. S. N. Lobo, *Phys. Rev. D* **105**(6), 064019 (2022).

[333] T. B. Goncalves, J. L. Rosa, F. S. N. Lobo, *Eur. Phys. J. C* **82**(5), 418 (2022).

[334] P. Bhar, P. Rej, M. Zubair, *Chin. J. Phys.* **77**, 2201-2212 (2022).

[335] J. Kumar, H. D. Singh, A. K. Prasad, *Phys. Dark Universe* **34**, 100880 (2021).

[336] P. Saha, U. Debnath, *Adv.High Energ. Phys.* **2018**, 3901790 (2018).

[337] T. Tangphati, S. Hansraj, A. Banerjee, A. Pradhan, *Phys. Dark Universe* **35**, 100990 (2022).

[338] T. Tangphati, I. Karar, A. Pradhan, A. Banerjee, *Eur. Phys. J. C* **82**(1), 57 (2022).

[339] M. Mondal, F. Rahaman, *Universe* **9**, 122 (2023).

[340] G. G. L. Nashed, *Euro. Phys. J. C* **83**, 698 (2023).

[341] H. Stephani et al., *Cambridge University Press, ISBN 978-0-521-46702-5, 978-0-511-05917-9*, (2003).

[342] K. D. Krori, J. Barua, *J. Phys. A Math. Gen.* **8**, 508 (1975).

[343] S. M. Carroll, V. Duvvuri, M. Trodden and M. S. Turner, *Phys. Rev. D* **70**, 043528 (2004).

[344] D. J. Einstein et al., *Astrophys. J.* **633**, 560-574 (2005).

[345] A. D. Felice, S. Tsujikawa, *Living Rev. Rel.* **13**, 3(2010).

[346] J. Harada, *Phys. Rev. D* **101**, 024053 (2020).

[347] G. J. Olmo, D. R. Garcia, A. Wojnar, *Phys. Rept.* **876**, 1 (2020).

[348] G. G. L. Nashed, S. Capozziello, *Eur. Phys. J. C* **80**(10), 969 (2020).

[349] C. Will, *Living Rev. Rel.* **17**, 4 (2014).

[350] J. G. Williams, S. G. Turyshev, D. H. Boggs, *Phys. Rev. Lett.* **93**, 261101 (2004).

[351] E. G. Adelberger et al., *Phys. Rev. Lett.* **98**, 131104 (2007).

[352] R. W. Romani, D. Kandel, A. V. Filippenko, T. G. Brink, WeiKang Zheng, *Astrophys. J. Lett.* **934**, L17 (2022).

[353] A. Tsokaros, M. Ruiz, S. L. Shapiro, *Astrophys. J.* **905**, 48 (2020).

[354] M. Bandyopadhyay, R. Biswas, *Mod. Phys. Lett. A* **36**, 7, 2150044 (2021).

[355] T. Harko, F. S. Lobo, S. I. Nojiri, S. D. Odintsov, *Phys. Rev. D* **84**, 024020 (2011).

[356] M. Mondal, F. Rahaman, K. N. Singh, *Eur. Phys. J. C* **81** , 84 (2021).

[357] P. H. R. S. Moraes, J. D. V. Arbanil, M. Malheiro, *J. Cosmol. Astropart. Phys.* **7**, 168 (2016).

[358] M. Bandyopadhyay, R. Biswas, *Int. J. Mod. Phys. D* **32**, 3 (2023).

[359] M. C. Millar et al., *Astrophys. J. Lett.* **887**(1), L24 (2019).

[360] L. Tolos, L. Fabbietti, *Prog. Part. Nucl. Phys.* **112**, 103770 (2020).

[361] J. M. Lattimer, *Ann. Rev. Nucl. Part. Sci.* **62**, 485-515 (2012).

[362] A. Sheykhi, *Phys. Rev. D* **86**, 024013 (2012).

[363] S. C. V. Ilijic, M. Sossich, *Phys. Rev. D* **98**, 064047 (2018).

[364] R. D'Agostino, R. C. Nunes, *Phys. Rev. D* **101**, 103505 (2020).

[365] R. Lobato et al., *J. Cosmol. Astropart. Phys.* **12**, 039 (2020).

[366] M. sharif, A. Waseem, *Eur. Phys. J. C* **78**, 868 (2018).

[367] P. Kaaret et al., *Astrophys. J. Lett.* **520**, L37 (1999).

[368] J. J. Darke et al., *Astrophys. J.* **572**, 996-1001 (2002).

[369] W. C. G. Ho et al., *Mon. Not. Roy. Astron. Soc.* **375**, 821-830 (2007).

[370] R. P. Mignani et al., *Mon. Not. Roy. Astron. Soc.* **465**(1), 492-500 (2017).

[371] X. Fan et al., *Eur. Phys. J. D* **71**, 308 (2017).

[372] D. Huterer, D. L. Shafer, *Rep. Prog. Phys.* **81**, 016901 (2018).

[373] K. V. Staykov et al., *arXiv: 1407.2180v1* (2014).

[374] G. Abbas et al., *Astrophys. Space Sci.* **357** 158 (2015).

[375] I. Bombaci, *Astron. Astrophys.* **305**, 871 (1996).

[376] H. Shabani, M. Farhoudi, *Phys. Rev. D* **90**, 044031 (2014).

[377] A. V. Astashenoka, S. Capozziello, S. D. Odintsov, *Phys. Lett. B* **742**, 160 (2015).

[378] R. C. Tolman, *Phys. Rev.* **55**, 364 (1939).

[379] B. Kuchowicz, *Acta Phys. Pol.* **33**,541 (1968).

[380] M. Javed, G. Mustafa, M. F. Shamir, *New Astron.* **84**, 101518 (2021).

[381] M. F. Shamir, T. Naz, *Phys. Dark. Universe* **27**, 100427 (2020).

[382] A. Majid, M. Sharif, *Universe* **6**, 124 (2020).

[383] M. F. Shamir, I. Fayyaz, *Int. J. Geom. Methods Mod. Phys.* **17**(09), 2050140 (2020).

[384] T. Naz, M. F. Shamir, *Int. J. Mod. Phys. A* **35**(09), 2050040 (2020).

[385] M. Linares, T. Sahabaz, J. Casares, *Astrophys. J.* **859**(1), 54 (2018).

[386] H. Abreu et al., *Class. Quant. Grav.* **24**, 4631 (2007).

[387] L. Herrera, *Phys. Lett. A* **165**, 206 (1992).

[388] Y. B. Zeldovich , I. D. Navikov, *Relativistic Astrophysics.*, Vol 1, Stars and Relativity (University of Chicago Press, Chicago) (1971).

[389] J. R. Oppenheimer, G. M. Volkoff, *Phys. Rev.* **55**, 374-381 (1939).

[390] L. D. Landau, E. M. Lifshitz, *The Classical Theory of Fieelds*(Pergamon, Oxford), (1998).

[391] R. C. Tolman, *Phys. Rev.* **35** 896 (1930).